PHD THESIS

THESIS SUBMITTED IN PARTIAL FULLFILLMENT OF THE REQUIREMENTS FOR THE DEGREE OF DOCTOR OF PHILOSOPHY

Investigating the role of centrosome amplification in extracellular vesicle secretion in pancreatic ductal adenocarcinoma

Author:

Sophie Danielle Adams

Bsc (hons)., MRes

September 2019

Centre for Molecular Oncology, Barts Cancer Institute

Queen Mary
University of London
Barts and The London

Statement of originality

I, Sophie Danielle Adams, confirm that the research included within this thesis is my own work or that where it has been carried out in collaboration with, or supported by others, that this is duly acknowledged below and my contribution indicated.

I attest that I have exercised reasonable care to ensure that the work is original, and does not to the best of my knowledge break any UK law, infringe any third party's copyright or other Intellectual Property Right, or contain any confidential material.

I accept that the College has the right to use plagiarism detection software to check the electronic version of the thesis. I confirm that this thesis has not been previously submitted for the award of a degree by this or any other university.

Signature: Sophie Adams

Date: 26/09/19

Acknowledgements

Firstly, I would like to express my sincere gratitude to my supervisor Dr. Susana Godinho, for her constant guidance, support and enthusiasm throughout my PhD. Thank you for pushing me to become a better scientist and giving me the freedom to pursue my own ideas. Thanks, should be given to my secondary supervisor Professor Hemant Kocher for his constant support and input over the years. I am blessed to have been mentored by such incredible scientists.

I would also like to thank all the members of the Godinho laboratory, past and present, for their support, guidance and friendship along the way. To members past, Alex, Teresa and Pedro, thank you for welcoming me into the lab, helping me find my feet and guiding me in those all-important early years. To the new members, Judit, Juidth and Bongwhan, thank you for your support and friendship these last few years. Working with you all has been a pleasure and ensured the lab was always a fun place to be.

Many thanks also go to our collaborator, Dr. Faraz Mardakheh for his assistance with our SILAC-based proteomics screen, to Hefin Rhys for mentoring me in vesicle research and statistical analysis and to the Medical Research Council and Cancer Research UK for funding my project.

To the PhD office, thank you for making my PhD a fun and sociable adventure and for supporting me through the difficulty times. Special thanks go to my friends Liz, Abi, Alejandro and Ed who have been on this journey with me from the start and without whom the journey wouldn't have been nearly as enjoyable or memorable. Thank you all for your friendship and support and for always knowing how to make me smile.

I would also like to thank my family, for always believing in me and providing unwavering support throughout my PhD. Thank you for the constant love and encouragement.

Abstract

Pancreatic Ductal Adenocarcinoma (PDAC) is characterised by a dense desmoplastic reaction that is attributed to the activation of pancreatic stellate cells (PSCs) in the stroma. This alteration of the tumour microenvironment is thought to contribute to PDAC aggressiveness and resistance to therapy. Recent studies have shown that exosomes (a subgroup of secreted extracellular vesicles) secreted by cancer cells facilitate cross talk between tumour cells and the microenvironment. However, the mechanisms that lead to the secretion of these vesicles remains elusive.

Here, we report for the first time, a novel role for centrosome amplification, a common feature of human tumours, in the secretion of small extracellular vesicles ($_s$EVs). We show that centrosome amplification significantly correlates with and is sufficient to induce the elevated secretion of $_s$EVs in PDAC cell lines. Furthermore, we demonstrate that oxidative stress in cells with supernumerary centrosomes is the driving force behind this altered $_s$EV secretion. An analysis of centrosome amplification-associated increases in cellular reactive oxygen species (ROS) demonstrated an impaired lysosome function and the prevention of MVB/lysosome fusion events. The results indicate that centrosome amplification induced ROS induces $_s$EV secretion by preventing MVB degradation by the lysosome, shifting their fate to fusion with the plasma membrane and subsequent secretion of their intraluminal vesicles (ILVs) as exosomes.

To understand if exosomes secreted from cells with amplified centrosomes could impact the tumour microenvironment, we subsequently investigated the role of these $_s$EVs on the activation of PSCs, as measured by the formation of fibres containing alpha-smooth muscle actin (α-SMA). We found that $_s$EVs isolated from cells with supernumerary centrosomes elicit significantly stronger activation of PSCs compared to $_s$EVs isolated from cells with a normal centrosome number, suggesting a difference in their biological cargo. SILAC based-proteomic analysis revealed the gain or loss of 6 EV protein in $_s$EVs isolated from cells upon the induction of centrosome amplification, that may have a role in the activation of PSCs. We hypothesise, that further understanding the role of centrosome amplification in $_s$EV-mediated PSC activation may help us to identify

innovative ways to block PSC activation and prevent the progression of PDAC, which could have major clinical implications for patients with this devastating disease.

Contents

List of Figures

List of Tables

Acronyms

α-SMA	Alpha-smooth muscle actin
ANOVA	Analysis of variance
ATP	Adenosine triphosphate
BAF. A1	Bafilomycin A1
BODIPY maleimide	Boron-dipyrromethene maleimide
BSA	Bovine serum albumin
CAF	Cancer-associated fibroblast
CA 19-9	Carbohydrate antigen 19-9
CDK	Cyclin-dependent kinase
CIN	Chromosomal instability
CPAP	Centrosomal P4.1-associated protein
DMEM	Dulbecco's modified Eagle's medium
DMEM:F12	Dulbecco's modified Eagle's medium/nutrient mixture F-12 Ham
DMSO	Dimethyl sulfoxide
DNA	Deoxyribonucleic acid
Dox	Doxycycline hyclate
ECL	Enhanced chemiluminescence reagent
ECM	Extracellular matrix
EGF	Epidermal growth factor
EGFR	Epidermal growth factor receptor
EMT	Epithelial-mesenchymal transition
EV	Extracellular vesicle
EXO	Exosome
FAP	Fibroblast activation protein
FBS	Foetal bovine serum
FGF2	Fibroblast growth factor 2
FITC	Fluorescein isothiocyanate
FOLFIRINOX	Folinic acid, 5-FU, irinotecan and oxaliplatin
GFP	Green fluorescent protein
GSH	Glutathione (reduced)
GSSG	Glutathione (oxidised)
GTP	Guanine triphosphate
HEPES	4-(2-hydroxyethyl)-1-piperazineethanesulfonic acid

HRP	Horseradish peroxidase
HER2	Human epidermal growth factor receptor 2
HIV	Human immunodeficiency virus
HPV	Human papillomavirus
H_2O_2	Hydrogen peroxide
IL	Interleukin
KO	Knockout
LATS 2	Large tumour suppressor kinase 2
LEVs	Large extracellular vesicles
M	Molar
MAPs	Microtubule associated proteins
mg	Milligram
min	Minutes
miRNA	Micro ribonucleic acid
mL	Millilitre
mM	Millimolar
MMP	Matrix metalloproteinase
MRI	Magnetic resonance imaging
mRNA	Messenger ribonucleic acid
MT	Microtubule
MV	Microvesicle
MVB	Multivesicular body
NAC	N-acetyl cysteine
NICE	National Institute for Health and Care Excellence
nm	Nanometer
NTA	Nanoparticle tracking analysis
OD	Optical densit
PanIN	Pancreatic intraepithelial neoplasia
PBS	Phosphate-buffered saline
PCM	Pericentriolar material
PCR	Polymerase chain reaction
PDAC	Pancreatic ductal adenocarcinoma
PDGF	Platelet-derived growth factor
PLK4	Polo like kinase 4
PSC	Pancreatic stellate cell
PTEN	Phosphatase and tensin homologue

PVDF	Polyvinylidene fluoride
Rac1	Ras-Related C3 Botulinum Toxin Substrate 1
Rb	Retinoblastoma
Rho(A)	Ras homolog gene family (member A)
RIPA	Radioimmunoprecipitation assay
RNA	Ribonucleic acid
RNAi	RNA interference
rpm	Revolutions per minute
RPMI	Roswell Park Memorial Institute medium
ROS	Reactive oxygen species
SAC	Spindle assembly checkpoint
SD	Standard deviation
SDS	Sodium dodecyl sulphate
SDS-PAGE	Sodium dodecyl sulphate polyacrylamide gel electrophoresis
SEC	Size exclusion chromatography
SEM	Standard error of the mean
sEVs	Small extracellular vesicles
Shh	Sonic hedgehog
siRNA	Small interfering RNA
SPB	Spindle pole body
SSC	Right angle light/side scatter
TβR	TGF-β receptor
TBST	Tris-buffered saline Tween-20
TetR	Tetracycline repressor
TGF-β	Transforming growth factor β
TP53	Tumour protein 53
UC	Ultracentrifugation
V	Volt
VEGF	Vascular endothelial growth factor
WT	Wild type
5-FU	5-fluorouracil
^{o}C	Degrees Celcius
µM	Micromolar
µg	Microgram
µm	Micrometer
γ-TURC	γ-tubulin ring complex

Chapter 1

Introduction

1.1 The centrosome

The centrosome is a small cytoplasmic organelle that constitutes the main microtubule organising centre (MTOC) in eukaryotic cells. Centrosomes are comprised of a pair of orthogonally poisitioned barrel shaped centrioles embedded in a dense proteinaceous matrix called the pericentriolar material (PCM), which provides the site for microtubule nucleation (Figure 1.1). The centrioles are cylindrical structures, that range from 100-400nm in length and 100-250nm in diameter (Carvalho-Santos *et al.*, 2011) and are characterised by a highly conserved triplet of microtubules that arrange in a nine-fold symmetry forming the centriole wall (Gönczy, 2012; Nigg and Holland, 2018). The two centrioles are structurally different with the older and more mature 'mother' centriole carrying subdistal and distal appendages that the younger 'daughter' centriole does not have (see Figure 1.1). These appendages are required for anchorage to microtubules and for membrane docking during ciliogenesis (Piel *et al.*, 2000; Bettencourt-Dias and Glover, 2007; Gogendeau, Guichard and Tassin, 2015; Nigg and Holland, 2018). Together, the two centrioles are crucial for recruiting the PCM which consists of concentric protein layers that surround the centrioles (Fu and Glover, 2012; Lawo *et al.*, 2012; Mennella *et al.*, 2012; Sonnen *et al.*, 2012). The inner layer of the PCM contains gamma-tubulin ring complexes (γ- TuRCs) which are fundamental for microtubule nucleation. During mitosis, this inner layer expands and recruits additional components resulting in a mature centrosome with peak MTOC activity (Fu and Glover, 2012; Mennella *et al.*, 2012).

In cycling cells, owing to its role as an MTOC, the centrosome is vital for generating the mitotic spindle, regulating cell shape, cell polarity and cell motility (Nigg and Raff, 2009; Bornens, 2012; Conduit, Wainman and Raff, 2015; Fu, Hagan and Glover, 2015). In many differentiated cell types, however, the mother centriole acts as a basal body and provides a template for the formation of cilia and flagella (Kim and Dynlacht, 2013; Ito and Bettencourt-Dias, 2018).

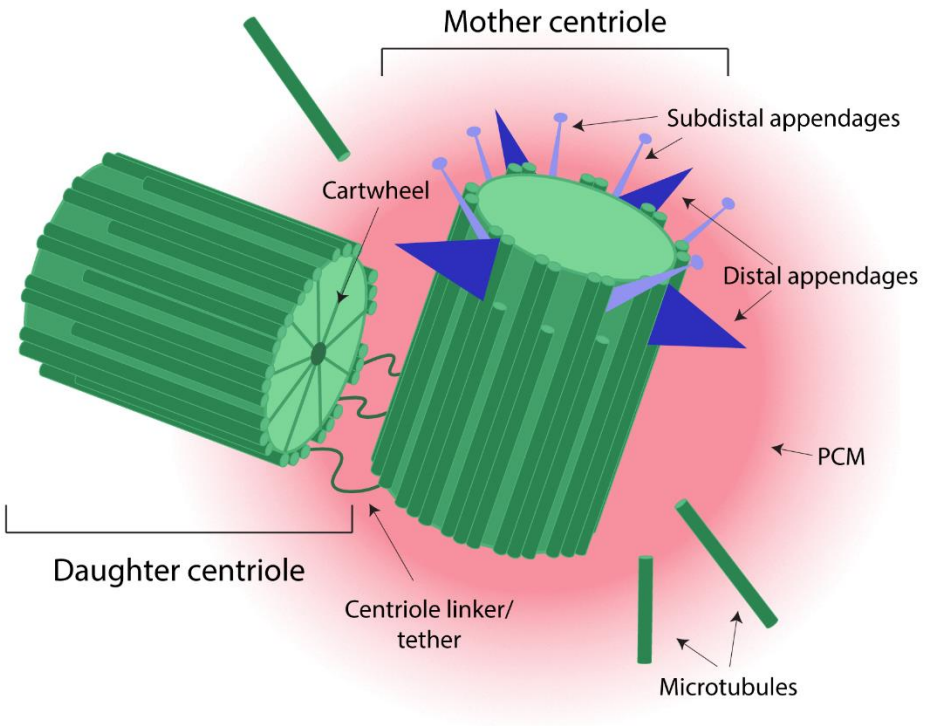

Figure 1.1 Centrosome structure. Schematic diagram of the centrosome structure. The centrosome consists of two orthogonally positioned centrioles which are comprised of a nine-fold symmetry of triplet microtubules. The older mother centriole carries distal and subdistal appendages that the younger daughter centriole lacks. The two centrioles are tethered together by a centriole linker and are surrounded by the pericentriolar material (PCM) which provides the site for microtubule nucleation.

1.1.1 Centrosomes and cell division

The centrosome, first described in 1887 by the German biologist Theodore Boveri as "the organ for cell division", has been shown to play a vital role in nucleating and organising spindle microtubules (MT) during mitosis to ensure faithful segregation of chromosomes (Paintrand *et al.*, 1992; Bignold, Coghlan and Jersmann, 2006; Boveri, 2008). However, more recent studies have revealed that many cells which lack centrosomes, such as higher plant cells and oocytes, still have a robust ability to form bipolar mitotic/meiotic spindles (Dumont and Desai, 2012; Masoud *et al.*, 2013). Additionally, it had been shown that in most cells, genetic or physical removal of the centrosome does not prevent the formation of a bipolar mitotic spindle and subsequent segregation of chromosomes (Lerit and Poulton, 2016). It is now understood that several non-centrosomal pathways exist which can nucleate MTs during mitosis in addition to or instead of centrosomal MT nucleation including: MT nucleation from mitotic

chromatin (Karsenti and Vernos, 2001; Gruss and Vernos, 2004; O'Connell and Khodjakov, 2007), the Augmin complex which nucleates MTs from existing MTs (Goshima *et al.*, 2008; Lawo *et al.*, 2009; Goshima and Kimura, 2010; Sánchez-Huertas and Lüders, 2015) and acentrosomal MTOCs (aMTOC) in which many components of the PCM self-organise in the absence of centrioles to nucleate MTs (Schuh and Ellenberg, 2007; Moutinho-Pereira, Debec and Maiato, 2009; Kleylein-Sohn *et al.*, 2012; Baumbach *et al.*, 2015). The importance of bipolar mitotic spindle assembly and faithful segregation of the chromosomes to maintain genomic stability makes it unsurprising that cells have more than one method of forming the mitotic spindle.

Interestingly, whilst it has been shown that the centrosome is not necessary for cell division to occur, the absence of functional centrosomes comes with a cost. In drosophila, research suggests that the centrosome is dispensable in most cells (Megraw, Kao and Kaufman, 2001; Basto *et al.*, 2006; Blachon *et al.*, 2008), however, as is seen with the developing fly wing disc, a significant fraction of cells without centrosomes develop increased rates of aneuploidy and DNA damage, often leading to apoptosis (Poulton, Cuningham and Peifer, 2014). Additionally, it has been demonstrated that the centrosome is required in early drosophila embryo development, specifically for the first division of a newly fertilised egg (Stevens *et al.*, 2007; Rodrigues-Martins *et al.*, 2008) and that embryos defective for key PCM proteins have aberrant mitotic spindles and damaged DNA (Megraw *et al.*, 1999; Vaizel-Ohayon and Schejter, 1999; Varmark *et al.*, 2007; Lerit *et al.*, 2015). Similar results have also been demonstrated in *C. elegans* where depletion of centrosome maturation factor Air-1 resulted in aberrant spindles, sever aneuploidy and embryonic lethality (Schumacher *et al.*, 1998). Although the centrosome appears non-essential to invertebrate cell division, in vertebrates, the lack of functional centrosomes has been shown to induce chromosome segregation errors, leading to loss of cell viability (reviewed in Conduit, Wainman and Raff, 2015). Indeed, centrosome loss in cultured chicken cells has been shown to result in slower rates of mitosis, perturbed chromosome segregation, DNA damage, aneuploidy and often leads to cell death (Sir *et al.*, 2013). Similarly, centrosome loss in mouse embryos and cultured mammalian cells has been shown to increase the rates of cell apoptosis (Bazzi and Anderson, 2014; Insolera *et al.*, 2014; Wong *et al.*, 2015). Furthermore, mouse embryonic tissues which

lack centrosomes have been shown to have significant mitotic delays which result in p53 activation and subsequent p53-mediated cell apoptosis (Bazzi and Anderson, 2014; Insolera *et al.*, 2014). Therefore, whilst cell division can occur in the absence of functional centrosomes, the centrosome facilitates the formation of the mitotic spindle and progression through mitosis in a timely manner preventing mitotic delays and maintaining cell viability. Moreover, centrosomes have been shown to play an important role in maintaining genomic stability and cell viability across many different species (Debec, 1978; Sir *et al.*, 2013).

1.1.2 The centrosome duplication cycle

In dividing cells, centrosomes are duplicated in a semi-conservative manner ensuring that at mitotic onset only two centrosomes are present to facilitate bipolar spindle formation. Failure to properly regulate the centrosome duplication cycle has been linked to several human diseases including cancer and microcephaly. The centrosome duplication cycle occurs in a 5 step process: in late M phase/ G1 the centrioles disengage from one another, in S-phase the centrioles duplicate, in G2 the centrioles elongate and the centrosome matures and finally in late G2/M-phase the centrosomes segregate and move to the poles of the cell in preparation for bipolar spindle formation (Nigg and Stearns, 2011; Mardin, 2014; Fu, Hagan and Glover, 2015) (Figure 1.1.2). Recent advances in imaging, proteomics, structural biology and genome editing have provided key insights into the centrosome duplication cycle including its regulation, centriole biogenesis and how alterations to the cycle can lead to human disease (reviewed by Nigg and Holland, 2018).

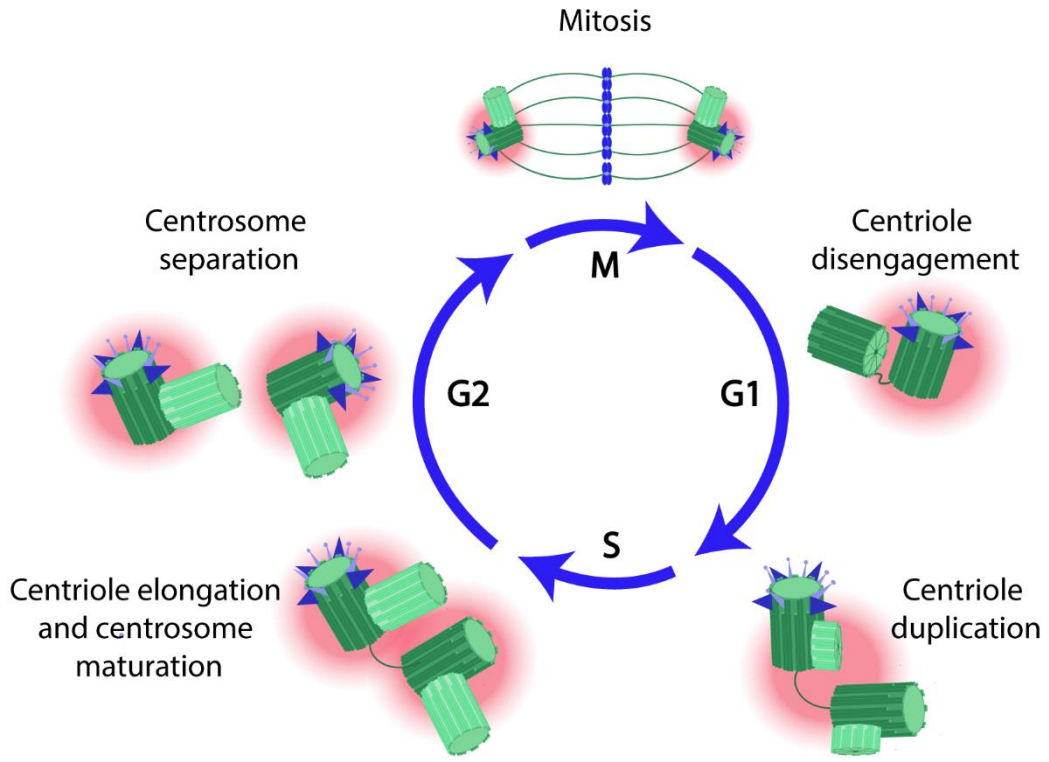

Figure 1.1.2 The centrosome duplication cycle. Schematic diagram of the centrosome duplication cycle. During the G1 phase of cell cycle the two centrioles disengage from one another but remain connected by a protein linker. At the transition from G1 to S phase, procentrioles form at the proximal end of each parent centriole. During S phase and G2, the procentrioles elongate into full sized centrioles and centrosome maturation takes place. In G2 the linker is removed and the two centrosomes segregate. Finally, during mitosis the newly formed mature centrosomes move to opposite poles and assemble the bipolar mitotic spindle.

1.1.2.1 Centriole disengagement

The centrosome duplication cycle begins at the end of mitosis when the two centrioles disengage from one another. Separation of the two centrioles is a crucial first step as the close proximity between the two centrioles is known to block duplication of the parent centriole (Tsou and Stearns, 2006; Loncarek *et al.*, 2008; Tsou *et al.*, 2009). Disengagement is controlled by the mitotic kinase Polo-like kinase 1 (PLK1) and the protein separase which likely cleaves the PCM component pericentrin (PCNT) promoting centriole separation (Tsou *et al.*, 2009; Lee and Rhee, 2012; Matsuo *et al.*, 2012). Importantly, PLK1-driven separase activity is required both for the separation of centrioles and the separation of sister chromatids during mitosis, linking the timing of these two events (Tsou *et al.*, 2009). Additionally, the cell cycle kinase Cdk2 is also

required for both DNA replication and centriole duplication, where its presence is necessary for centriole disengagement and the initiation of centriole duplication (Hinchcliffe *et al.*, 1999; Lacey, Jackson and Stearns, 1999). Synchronising centriole disengagement and the DNA cycle ensures that centrosomes cannot duplicate before chromosome segregation has taken place, eliminating the possibility of multipolar spindles forming and subsequent chromosome missegregation. Upon separation of the centrioles, a proteinaceous tether forms between the two ensuring they remain localised near one another until the two newly formed centrosomes are finally separated in G2 (Mardin and Schiebel, 2012).

1.1.2.2 Centriole duplication

During G1/S transition, once the centrioles have successfully disengaged, centriole duplication begins with the assembly of a procentriole (which will form the new daughter centriole) perpendicular to the parent centriole. Centriole duplication is initiated by the centrosomal proteins CEP192 and CEP152 which recruit PLK4, the master regulator of centriole duplication, to the proximal end of the mother centriole (Bettencourt-Dias *et al.*, 2005; Habedanck *et al.*, 2005; Pelletier *et al.*, 2006; Kim *et al.*, 2013; Sonnen *et al.*, 2013; Park *et al.*, 2014). PLK4 subsequently phosphorylates the conserved centriole duplication factor SCL/TAL-interrupting locus protein (STIL) which triggers the recruitment of the spindle assembly abnormal protein 6 homologue (SAS-6) to the centriole (Dzhindzhev *et al.*, 2014; Ohta *et al.*, 2014; Kratz *et al.*, 2015; Moyer *et al.*, 2015). Recruitment of SAS-6 results in the formation of the procentriole scaffold structure known as the cartwheel. The cartwheel consists of an internal ring composed of nine SAS-6 homodimers from which nine ‘spokes’ protrude to connect the nine triplets of microtubules that make up the centriole wall (Nakazawa *et al.*, 2007; Gopalakrishnan *et al.*, 2010; Kitagawa *et al.*, 2011; van Breugel *et al.*, 2011, 2014; Guichard *et al.*, 2012; Arquint and Nigg, 2016; Marteil, Dias Louro and Bettencourt-Dias, 2017). Thus PLK4, STIL and SAS-6 are crucial regulators of centriole duplication.

1.1.2.3 Centriole elongation

During S-phase, following the formation of the procentriole cartwheel structure, the procentriole elongates to form a full-length centriole. Elongation begins with the recruitment of centrosomal P4.1-associated protein (CPAP) to the cartwheel where it binds centrosome-associated protein 135 (CEP135) and stabilises the cartwheel structure (Lin *et al.*, 2013). CPAP, along with CEP135 and γ-tubulin, then regulate the deposition of centriolar microtubules around the cartwheel (Kleylein-Sohn *et al.*, 2007). CEP135 connects SAS-6 to CPAP, bridging the gap between the SAS-6 homodimers and the microtubules (Lin *et al.*, 2013). Importantly, CP110 localises to the distal end of the elongating procentriole and acts as a cap to limit microtubule growth, thereby regulating centriole size (Tsang *et al.*, 2008; Lee *et al.*, 2017).

1.1.2.4 Maturation of the centrosome

Towards the end of G2, following centriole elongation, the PCM expands significantly in a process termed centrosome maturation. Maturation of the centrosomes is governed by PLK1 which localises Cep192, CDK5RAP2, pericentrin, Nedd1 and γ-tubulin to the centrosome (Haren, Stearns and Lüders, 2009; Zhang *et al.*, 2009; Lee and Rhee, 2011; Fu and Glover, 2012). Furthermore, Aurora A has been shown to play a role in both the phosphorylation/activation of PLK1 and additionally in the enrichment of multiple centrosomal factors, including the transforming acidic coiled-coil protein 3 (TACC3) to the centrosome (Giet *et al.*, 2002; Barros *et al.*, 2005; Kinoshita *et al.*, 2005; Macůrek *et al.*, 2008). The recruited PCM proteins then activate the γ-TuRCs which are required for microtubule nucleation and mitotic spindle assembly (reviewed by Ito and Bettencourt-Dias, 2018). Importantly, the PCM is only present around the mother centriole, however, during disengagement of the centrioles at G1 phase, PLK1 regulates the daughter centriole becoming competent and recruiting a PCM of its own (reviewed by Fu, Hagan and Glover, 2015). Additionally, in G2/M-phase the daughter centriole becomes fully mature by acquiring the appendages that are characteristic of a mother centriole in a process that is once again regulated by PLK1 (Kong *et al.*, 2014).

1.1.2.5 Centrosome segregation

At the end of G2, in preparation for mitosis, the two newly formed centrosomes separate and move to either pole of the cell to facilitate formation of the bipolar spindle. Centrosome segregation entails a two-step process, first the physical linker that binds the two centrosomes via their mother centrioles is severed and then force-dependent separation and movement of the two centrosomes occurs.

The centrosomal linker is composed of several proteins including C-Nap1 (CEP250), rootletin, CEP68 and LLRC45 (Mayor *et al.*, 2000; Bahe *et al.*, 2005; Yang, Adamian and Li, 2006; Graser *et al.*, 2007; He *et al.*, 2013). At the proximal ends of the two mother centrioles is a CEP250 ring which acts as an anchor for the filament-like proteins rootletin and LLRC45 which form the body of the linker (Yang, Adamian and Li, 2006; He *et al.*, 2013; Panic *et al.*, 2015; Vlijm *et al.*, 2018). Specifically, a rootletin ring is organised at the CEP250 ring from which additional rootletin/Cep68 fibres and LLRC45 emanate and form a web like structure which provides flexibility to the linker (Vlijm *et al.*, 2018). During the G2/M transition, the centrosomal linker is severed by the NIMA-related kinase 2A (Nek2A) which phosphorylates the linker proteins resulting in their disassociation from the centrosome and subsequent dissolution of the linker (Mayor *et al.*, 2000; Bahe *et al.*, 2005; Graser *et al.*, 2007; Nigg and Stearns, 2011; Mardin and Schiebel, 2012; He *et al.*, 2013). Following removal of the linker, force-dependent separation and movement of the centrosomes occurs under the control of motor proteins. The kinesin related plus-end-directed motor Eg5 is the main force generator responsible for centrosome separation, acting through anti-parallel microtubule sliding to physically push the centrosomes apart from one another (reviewed in Mardin and Schiebel, 2012). In fact, the strong force generated by Eg5 is sufficient to separate the two centrosomes even in the presence of an intact centrosomal linker (Mardin *et al.*, 2010). Inhibition of Eg5 results in prometaphase arrest and the formation of a monopolar spindle (Whitehead and Rattner, 1998; Kapoor *et al.*, 2000). The activity of Eg5 is regulated by PLK1, which during prophase phosphorylates and activates the NIMA-related kinase Nek9, which in turn phosphorylates Nek6 and Nek7. Activated Nek6 then phosphorylates Eg5 targeting it to the centrosome resulting in Eg5 binding to MTs and enabling centrosome separation (Blangy *et al.*, 1995; Roig *et al.*, 2002, 2005;

Belham *et al.*, 2003; Bertran *et al.*, 2011; Mardin *et al.*, 2011; Smith *et al.*, 2011). In addition, nuclear envelope (NE)- associated dynein works in conjunction with Eg5 to separate centrosomes by pulling the centrosomes along the NE (Raaijmakers *et al.*, 2012; Raaijmakers and Medema, 2014). Following successful separation of the centrosomes and movement to opposite poles, each centrosome nucleates a microtubule array, forming a bipolar spindle which connects to and faithfully segregates the chromosomes into two daughter cells.

1.2 Centrosome amplification and cancer

A link between centrosome abnormalities and cancer was first proposed in the 19th century by Theodore Boveri who hypothesised that supernumerary centrosomes would lead to multipolar cell division resulting in malignant transformation due to genomic instability (Boveri, 1888, 2008). Using dispermic sea urchin eggs, which harbour extra centrosomes (as the sperm provides the centrosome during embryogenesis), Boveri observed the development of multipolar spindles and the subsequent asymmetric division of chromosomes into 3 or more highly aneuploid daughter cells (Figure 1.2).

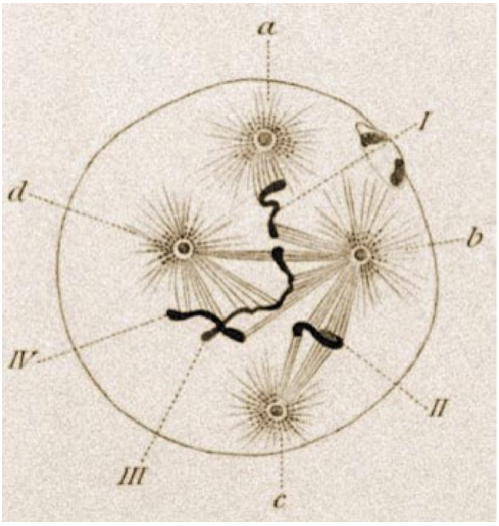

Figure 1.2 Theodor Boveri drawing of dispermic sea urchin eggs based on his microscopy observations. Theodor Boveri's observation that amplified centrosomes (a-d) in a fertilised sea urchin egg resulted in uneven chromosome distribution (I-IV) and multipolar cell division, resulting in aneuploid daughter cells. He therefore hypothesised that supernumerary centrosomes could generate genetic instability and facilitate tumourigenesis (Boveri, 1888).

He found the resultant progeny to have different developmental characteristics which provided the first ever indication that chromosomes are important for cellular traits (Boveri, 1887, 1888). This finding, along with the contribution of his contemporaries Gino Galeotti and David von Hansemann who showed abnormal cell division to be a common feature of human tumours, led to Boveri's later hypothesis that supernumerary centrosomes drive tumourigenesis by triggering aneuploidy (Hansemann, 1890; Galeotti, 1893; Boveri, 2008). However, whilst Hansemann's work did show the frequent presence of asymmetric cell division and aneuploid progeny in tumours, he also observed faulty mitoses in benign lesions and therefore suggested they were not the cause of cancer (Hardy and Zacharias, 2005). Thus, whilst Boveri was in favour of chromosome segregation errors driving tumourigenesis, Hansemann was not. Indeed, many remained sceptical of the role of abnormal mitoses in the development of cancer and instead research remained focussed on the discovery of cancer-causing mutations. In the late 1990s, however, it was discovered that the loss of the key tumour suppressor p53 was associated with centrosome defects which led to renewed interest in the role of centrosome defects in tumourigenesis (Fukasawa *et al.*, 1996). Following this discovery, extensive research has established centrosome abnormalities to be a common feature of both solid and haematological malignancies (reviewed in Chan, 2011).

1.2.1 Centrosome abnormalities in cancer

Centrosome abnormalities can be classified as either structural or numerical aberrations where structural aberrations constitute defects in either centriole size/structure or alterations in the amount of PCM surrounding the centrosomes and numerical aberrations can include centrosome amplification or centrosome loss (reviewed by Nigg, 2006). Currently numerical aberrations are far better characterised than structural ones owning to the difficulties in identifying structural abnormalities. As Centrioles are close to the limits of optical resolution of light microscopy at 0.2-0.5µM in length, specialised fluorescence microscopy is required to identify differences between structural and numerical anomalies. Historically, PCM markers have been used to analyse centrosomal

changes, however interpreting these changes as purely structural or numerical is difficult. For example, although increases in PCM is a characteristic of structural abnormalities, similarly increased PCM is observed when supernumerary centrosome cluster together in interphase constituting a numerical defect (D'Assoro *et al.*, 2002a; Lingle *et al.*, 2002; Nigg, 2006; Guo *et al.*, 2007; Godinho *et al.*, 2014). Thus, PCM markers alone cannot distinguish structural from numerical aberrations. As many studies analysing centrosome anomalies in tumour samples use PCM markers only, it is difficult to distinguish between the role of numerical and structural aberrations in cancer development and progression. To aid in the distinction between numerical and structural aberrations, it is now widely accepted that the use of bona fide centriole labelling is necessary. However, as structural abnormalities caused by increased centriole length can also result in centriole fragmentation, it is still possible to confuse the presence of fragmented centrioles with amplified centrioles (Kohlmaier *et al.*, 2009). Therefore, more accurate methods to distinguish and classify centrosome abnormalities are required to gain further insight into how different centrosome aberrations affect the tumour landscape.

Currently numerical aberrations, specifically centrosome amplification have been described as the most prevalent centrosomes defect in human cancers where the presence of extra centrosome has been identified in the majority of human tumour types including breast, prostate, colon, ovarian and pancreatic cancers (Lingle *et al.*, 1998; Pihan *et al.*, 1998; Sato *et al.*, 1999; Nigg, 2002; Giehl *et al.*, 2005; Hsu *et al.*, 2005; Krämer, Neben and Ho, 2005; Chan, 2011). Furthermore, centrosome amplification has been shown to correlate with high-grade tumours and poor prognosis as well as tumour recurrence and metastasis (Pihan *et al.*, 2001; D'Assoro *et al.*, 2002a; Yamamoto *et al.*, 2004; Reiter *et al.*, 2009; Chan, 2011). Currently the exact role of supernumerary centrosomes in tumour development and progression is unclear. However, amplified centrosomes have also been observed in early, low-grade lesions indicating that supernumerary centrosomes may play a driving role in tumourigenesis (Lingle *et al.*, 2002; Pihan *et al.*, 2003; Segat *et al.*, 2010; Lopes *et al.*, 2018). Thus, understanding the link between centrosome amplification and disease progression may provide important new targets for therapy and biomarker development.

1.2.2 Causes of centrosome amplification

Whilst it is still unclear how centrosome amplification arises in cancer; a few different methods have been shown to lead to its initiation. An important contributor to the overduplication of centrosomes is the dysregulation of the centrosome cycle, which can lead to centriole overduplication or overexpression of PCM proteins (reviewed in Godinho and Pellman, 2014). As previously described in this chapter, the centrosome duplication cycle is tightly regulated by crucial positive and negative regulators to ensure centrosomes are duplicated in a timely manner and only once per cell cycle (Nigg and Stearns, 2011; Brownlee and Rogers, 2013). Although these regulators are rarely mutated, centrosomal proteins are often found to be over or under expressed in cancer (Nigg and Raff, 2009; Chan, 2011; Gönczy, 2015). One major route to supernumerary centrosomes is dysregulation of centriole duplication through destabilisation of key centriolar proteins. For example, overexpression of PLK4, the master regulator of centriole duplication, leads to over duplication of centrioles and subsequent centrosome amplification (Habedanck *et al.*, 2005; Kleylein-Sohn *et al.*, 2007). Conversely, loss of PLk4 results in decreased centriole numbers (O'Connell *et al.*, 2001; Bettencourt-Dias *et al.*, 2005; Habedanck *et al.*, 2005). Levels of PLK4 are tightly regulated throughout the cell cycle via its own autophosphorylation which leads to $SCF\beta^{TrCP}$/ubiquitin-dependent proteolysis (Cunha-Ferreira *et al.*, 2009; Rogers *et al.*, 2009; Guderian *et al.*, 2010; Holland *et al.*, 2010; Sillibourne *et al.*, 2010; Brownlee *et al.*, 2011). In fact, it has been suggested that in some tumours, supernumerary centrosomes may arise from deregulation of ubiquitin regulators leading to over or under expression of centriolar components. For example, decreased expression of the ubiquitin ligase βTrCP has been shown to result in PLK4 stabilisation leading to amplified centrosomes (Wojcik, Glover and Hays, 2000; Guardavaccaro *et al.*, 2003; Cunha-Ferreira *et al.*, 2009; Rogers *et al.*, 2009). Additionally, levels of the centriole capping protein CP110 are regulated by $SCF^{cyclinF}$/ubiquitin-dependent proteolysis and the deubiquitinating enzyme USP33. Overexpression of USP33 has been shown to induce centrosome amplification through increased CP110 levels (Li *et al.*, 2013). Supporting the notion that deregulation of ubiquitin regulators leads to amplified centrosomes through stabilisation of key centriolar proteins.

Another instance of centriole overduplication resulting in centrosome amplification is in High-risk human papillomavirus (HPV)-associated tumours. The HPV-16 E7 oncogene has been shown to induce centriole overduplication by increasing PLK4 mRNA levels (Korzeniewski, Treat and Duensing, 2011). Thus, regulation of centriole duplication can be affected at the transcriptional level. Importantly, the levels of PLK4 mRNA are negatively regulated through p53 which recruits histone deacetylases (HDAC) to the promoter of PLK4 repressing transcription (Li *et al.*, 2005). Therefore, indicating that p53 loss could lead to increased PLK4 levels, a view that has been supported by the observation that p53 loss in mouse fibroblasts is associated with centrosome amplification (Fukasawa *et al.*, 1996). On the converse however, analysis of p53-/- mouse brains indicated no change in centrosome number (Marthiens *et al.*, 2013). Highlighting that whilst p53 loss may play a contributory role in the development of centrosome amplification, it is not sufficient to induce it alone.

In addition to centriole overduplication, overexpression of key PCM components such as pericentrin and γ-tubulin can also induce centrosome amplification (Loncarek *et al.*, 2008). It has been demonstrated that upon loss of the tumour suppressor BRAC1, γ-tubulin levels become elevated resulting in supernumerary centrosomes (Starita *et al.*, 2004). Disruption of cell cycle progression can lead to re-duplication of centrioles. Prolonged G2 arrest can lead to PLK1 activation which promotes premature centrosome maturation and disengagement prior to mitosis resulting in reduplication of centrioles (Lončarek, Hergert and Khodjakov, 2010). Therefore, DNA damage may induce centrosome amplification by elongating the time spent in G2 phase. Another mechanism of generating supernumerary centrosomes is through the formation of tetraploid cells, which can arise from cytokinesis failure, mitotic slippage or cell-cell fusion (Andreassen *et al.*, 2001; Fujiwara *et al.*, 2005) . Furthermore, over-elongation of the centrioles can result in their fragmentation which also promotes centrosome amplification (Marteil *et al.*, 2018).

1.2.3 p53 activation

Despite the maintained presence of centrosome amplification in cell lines and tumours, extra centrosomes have been shown to have a deleterious effect on cell proliferation and survival. This fitness disadvantage appears to arise from centrosome amplification-associated p53 and subsequent p21 stabilisation resulting in G1 cell cycle arrest and decreased proliferation (reviewed in Rhys and Godinho, 2017; Nigg and Holland, 2018). In fact, it has been shown that supernumerary centrosomes arising from both centriole over-duplication and tetraploidisation trigger cell cycle arrest through p53 stabilisation (Holland *et al.*, 2012; Ganem *et al.*, 2014). Thus, highlighting that regardless of the method of amplification, extra centrosomes on their own confer a survival disadvantage to cells in culture. Interestingly, however, tetraploid cells have been shown to maintain a growth advantage and induce tumourigenesis, with strong evidence now indicating that a large proportion of human tumours may originate from tetraploid cells (Zack *et al.*, 2013). Additionally, the established presence of supernumerary centrosomes in cell lines and human tumours indicates that cells must acquire further genetic alterations to enable them to overcome the fitness disadvantage associated with extra centrosomes. One important genetic alteration is loss of p53 which has been shown to rescue the detrimental effects of centrosome amplification enabling cells to not only survive and proliferate in the presence of but also maintain supernumerary centrosomes (Holland *et al.*, 2012). Furthermore, work performed to identify modulators of p53-mediated arrest in tetraploid cells with amplified centrosomes revealed a role for the large tumour suppressor kinase 2 (LATS2) in arresting tetraploid cells in G1. LATS2 was found to be phosphorylated in cells with extra centrosomes which lead to activation of the Hippo pathway and subsequent proliferation defects (Ganem *et al.*, 2014) (See Figure 1.2.3). Additionally, decreased RhoA activity has been observed in cells with extra centrosomes, which also leads to activation of the Hippo pathway (Ganem *et al.*, 2014; Godinho *et al.*, 2014). Decreased RhoA activity is likely due to centrosome amplification-associated increases in microtubule nucleation which results in the hyperactivation of the RhoA antagonist Rac1 (Sander *et al.*, 1999; Godinho *et al.*, 2014). Similarly, amplified centrosomes have been found to activate PIDDosome components which leads to p53 stabilisation through Caspase-2 mediated cleavage of the p53 regulator MDM2 (Fava *et*

al., 2017) (See Figure 1.2.3). Thus, it is possible that disruption of the Hippo pathway or PIDDosome activation may facilitate survival of cells with extra centrosomes.

Although cancer cells can overcome the deleterious effects of amplified centrosomes through additional genetic alterations, it is still somewhat surprising that supernumerary centrosomes are such a common feature of human malignancies. Therefore, their maintained presence may suggest amplified centrosomes confer an advantage to tumourigenesis that outweighs their detrimental effects and warrants their preservation.

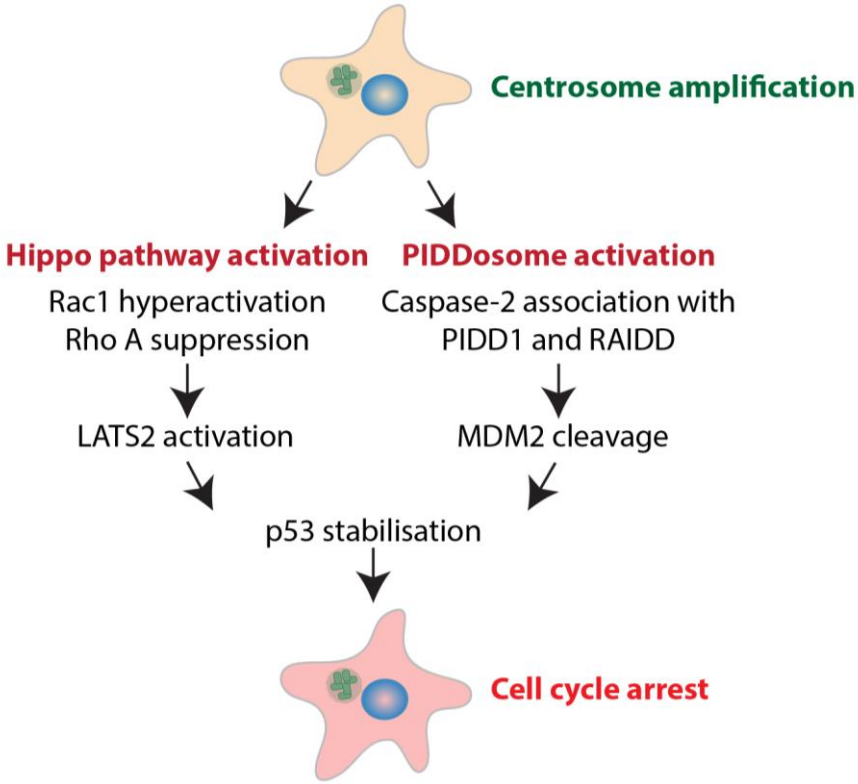

Figure 1.2.3 Mechanisms of centrosome amplification-induced p53-mediated cell cycle arrest. Supernumerary centrosomes can result in Hippo pathway or PIDDosome activation leading to p53 stabilisation and cell cycle arrest.

1.2.4 Coping with extra centrosomes

In the 18th century, Theodore Boveri hypothesized that supernumerary centrosomes would cause multipolar mitoses, inducing high levels of genetic instability and facilitating the formation of tumours (Boveri, 2008). It is unlikely, however, that this correlation is a result of centrosome amplification-induced multipolar cell division as recent studies have shown multipolar mitoses to result in catastrophic levels of aneuploidy and subsequent cell death (Ganem, Godinho and Pellman, 2009; Godinho and Pellman, 2014) (Figure 1.2.4). In fact, it has been demonstrated that in mouse neuronal stem cell where centrosome amplification leads to multipolar mitosis's, the resultant high levels of aneuploidy lead to developmental defects but not cancer (Marthiens *et al.*, 2013). Therefore, multipolar cell division render a significant barrier to the survival of cells with supernumerary centrosomes and are thus detrimental to tumour formation. Instead, cells with extra centrosomes have been found to supress multipolar cell division thorough a process termed "centrosome clustering", where centrosomes are coalesced into two poles. This phenomenon was first discovered through work performed in the N1E-115 mouse neuroblastoma cell line in which almost 100% of cells have extra centrosomes (Ring, Hubble and Kirschner, 1982). Amplified centrosomes were shown to cluster into two poles, enabling the formation of a bipolar spindle allowing chromosome segregation into two daughter cells (Ring, Hubble and Kirschner, 1982) (see Figure 1.2.4). Following this finding, many cancer cell lines with high levels of centrosome amplification (>30% of cells with supernumerary centrosomes) have been shown to efficiently cluster centrosomes (Ring, Hubble and Kirschner, 1982; Brinkley, 2001; Quintyne *et al.*, 2005; Kwon *et al.*, 2008; Ganem, Godinho and Pellman, 2009). In fact, to date, centrosome clustering is the best characterised mechanism employed by cells with amplified centrosomes, to avoid the detrimental effects of multipolar mitoses.

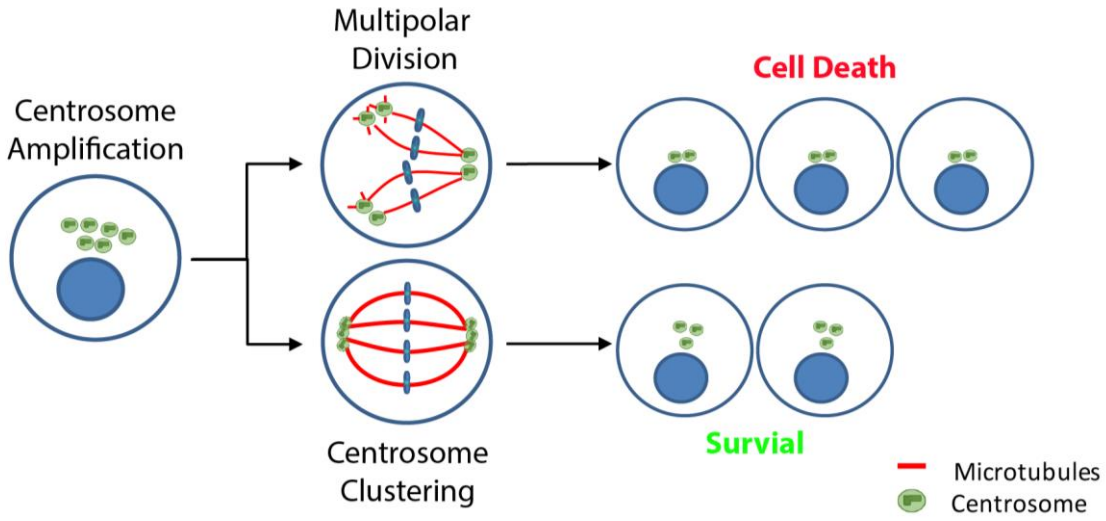

Figure 1.2.4 Coping with supernumerary centrosomes. Supernumerary centrosomes can result in i) multipolar cell division, where chromosomes are separated into three or more daughter cells resulting in gross aneuploidy and poor survival or ii) pseudo-bipolar cell division, facilitated by centrosome clustering, where chromosomes are segregation into two daughter cells only resulting in little to no aneuploidy and cell survival.

1.2.5 Centrosome amplification and tumourigenesis

1.2.5.1 Chromosome instability (CIN)

Since Boveri's initial hypothesis, a strong correlation has been identified between centrosome amplification and chromosome instability (CIN) in human cancers and aneuploidy and CIN have been shown to facilitate the formation of tumours (Weaver *et al.*, 2007; Zyss and Gergely, 2009; Chan, 2011). However, as centrosome amplification induced multipolar mitoses are detrimental to cell viability and proliferation, they do not explain the link between centrosome amplification and CIN, suggesting another mechanism is involved. In fact, centrosome clustering is now known to induce low levels of aneuploidy and CIN due to the increased formation of erroneous merotelic attachments, which can result in the formation of lagging chromosomes (Cimini, 2008; Ganem, Godinho and Pellman, 2009; Silkworth *et al.*, 2009). If undetected by the spindle assembly checkpoint (SAC), lagging chromosomes can result in DNA damage, chromothripsis and the formation of micronuclei (Cimini, 2008; Janssen *et al.*, 2011; Stephens *et al.*, 2011; Crasta *et al.*, 2012; Wang *et al.*, 2014). Therefore, centrosome clustering enables cell survival, whilst also affording the cells losses or gains of genetic

material, which explains the observed correlation between centrosome amplification and CIN in tumours (Chan, 2011; Gönczy, 2015). Importantly, these centrosome amplification-associated chromosomal defects, both numerical and structural may facilitate tumourigenesis (Weaver *et al.*, 2007; Holland and Cleveland, 2012). Whilst the exact mechanism behind this is unknown, it is believed that these defects drive genetic instability and heterogeneity which provides cancer cells with advantageous features that enable tumours to evolve and avoid cell death (reviewed in Nigg and Holland, 2018).

1.2.5.2 Microtubule nucleation, cell polarity and motility

In non-dividing cells, the centrosome plays an important role in organising microtubule (MT) arrays which affect cell polarity, cell motility and cell signalling (Bettencourt-Dias and Glover, 2007). During interphase, amplified centrosomes can be clustered into one "super centrosome" which recruits a large PCM affording these cells a heightened capacity for MT nucleation (D'Assoro *et al.*, 2002b; Lingle *et al.*, 2002). Therefore, amplified centrosomes may also influence tumour biology by affecting MT nucleation and altering the subsequent associated cellular processes (Godinho and Pellman, 2014). Indeed, centrosome amplification-linked increases in MT nucleation have been correlated with high grade breast cancer independent of aneuploidy generation (Salisbury, D'Assoro and Lingle, 2004). Centrosome position and the direction of MT nucleation plays a major role in establishing cell polarity, determining cell shape and motility (Tang and Marshall, 2012). In fact in neurons, the direction of MT nucleation can determine the site of axon outgrowth and can affect the direction of migration by altering the positioning of the Golgi to the leading edge (Tang and Marshall, 2012). Additionally, increase MT nucleation can alter focal adhesion (FA) disassembly which is key for cell migration and regulated by MTs (Stephens *et al.*, 2012). Therefore, whilst further study is necessary, in theory, super centrosomes have the potential to induce stronger polarisation and subsequently alter cell motility (Godinho and Pellman, 2014).

1.2.5.3 Cell Invasion

The ability of a super centrosome to nucleate more MTs may also affect cell invasion through activation of the Rho GTPases (Lozano, Betson and Braga, 2003). For example, MT depolymerization induces RhoA activation and MT polymerisation activates Rac1 resulting lamellipodia formation and cell migration by inducting Arp2/3-mediated actin polymerisation (Waterman-Storer *et al.*, 1999; Yuan-Chen *et al.*, 2008). Indeed using a 3D culture model, Godinho *et al* have demonstrated that increased MT nucleation as a result of centrosome amplification leads to increased Rac1 activity, the formation of invadopodia, decreased cell-cell adhesion and subsequent cell invasion. Importantly, this result was shown to be independent of the degree of aneuploidy (Godinho *et al.*, 2014). Furthermore, recent work performed by Ganier *et al* has demonstrated that centrosome structural abnormalities also result in the formation of invasive protrusions. The authors show that the induction of centrosome structural aberrations trigger basal cell extrusion of damaged cells (Ganier, Schnerch and Nigg, 2018), suggesting that centrosome aberrations as a whole have the capacity to induce invadopodia formation and cell invasion.

Importantly, a more recent study from our laboratory has shown centrosome amplification to drive non-cell-autonomous invasion in 3D mammary organoids and zebrafish models (Arnandis *et al.*, 2018). Our work shows cells with extra centrosomes have an extra centrosomes-associated secretory phenotype (ECASP) which includes increased secretion of interleukin-8 (IL-8) and results in paracrine cell invasion through activation of human epidermal growth factor receptor 2 (HER-2) signalling. Moreover, we show that centrosome amplification induces oxidative stress in the human breast cell line MCF10A through increased levels of reactive oxygen species (ROS). These increases in ROS were shown to be responsible for the ECASP and subsequent paracrine-mediated cell invasion (Arnandis *et al.*, 2018). Crucially our work highlights that cells with supernumerary centrosomes have the capacity to alter the behaviours of surrounding cells, indicating that these cells may have further and more far-reaching impact on tumourigenesis.

Therefore, the ability of cells with amplified centrosomes to increase cell invasion, whether it be autocrine or paracrine, may at least in part, explain the observed

association between centrosome amplification and advanced disease and metastasis (Godinho and Pellman, 2014).

1.2.5.4 Cell signalling

The centrosome has been established as a cellular signalling platform for many years, where it has been shown to concentrate signalling molecules and enhance signalling specificity (reviewed in Godinho and Pellman, 2014). One clear example, is the regulation of mitotic entry in fission yeast, where the centrosome/spindle body pole acts as a hub to regulate mitotic entry by amplifying cyclinB/cdk1 activity and circulating the signal throughout the cell (Hagan and Grallert, 2013). Centrosomal regulation of mitotic entry appears to be a widely conserved mechanism as it has been observed in *C.elegans, Xenopus* eggs and in human cells.

The role of the centrosome as a signalling platform has been strengthened by proteomic analysis of purified centrosomes, which identified members of multiple signalling pathways as being associated with the centrosome (Andersen *et al.*, 2003; Jakobsen *et al.*, 2011). In fact, components of the Wnt, NF-κ B and integrin signalling pathways which can affect tumourigenesis, can associate with the centrosome (Fielding *et al.*, 2008; Kfoury *et al.*, 2008; Itoh *et al.*, 2009). In addition, the centrosome is a known core for ubiquitin-mediated proteolysis (Wigley *et al.*, 1999). For example, upon bone morphogenic protein (BMP) signalling, phosphorylated and polyubiquitinated Smad1 becomes localized at the centrosome. In fact, following inhibition of the proteasome, the levels of phospho-Smad1 at the centrosomes greatly increases, therefore indicating that the centrosome may also act as a platform for proteasome-mediated degradation (Fuentealba *et al.*, 2007). The centrosome, therefore, has been shown to act as a signalling hub, sequestering signalling proteins and promoting phosphorylation and degradation as necessary. Thus, it is likely, that centrosome aberrations would affect centrosome-mediated cellular signalling and contribute to the deregulated signalling often observed in cancer (Godinho and Pellman, 2014).

1.2.5.5 Transgenic mouse models

Whilst a link between centrosome amplification and tumourigenesis has been postulated for many years, the role of extra centrosomes on tumour initiation and development remained largely untested in mammalian models until recently. However, the development of transgenic mouse models in which overexpression of PLK4 can be exploited to induce centrosome amplification has enabled further investigation into the role of supernumerary centrosomes in cancer development and progression. These models revealed that transient PLK4 overexpression leading to centrosome amplification in mice accelerates tumourigenesis in absence of the tumour suppressor p53 (Coelho *et al.*, 2015; Serçin *et al.*, 2015). Specifically, Serçin *et al* showed that in p53 deficient mice, transient PLK4 overexpression in the mouse epidermis resulted in centrosome amplification and subsequent formation of tumours in the skin. Interestingly, prior to tumour formation, centrosome amplification in epidermal cells significantly decreased. The relatively short-lived presence of amplified centrosomes in the mouse epidermis, was sufficient to induce aneuploidy and resulted in spontaneous tumours in the absence of p53. Suggesting therefore that centrosome amplification may play a role in the development of these skin tumours (Serçin *et al.*, 2015). Similarly, work performed by Coelho *et al* utilising inducible ubiquitous overexpression of PLK4 in p53 knock out mice, revealed that centrosome amplification advanced the onset of tumours, primarily lymphomas and sarcomas (Coelho *et al*., 2015). In this study, hyperplasia of the pancreas and skin was also observed, although tumours did not develop in these areas. It is possible, however, that tumours did not form in these areas as the mice succumb early to lymphoma and sarcoma, preventing sufficient time for pancreatic cancer and/or skin cancer development (Coelho *et al*., 2015). Together these studies indicate that upon loss of p53, centrosome amplification accelerates tumourigenesis.

Conversely, however, when an alternative mouse model was used to generate extra centrosomes, where PLK4 overexpression was ubiquitous, centrosome amplification did not induce or accelerate tumourigenesis even in the absence of p53 (Vitre *et al.*, 2015). The exact reasons for these different observations are unknown, however, the different method for generating amplified centrosome may be accountable. It is possible that whilst transient overexpression of PLK4 is permissive to tumourigenesis, ubiquitous

overexpression is detrimental to the process. Furthermore, an additional study evaluating centrosome amplification on tumour formation in the mouse brain, found that extra centrosomes do not induce brain tumours but instead leads to microcephaly (Marthiens *et al.*, 2013). Thus, indicating that centrosome amplification associated tumourigenesis is tissue dependent.

Interestingly, a more recent study performed by (Levine *et al.*, 2017) demonstrated that centrosome amplification was sufficient to promote tumourigenesis in mice with wild-type (WT) p53. The authors showed that transient overexpression of PLK4 throughout the mice leads to centrosome amplification and subsequently results in the development of spontaneous tumours with high levels of genomic instability that have lost p53. These genomic effects strongly suggest that supernumerary centrosomes are not mere by-standers, but induce mitotic errors resulting in malignant karyotypes promoting tumourigenesis (Levine *et al.*, 2017). These contradictory observations on the necessity of a p53 null background may be attributed to the use of different mouse models in the studies. Spontaneous tumour formation in the presence of WT p53 was induced by a single copy of the PLK4 transgene knocked into the COI1a1 locus resulting in a modest increase in PLK4 levels and relatively low levels of centrosome amplification (Levine *et al.*, 2017). In the other models (described above), the PLK4 transgene is expressed at much higher levels leading to higher centrosome amplification. It is possible that small increases in centrosome number facilitate tumour development in a WT p53 background, whereas larger increases in centrosome number may be detrimental to cells (Levine *et al.*, 2017). Furthermore, Lopes *et al* demonstrated the presence of amplified centrosomes in during Barrett's esophagus tumourigenesis, where extra centrosomes were identified in the premalignant condition through to dysplasia and throughout malignant transformation and metastasis. This work showed, as has been previously described, that widespread centrosome amplification required p53 loss (Chan, 2011; Lopes *et al*., 2018), however, low incidence of centrosome amplification does arise in a p53 WT background (Lopes *et al*., 2018). Providing further evidence to suggest a role for centrosome amplification in the initiation and progression of tumourigenesis.

The work performed using mouse models of centrosome amplification highlights potential roles for supernumerary centrosomes in both initiating tumour formation and cancer progression. The presence of extra centrosomes in both early and late stages of disease indicate that centrosome amplification may be a promising marker for both early and late stage cancer development, highlighting the potential benefit of developing a biomarker for centrosome amplification.

1.3 Pancreatic cancer

1.3.1 Incidence and mortality rates

Pancreatic cancer, one of the most aggressive solid malignancies, is the 5th leading cause of cancer related deaths in the UK (Cancer Research UK, 2019). This highly lethal cancer is associated with very poor prognosis, and mortality rates associated with the disease closely parallel incidence rates (Kamisawa *et al.*, 2016). In fact, following diagnosis, patients suffering from pancreatic cancer have a median survival rate of 6 months and a 5-year survival rate of only 3% (Siegel, Miller and Jemal, 2019). This dismal prognosis is attributed to the absence of detectable symptoms during early stages of the disease, a lack of reliable biomarkers and aggressive metastasis which leads to poor response to treatment (Maitra and Hruban, 2008). As early stages of the disease are symptomless, at diagnosis, around 50% of patients present with late stage metastatic disease (Adamska, Domenichini and Falasca, 2017). Furthermore, autopsy reports have indicated that around 90% of pancreatic cancer related deaths are attributed to complications due to distant metastasis (Kamisawa *et al.*, 1995). Shockingly, whilst significant strides have been made to improve the 5-year survival rates of patients suffering from other common cancers such as breast, prostate and bowel, survival rates for patients with pancreatic cancer have not improved (see Figure 1.3.1; Cancer Research UK, 2019). Moreover, incidences of pancreatic cancer have risen by 15% over the past 30 years (Rahib *et al.*, 2014). With the current lack of significant advances in detection or treatment, pancreatic cancer is predicted to become the second leading cause of cancer related deaths, behind lung cancer, by 2030 (Rahib *et al.*, 2014). Clearly, pancreatic cancer represents an area of unmet clinical need, where advancements in

early detection and novel therapeutics are desperately required to improve clinical outcome.

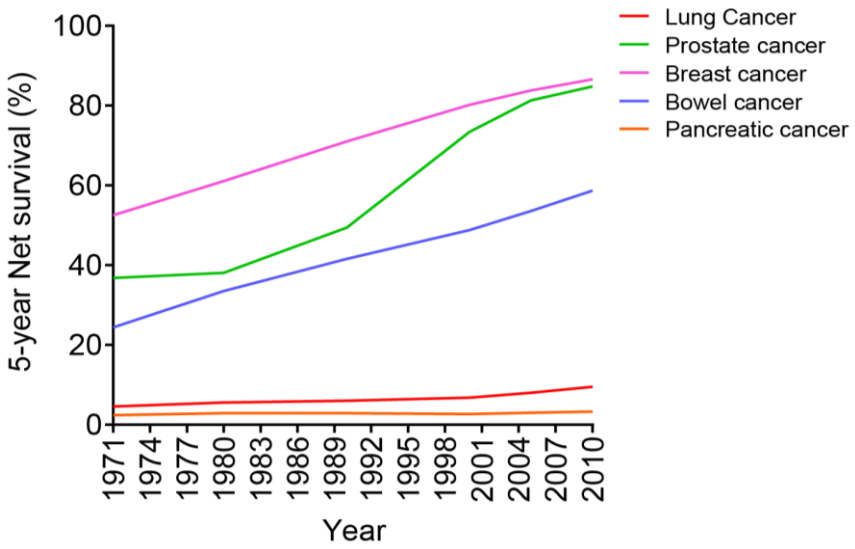

Figure 1.3.1 Improvements in cancer 5-year survival rates. Changes in 5-year survival rates for the 5 most common UK cancers from 1981-2010. Significant improvement is observed in the 5-year survival of patients suffering prostate, breast and bowel cancer. Little improvement is observed in patients suffering lung or pancreatic cancer (data from Cancer Research UK, 2019).

1.3.2 Risk factors for pancreatic cancer

To date, the development of pancreatic cancer is largely unexplained by any known risk factors, and around 90% of cases arise from spontaneous somatic oncogenic mutations (Raimondi, Maisonneuve and Lowenfels, 2009; Kamisawa *et al.*, 2016). Pancreatic cancer predominately affects the elderly, with the majority of diagnosis occurring in patients over 50 and over half of these patients being 70-80 years of age (Kleeff *et al.*, 2016). Thus, ageing is considered the greatest risk factor for pancreatic cancer. This is likely due to advanced age providing time for DNA damage to occur and facilitate oncogenic mutations (Raimondi, Maisonneuve and Lowenfels, 2009). Several other risk factors have been identified, however, including family history, personal history and underlying medical conditions. Around 5-10% of pancreatic cancer incidences are familial in origin, and several genetic syndromes are known to result in development of the disease (Klein *et al.*, 2004; Hruban *et al.*, 2010). Such hereditary conditions include:

Peutz-Jeghers syndrome which is caused by germline alterations in *STK11* (LBK1) (Giardiello *et al.*, 1987), familial atypical mole-multiple melanoma (FAMMM) syndrome which arises as a result of *CDKN2A* (p16) mutation (A. M. Goldstein *et al*., 1995), familial pancreatic cancer caused by *PALB2* or *ATM* germline mutations (Jones *et al.*, 2009; Roberts *et al.*, 2012) and hereditary pancreatitis caused by germline mutations in *PRSS1* and *SPINK1* (Lowenfels *et al.*, 1997). Additionally, mutations in the *BRCA1* gene have been shown to increase the risk of breast, ovarian and pancreatic cancer (Couch *et al.*, 2007; Kamisawa *et al.*, 2016).

Lifestyle risk factors are believed to be accountable for around 37% of pancreatic cancer incidences in the UK (Brown *et al.*, 2018). Smoking tobacco increases the risk of developing pancreatic cancer by 75% and around 15-30% of pancreatic cancer cases are associated with smoking (Iodice *et al.*, 2008; Parkin, 2011; Bosetti *et al.*, 2012; Whiteman *et al.*, 2015). Thus, smoking is the biggest avoidable cause of pancreatic cancer. Heavy alcohol consumption has also been shown to increase the risk of developing pancreatic cancer (Tramacere *et al.*, 2010; Lucenteforte *et al.*, 2012). This is believed to be due to the alcohol-associated development of chronic pancreatitis which is known to increase the risk of pancreatic cancer by more than 10-fold (Raimondi *et al.*, 2010). Whilst pancreatitis can be hereditary, it accounts for only 1% of the disease, whereas 70% of chronic pancreatitis is caused by heavy alcohol consumption. Obesity, low physical activity and poor diet including high intake of saturated fats and red and processed meat have also been linked to an increased risk of pancreatic cancer (Larsson and Wolk, 2012; Bosetti *et al.*, 2013; Rohrmann *et al.*, 2013; Behrens *et al.,* 2015; Genkinger *et al.*, 2015). Furthermore, type 2 diabetes mellitus has been associated with an approximate 30% increase in the risk of pancreatic cancer (Sah *et al.*, 2013; Bosetti *et al.*, 2014). In fact, long term diabetes is believed to double the risk of pancreatic cancer (Bosetti *et al.*, 2014). However, diabetes, specifically type 3c diabetes, can also be caused by pancreatic cancer itself. Therefore, the development of diabetes in elderly patients can lead to a pancreatic cancer diagnosis (Chari *et al.*, 2008; Bosetti *et al.*, 2014). Thus, whilst most pancreatic cancer incidences are unexplained, a proportion of cases could be prevented by altering certain lifestyle choices.

1.3.3 Types of pancreatic cancer

The pancreas is a highly specialised organ that carries out two key biological functions; the exocrine function and the endocrine function. The exocrine function, facilitated by the exocrine cells of the pancreas including acinar and ductal cells, involves the secretion of enzymes into the intestine to aid digestion (reviewed by Pandol, 2011). The endocrine function, facilitated by endocrine cells that are contained within the pancreatic islets of Langerhans, involves the secretion of pancreatic hormones such as insulin and glucagon into the bloodstream to regulate blood glucose levels (reviewed by Nussey and Whitehead, 2001). The exocrine pancreas accounts for up to 98% of the pancreas volume, whereas the endocrine pancreas constitutes only 2-3% of the pancreas volume (Rahier, Wallon and Henquin, 1981).

Pancreatic cancer consists of multiple different cancer subgroups that are classified based on the pancreatic cells from which they arise. The majority of pancreatic cancers are adenocarcinomas that originate from cells of the exocrine pancreas. In fact, pancreatic ductal adenocarcinoma (PDAC), which commonly arises from the ductal epithelium in the head of the pancreas, accounts for over 85% of all pancreatic cancer cases (Ryan, Hong and Bardeesy, 2014; Ilic and Ilic, 2016). Thus, when referring to pancreatic cancer, most studies focus on PDAC (reviewed by Kleeff *et al.*, 2016).

Less common exocrine tumours include acinar carcinomas (Chaudhary, 2015), pancreatoblastomas (Terino, Plotkin and Karagozian, 2018), colloid carcinomas (Liszka *et al.*, 2008) and solid pseudopapillary neoplasms (Dinarvand and Lai, 2017). Tumours arising from the endocrine pancreas, including pancreatic neuroendocrine tumours (PNETs), are rare in comparison and account for merely 5% of pancreatic cancer cases (Ilic and Ilic, 2016). These tumours arise from the islets of Langerhans and can result in the unregulated secretion of pancreatic hormones. Importantly, patients diagnosed with these tumours have significantly better prognosis with a 5-year survival rate of 59% compared to those diagnosed with PDAC who have a 3% 5-year survival rate (Bilimoria *et al.*, 2008; Siegel, Miller and Jemal, 2019). Due to the high mortality rates and poor 5-year survival rates, most pancreatic cancer research now focuses on gaining a better

understanding of PDAC and developing novel therapies to address the unmet clinical need this disease poses.

1.4 Pancreatic ductal adenocarcinoma (PDAC)

1.4.1 PDAC precursor lesions

Histological studies have shown that PDAC evolves in a stepwise manner developing from non-malignant precursor lesions into an invasive cancer (Bardeesy and DePinho, 2002; Maitra *et al.*, 2005; Wood and Hruban, 2012). To date, 5 different precursor lesions have been identified in the development of human PDAC: pancreatic intraepithelial neoplasias (PanINs), intraductal papillary mucinous neoplasms (IPMNs), intraductal tubular papillary neoplasms (ITPNs), intraductal oncocytic papillary neoplasms (IOPNs) and mucinous cystic neoplasms (MCNs) lesions (reviewed in by Kim and Hong, 2018). These lesions can be further categorised as low- or high-grade on the basis of atypia (Kamisawa *et al.*, 2016). Typically, pancreatic cancer most frequently arises from PanIN precursor lesions. PanINs are small (< 0.5 cm), non-invasive lesions consisting of cuboidal or columnar epithelial cells confined within the pancreatic ducts (reviewed in Kim and Hong, 2018). Whilst PanINs are curable, the microscopic size of these lesions makes them difficult to detect by radiological modalities including magnetic resonance imaging (MRI) and computerized tomography (CT) scans (Canto *et al.*, 2012). PanINs are stratified into low-grade and high-grade lesions based on the varying degrees of structural and cytological atypia and expression of mucin. Low-grade PanINs are flat or papillary lesions with mild to moderate atypia that typically have basally located nuclei (reviewed in Kim and Hong, 2018). High-grade PanINs, however, are categorized by the presence of papillary lesions, severe atypia, loss of polarity, tufting and in some cases the presence of intraluminal necrosis (reviewed in Kim and Hong, 2018).

1.4.2 Molecular pathology of PDAC

The molecular pathology of PDAC is predominantly characterised by activating mutations in the KRAS GTPase, typically $KRAS^{G12D}$, $KRAS^{G12R}$, $KRAS^{G12V}$or $KRAS^{G12C}$ (Pellegata *et al.*, 1994), which are observed in over 90% of tumours (Kleeff *et al.*, 2016). Further genetic alterations associated with the development of PDAC include inactivating mutations in *TP53*, *CDKN2A* and *SMAD* which occur in 50-80% of cases (Kleeff *et al.*, 2016). As the PanIN model of PDAC progression is the most frequently observed and studied, the molecular pathology of PDAC will be discussed in terms of this model. The PanIN model involves three PanIN stages which increase in degree of cellular atypia, from the low-grade PanIN-1A/B and PanIN-2 to the development of high-grade PanIN-3 and invasive PDAC (reviewed in Hruban, Maitra and Goggins, 2008). Low-grade PanIN-1A/B lesions are associated with oncogenic KRAS mutations, which occur in 36% of PanIN-1A lesions and 44% of PanIN-1B lesions (Pellegata *et al.*, 1994; Löhr *et al.*, 2005). KRAS mutations, causing constitutive activation of KRAS, results in constitutive signalling between KRAS and its multiple effector pathways resulting in dysregulated cell proliferation, differentiation and survival (reviewed in Liu, Wang and Li, 2019). HER-2 mutations are also observed in most of these early PanINs (Hruban *et al.*, 2000) in addition to KRAS allele changes. Overexpression of HER-2 results in uncontrolled cell growth and tumourigenesis, also through activation of KRAS (Iqbal and Iqbal, 2014). Thus, KRAS and/or HER-2 mutation are the earliest genetic events associated with the development of PDAC and likely facilitate deregulated cell proliferation and survival. The second low-grade lesion, PanIN-2, is characterised by flat and papillary ducts with atypia (Hruban, Maitra and Goggins, 2008) and is associated with inactivation of CDKN2A (or loss of p16) in 55% of cases. The percentage of p16 loss increases during later stages of the disease with 71% loss in PanIN-3 and 85-98% loss in full-blown PDAC (Caldas *et al.*, 1994; Schutte *et al.*, 1997; Wilentz *et al.*, 1998). Due to the apparent loss of p16 in later stages, CDKN2A inactivation is believed to occur after KRAS mutation. The p16 protein is important for cell cycle progression and its expression is enhanced in times of DNA damage, oxidative stress or oncogene activation and usually results in senescence (Rayess, Wang and Srivatsan, 2012). Loss of p16 therefore enables cancer (the transformed) cells to by-pass senescence. The development of the high-

grade PanIN-3 lesions are characterised by significant cytological and architectural atypia including nuclear atypia and involves budding of cells into the ductal lumen (Hruban, Maitra and Goggins, 2008). In fact, PanIN-3 lesions are often considered carcinomas *in situ*. Since PanIN-3 lesions are usually observed in the presence of invasive PDAC, the progression from PanIN-3 to PDAC is unclear. As with PDAC, PanIN-3 lesions are associated with mutation in the *TP53* and *BRCA2* genes (Hruban *et al.*, 2000), but, interestingly, only 20% of PanIN-3 lesions have *TP53* mutation (Yokode *et al.*, 2018). Since *TP53* mutation is observed in 50-70% of PDAC tumours, it is possible that *TP53* mutation may predominantly occur in PDAC and not PanIN-3 (Scarpa *et al.*, 1993; Rozenblum *et al.*, 1997). *TP53* is arguably the most potent tumour suppressor gene and is involved in the regulation of numerous physiological processes including; cell cycle and senescence, survival/apoptosis, autophagy and responses to stress stimuli such as DNA damage, oxidative stress and oncogene activation (Zilfou and Lowe, 2009). Thus, regardless of when *TP53* mutation occurs, loss of the functional p53 protein could advance tumourigenesis in many ways. Interestingly, whilst loss of BRCA2 is associated with PanIN-3, it has been shown that alone, it does not facilitate progression into PDAC. In fact, whilst deletion of this gene in developing mice did promote PanIN formation, only 15% of mice developed PDAC (Feldmann *et al.*, 2011). Crucially, however, when BRCA2 loss was analysed in combination with p53 mutation, most mice progressed to PDAC, indicating that loss of BRCA2 alone is not sufficient to induce PDAC progression (Feldmann *et al.*, 2011). Finally, progression to full blown PDAC, which is characterised by invasive growth and marked desmoplasia, is associated with loss of SMAD4 (Hruban, Maitra and Goggins, 2008; Y. W. Chen *et al.*, 2014; Wang *et al.*, 2017). SMAD4 is commonly lost through homozygous deletion and is observed in 50% of PDAC tumours (Hahn *et al.*, 1996; Kleeff *et al.*, 2016). Since SMAD4 is required for TGF-β mediated PDAC cell cycle arrest and apoptosis, loss of this protein promotes many cellular processes including cell proliferation and differentiation (Kleeff *et al.*, 2016; Ahmed *et al.*, 2017). PDAC progression stages and associated mutations are summarised in table 1.4.2

Table 1.4.2 Stages of PDAC progression and associated mutations

Stage	Associated mutations
PanIN-1A/B	*KRAS*^{G12D}, *KRAS*^{G12R}, *KRAS*^{G12V}, *KRAS*^{G12C} *and HER-2*
PanIN-2	*CDKN2A* (p16)
PanIN-3	*TP53* and *BRCA2*
PDAC	*TP53* and *SMAD4*

1.4.3 Clinical presentation and diagnosis

The exceptionally poor prognosis associated with PDAC is due in part to late/advanced stage diagnosis, and the lack of effective therapeutic options for metastatic disease. To date, surgical resection remains the most successful treatment option for pancreatic cancer patients, however at diagnosis, only 8% of patients have stage I tumours and are suitable for this potentially curative surgery (Kimura *et al.*, 2015). Whilst most patients present with metastatic disease, the time frame for the development of advanced stage pancreatic cancer is slow. In fact, it can take up to 10 years for the initiating oncogenic mutation to develop in the parental, non-metastatic founder cell (Yachida *et al.*, 2010). From this founder cell, a further 5 years are required for the development of a metastatic phenotype (Yachida *et al.*, 2010). Thus, there is a significant window for early detection of pancreatic cancer. Diagnosis during the localised stage of disease markedly increases patient 5-year survival rate to 34%, compared to 12% in patients diagnosed with locally advanced disease and 3% for those diagnosed with metastatic disease (Siegel, Miller and Jemal, 2019). Furthermore, it is estimated that patients diagnosed during stage I of the disease, where surgical resection is possible have a 5-year survival rate of between 37 and 59% (Tsuchiya *et al.*, 1986; Shimizu *et al.*, 2005). Whilst survival is still fairly low for these patients, diagnosis at an early stage may provide a window where therapeutic intervention could be potentially curative.

As the majority of PDAC patients do not present with symptoms until late stage disease, early diagnosis is difficult due to our current lack of sensitive and specific tumour markers, difficulties in imaging early tumour lesions and the absence of screening methods (Kleeff *et al.*, 2016; Siegel, Miller and Jemal, 2019). To date, standard screening programmes are not possible for the detection of pancreatic cancer, even for those with higher risk of developing the disease. Mounting evidence, however, suggests that implementing screening regimes for individuals who are high-risk (with at least 2.5 times increased risk) could save lives (Pandharipande *et al.*, 2015). Due to the small size of PanINs, however, detection by imaging is difficult and distinctions cannot be made between low and high-grade lesions (Kleeff *et al.*, 2016). The development of a rapid process for monitoring specific biomarkers for pancreatic cancer is one possible route to improving early detection. Currently, specific biomarkers for the detection of pancreatic cancer do not exist. Historically, serum carbohydrate antigen 19-9 (CA 19-9) has been used as a marker for pancreatic cancer, however, it is not specific to pancreatic cancer and lacks the sensitivity to be used for early diagnosis (Poruk *et al.*, 2013). CA 19-9 can, however, be used to monitor the progression of PDAC after diagnosis . Other promising biomarkers have emerged in recent years including (i) circulating tumour DNA encoding mutant KRAS which can be detected in 43% of patients with localised disease (Sausen *et al.*, 2015), (ii) a highly specific protein signature of oestrogen receptor 1, HER-2 and tenascin C (Mirus *et al.*, 2015) and (iii) the presence of the heparin sulfate proteoglycan glypican 1 on the surface of exosomes (Melo *et al.*, 2015)(discussed further in section 1.7). Despite initial success in both GEMM of pancreatic cancer and patient samples, these promising biomarkers are still in early stages of development and are not yet clinically available .

1.4.4 Treatment of PDAC

Where surgical resection is not possible, chemotherapy is the only remaining treatment option for PDAC patients but unfortunately it is not curative and offers only a modest survival increase. Currently, the most successful chemotherapeutic options available include gemcitabine (as a single agent), FOLFIRINOX (folinic acid, fluorouracil, irinotecan

and oxaliplatin) or gemcitabine nab-paclitaxel (Burris *et al.*, 1997; Berlin *et al.*, 2000; Conroy *et al.*, 2011; Von Hoff *et al.*, 2013; Goldstein *et al.*, 2015). For roughly 20 years, 5-fluorouracil (5-FU) was the only chemotherapeutic agent available for PDAC. In 1997 however Gemcitabine was introduced after a significant increase in patient survival was demonstrated, where 1-year survival rose from 2% in 5-FU treated patients to 18% in gemcitabine treated patients (Burris *et al.*, 1997; Berlin *et al.*, 2000). To date, single agent gemcitabine is the gold standard chemotherapeutic treatment for PDAC, however, it is relatively ineffective and merely shrinks tumours, temporarily reducing the devastating symptoms of PDAC. The lack of any significant improvement in outcome is in part due to the rapid development of resistance to gemcitabine, which arises within weeks of administration (Binenbaum, Na'ara and Gil, 2015).

More recently, treatment with the FOLFIRNOX regime was shown to offer the most significant survival benefit for PDAC patients, where median survival is 11.1 months compared to 6.8 months with gemcitabine (Conroy *et al.*, 2011; Vaccaro, Sperduti and Milella, 2011). Furthermore, progression free survival rose from 3.3 month to 6.4 months and 1-year survival rates rose from 21% to 48% for those treated with FOLFIRNOX compared to gemcitabine. Unfortunately, however, FOLFIRNOX is associated with high levels of toxicity and so is reserved for use in patients with good performance status only (Conroy *et al.*, 2011; Vaccaro, Sperduti and Milella, 2011). More recently, combination treatment with gemcitabine and nab-paclitaxel has been shown to increase median survival from 6.8 months (gemcitabine alone) to 8.5 months (Goldstein *et al.*, 2015). The use of combination therapy also resulted in adverse side effects. Thus, treatment with gemcitabine nab-paclitaxel is also limited to patients with good performance status (Von Hoff *et al.*, 2013).

The survival benefit associated with gemcitabine, FOLFIRINOX and gemcitabine plus nab-paclitaxel, is modest and only increases life expectancy by mere months. In addition, the toxicities associated with these treatments mean that patient quality of life is greatly decreased and may outweigh survival benefit and often palliative care is preferential. These poor patient outcomes highlight the inadequacies of current therapies targeting PDAC and emphasises the desperate need for new and more successful treatments.

1.4.5 Centrosome amplification and PDAC

Centrosome amplification has been identified as a hallmark of most human cancers including pancreatic cancer. A study performed in 1999 examined surgically resected human pancreas tissues for the presence of centrosome abnormalities including amplification. Analysis of 13 pancreatic ductal adenocarcinoma identified the presence of supernumerary centrosomes in 85% of samples (see Figure 1.4.5.1) (Sato *et al.*, 1999). Furthermore, no amplification was observed in any of the 12 normal duct and stromal tissues. Amplified centrosomes were observed in adenocarcinomas with varying degrees of atypia and so it has been suggested that centrosome amplification may occur early on in the multi-step progression of PDAC (Sato *et al.*, 1999; Ansari *et al.*, 2018). Interestingly, amplified centrosomes were not observed in pancreatic endocrine tumours. Endocrine tumours are often well differentiated and have few areas of atypia and mitotic activity in comparison to adenocarcinomas and are not associated with loss of cell polarity. It is therefore possible that the underlying drivers of endocrine tumours differ from those associated with adenocarcinomas (exocrine tumours) and are not associated with centrosome amplification (Sato *et al.*, 1999; Ansari *et al.*, 2018).

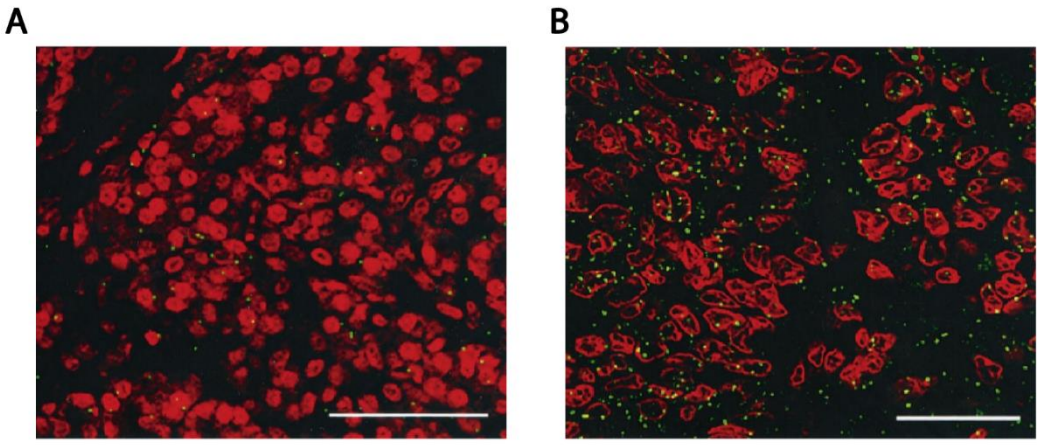

Figure 1.4.5.1 Immunofluorescent staining of centrosomes in pancreatic tissues A) Centrosome staining (as defined by ϒ-tubulin staining) in normal pancreas duct, showing little to no centrosome amplification. B) Centrosome staining (as defined by ϒ-tubulin staining) in poorly differentiated pancreatic ductal adenocarcinoma, showing high centrosome amplification. Samples are formalin-fixed, paraffin embedded human pancreas tissue. ϒ-tubulin in green, propidium iodide in red. Scale bar represents 50 µm (taken from Sato *et al.*, 1999).

More recent studies have linked centrosome amplification in pancreatic tumours to rapid disease progression, metastasis and worse clinical outcome (Sato *et al.*, 2001; Shono *et al.*, 2001; Mittal *et al.*, 2015). Crucially, centrosome amplification was shown to enhance the motility and invasiveness of pancreatic cancer cells (Mittal *et al.*, 2015). Whilst the exact mechanisms underlying the induction of centrosome amplification in pancreatic cancer remain elusive, the overexpression of PLK4 in mouse models has been shown to induce centrosome amplification and enhance tumour formation and progression (Coelho *et al.*, 2015; Serçin *et al.*, 2015; Levine *et al.*, 2017). In fact using a transgenic mouse model, Coelho *et al.* showed that in a p53 null background, transient PLK4 overexpression lead to the development of centrosome amplification in the pancreas, resulting in the hyperproliferation of cells in the pancreas and advancing the formation of pancreatic tumours. Furthermore, analysis of PLK4 expression in pancreatic cancer patients using the pancreatic expression database (PED) (Marzec *et al.,* 2018) revealed patients with high PLK4 expression had a significantly lower survival probability ($p=0.048$) compared to patients with low expression (see Figure 1.4.5.2). Therefore, it is possible that centrosome amplification in PDAC is caused by PLK4 overexpression.

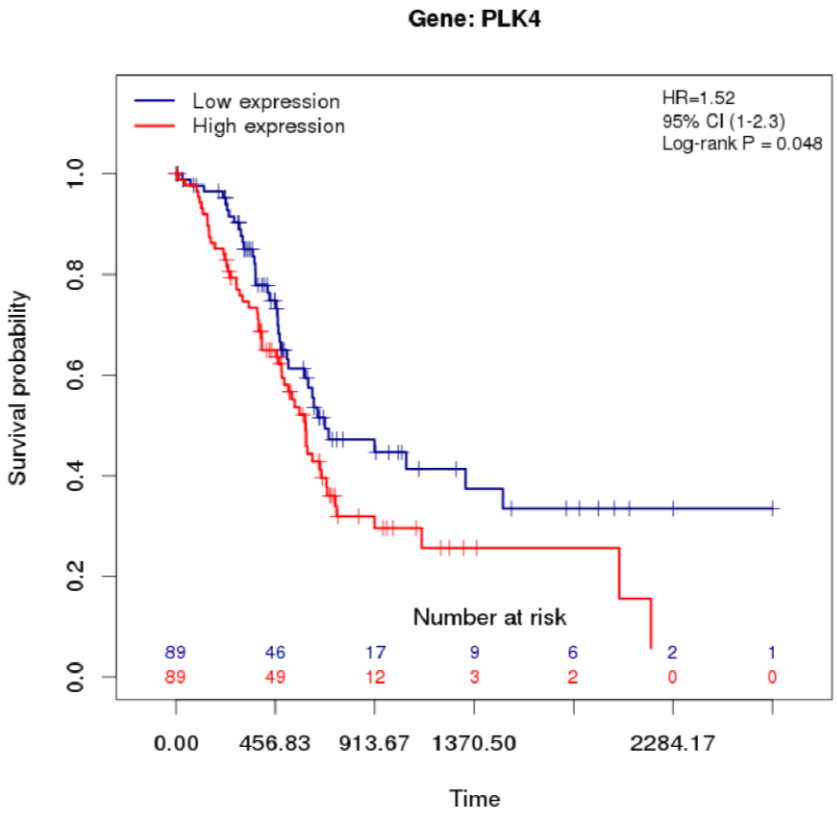

Figure 1.4.5.2 Survival probability of pancreatic cancer patients and PLK4 expression. Survival probability curves generated using the pancreatic expression data base, analysing relationship between PLK4 expression and predicted pancreatic cancer patient survival. Survival probability is significantly lower (p=0.048) for patients with high PLK4 expression compared to low PLK4 expression (data from PED http://www.pancreasexpression.org).

In support of this hypothesis, a number of centrosome related proteins have been shown to be over-expressed in pancreatic cancer (Weng *et al.*, 2012; Xie *et al.*, 2016; Peng *et al.*, 2017). For example, CEP70, a protein that induces centrosome amplification upon its overexpression (Xie *et al.*, 2016), and the centrosome related protein phosphatase 4 (PP4) which plays a role in centrosome organisation and maturation (Weng *et al.*, 2012) and is considered a prognostic factor for pancreatic cancer. Centrosomal protein 55 (CEP55), a microtubule bundling protein, is also over-expressed in pancreatic cancer (Peng *et al.*, 2017) and has been shown to promote pancreatic cancer cell proliferation, migration and invasion *in vitro* and accelerated tumourigenicity *in vivo* through the activation of NF-κB signalling (Peng *et al.*, 2017). CEP55 may be valuable as a prognostic marker for pancreatic cancer and may also represent a novel target for therapy.

The presence of amplified centrosomes in both early and late stage pancreatic cancer makes them intriguing targets for biomarker development and/or therapeutic intervention. Whilst detection of centrosomal abnormalities as a biomarker is a relatively unexplored area, the development of therapeutics targeting amplified centrosomes are in progress. Many of these therapeutics centre around centrosome de-clustering, forcing cancer cells into multipolar mitoses, resulting in gross aneuploidy and cell death. The identification of the kinesin-14 family protein HSET as a key mediator of centrosome clustering has led to the development of a number of new therapeutics targeting HSET in cancer cells (Mountain *et al*., 1999; Cai *et al*., 2008; Kwon *et al*., 2008; Watts *et al*., 2013; Wu *et al*., 2013; Zhang *et al*., 2016). For example, the allosteric inhibitor CW069 gives rise to multipolar mitoses in cells with supernumerary centrosomes and shown promise as an HSET inhibitor *in vitro* (Watts *et al.*, 2013). More recently, two more small molecule inhibitors, AZ82 and SR31527 have shown centrosome de-clustering and subsequent multipolar mitoses in cells with amplified centrosomes (Wu *et al.*, 2013; Zhang *et al*., 2016). Further study into the biological efficacy and off target toxicity of these inhibitors however, revealed all three to have HSET-independent cytotoxicity (Yukawa *et al.*, 2018). Despite the observed toxicities however, AZ82 was shown to have potent neutralising activity against HSET induced lethality in fission yeast (Yukawa *et al.*, 2018). Thus, whilst further investigation and development is still required HSET inhibitors show promise as future centrosome amplification targeting therapeutics.

1.5 The tumour microenvironment

The current failures of pancreatic cancer therapeutics may be attributed to an important element of the tumour being largely ignored; the tumour stroma. Pancreatic cancer is characterised by a strong desmoplastic stromal reaction resulting in dense fibrosis around the tumour. The tumour stroma however is not accurately replicated in most of the experimental models used to develop new therapeutics for PDAC (Apte and Wilson, 2012; Apte *et al.*, 2013). Therefore, over the last decade researchers have directed their

attentions to understanding the pancreatic tumour stroma and its role in tumour progression and drug resistance.

In normal tissues, the microenvironment is composed of numerous cellular and acellular components that form an organized niche to regulate homeostasis (Alderton, 2014; Hui and Chen, 2015). In a tumour setting, the stromal compartment consists of several extracellular matrix (ECM) proteins, signalling molecules, endothelial cells, immune cells, cancer associated fibroblasts (CAFs) and pancreatic stellate cells (PSCs) (Erkan, Hausmann, *et al.*, 2012; Neesse *et al.*, 2015) (see Figure 1.5). PDAC tumours have a significant, highly fibrotic, stromal compartment that can account for over 90% of the total tumour, making PDAC one of the most stroma-rich cancers (Neesse *et al.*, 2011). Furthermore, the PDAC tumour microenvironment (TME) is known to facilitate cancer cell growth and survival, EMT, cell migration, metastasis and chemoresistance (Neesse *et al.*, 2015; Nielsen, Mortensen and Detlefsen, 2016; Thomas and Radhakrishnan, 2019). Thus, the TME plays a key role in the progression of pancreatic cancer .

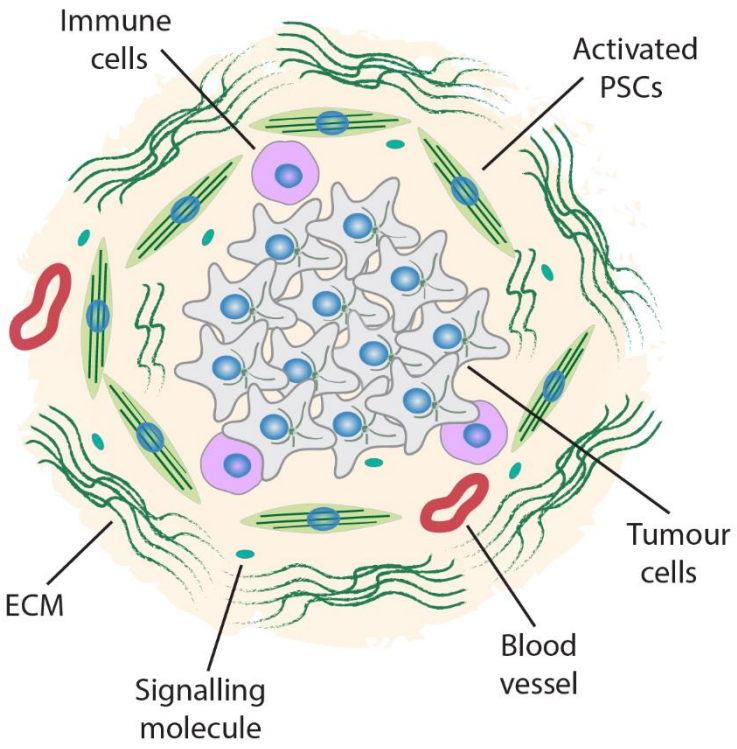

Figure 1.5 Pancreatic tumour microenvironment. Pancreatic cancer cells are surrounded by a dense stromal compartment consisting of ECM proteins, blood vessels, immune cells, activated PSCs and signalling molecules. ECM= extracellular matrix, PSC= pancreatic stellate cells.

1.5.1 Pancreatic stellate cells (PSCs)

First identified in the liver in 1975, stellate cells have since been shown to frequent the pancreas of mice and humans. Stellate cells are star-shaped fibroblast like cells with long cytoplasmic projections that are woven into tissues. In the normal healthy pancreas PSCs account for roughly 4-7% of parenchymal cells and exist in a quiescent state. PSC quiescence is characterised by their ability to store retinoids (vitamin A) in the form of droplets in the cytoplasm and little to no detectable α-smooth muscle actin (α-SMA) (Apte *et al.*, 1998; Friedman, 2008). In their quiescent state, PSCs have a low mitotic index, have limited migratory capacity and function to synthesise and maintain the ECM (Apte *et al.*, 1998; Phillips, McCarroll, *et al.*, 2003). Upon injury or inflammation, PSCs become activated, transitioning into myofibroblast-like cells which are characterised by loss of vitamin A droplets and increased expression of α-SMA stress fibres (Apte *et al.*, 1998; Erkan, Adler, *et al.*, 2012). Once activated, PSCs adopt a spindle like shape and exhibit heightened migratory and proliferative capabilities (Bachem *et al.*, 1998; Schneider *et al.*, 2001; Mews *et al.*, 2002; Phillips, Wu, *et al.*, 2003; Omary *et al.*, 2007; Keogh *et al.*, 2011), increased contractility, excessive deposition of ECM proteins including collagens I, II and XI and fibronectin and remodelling of the ECM through secretion of matrix metalloproteinases (MMPs) and tissue inhibitors of matrix metalloproteinases (TIMPs) (Apte *et al.*, 1999, 2004; Schneider *et al.*, 2001; Phillips, McCarroll, *et al.*, 2003; Bachem *et al.*, 2005). During injury, activated PSCs function to heal wounds in the tissue by substituting damaged cells with fibrotic tissue, thus generating a quick fix to maintain organ integrity (Ferdek and Jakubowska, 2017). The extended presence of activated PSCs, however, may become pathological with PSCs depositing excessive amounts of ECM proteins resulting in fibrosis. In fact, the desmoplastic stromal reaction/ fibrosis that is characteristic of PDAC has been attributed to chronic and sustained activation of PSCs during tumour progression (Erkan, *et al.*, 2012).

PSCs are activated in response to a number of different factors and stimuli including inflammatory cytokines such as TNF-α and IL-8, growth factors including platelet-derived growth factor (PDGF), the transforming growth factors TGF-α and TGF-β, and oxidative stress and alcohol metabolites (Apte *et al.*, 1999, 2000; Andoh *et al.*, 2000; Schneider *et*

al., 2001; Mews *et al.*, 2002; Shek *et al.*, 2002; Gao and Brigstock, 2005; Kordes *et al.*, 2005; Vonlaufen *et al.*, 2010; Tahara *et al.*, 2013). Many of these PSC activating factors are secreted by neighbouring cells including endothelial cells, acinar cells, infiltrating cells such as macrophages, platelets and pancreatic cancer cells (Masamune and Shimosegawa, 2009; Erkan, *et al.*, 2012). In the normal pancreas, activation is transient, and PSCs will revert back to their quiescent state upon tissue restoration. In PDAC, however, once activated, PSCs remain in a chronic state of activation via both paracrine stimuli and autocrine signalling (Shek *et al*., 2002; Ohnishi *et al.*, 2003; Aoki *et al*., 2005; Omary *et al*., 2007; Jiang *et al*., 2009). A summary of PSC activation is shown in figure 1.5.1.

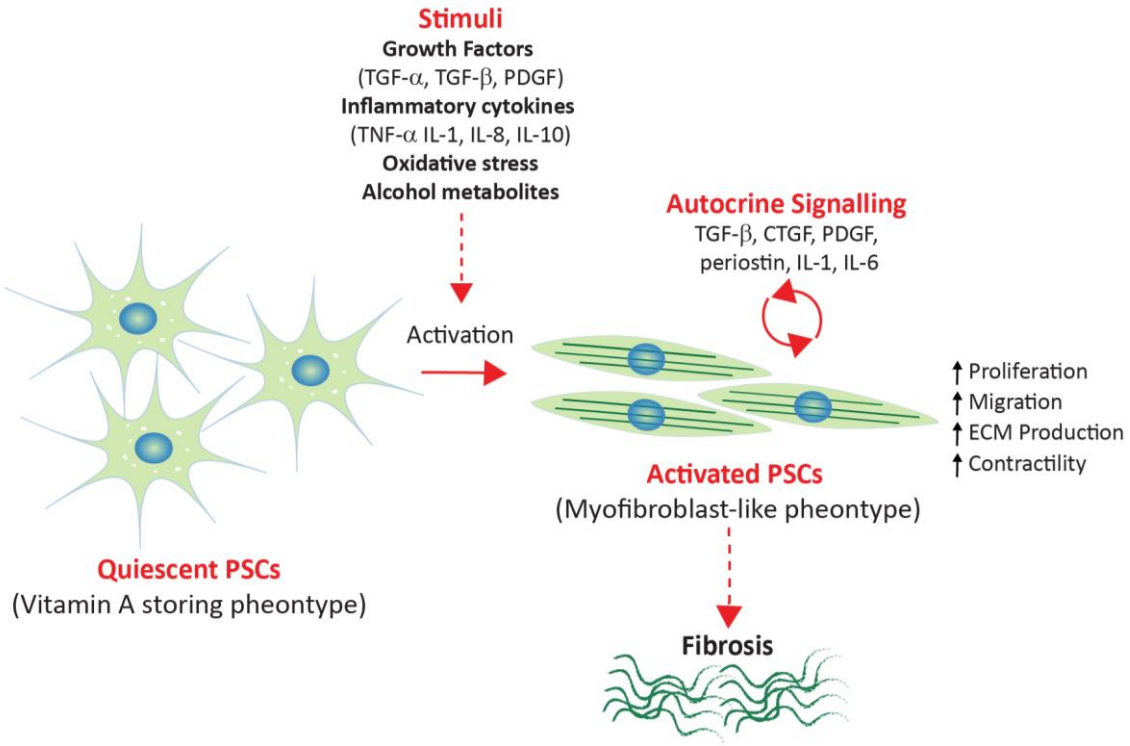

Figure 1.5.1 Paracrine and autocrine-mediated activation of pancreatic stellate cells (PSCs). PSCs transition from a quiescent state (vitamin A storing) to an activated state (myofibroblast-like phenotype) in response to paracrine signalling from neighbouring cells including pancreatic cancer cells. PSCs perpetuate their own activation through subsequent autocrine signalling. This PSC activation results in increased proliferation and migration and excessive ECM synthesis resulting in extensive fibrosis.

1.5.2 Activated PSCs and cancer

Mounting evidence now suggests that the increased presence of activated PSCs within a tumour correlates with poor clinical outcome. In fact, a study of 233 patients reported an association between the number of activated PSCs and poorest prognosis (Erkan *et al.*, 2008). In addition, PSC activation has been observed during the PanIN stages, resulting in fibrosis surrounding these precursor lesions (Bynigeri *et al.*, 2017). An additional study analysing prognosis of 145 patients in early stages of pancreatic cancer found that moderate-to-strong α-SMA expression in PSCs was associated with poorer progression-free survival (L. M. Wang *et al.*, 2016). These findings indicate that the activation of PSCs may be an early event in the development of pancreatic cancer and chronic or sustained activation is associated with poorer clinical outcomes. Furthermore, two studies analysing orthotopic injection of human PDAC cells alone or in combination with PSCs into mouse pancreas demonstrated that the presence of PSCs induced fibrosis, increased tumour growth, and advanced invasion and metastasis. Therefore, PSC activation appears to have multiple roles in advancing PDAC.

The strong desmoplastic reaction caused by activated PSCs results in the formation of a solid tumour with growth induced solid stress (GISS) which results in blood vessel compression and impairs the delivery of intravenous drugs to the tumour (Provenzano *et al.*, 2012; Chauhan *et al.*, 2013; DuFort, Christopher. C DelGiorno and Hingorani, 2016). Furthermore, the presence of PSC deposited fibrillar collagen in the stroma inhibits concentration-driven delivery of cancer therapeutics to the cancer cells, by providing a physical barrier to drug diffusion (Provenzano *et al.*, 2012; DuFort, Christopher. C DelGiorno and Hingorani, 2016). Thus, the extensive stroma associated with PSC activation creates a significant barrier to drug delivery.

Importantly, GEMM of PDAC have demonstrated that stromal depletion can enhance drug delivery. In fact, in KPC mice with pancreatic tumours, treatment with the hyaluronidase PEGPH20, which degrades stromal components, was found to promote vascularisation of the tumours. This enhanced the intra-tumoural delivery of chemotherapeutic agents and improved overall survival of the mice (Provenzano *et al.*, 2012; Jacobetz *et al.*, 2013). An additional study also demonstrated that stromal

depletion with the angiotensin inhibitor losartan resulted in reduced solid stress and increased vasculature of the tumour, facilitating oxygen and drug delivery (Chauhan *et al.*, 2013). Stromal depleting therapies have therefore been highlighted as strong candidates for the development of novel therapeutics. Unfortunately, despite numerous stromal depleting therapies reaching clinical trials, they have not translated well in the clinic, are often associated with toxicities and offer no survival benefit (reviewed in Kota *et al.*, 2017). In fact, mounting evidence now indicates that the stroma has important anti-tumour properties, since its ablation has been shown to promote tumour progression and decrease survival (Özdemir *et al.*, 2014; Rhim *et al.*, 2014). For example, whilst the depletion of Shh in the *dx1-Cre;Kras*$^{LSL\text{-}G12D/+}$*;p53*$^{fl/+}$*;Rosa26*$^{LSL\text{-}YFP/+}$ (PKCY) mouse model resulted in the depletion of stromal cells from PDAC tumours, this stromal depletion resulted in increased tumour vasculature, tumour cell proliferation and reduced survival (Rhim *et al.*, 2014). Additionally, depletion of myofibroblasts in the *Ptf1a*$^{cre/+}$;*LSL-Kras*$^{G12D/+}$;*Tgfbr2*$^{flox/flox}$ (PKT) mouse model of pancreatic cancer decreased fibrosis but enhanced cancer cell EMT leading to more invasive tumours (Özdemir *et al.*, 2014). The failure of stroma ablating therapies highlights the need to further understand the molecular mechanisms associated with PDAC stromal biology before stromal therapies can be implemented. Efforts are now focussed on the development of therapies that modulate the tumour stroma rather than fully ablating it. Indeed, recent studies are now analysing the potential therapeutic advantage of inducing stromal quiescence over stromal ablation. For example, treatment of PSCs with all-trans retinoic acid (ATRA) was shown to induce PSC quiescence which slowed tumour progression by reducing cancer cell proliferation and invasion in the *LSL-Kras*$^{G12D/+}$; *Trp53*$^{fl/+}$; *Pdx1-Cre* (KPC) mouse model (Froeling *et al.*, 2011). Furthermore, combination therapy of gemcitabine and ATRA was shown to reduce cancer cell proliferation and invasion in KPC mice compared to those treated with gemcitabine alone (Carapuça *et al.*, 2016). The success of ATRA/gemcitabine treatment in KPC mice lead to the development of the currently ongoing phase I STAR_PAC clinical trial in which patients with locally advanced or metastatic PDAC are treated with ATRA in combination with either gemcitabine or nab-paclitaxel (NCT03307148).

1.5.2.1 Activation of PSCs by PDAC cells

Within the tumour setting, PDAC cells have been shown to activate PSCs and modulate their activity through a multitude of paracrine signals (Bachem *et al.*, 2005). TGF- β is a key mediator of PSC activation and can be supplied to PSCs by the cancer cells. PSCs respond to TGF-β signalling in a SMAD-dependent manner resulting in the synthesis and deposition of excessive ECM components that can lead to fibrosis in the tumour (Apte *et al.*, 1999; Löhr *et al.*, 2001; Ohnishi *et al.*, 2004). In addition, TGF-β signalling has been shown to enhance the proliferative capabilities of stellate cells (Pinzani *et al.*, 1989). Interestingly, in addition to responding to PDAC-derived TGF-β1 signalling, PSCs themselves have been identified as a source of TFG-β1 (Ohnishi *et al.*, 2004). Thus, PSCs can sustain their own activation through TGF-β1 autocrine signalling. Connective tissue growth factor (CTGF) has also been shown to induce stellate cell activation and was found to promote migration and extracellular matrix production through interaction with TGF-β 1 (Huang and Brigstock, 2012; Hao *et al.*, 2014). PDAC cells can also induce accelerated ECM synthesis by PSCs via secretion of PDGF and/or, fibroblast growth factor 2 (FGF2) (Bachem *et al.*, 2005). Additionally, PDAC cells secrete ECM metalloproteinase inducer (EMMPRIN) which induces PSCs to synthesise MMP-2, an important basement membrane degradation protein (Schneiderhan *et al.*, 2007). As ECM re-modelling and basement membrane degradation are important steps in tumour progression, PDAC cells may be aiding their own metastasis through modulation of PSCs.

Another key factor secreted by PDAC cells that can activate PSCs is sonic hedgehog (shh). Whilst shh is not usually present in the healthy adult pancreas, it has been detected in up to 70% of patient tumours (Thayer *et al.*, 2003). Secretion of shh by PDAC cells has been shown to mediate activation of the surrounding PSCs, enhancing PSC proliferation, differentiation and motility (Bailey *et al.*, 2008; Fendrich *et al.*, 2011). Moreover, shh has been shown to enhance ECM deposition by PSCs (Bailey *et al.*, 2008; Fendrich *et al.*, 2011; Rhim *et al.*, 2014). Other PDAC secreted factors including PDGF, trefoil factor 1 (TFF1), insulin-like growth factor 1 (IGF1) and interleukin 6 (IL-6) have also been shown to enhance PSC proliferation and migration (Phillips, Wu, *et al.*, 2003; Bachem *et al.*, 2005; Arumugam *et al.*, 2011; Rosendahl *et al.*, 2015; Fu *et al.*, 2018; Marzoq *et al.*, 2019). Interestingly, whilst TFF1 is not expressed by normal pancreatic

cells, it is highly upregulated in pancreatic cancer cells. TFF1 is also significantly upregulated in PanINs (Arumugam *et al.*, 2011) and so may play a role in the early stages of PDAC development.

Pancreatic cancer cells are a significant source of reactive oxygen species (ROS). In fact, high levels of ROS, produced during oxidative stress, have been identified in many different cancers and are believed to promote tumour aggressiveness (Martinez-Useros *et al.*, 2017). Interestingly, ROS and lipid peroxidation products have been shown to induce hepatic stellate cell (HSC) activation, promoting HSC proliferation and deposition of ECM components (reviewed in Gandhi, 2012). Recently, exosomes have been shown to deliver ROS to injured neurons through transfer of NADPH2 oxidase, thereby promoting neuronal regeneration (Hervera *et al.*, 2018). Thus, it is possible that pancreatic cancer cells may induce stellate cell activation through the transfer of secreted ROS.

1.5.2.2 Effect of PSC activation on PDAC cells

Current data suggests that PDAC cells and PSCs interact in a bidirectional manner, where PDAC cells recruit and activate PSCs, and in turn PSCs facilitate cancer cell growth, invasion and chemoradiation resistance (Bachem *et al.*, 2005; Rosa F Hwang *et al.*, 2008; Mantoni *et al.*, 2011). In fact, the extensive bidirectional interplay between pancreatic cancer cells and PSCs has been shown to facilitate tumour progression (see Figure 1.5.2.2) (Apte *et al.*, 2004; Bachem *et al.*, 2005; Rosa F Hwang *et al.*, 2008; Vonlaufen *et al.*, 2008; Xu *et al.*, 2010).

Studies have shown that paracrine signalling from PSCs stimulates PDAC proliferation and inhibits apoptosis (Bachem *et al.*, 2005; Rosa F. Hwang *et al.*, 2008; Vonlaufen *et al.*, 2008). Secretion of epidermal growth factor (EGF), connective tissue growth factor (CTGF), PDGF, Galectin-1 and adrenomedullin by PSCs have all been shown to enhance PDAC cell proliferation (Marzoq *et al.*, 2019; Thomas and Radhakrishnan, 2019). Likewise, PSC secretion of C-X-C motif chemokine ligand 13 (CXCL13) recruits B cells to the TME, which in turn secrete IL-35 inhibiting PDAC cell apoptosis and stimulating proliferation (Nicholl *et al.*, 2014; Pylayeva-Gupta *et al.*, 2016).

PSCs have also been shown to induce EMT in PDAC cells, possibly facilitating PDAC cell invasion and metastasis. PDAC cells co-cultured with PSCs were reported to have decreased E-cadherin and beta-catenin expression, and increased vimentin and snail expression which is consistent with EMT (Kikuta *et al.*, 2010). Interestingly, hypoxia has been shown to induce secretion of CTGF by PSCs which mediates PDAC cell EMT, facilitating cancer cell invasion (Eguchi *et al.*, 2013). Additionally, the secretion of MMPs by PSCs has been shown to enhance the migration of PDAC cells and accelerate tumourigenesis (Schnelderhan *et al.*, 2007; Tjomsland *et al.*, 2016). Furthermore, Galectin-1 driven up-regulation of stromal cell-derived factor 1 (SDF-1) in PSCs has been shown to induce PDAC metastasis (Qian *et al.*, 2017; Orozco *et al.*, 2018).

PSCs have been shown to mediate PDAC cell resistance to chemotherapy and radiotherapy for example by supporting PDAC cell resistance to gemcitabine, through the secretion of IGF1 and IGF2 which activate IGF receptors on the cancer cells (Ireland *et al.*, 2016). Indeed, *in vivo* studies revealed that pharmacological blockage of IGF resulted in re-sensitisation to gemcitabine (Ireland *et al.*, 2016). Secretion of fibronectin by PSCs has also been shown to promote PDAC cell chemoresistance to gemcitabine (Amrutkar *et al.*, 2019). Similarly, PSCs are thought to mediate chemoresistance in PDAC cells through nitric oxide (NO) and IL-1β secretion (Haqq *et al.*, 2014). PSCs may also confer chemoresistance by increasing the expression of the stem cell related genes nestin, LIN28 and ABCG2 in PDAC cells, thereby inducing the establishment of stem cells within the tumour (Hamada *et al.*, 2012; Lonardo *et al.*, 2012). In conclusion, the significant bidirectional cross talk exhibited by PSCs and PDAC cells has a profound effect on PDAC cell proliferation, invasion, metastasis and chemoresistance (see Figure 1.5.2.2).

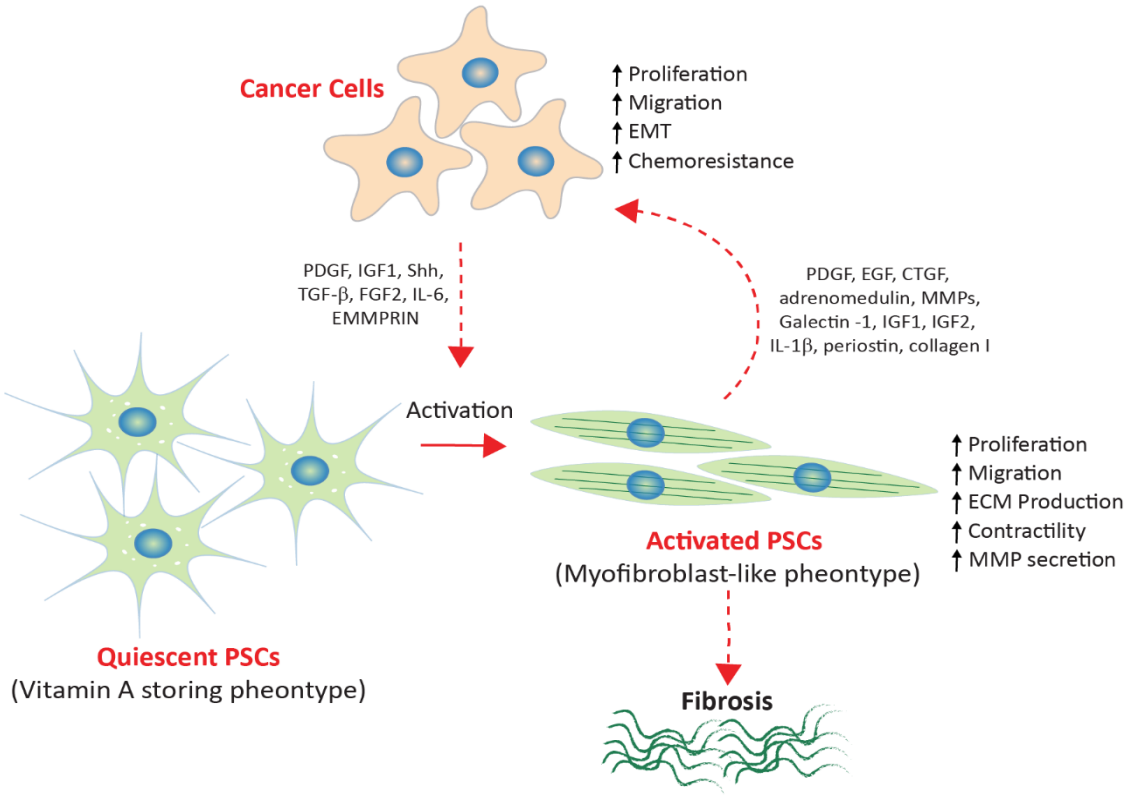

Figure 1.5.2.2 Bidirectional cross talk between activated pancreatic stellate cells (PSCs) and pancreatic cancer cells. Pancreatic cancer cells stimulate PSC activation resulting in increased proliferation, migration, deposition of ECM, contractility and MMP secretion. In response, through paracrine signalling, activated PSCs stimulate proliferation, migration, EMT and chemoresistance in PDAC cells. Perpetual cross talk between PSCs and Pancreatic cancer cells results in tumour progression

1.6 Extracellular vesicles

1.6.1 Extracellular vesicles: classes and biogenesis

Extracellular vesicles (EVs) are small, membrane-bound vesicles that are secreted by cells into the extracellular environment. Secretion of EVs appears to be conserved throughout evolution and all eukaryotic cell types demonstrate EV release (Raposo and Stoorvogel, 2013). EVs contain a biological cargo specific to their cell of origin that can influence the behaviours of surrounding cells upon interaction with neighbouring cells (Colombo, Raposo and Théry, 2014). Once released, EVs can enter the circulation and pass into most bodily fluids including blood, urine, saliva and breast milk (Crawford,

1971; Vlassov *et al.*, 2012), thus EVs can communicate biological information with distant cells.

Classically, the secretory pathway in eukaryotic cells involves packaging of cargo proteins into secretory vesicles via the endoplasmic reticulum (ER)-Golgi route (reviewed in Kim *et al.*, 2018). Proteins targeted for secretion in this manner contain a recognition signal peptide at the N-terminus or transmembrane domain, which directs their translocation into the lumen of the ER (reviewed in Grieve and Rabouille, 2011). Secretory proteins are then transferred to the Golgi, where they are moved by cisternal migration to the trans-Golgi and into the trans-Golgi reticulum, where they are sorted into secretory vesicles (Grieve and Rabouille, 2011; Kim, Gee and Lee, 2018). Upon the recognition of a stimulus for exocytosis, these vesicles are trafficked to and fuse with the plasma membrane resulting in the release of their contents into the extracellular milieu (Bonifacino and Glick, 2004). EVs however, represent an unconventional secretory pathway that differs significantly from the 'classical' secretory pathway. These alternative pathways are detailed below.

Eukaryotic cells secrete a range of different EV types which differ in their size, biogenesis, cargo and function. Whilst the nomenclature of these different vesicle types is in constant debate, broadly speaking, secreted vesicles can be separated into three main groups, i) the plasma membrane secreted apoptotic bodies and microvesicles and ii) the intracellularly generated exosomes. Apoptotic bodies, which are 1-5 µm in size, are released from dying cells through outward membrane blebbing and are thought to contain the potentially toxic debris of apoptotic cells preventing leakage of these factors into the extracellular milieu (Wickman, Julian and Olson, 2012). Microvesicles and exosomes, on the other hand, play critical roles in intercellular communication and have become the focus of many subsequent studies (Mathivanan, Ji and Simpson, 2010; György *et al.*, 2011).

Critically, the distinction between microvesicles and exosomes is dependent on which arm of the secretory pathway they originate from (György *et al.*, 2011; Meckes and Raab-Traub, 2011). Microvesicles, generally considered the larger of the two EVs measuring between 100-1000 nm in diameter, are formed through outward budding or "shedding" of the plasma membrane into the extracellular space (Voichitoiu *et al.*,

2019). Initially, it was assumed that all secreted EVs were generated in this manner, until the 1980s when a secondary more complex EV secretion pathway was described (Clifford Harding, Heuser and Stahl, 1983; Pan and Johnstone, 1983). It was discovered, that the smaller EVs, now termed exosomes, which range from 30-150 nm in diameter, form intracellularly within multivesicular bodies (MVBs) or early endosomes (Voichitoiu *et al.*, 2019). In short, exosomes form as intraluminal vesicles (ILVs), through inward budding into MVBs, which can then fuse with the plasma membrane releasing the exosomes into the extracellular space. Conversely, these MVBs can fuse with lysosomes resulting in degradation and recycling of the vesicles and their contents (C Harding, Heuser and Stahl, 1983; Pan and Johnstone, 1983; Pan *et al.*, 1985; Sun and Liu, 2014). A summary schematic of microvesicle and exosome biogenesis is shown in figure 1.6.1.

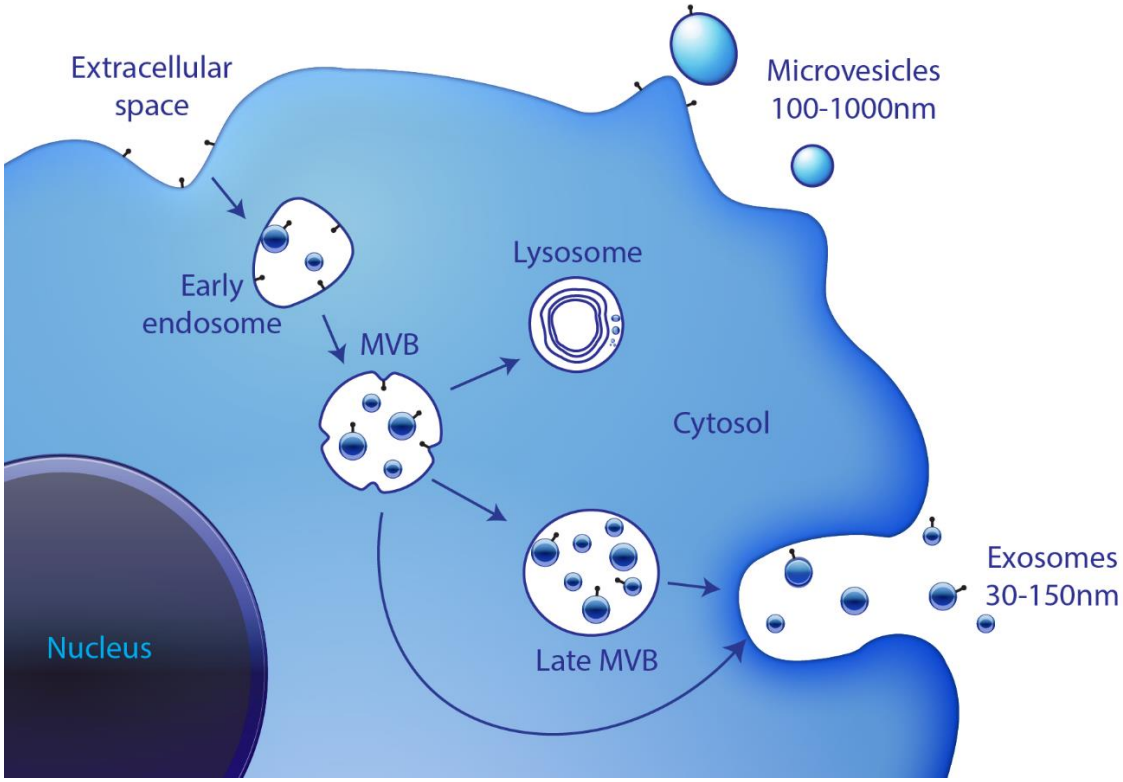

Figure 1.6.1 Extracellular vesicle biogenesis and secretion. Exosomes: Early endosomes are formed through inward budding of the plasma membrane. Exosomes are synthesised by subsequent intraluminal budding inside early endosomes and multivesicular bodies (MVBs). Early endosomes mature into MVBs and late MVBs. MVB fate is either fusion with lysosomes and subsequent degradation of vesicle contents or fusion with the plasma membrane. Exosomes are secreted upon MVB or late MVB fusion with the plasma membrane. Microvesicles: microvesicles are formed through outward budding of the plasma membrane.

Microvesicles and other EV types that are similar in size to exosomes share similar characteristics, including density and membrane orientation. As a result of this, EV isolation methods struggle to efficiently separate the different types of vesicles and most protocols used to isolate exosomes also contain other EVs of non-endosomal origin and lipoproteins (lipid-based non-vesicular structures) (Kowal *et al.*, 2016a; Karimi *et al.*, 2018). Recent investigation into the heterogeneity of exosome populations themselves revealed the existence of an additional non-membranous nano-particle termed 'exomeres' (~ 35 nm in diameter) that may further contribute to the heterogeneity of EV samples (Zhang *et al.*, 2018).

To date, many studies have identified roles for exosomes in a multitude of pathophysiological situations, including cancer, cardiovascular diseases, immune responses, regeneration and stem cell-based therapies (Mathieu *et al.*, 2019). The heterogeneity of isolated EV populations, however, means that we cannot specifically attribute these roles to specific vesicle types. To combat the issue of vesicle identification, many studies have been performed to identify markers specific for exosomes. However, Plasma membrane-derived and endosomal-derived EVs are both formed through membrane budding away from the cytosol, so they share the same membrane orientation, with similar membrane associated proteins and enclose cytosolic components. Identification of exosome specific markers has therefore proved a difficult task. More recently, however, it was demonstrated that the tetraspanins CD63, CD81 and CD9 are enriched on exosomes (Kowal *et al.*, 2016a). Whilst further validation is required, these findings suggest that the presence of CD63, CD81 and CD9 together on EVs within the correct size range (30-150 nm) could be indicative of exosomes (Mathieu *et al.*, 2019).

1.6.2 Exosomal cargo

Exosomes contain a broad range of cargos that can be transferred to recipient cells though fusion with target cell plasma membranes (Montecalvo *et al.*, 2012) or through exosome uptake into endocytic or phagocytic compartments (Morelli, 2006; Barrès *et al.*, 2010; Tian *et al.*, 2010). This cargo has been shown to be functional in target cells

and can regulate a number of cellular activities. Exosomal cargo is sequestered and packaged in the cells from which the exosomes originate, therefore, exosomes may in part, reflect the contents of the cells from which they are synthesised. Numerous different proteins have been identified in exosomes. These proteins can be ubiquitous and act as possible universal markers of exosomes, or they can be cell-specific and may prove useful in identifying characteristics of the cells that the exosomes originate from. Proteins that are ubiquitously expressed in all exosomes include the membrane-associated tetraspansins CD9, CD63, CD81 and CD82, the cytoplasmic heat shock proteins Hsp70 and Hsp90, the endosomal sorting complex required for transport (ESCRT) associated proteins TSG101 and ALIX, and transport/fusion associated Annexins and the RAB small GTPases (Théry, Ostrowski and Segura, 2009; Mincheva-Nilsson and Baranov, 2010; Mathivanan *et al.*, 2012; Vlassov *et al.*, 2012). Examples of cell specific proteins sequestered into exosomes include the major histocompatibility complex (MHC) class-I and class-II secreted by MHC presenting cells (Denzer *et al.*, 2000). Similarly, exosomes derived from tumour cells have been shown to contain many adhesion molecules, metalloproteinases and a number of oncogenic proteins that play a role in tumourigenesis and metastasis (Raimondo *et al.*, 2011; Liang *et al.*, 2013; Kruger *et al.*, 2014). In addition to proteins, exosomes are rich in lipids and lipid-raft cholesterol (Théry, Ostrowski and Segura, 2009; Yuyama *et al.*, 2012).

Nucleic acids including DNA, long non-coding RNA (lncRNA), mRNA and microRNA (miRNA) are also present in exosomes. In general, RNA can be easily degraded by RNases present in the ECM, however RNA present in exosomes is significantly more stable (Ge *et al.*, 2014) due to its compartmentalisation 'stable' exosomal mRNAs are functional and can be translated in recipient cells (Valadi *et al.*, 2007). To date, thousands of different miRNAs have been identified within exosomes and the transfer of miRNAs has been shown to regulate gene expression and cellular activities in target cells(W. X. Chen *et al.*, 2014). It is reported that the majority of miRNA present in serum and saliva are contained within exosomes and evidence suggests that exosomal miRNA is more biologically active than others in circulation (Turchinovich *et al.*, 2011; Gallo *et al.*, 2012; Zhang and Grizzle, 2014). Recent work has shown an increase in exosomal miRNA in the sera of cancer patients, highlighting the potential for exosomal miRNAs as diagnostic

biomarkers for cancer (Rabinowits *et al.*, 2009; Tanaka *et al.*, 2013; Eichelser *et al.*, 2014). Similarly, evidence also supports the potential of exosomal lncRNA and double-stranded DNA (dsDNA) as biomarkers for cancer (Kahlert *et al.*, 2014; Takahashi *et al.*, 2014; Thakur *et al.*, 2014; Q. Li *et al.*, 2015).

1.6.3 The formation and secretion of exosomes

1.6.3.1 ILV formation inside MVBs

Exosome biogenesis and secretion have been studied a great deal in recent years leading to significant advances in our understanding of the mechanisms involved. The best described method involves the ESCRT driven sorting and formation of ILVs (reviewed in Colombo, Raposo and Théry, 2014). The ESCRT machinery is composed of four complexes and associated proteins: ESCRT-0, ESCRT-I, ESCRT-II and ESCRT-III which associate at MVB membranes and regulate cargo targeting and the formation of ILVs in a successive manner (Hurley, 2015).

The ESCRT-0 complex is involved in the identification and sequestering of ubiquitinated proteins into the endosomal membrane. This complex contains hepatocyte growth factor-regulated tyrosine kinase substrate (HRS) (encoded by HSG) which associates with other ESCRT-0 associated proteins including signal transducing adaptor molecule 1 (STAM1) and the non ESCRT protein Eps15 and clathrin (Colombo, Raposo and Théry, 2014). Components of the ESCRT-0 complex are generally not associated with vesicle budding from the plasma membrane and thus, their presence in EVs may indicate endosomal origin (Mathieu *et al.*, 2019). HRS from ESCRT-0 then recruits the ESCRT-I complex protein TSG101, which subsequently recruits ESCRT-III through association with either ESCRT-II or the ESCRT associated protein ALIX (encoded by PDCD6IP). The ESCRT-I and ESCRT-II complexes are then responsible for membrane deformation, inducing intraluminal budding and the ESCRT-III complex drives vesicle scission (Hanson and Cashikar, 2012; Henne, Stenmark and Emr, 2013). Furthermore, vesicle budding has been shown to involve a number of cone shaped lipids including ceramide which is generated by sphingomyelinases (Trajkovic *et al.*, 2008; Bianco *et al.*, 2009). Finally, vacuolar protein sorting associated protein 4 (VPS4) is required for the disassociation

and recycling of the ESCRT machinery (Colombo, Raposo and Théry, 2014; Jackson *et al.*, 2017).Interestingly, the ESCRT-associated protein ALIX has been shown to play a role in ILV formation by promoting intraluminal budding (Baietti *et al.*, 2012; Romancino *et al.*, 2013).

The mechanisms of cytosolic protein cargo sorting into ILVs are less well understood. However, a role for the ESCRT-0 associated protein HRS has been identified, whereby HRS recognises ubiquitin moieties on cargo proteins and sequesters ubiquitinated proteins into the ILVs (Colombo, Raposo and Théry, 2014). Additionally, a role for the heat shock protein HSC70 has been identified. HSC70 was shown to bind to phosphatidylserine on outer membranes of MVBs and to cytosolic proteins with a KFERQ sequence resulting in the inclusion of this protein and its binding partners in ILVs in a process that was found to be TSG101 and VPS4- dependent (Sahu *et al.*, 2011). Furthermore, multiple roles have been identified for the ESCRT associated protein ALIX in cargo sorting. ALIX binding to the cytoplasmic domain of transferrin receptor (TfR) in reticulocytes was shown to induce the sorting of TfR into ILVs (Géminard *et al.*, 2004) in what appears to be a competitive manner with HSC70 binding (Géminard *et al.*, 2004). ALIX has also been shown to induce the sorting of syndecans via syntenin interaction into ILVs in an ESCRT-II, ESCRT-III and VPS4 dependent manner, resulting in the formation of syndecan, syntenin and ALIX containing exosomes (Baietti *et al.*, 2012).

Studies into the loading of miRNAs into exosomes have revealed a few different mechanisms by which miRNAs are sequestered into vesicles. One possible mechanism involves sphingomyelinase2 (nSMase2) which is believed to promote miRNA trapping in exosomes through the catalysation of ceramide (Kosaka *et al.*, 2010). Additionally, miRNA packaging has been shown to be mediated through chaperone proteins such as hnRNPA2B1 (Batagov, Kuznetsov and Kurochkin, 2011; Villarroya-Beltri *et al.*, 2013). Mechanistic studies have revealed that specific sequences at the 3’ end of miRNAs are recognised by effector proteins and thus determine which miRNAs are packaged into exosomes. For instance, the presence of 1,2, or 3 uridine or adenosine nucleotides at the 3’ end of miRNA specifically direct them to exosomes (Koppers-Lalic *et al.*, 2014).

1.6.3.1 MVB trafficking and exosome secretion

Mechanisms that drive exosome secretion have also been widely studied. The Rab family of small GTPases are known to play key roles in intracellular vesicle trafficking and so it is unsurprising that they have been implicated in various steps of MVB trafficking to the plasma membrane and subsequent exosome release (Stenmark, 2009). Impairment of Rab27a or Rab27b has been shown to alter the ability of MVBs to dock to the plasma membrane resulting in decreased exosome secretion (Ostrowski *et al.*, 2010). Rab11, Rab35, Rab5a, Rab9a, Rab2b and Rab7 have also been identified as major players in exosome secretion, albeit in a cell line dependent manner(Savina *et al.*, 2005; Hsu *et al.*, 2010; Ostrowski *et al.*, 2010; Baietti *et al.*, 2012; Abrami *et al.*, 2013; Frühbeis *et al.*, 2013).

In addition to the Rab GTPases, a number of ESCRT associated proteins have been shown to play a role in exosome secretion. Depletion of the ESCRT-0 associated HRS and STAM1 have been implicated in exosome secretion, since their inhibition decreased exosome release (Tamai *et al.*, 2010; Gross *et al.*, 2012; Colombo *et al.*, 2013; Hoshino *et al.*, 2013). However, some evidence suggests that a confounding effect may also result in the decreased secretion of microvesicles. For instance, HRS depletion during HIV infection prevented viral release from the plasma membrane by inhibiting degradation of tetherin (Janvier *et al.*, 2011). Tetherin, which holds viral particles at the membrane, is also found to be present on microvesicles and exosomes (Edgar *et al.*, 2016). Thus, HRS depletion may lead to a decrease in both exosome and microvesicle secretion. Furthermore, the ESCRT-I associated protein TSG101 has also been implicated in exosome secretion, as evidenced by decreased exosome secretion upon its depletion (Baietti *et al.*, 2012; Colombo *et al.*, 2013). Whilst common mechanisms of exosome secretion have been demonstrated (including involvement of HRS and TSG101), many studies have revealed different secretion mechanisms that are dependent on cell type (Baietti *et al.*, 2012; Abrami *et al.*, 2013; Colombo *et al.*, 2013; Romancino *et al.*, 2013). For example, whilst Colombo *et al.*, found silencing of VPS4B to induce the secretion of exosomes in HeLa cells, Baietti *et al.*, reported decreased exosome secretion in MCF7 cells upon its depletion. Additionally, they showed that ALIX depletion in MCF7A decreased exosome secretion, however, no change in secretion was observed in HeLa

cells (Baietti *et al.*, 2012; Colombo *et al.*, 2013). Highlighting therefore, that some secretion mechanisms are cell dependent.

Other important mediators of MVB-plasma membrane fusion are the soluble N-ethylmaleimide-sensitive fusion attachment protein receptors (SNARES). SNAREs form complexes with the synaptosomal-associated proteins (SNAPs) on the membranes of different membrane bound organelles mediating the fusion of their membranes (Colombo, Raposo and Théry, 2014). SNAREs have since been shown to play a role in MVB fusion at the plasma membrane. For example, the Ykt6 SNARE has been shown to be required for the secretion of Wnt-containing exosomes (Gross *et al.*, 2012), the syx-5 (STX5 in humans) SNARE was shown to target MVBs to the plasma membrane via Ral-1 small GTPase in *C.elegans* (Hyenne *et al.*, 2015) and the neurone specific snare Syntaxin 1a (STX1 in humans) alters exosome secretion in *Drosophilla* (Koles *et al.*, 2012). Furthermore, the plasma membrane associated SNAP, SNAP23 was shown to be important for the fusion of both MVBs and secretory lysosomes with the plasma membrane (Puri and Roche, 2008; Tiwari *et al.*, 2008; Verweij *et al.*, 2018).

Finally, the cytoskeleton is believed to play a role in the formation and secretion of extracellular vesicles. Actin has a well characterised role in clathrin-mediated endocytosis at the plasma membrane, where actin polymerisation stabilises and elongates the newly formed endosomal neck by exerting force against the membrane (Collins *et al.*, 2011; Mooren, Galletta and Cooper, 2012). Additionally, depolymerisation of cortical actin at the plasma membrane is hypothesized to be required for MVB docking and subsequent exosome secretion (Antonyak, Wilson and Cerione, 2012; Sedgwick and D'Souza-Schorey, 2018). Furthermore, microtubule networks are required for the trafficking of MVBs and their transport to the plasma membrane, as pharmacological inhibition of microtubules results in decreased exosome secretion (Granger *et al.*, 2014; Jackson *et al.*, 2017). It is well established that endosomes are trafficked along microtubules by microtubule motors including dynein which directs minus-end directed transport (minus end is anchored to the MTOC) (Allan, 2011) and the kinesins which direct plus-end directed transport (plus ends emanate to the periphery of the cell) (Jon Kull and Endow, 2013). In fact, inhibition of dynein was shown to result in the scattering of early endosomes, late endosomes and lysosomes

throughout the cytosol, highlighting that dynein plays a key role in the inward trafficking of endosomes (reviewed in Granger *et al.*, 2014). Interestingly, dynein is believed to be loaded onto endosomes by the Rab7 interacting lysosomal protein (RILP) which is known to bind to the HOPs complex (van der Kant *et al.*, 2013). Crucially, the HOPs complex is known to play a key role in late endosome/lysosome fusion and so RILP and dynein may direct endosomes to lysosomes for cargo degradation (Balderhaar and Ungermann, 2013). Thus, microtubule motors are key mediators of endosomal transport along microtubules and bidirectional movement of endosomes is facilitated by the presence of both plus-end and minus-end directed motors. Directional switching has been observed through a "tug of war"- like mechanism, where the endosome is subjected to opposing forces from microtubule motors until one prevails and trafficking resumes (reviewed in Granger *et al.*, 2014). Whilst the exact mechanisms of directional switching are still under investigation, evidence suggests a potential role for posttranslational modification. For example, in neurons the regulatory factor for vesicular transport, huntingtin (htt) protein, was shown to favour retrograde movement until phosphorylation by the protein kinase Akt, which resulted in switching to plus-end directed movement (Colin *et al.*, 2008).

1.6.4 Targeting and uptake of extracellular vesicles by acceptor cells

The ability of extracellular vesicles such as exosomes to trigger phenotypical changes in acceptor cells is well established and has resulted in numerous studies investigating their uptake by acceptor cells and the delivery of their cargo. Whilst EVs have been shown to influence recipient cells simply by acting at the surface without delivery of their contents (Raposo *et al.*, 1996; Tkach *et al.*, 2017), the majority of studies have revealed the full delivery of EV cargo. The exact mechanism behind EV uptake and cargo delivery, however, is still to be resolved.

Recently, targeting of EVs to specific acceptor cells has been proposed in addition to non-specific uptake. For example, whilst Hela cells are able to internalise a wide variety of EVs from many different cell types (Svensson *et al.*, 2013; Costa Verdera *et al.*, 2017), EVs secreted by oligodendrocytes were found to be preferentially engulfed by microglia

compared to neurons (Fitzner *et al.*, 2011). Likewise, EVs secreted by primary neurons were found to specifically target other neurons, whilst neuroblastoma-derived EVs were taken up by astrocytes (Chivet *et al.*, 2014).

A growing body of evidence now suggests that interplay between tetraspanins, integrins and other associated proteins within EV and cell membranes may regulate EV targeting and uptake. For instance, whilst EVs derived from the rat pancreatic adenocarcinoma cell line BSp73ASML were found to selectively target lung fibroblasts and lymph node stromal cells, upregulation of Tspan8 in these EVs resulted in preferential targeting to endothelial cells (Rana *et al.*, 2012). Upon transfection of Tspan8 and integrin β4, the selective targeting of the secreted EVs was altered again. This time, the EVs gained an increased metastatic capacity and were preferentially taken up by stromal cells in the liver and lung after intravenous injection (Yue *et al.*, 2015). Evidence now suggests that tumours produce distinct EVs or subpopulations of EVs that facilitate metastasis to specific organs. For instance, the presence of the integrins α6β1 and α6β4 on EVs was found to target them to lung fibroblasts and epithelial cells, thus facilitating lung metastasis (Hoshino *et al.*, 2015). The presence of αvβ5, however, directs EV binding to Kupffer cells in the liver and therefore induces metastasis to the liver (Hoshino *et al.*, 2015). Similarly, the presence of CD47 on the surface of exosomes has been shown to prevent EV capture by immune cells, thereby increasing vesicle duration in circulation and enhances delivery of these EVs to pancreatic cells (Kamerkar *et al.*, 2017)

Furthermore, it has been demonstrated that neuroblastoma cells secrete two distinct subpopulations of EVs that selectively target different cell types depending on the expression of CD63 or amyloid precursor protein (APP) in the EV membrane (Laulagnier *et al.*, 2018). The $CD63^+$ subpopulation, generated via ESCRT-independent mechanisms, indifferently bound to neurons and glial cells, whereas the APP^+ EVs, generated in an ESCRT-dependent manner, preferentially bound neurons (Laulagnier *et al.*, 2018). Thus, an increasing body of evidence now suggests that tumour cells secrete different subpopulations of EVs that preferentially target acceptor cells through the altered expression of tetraspanins and integrins on the EV surface.

Once EVs reach their target, they dock onto the surface of the cell through interaction with membrane-exposed proteins, lipids and/or sugars (Mathieu *et al.*, 2019). Following

docking, the EV cargo can be transferred to the recipient cell. Whilst the mechanisms of EV cargo delivery are not fully characterised, two distinct pathways have been described (see Figure 1.6.4). The first involves direct fusion of the EV with the plasma membrane of the recipient cell and the subsequent transfer of EV cargo into the cell cytosol (Parolini *et al.*, 2009). This method of transfer is believed to be utilised by the larger, plasma-membrane-derived EVs (Kanada *et al.*, 2015). The second, more well characterised mechanism involves EV internalisation by the acceptor cell through endocytosis prior to cargo delivery. Following endocytosis, EVs can either i) fuse with the endosomal membranes releasing their contents into the cell cytosol ii) be targeted for degradation by the lysosome, or iii) be recycled and re-secreted (Svensson *et al.*, 2013; Mulcahy, Pink and Carter, 2014; Costa Verdera *et al.*, 2017; Horibe *et al.*, 2018; Mathieu *et al.*, 2019).

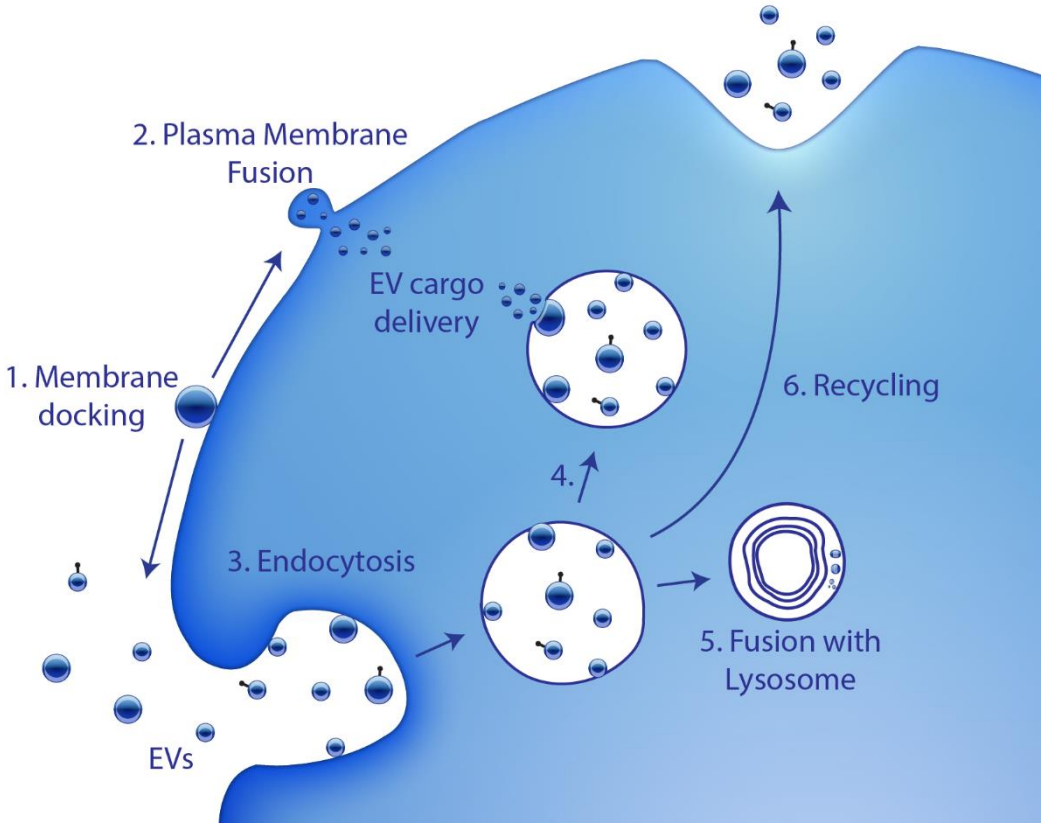

Figure 1.6.4 Mechanisms of extracellular vesicle uptake by acceptor cells. 1) EVs are targeted to the acceptor cell and dock through interaction with membrane proteins, lipids or sugars. 2) EVs directly fuse with the plasma membrane releasing their cargo into the acceptor cell cytosol. 3) EVs can be endocytosed by acceptor cells into endosomes. EVs can then either fuse with the endosomal membrane releasing their cargo into the acceptor cell cytosol (4), fuse with the lysosome resulting in degradation (5), or the EVs can be recycled and re-secreted (6).

1.7 Extracellular vesicles and cancer

It is now widely accepted that cancer-derived EVs play key roles in the development and progression of cancer. In recent years, proteomic studies have revealed tumour-derived EVs to have significantly altered protein cargoes compared to EVs derived from non-malignant cells (Hurwitz *et al.*, 2016). Additionally, studies comparing the cargoes of EVs derived from different cancer types have identified a number of proteins that are common to all EVs (proteins involved in biogenesis) as well as a number of proteins that were uniquely packaged and representative of the cells from which they were derived (Hurwitz *et al.*, 2016). Furthermore, analysis of pancreatic cancer-derived exosomes, revealed the presence of 362 cancer-related proteins that are known to have roles in tumour cell proliferation, invasion, metastasis and premetastatic niche formation (Emmanouilidi *et al.*, 2019).

1.7.1 The role of exosomes in tumourigenesis

Many studies have analysed the effects of PDAC-derived exosomes on tumourigenesis, and recent evidence suggests that EVs can play a role in transforming normal cells into malignant cells through the transfer of oncogenic material (Al-Nedawi *et al.*, 2008). For example, the transfer of mRNAs from metastatic cells have been shown to facilitate cancerous development in previously non-cancerous cells through modulation of target genes such as *PTEN* and *HOXD10* (Melo *et al.*, 2014; L. Zhang *et al.*, 2015). Similarly, gastric cancer (GC)-derived exosomes have been shown to promote tumour growth through activation of PI3K/Akt and MAPK/ERK signalling pathways (Qu *et al.*, 2009). Cancer-derived exosomes have also been shown to promote tumour growth through expression of TGF-β activated kinase 1 (TAK1) signalling which exerts anti-apoptotic effects on the cancer cells promoting their proliferation (Kogure *et al.*, 2011).

Cancer-derived exosomes have also been shown to play a role in ECM remodelling and local tumour invasion (Becker *et al.*, 2016). For example, cancer-derived exosomes containing the ECM protein fibronectin were found to promote increased cancer cell motility (Sung *et al.*, 2015) and secretion of tumour-derived exosomes enriched in

annexins, α3 integrins and ADAM10 all correlated with increased cell migration and local invasion (Keerthikumar *et al.*, 2015). Furthermore, exosomes carrying Hsp90 released by metastatic cancer cells via Rab27b-mediated exocytosis have been shown to promote cancer cell invasion through activation of MMP2 resulting in ECM degradation (Hendrix *et al.*, 2010).

Tumour-derived exosomes have also been shown to play key roles in mediating angiogenesis. For instance, cancer-EVs enriched in Tspan8 have been shown to upregulate angiogenesis-related genes in endothelial cells, thereby inducing angiogenesis in tumours (Nazarenko *et al.*, 2010). Similarly, cancer-exosomes containing miR-17-92 clusters have been shown to induce endothelial cell migration and tube formation (Umezu *et al*., 2013). Thus, cancer-exosomes have been shown to re-educate endothelial cells enhancing their motility and inducing formation of blood vessels to feed solid tumours.

Significant evidence now also indicates a role for cancer-exosomes in communication with immune cells including macrophages, dendritic cells, neutrophils, natural killer cells and T cells. For example macrophage polarization towards tumour-promoting M2 macrophages can be mediated through exosomal transfer of miR222-3p which activates SOCS3/STAT3 signalling (Ying *et al.*, 2016). In addition, acute myelogenous leukaemia -derived exosomes were found to decrease natural killer cell cytotoxicity through increased SMAD phosphorylation and decreased expression of the NKG2D receptor (Whiteside, 2013) indicating that cancer-derived exosomes can attenuate immune responses.

1.7.2 Cancer-exosomes and metastasis

Following secretion, tumour-derived exosomes may enter the circulation and transferred to distant sites throughout the body. In light of this, mounting evidence suggests a role for tumour-derived exosomes in the development of pre-metastatic niches and cancer cell metastasis. For example, PDAC-derived exosomes have been shown to initiate pre-metastatic niche formation in the liver in a stepwise manner (Costa-Silva *et al.*, 2015). Kupffer cells, the resident macrophages of the liver, are

activated by PDAC exosomes containing elevated levels of macrophage migration inhibitory factor (MIF). Once activated, Kupffer cells secrete TGF-β causing hepatic stellate cells to secrete fibronectin and recruit bone marrow-derived cells to the site forming the pre-metastatic niche (Costa-Silva *et al.*, 2015). Similarly, tumour-derived exosomes carrying the crucial ECM remodelling proteins MMP2 and MMP9 were found to degrade the ECM which subsequently enabled cancer cell invasion and metastasis (Ge *et al.*, 2012). Furthermore, tumour-derived exosomal RNAs were found to promote metastatic niche formation in the lung by activating lung epithelial cells to recruit neutrophils, a critical first step in lung premetastatic niche formation (Liu *et al.*, 2016).

Interestingly, the enrichment of certain integrins on the surface of EVs has been shown to determine organotrophic metastasis. For instance, the presence of α6β1 and α6β4 on breast cancer exosomes preferentially targets them to fibroblasts and epithelial cells in the lung, governing lung metastasis (Hoshino *et al.*, 2015). Whereas αvβ5 on pancreatic cancer exosomes results in the preferential targeting of the Kupffer cells in the liver, facilitating metastasis to the liver (Hoshino *et al.*, 2015). Likewise, PDAC tumour-derived exosomes positive for the cell surface adhesion receptor CD44 were found to aid the establishment of a premetastatic niche in the lung and lymph node (Jung *et al.*, 2009). Thus, an increasing body of evidence now suggests that tumour-derived EVs initiate premetastatic niche formation and facilitate cancer cell metastasis.

1.7.3 Tumour-derived exosomes in stromal cell reprogramming

During tumourigenesis, fibroblasts and stellate cells differentiate into an activated phenotype. Upon activation, these cells exhibit heightened migratory and invasive capacities and contribute to tumour growth and metastasis. Interestingly, cancer-derived exosomes have been found to mediate the activation/differentiation of these stromal cells. For example, exosomal transfer of TGF-β (a known fibroblast differentiation initiator) to fibroblasts was shown to promote conversion into myofibroblasts, resulting in tumour growth, local invasion and vascularization (De Wever *et al.*, 2008; Webber *et al.*, 2010a; Cho *et al.*, 2012; Ringuette Goulet *et al.*, 2018). Exosomal TGF-β was found to account for up to 86% of the TGF-β present in cancer cell

supernatants, thus exosomes may be a primary extracellular source of TGF-β. Additionally, it was demonstrated that exosomal TGF-β, as opposed to secreted TGF-β, was responsible for SMAD signalling in the target fibroblasts and subsequent fibroblast to cancer associated fibroblast transition (Ringuette Goulet *et al.*, 2018).

Recent studies have also revealed a role for tumour-derived exosomes in the activation of PSCs. For example, exosomes derived from PDAC cells were shown to activate PSCs, resulting in increased proliferation and migration, activation of ERK/Akt signalling, upregulation of fibrosis-related genes and enhanced production of procollagen type I C-peptide (Masamune *et al.*, 2018). Subsequent pathway analysis identified TGF-β1 and tumour necrosis factor (TNF) as the top upstream regulators commonly altered following treatment with PDAC-derived exosomes. During tumourigenesis, activated fibroblasts and PSCs are recruited to the premetastatic site to facilitate cancer cell metastasis. Interestingly, exosomes secreted by the pancreatic cancer cell lines PANC-1 and MIA PaCa-2 have been shown to promote the recruitment of PSCs through the transfer of exosomal protein Lin28B (Zhang *et al.*, 2019). Thus, cancer-derived exosomes have been shown to promote tumourigenesis by both activating stromal cells and promoting their recruitment.

1.7.4 Exosomes as potential biomarkers for cancer.

Due to their active role in tumour formation and abundance in biological fluids, circulating tumour exosomes have emerged as promising candidates for biomarker development. In light of this, identifying proteins and RNAs that are unique to cancer-derived exosomes has become a key focus of the exosome field. Many potential exosomal markers have already been identified and have promising clinical applications. For example, EpCAM positive exosomes are elevated in ovarian cancer and their abundance can distinguish cancer patients from those with benign conditions and healthy donors (Taylor and Gercel-Taylor, 2008). Similarly, plasma isolated exosomes from melanoma patients are enriched in caveolin-1 compared to healthy donors, highlighting the potential of caveolin-1 as a biomarker for melanoma (Logozzi *et al.*, 2009). Additionally, exosomal integrin combinations appear to dictate organ specific

metastasis and may mark for both the presence of cancer and the metastatic tendency (Hoshino *et al.*, 2015b). Major advances have also been made in identifying potential biomarkers for pancreatic cancer with two studies in particular presenting promising candidates for PDAC. For example, Glypican-1 (GPC1) has been shown to be enriched in pancreatic cancer exosomes compared to exosomes secreted by the normal pancreas (Melo., *et al.*, 2015a; Frampton *et al.*, 2018). However, whether or not GPC1 can distinguish between cancer patients and sufferers of benign pancreatic disease is still in debate (Melo *et al.*, 2015; Frampton *et al.*, 2018). Additionally, Costa-Silva. *et al.* identified exosomal MIF as a potential prognostic biomarker for PDAC. They reported that stage I PDAC patients who go on to develop liver metastases have increased levels of exosomal MIF compared to patients who did not present with metastasis and normal healthy controls (Costa-Silva., *et al.*, 2015).

The genetic material contained within exosomes also shows promise as diagnostic biomarkers for cancer. dsDNA present in exosomes has been shown to reflect the oncogenic mutation status of the cells they originate from (Kahlert *et al.*, 2014; Thakur *et al.*, 2014; Melo *et al.*, 2015). For example, the p53 and KRAS mutational states of PDAC cells has been observed in the dsDNA contained within the exosomes secreted by these cells (Melo *et al.*, 2015). The presence of miRNA in cancer-derived exosomes may also serve as diagnostic and prognostic biomarkers. In colon cancer patients, the presence of exosomal miR-17-92a correlates with disease recurrence whereas miR-19a is associated with poor prognosis (Matsumura *et al.*, 2015). In metastatic prostate cancer, the presence of exosomal miR-141 and miR-375 is observed (Bryant *et al.*, 2012; Z. Li *et al.*, 2015) whereas low levels of miR125a are observed in advanced melanoma (Alegre *et al.*, 2014). These observations highlight the potential of exosomal genetic material in the development of new biomarkers for cancer.

1.8 Project aims

Human tumours are formed from a heterogenous population of cancer cells. Whilst being considered “less fit” cells and offering no proliferative advantage, cells with extra centrosomes are maintained in most human tumours. In recent years, cells with centrosome amplification have been shown to have an active role in the development and progression of cancer. Therefore, it is possible that these “less fit” cells are maintained because they offer a survival advantage to the tumour as a whole.

Recent work from our laboratory has demonstrated that cells with extra centrosomes have an altered secretome which enhances tumour progression. Proteomic analysis of this altered secretome revealed that cells with extra centrosomes secrete several proteins associated with extracellular vesicles. Interestingly, whilst the roles of cancer exosomes, including PDAC-derived exosomes, on tumour progression and metastasis have been widely studied, it is not currently known if all cancer cells or a subtype of cancer cells are responsible for the secretion of cancer-promoting EVs. We therefore hypothesised that cancer cells with extra centrosomes may secrete more extracellular vesicles with the capacity to aid tumourigenesis. Identifying the role of vesicles secreted by specific cell subtypes may provide us with new targets for cancer therapeutics. The aims of this project were to:

1. Determine if the presence of extra centrosomes is sufficient to increase extracellular vesicle secretion in PDAC cell lines.
2. Identify key mechanisms involved in the increased secretion of extracellular vesicles by cells with extra centrosomes.
3. Identify the role of extracellular vesicles secreted by cells with supernumerary centrosomes on tumour progression.
4. Determine the exosomal cargo or cargos responsible for the cancer promoting activity of the vesicles.

Chapter 2

Materials and Methods

2.1 Cell culture

2.1.1 Cell culture reagents

Dulbecco's modified Eagle's medium (DMEM): with 4.5 g/L glucose, 4mM L-glutamine and 110 mg/L sodium pyruvate. Sterile filtered. Stored at 4°C (Thermo Fisher Scientific, 41966).

Dulbecco's modified Eagle's medium/nutrient mixture F-12 Ham (DMEM F-12): with 3.15 g/L glucose, 0.365 g/L L-glutamine, 15 mM HEPES, 14.2 mM sodium bicarbonate and 55 mg/L sodium pyruvate. Sterile filtered. Stored at 4°C. (Sigma Aldrich, D8437).

RPMI-1640 medium (RPMI): with 2 g/L glucose, 2mM L-glutamine, 2 g/L sodium bicarbonate. Sterile filtered. Stored at 4°C (Thermo Fisher Scientific, 11875093).

Keratinocyte serum free medium (1X): with L-Glutamine and supplemented with 0.2 ng/ml human recombinant Epidermal Growth Factor (rEGF) 1- 53 and 30 µg/ml Bovine Pituitary Extract (BPE). Sterile filtered. Stored at 4°C (Thermo Fisher Scientific, 17005042).

Opti-MEM® reduced serum medium: with L-glutamine and 2.4 g/L sodium bicarbonate. Stored at 4°C (Thermo Fisher Scientific, 31985070).

Gibco ™ 0.05% Trypsin-ethylenediaminetetraacetic acid (Trypsin-EDTA) (1X): with phenol red. Stored at 4°C (Thermo Fisher Scientific, 25300-054).

Gibco ™ Foetal Bovine Serum (FBS): Heat inactivated. 50 ml aliquots were stored at -20°C. Prior to use aliquots were thawed at 37°C (Thermo Fisher Scientific, 10500064).

HyClone ™ Foetal Bovine Serum, Tetracycline Screened (Tet-FBS): 50 ml aliquots were stored at -20°C. Prior to use aliquots were thawed at 37°C (GE Healthcare, SH30070.03T).

Penicillin-Streptomycin (pen/strep): 100 U/ml was added to growth media. Stored at -20 °C long term and 4 °C for short term use, (Thermo Fisher Scientific, 15140122).

EZSolution ™ Blasticidin S hydrochloride (Blasticidin): 10 mg/ml Blasticidin hydrochloride in 20 mM HEPES at pH 7.5. Sterile filtered. Blasticidin was used at a final concentration of 2.5-20 µg/ml. Stored at -20 °C (EZSolution ™, 2805).

Geneticin® (G418) Sulphate: A stock solution of 50 mg/ml was stored at -20 °C. G418 was used at a final concentration of 0.5-1 mg/ml (108321-42-2, Santa Cruz).

Puromycin: A stock solution of 10 mg/ml was stored at -20 °C. Puromycin was used at a final concentration of 1-5 µg/ml (InvivoGen, ant-pr-1).

2.1.2 Mainenance of a 2D cell monolayer

The cell lines used in this thesis are detailed in Table 2.1.2. Adherent cell lines were cultured in the appropriate growth medium (supplemented with FBS and Pen/Strep as per Table 2.1.2) and incubated at 37°C and 5% humidified CO_2. To maintain cells in a 2D monolayer, cells were passaged once they reached 70-80% confluency. To passage cells, the cell growth medium was aspirated, and cells were washed with 15ml of autoclaved phosphate-buffered saline (PBS). The PBS was then aspirated, and the cells were incubated with 0.05% Trypsin-EDTA at 37°C for approximately 5 minutes until the cells detached. The enzymatic activity of Trypsin-EDTA was then inhibited by adding the appropriate cell culture medium complete with FBS. The cell suspension was then centrifuged at 1200 rpm for 3 minutes to pellet the cells. The supernatant was then aspirated, and the cell pellet resuspended in fresh cell culture medium. Approximately 0.5-1 ml of the cell suspension was then transferred into a fresh cell culture flask, or cells were counted using a haematocytometer and seeded accordingly depending on doubling times and experimental need. Growth medium was then added to the freshly seeded cells. The flasks were then gently agitated, to evenly distribute cells and incubated once again at 37°C, 5% CO_2.

Table 2.1.2 Cell lines

Cell line	Growth medium	Cell type	Source
PaTu-8988T	DMEM + 10% FBS + 1 % Pen/Strep	Pancreatic cancer (adenocarcinoma)	Professor Hemant Kocher (BCI)
PaTu-8988S	DMEM + 10% FBS + 1 % Pen/Strep	Pancreatic cancer (adenocarcinoma)	Professor Yaohe Wang (BCI)
Panc-1	DMEM + 10% FBS + 1 % Pen/Strep	Pancreatic cancer (adenocarcinoma)	Professor Hemant Kocher (BCI)
CFPAC-1	DMEM + 10% FBS + 1 % Pen/Strep	Pancreatic cancer (adenocarcinoma)	Professor David Pellman (Harvard)
Hs766T	DMEM + 10% FBS + 1 % Pen/Strep	Pancreatic cancer (carcinoma)	Professor Hemant Kocher (BCI)
BxPC3	DMEM + 10% FBS + 1 % Pen/Strep	Pancreatic cancer (adenocarcinoma)	Professor Hemant Kocher (BCI)
Capan-1	RPMI + 10% FBS + 1 % Pen/Strep	Pancreatic cancer (adenocarcinoma)	Professor Hemant Kocher (BCI)
Capan-2	DMEM + 10% FBS + 1 % Pen/Strep	Pancreatic cancer (adenocarcinoma)	Professor Hemant Kocher (BCI)
Panc0403	DMEM + 10% FBS + 1 % Pen/Strep	Pancreatic cancer (adenocarcinoma)	Professor Hemant Kocher (BCI)
HPAF-II	DMEM + 10% FBS + 1 % Pen/Strep	Pancreatic cancer (adenocarcinoma)	Professor Hemant Kocher (BCI)
MIA-PaCa-2	DMEM + 10% FBS + 1 % Pen/Strep	Pancreatic cancer (carcinoma)	Professor Hemant Kocher (BCI)
AsPC-1	RPMI + 10% FBS + 1 % Pen/Strep	Pancreatic cancer (adenocarcinoma)	Professor Hemant Kocher (BCI)
DEC-hTERT	DMEM + 10% FBS + 1 % Pen/Strep	Normal pancreas	Professor Hemant Kocher (BCI)
HPDE	keratinocyte-SFM (1X) serum free media +30ug/ml (BPE)+ 0.2ng/ml rEGF	Normal pancreas	Professor Yaohe Wang (BCI)
PS1	DMEM: F12 + 10% FBS + 1 % Pen/Strep	Normal pancreas	Professor Hemant Kocher (BCI)
HEK-293M	DMEM + 10% FBS + 1 % Pen/Strep	Embryonic kidney	David Pellman (Harvard)

2.1.3 Drug treatments

Doxycycline hyclate (Dox): Dox is a synthetic oxytetracycline derivative used to induce overexpression of PLK4 in the TetR.PLK4 cell lines. Stock solutions of 2 mg/ml were generated in autoclaved deionised water and aliquots stored at -20°C. To induce PLK4 overexpression, 2 µg/ml of Dox was added to cell culture medium for 48 hours (Sigma-Aldrich, D9891).

Hydrogen peroxide (H_2O_2): H_2O_2 30%(w/w) in H_2O was used to induce ROS production in our cells. The H_2O_2 stock was stored at 4°C. For use in cell culture, H_2O_2 was diluted in cell culture medium and sterile filtered before being used at a final concentration of 100 µM (Sigma Aldrich, H1009). Cells were treated with H_2O_2 for a maximum of 48 hours.

N-acetyl cysteine (NAC): NAC is a scavenger of ROS and so was used to quench ROS in our cells. NAC powder (stored at 4°C) was dissolved in autoclaved deionised water to generate a stock concentration of 613 mM. The NAC stock was aliquoted and stored at -20°C until needed. Prior to use in cell culture, the acidity of the NAC stock solution was neutralised to pH7 using sodium hydroxide (NaOH). The neutralised NAC was then sterile filtered, and used in cell culture at a final concentration of 5 mM (Sigma-Aldrich, A9165). Cells were treated with NAC for a maximum of 48 hours.

Bafilomycin A1: Bafilomycin A1 (from *Streptomyces* griseus) is a vacuolar type H+-ATPase inhibitor and was used to prevent the acidification of lysosomes, diminishing their degradative capacity. Bafilomycin A1 was dissolved in DMSO to generate a stock solution of 0.1 mg/ml and aliquots were stored at -20°C. Bafilomycin A1 was used in cell culture at a final concentration of 20 nM (Sigma-Aldrich, B1793-10UG). Cells were treated with Bafilomycin A1 for a maximum of 24 hours.

2.1.4 Small interfering RNA (siRNA) transfection

PaTu-S.PLK4 and HPAF-II.PLK4 cells for siRNA transfection were seeded into 6 well tissue culture plates at a density of 2 x 10^5 and 5 x 10^5 cells per well respectively in antibiotic free growth medium. The following day, transfection was performed by diluting the appropriate siRNA and 10 µl of the transfection reagent Lipofectamine® RNAiMAX (Thermo Fisher Scientific, 13778030) in 500 µl of Opti-MEM® reduced serum medium.

The solution was incubated at room temperature for 20 minutes to enable to formation of liposomes before being added in a dropwise fashion onto the cells. For SAS-6 knock down experiments siNegative control (siNegative, Qiagen, 1027310) and siSAS-6 (siSAS6 on-TARGET smart pool, Dharmacon, M-004158-02) were used. 20 nM of siRNA was used for PaTu-S.PLK4 cells and 50 nM for HPAF-II.PLK4 cells as PaTu-S.PLK4 cells were found to be more sensitive to SAS-6 depletion. siRNA stocks were diluted in RNase-free water to a concentration of 20 µM and stored at -20^{o}C. 24 hours post transfection, the cells were trypsinised and seeded onto coverslips for analysis by immunofluorescence or into 15 cm dishes for exosome harvest experiments.

2.1.5 Measureing cellular reactive oxygen species (ROS)

Cellular ROS levels were measured using the GSH/GSSG-Glo™ Assay (Promega, V6611). This Promega kit measures glutathione in its reduced (GSH) and oxidised (GSSG) forms. As glutathione is converted from its reduced from to its oxidised form upon oxidative stress, the ratio between the two forms of glutathione is a good read out for ROS in cells and tissues (Carelli et al., 1997; Locigno and Castronovo, 2001; Noctor and Foyer, 2002; Townsend, Tew and Tapiero, 2003). The GSH/GSSG-Glo™ Assay is a luminescence-based assay, which relies on GSH-mediated conversion of the GSH probe Luciferin-NT to luciferin by a glutathione S-transferase enzyme. This reaction is coupled to a firefly luciferase reaction resulting in a luminescent signal that is proportional to the amount of GSH present in the sample. Parallel reactions are performed to determine total and oxidised levels of glutathione. The first utilises a reducing agent to convert all glutathione to the reduced form and gives a readout of total glutathione. The second reaction measures only the oxidised form by blocking the GSH present in the sample, a reducing step is then used to convert the GSSG to GSH for quantification. The ratio of GSH to GSSG can then be calculated to give a read out of oxidative stress in the cells, where a decrease in the ratio indicates an and increase in oxidative stress. All reactions and calculations were carried out as per the manufacturer's instructions. Finally, the amount of protein present in each reaction was quantified using the Pierce™ BCA Protein Assay Kit (Thermo Fisher Scientific, 23227) as per the manufacturer's

instructions. The final ratio of GSH/GSSG was then normalised to protein content to control for any changes in cell number.

2.2 Lentivirus and Generation of PLK4 inducible cells

As lentiviruses (a class of retrovirus) have the capacity to integrate viral DNA into the genome of both dividing and non-dividing cells, a lentiviral delivery system was used to generate genetically modified cell lines.

2.2.1 Lentivirus production and infection

To generate lentivirus, HEK-293M cells were seeded into a 6-well plate in growth medium without antibiotic supplementation. Once cells reached 50% confluency, transfection was performed. Cells were transfected with a transfection mixture consisting of 500 µl Opti-MEM, 10 µl lipofectamine® 2000 (Thermo Fisher Scientific, 11668027), 2 µg of plasmid DNA, 1 µg of Gag-Pol DNA (Gag-Pol: psPAX2, Addgene, 12260) and 0.5 µg VSV-G DNA (VSV-G: pMD2.G, Addgene, 12259). The transfection mixture was incubated at room temperature for 20 minutes to allow for the formation of liposomes before being added in a dropwise manner to the cells. 6 hours post transfection, the medium was replaced with 1.5 ml of fresh growth medium. Virus was collected 24- and 48-hours post-transfection, filtered using a 0.4 µM syringe filter and stored in cryovials at -80^{o}C until needed.

For lentiviral infection, PaTu-S or HPAF-II cells were plated in a 6-well plate. The following day, growth medium was replaced with 1 ml of medium without antibiotic supplementation. The appropriate lentivirus was then mixed with 8 µg/ml polybrene (Sigma-Aldrich, TR-1003-G) before being added to the cells in a dropwise fashion. An 8 mg/ml stock solution of polybrene was generated in autoclaved deionised water and stored at -20^{o}C. 6 hours post-infection, the virus was removed and replaced with normal growth medium. Infection was repeated the following day and antibiotic selection started 24 hours after final infection.

2.2.2 Generation of cells with inducible PLK4 overexpression

To generate PaTu-S and HPAF-II cell lines with an inducible PLK4-overexpression system, cells were initially infected with lentivirus containing a Tetracycline repressor (TetR), pLenti-CMV-TetR-Blast lentiviral vector (Addgene, 17492). Following viral infection, cells successful for transduction were selected for using Blasticidin (10 µg/ml). Post-selection, cells were then infected with a lentiviral vector containing PLK4 cDNA which had been previously cloned into the pLenti-CMV/TO-Neo-Dest vector using the gateway system by Susana Godinho (Godinho *et al.*, 2014). Following infection with PLK4 lentivirus, cells were selected with Geneticin (200 µg/ml) for two weeks. The presence of the TetR ensures that PLK4 overexpression only occurs upon the addition of the tetracycline analogue doxycycline. This method allowed the generation of PaTu-S.PLK4 and HPAF-II.PLK4 cell lines in which the PLK4 transgene is induced using 2 µg/ml of Doxycycline for 48 hours.

2.3 2D Immunofluorescent microscopy

2.3.1 Reagents

Methanol: ≥99.9% methanol was stored and used at -20^{o}C (Sigma-Aldrich, 154903).

Formaldehyde: Pierce™ 16% Formaldehyde (w/v), Methanol-free (Thermo Fisher Scientific, 28906). Stored at room temperature.

Cell permeabilisation buffer: 0.02% v/v Triton X-100 diluted in PBS. Stored at room temperature.

Blocking solution: 5% w/v Bovine Serum Albumin and 0.1% v/v Triton X-100 in PBS. Prior to use, blocking solution was filtered through a 0.2µM 500ml Rapid Flow Filter Unit (Thermo Fisher Scientific, 156-4020). Stored at 4^{o}C.

ProLong™ Gold Antifade Mountant: Ready to use and stored at room temperature (Thermo Fisher Scientific, P36934).

2.3.2 Cell fixation

For immunofluorescent staining, cells were plated on 1.5 thickness, 18mm round glass coverslips (Warner Scientific, CS-18R15) at least 24 hours prior to fixation. Cells were then treated for up to 48 hours with the appropriate drug treatments (controls left untreated). Post treatment, cells were washed twice in PBS and fixed in 4% Formaldehyde (diluted from 16% Formaldehyde stock in PBS) for 20 minutes at room temperature. Cells to be stained for the centrosomal protein centrin, however, were instead fixed in ice-cold methanol for 10 minutes at -20 ^{o}C. Following fixation, cells were washed twice in PBS and stored at 4^{o}C until needed.

2.3.3 Immunofluorescent staining

Following fixation, cells were permeabilised for 5 minutes using our cell permeabilisation buffer and then blocked for 30 minutes in the previously generated blocking solution. The cells were then incubated with primary antibody diluted in blocking solution (See Table 2.3.2 for primary antibodies and dilutions) for 1 hour at room temperature. Cells were then washed twice with PBS to remove any residual/non-specifically bound primary antibody. Cells were then incubated with the appropriate secondary antibody conjugated to an Alexa Flour fluorophore diluted in blocking solution for 50 minutes at room temperature in the dark (see Table 2.3.2 for secondary antibodies and dilutions). Where phalloidin was used to stain for F-actin, cells were incubated with phalloidin in blocking solution for 1 hour only. To remove any non-specifically bound secondary antibody, cells were then washed twice in PBS. DNA was then stained with Hoechst diluted in PBS for 5 minutes at room temperature. After a final PBS wash step, coverslips were mounted using ProLong™ Gold Antifade Mountant. Details of all antibodies and stains used for immunofluorescence staining can be found in table 2.3.2.

Table 2.3.2 Antibodies for immunofluorescence staining

Primary Antibodies	**Product number**	**Supplier**	**Species raised**	**Dilution**
Anti-centrin 2 (N-17-R)	sc-27793-R	Santa Cruz	Rabbit	1:100
Anti α-tubulin (DM1 α)	T9026	Sigma-Aldrich	Mouse	1:1000
Anti LBPA (6C4)	MABT837	Merck Millipore	Mouse	1:100
Anti LC3B (D11) XP ®	3868S	Cell signalling	Rabbit	1:200
Anti α-SMA	A2547	Sigma-Aldrich	Mouse	1:300
Secondary Antibodies	**Product number**	**Supplier**	**Species raised**	**Dilution**
Anti-Rabbit Alexa Flour 488	A11008	Life Technologies	Goat	1:1000
Anti-Rabbit Alexa Fluor 568	A11011	Life Technologies	Goat	1:1000
Anti-Mouse Alexa Fluor 488	A11001	Life Technologies	Goat	1:1000
Other	**Product number**	**Supplier**	**Species raised**	**Dilution**
Alexa Fluor 568 Phalloidin	A12380	Life Technologies	-	1:250
Hoechst 33342	H3570	ThermoFisher Scientific	-	1:5000

2.3.4 Analysis

Images were acquired using an inverted Nikon microscope coupled with a spinning disk confocal head (Andor). Unless otherwise stated, imaging of cancer cells was performed using a 100x objective and imaging of stellate cells with a 40x objective. Images/projection images (from z-stacks) were subsequently generated and analysed with Image J (please see each experiment for details). Where Z-stack images were required to analyse fluorescence intensity, Z-stack parameters were determined using the following equation: Zmin = 1.4λn/(NAobj)2. λ = the emission wavelength, n= refractive index of the immersion media, NAobj = the numerical aperture of the objective. This equation calculates the ideal z stack step size to minimise overlap between each step of the stack. Sum intensity projection images were subsequently generated using Image J and fluorescence intensity was quantified using Image J.

2.3.5 Magic Red ™ Cathepsin B analysis

The Magic Red™ Cathepsin B kit (Bio-Rad, ICT937) was used to analyse the protease activity of Cathepsin B in lysosomes as a proxy to lysosome function. Cells were plated on coverslips and treated with Dox, Dox +NAC, H_2O_2, Bafilomycin A1 or left untreated as described previously. One hour prior to the end of the experiment, cells were given the Magic Red substrate and returned to the incubator. Magic Red is a cell-permeable and non-toxic reagent consisting of a cathepsin B target sequence peptide $(RR)_2$ which has been linked to a Cresyl Violet fluorescent probe. In the presence of functional cathepsin B, Magic Red is cleaved allowing the Cresyl violet fluorophore to fluoresce red upon excitation at 550-590 nm. A stock solution of Magic Red was reconstituted in 50 µl of DMSO and stored thereafter at -20^{o}C. Prior to use in cell culture, the reconstituted Magic Red was diluted 1 in 10 in deionised water and 20µl per 300µl of growth media was added to each coverslip as per the manufacturer's instructions. One hour later, cells were fixed in 4% Formaldehyde as previously described. Cresyl Violet fluorescence was detected using an inverted Nikon microscope coupled with a spinning disk confocal head (Andor). Z-stack images were acquired, and sum intensity image projections were generated using Image J. Fluorescence intensity was then quantified per cell with ImageJ.

2.4. Extracellular vesicle (EV) isolation and quantification

2.4.1 Materials and reagents

Ultracentrifugation tubes: Tube, Thinwall, Ultra-Clear™, 38.5 mL, 25 x 89 mm (Beckman coulter, 344058).

Dulbecco's Phosphate Buffered Saline (PBS): Sterile PBS (Sigma-Aldrich, D8537), filtered through two 0.22 μm filters before use.

qEV original Size Exclusion Chromatography (SEC) columns: qEVoriginal/70 nm pore size SEC columns for exosomes separation and purification, 10ml volume. Stored at 4^{o}C (izon, SP1).

BODIPY® FL Maleimide (BODIPY® FL N-(2-Aminoethyl))Maleimide) (BODIPY): BODIPY was reconstituted in DMSO generating a stock solution of 5 mM (Thermo Fisher Scientific, B10250). Aliquots of the stock solution were stored at -20^{o}C. BODIPY was used at a working dilution of 1/200.

2.4.2 Extracellular vesicle harvest

Prior to culturing cells for EV harvest, the FBS supplement added to the media first had to be depleted of naturally occurring EVs. Vesicle depletion in FBS was performed via ultracentrifugation at 100,000 x g at 4^{o}C. As is described in Chapter 3 Results I section 3.2.2, Gibco FBS required 2 hours of ultracentrifugation at 100,000 x g, whereas GE Healthcare FBS required 18 hours of ultracentrifugation at 100,000 x g to successfully deplete contaminating EVs.

To harvest exosomes, cells were grown for 48 hours in vesicle depleted media. Where induction of centrosome amplification was necessary, cells were treated with Dox for 48 hours, before cells were washed in PBS and subsequently cultured in EV depleted media. Where drug treatments were required, cells were treated for the duration of the exosome harvest (48 hours post addition of vesicle depleted media). After 48 hours, the conditioned medium was collected from the cells and a final cell count was performed

to ensure the final cell count always remained the same between cell types and experimental conditions.

2.4.3 Extracellular vesicle isolation

2.4.3.1 Serial ultracentrifugation (UC)

Extracellular vesicles were isolated from the conditioned media via serial ultracentrifugation steps at 4°C (similar to Costa-Silva *et al.*, 2015). Initially, the cell culture medium was subjected to a low speed centrifugation of 500 x g for 10 minutes to remove debris. The supernatant was then centrifuged at 12,000 x g for 20 minutes to pellet the large EVs ($_{L}$EVs), after removal of the supernatant the $_{L}$EVs were re-suspended in 500µl of PBS. The supernatant was then subjected to a high-speed ultracentrifugation at 100,000 x g for 70 minutes to pellet the smaller EVs ($_{s}$EVs). The resultant pellet was washed in PBS and a second high-speed ultracentrifugation was performed at 100,000 x g for 70 minutes to aid in removal of non-EV contaminants. The isolated $_{s}$EV pellet was then re-suspended in 500 µl of PBS. Where necessary EV isolates were stored in PBS at -80°C and where possible isolates were used for further analysis or functional assays immediately.

2.4.3.2 Size exclusion chromatography (SEC)

To further purify EVs isolated by serial ultracentrifugation, size exclusion chromatography (SEC) was performed. Prior to use, size exclusion chromatography (SEC) columns were removed from 4°C and incubated at room temperature for 1 hour to equilibrate the column. The columns were then flushed with 5ml of buffer (PBS filtered twice through 0.22 µM filters). Once ready for use, any buffer present above the top filter was pipetted out and 500 µl of concentrated exosomes (isolated by serial ultracentrifugation) was added to the top of the column. The eluted fractions were immediately collected in 500 µl volumes. To prevent unintentional dilution of the samples, the sample was allowed to pass fully into the top filter before additional buffer was added. The column is then kept topped up with buffer (500 µl at a time) throughout

the experiment ensuring that the top filter never runs dry. The first six fractions collected contain the void volume which do not have EVs. The subsequent fractions, fraction 7-12 contain the eluting EVs. Following collection of the EVs, the columns were flushed with 10ml of buffer and stored at 4^{o}C in storage buffer as per the manufacturer's instructions. Columns were reused a maximum of 5 times before being discarded.

2.4.4 Quantification of isolated vesicles

2.4.4.1 Amins ImageStream® Mark II Imaging Flow Cytometer (ImageStream)

Samples to be analysed by ImageStream were prepared in 50 µl volumes in Eppendorf tubes. Vesicles were labelled with the fluorescent lipid dye BODIPY (used at a 1/200 dilution) and incubated at room temperature in the dark 10 minutes prior to analysis. In addition to vesicle samples, a control sample that had been processed and stained with BODIPY as if containing vesicles was also run to ensure that BODIPY alone did not contribute to the observed vesicle populations. Upon loading of the samples, the ImageStream uses syringe driven sample injection to accurately measure the volume of sample injected into the flow cell. This enables the software to accurately report the number of objects/ml that pass through the flow stream. Once loaded, vesicles were acquired at a slow flow rate with 60x magnification, a 488 nm excitation laser (BODIPY detection) and 765 nm laser (side scatter). The "remove bead" function was turned off and the flow rate allowed to stabilise before acquisitions began. For acquisition, the storage gate was set to collect all events and the stopping gate set to the vesicle population (low to mid BODIPY intensity and low side scatter). The stopping gate was set to ensure that at least 20,000 objects were analysed per acquisition. Three separate acquisitions were collected per sample. Analysis was then performed using the IDEAS software. To quantify objects/ml, a graph was generated plotting channel 02 fluorescence intensity (BODIPY) against channel 12 scatter intensity (side scatter) and a vesicle gate was re-applied to select the population at the correct BODIPY and side scatter intensities to be EVs. Where necessary the gate was adjusted using the Image library to eliminate noise and artefacts from the vesicle population. The objects/ml statistic was then used to quantify the number of objects/ml in the gated region. The

average objects/ml was then calculated from the three separate acquisitions from each sample.

2.4.4.2 Nanoparticle tracking anlaysis (NTA)

Small particle analysis was also performed by NTA using a NanoSight NS300 with a high sensitivity camera and a syringe pump. As previously described, isolated EVs were resuspended (UC) or eluted (SEC) in Dulbecco's PBS filtered twice through 0.22 µM filters. Prior to loading samples, the NS300 chamber was flushed first with 0.22 µM filtered deionised water and then again with 500 µl of PBS (Dulbecco's PBS filtered twice through 0.22 µM filters) until the chamber is free of any particle matter. Using a 1 ml syringe 400 of EV samples was then flushed through the chamber until vesicles were visible on the camera to allow the focus and gain settings to be optimised. The sample was the injected into the flow cell at speed 50 and 3 recordings of 60 seconds each were acquired. Between samples filtered PBS was used again to flush the chamber ensuring no residual particles remained. The data was then analysed using the NTA 3.2 analysis software and averages of the three technical replicates were plotted per experiment. This analysis provides both a measure of vesicle concentration (objects/ml) and vesicle size.

2.5 Western blotting

2.5.1 Reagents

Radioimmunoprecipitation assay (RIPA) lysis and extraction buffer: Ready to use, stored at 4^{o}C (Thermo Fisher Scientific , 89901).

RIPA buffer with Protease Inhibitors: One cOmplete™ Mini Protease Inhibitor Cocktail tablet (Roche, 11836153001) was added to 10mls of RIPA buffer and vortexed until fully dissolved. Aliquots were stored at -20^{o}C until required.

Bovine serum albumin (BSA): Protein Standards for Bradford assay were generated from a stock of 10 mg/ml BSA (Sigma-Aldrich, A2153) dissolved in deionised water. Standards ranged from 0-6 mg/ml BSA and were stored at 4^{o}C.

Bio-Rad Protein Assay Dye Reagent Concentrate: Bio-Rad Protein Assay Dye Reagent (Bio-Rad, 500-0006) was used to quantify protein using a colorimetric assay based on the Bradford method. Stored at 4^{o}C.

Laemmli SDS sample buffer, reducing 4x: Containing 250 mM Tris-HCL, 8% SDS, 40% glycerol, 8% beta-mercaptoethanol and 0.02% bromophenol blue. Used at 1x concentration. Stored at room temperature (Alfa Aesar, J60015).

NuPAGE™ 10% Bis-Tris Protein Gels, 1.0 mm, 10-well: Precast polyacrylamide gels with a neutral pH. Stored at 4^{o}C (Thermo Fisher Scientific, NP0301BOX).

PageRuler™ Plus Prestained Protein Ladder: Ready to use ladder for use as size standards in SDS-Page, showing 10 to 250 kDa. Stored at -20^{o}C (Thermo Fisher Scientific, 26619).

Running buffer: NuPAGE™ MOPS SDS Running Buffer (20X) (Thermo Fisher Scientific, NP0001). Stored at room temperature. Diluted to 1X in deionised water.

Transfer buffer: 10X Tris Glycine (Severn Biotech, 20630050) diluted to 1X in deionised water and 20% (final concentration) methanol. Stored at room temperature.

Polyvinylidene fluoride (PVDF) western blotting membrane: PVDF western blotting membrane with 0.2 µm pore size (Merck, 3010040001). Activated with methanol 5 minutes prior to use.

TWEEN® 20: Stored at room temperature (Sigma- Aldrich).

Tris buffered saline (TBS)- Tween (TBS-T): TBS (Severn Biotech , 20730110) was diluted to 1X in deionised water and supplemented with 0.1% v/v Tween-20 to generate TBS-T.
Blocking solution: Blocking solution was generated by dissolving 5% w/v skimmed milk powder (Sigma-Aldrich, 70166) in TBS-T. Blocking solution was made fresh prior to each use.

Pierce™ enhanced chemiluminescence reagent (ECL) Western Blotting Substrate: ECL Western Blotting Substrate was used to detect HRP on immunoblots (Thermo Fisher Scientific, 32106). Stored at 4°C.

X-Ray Film: 18x24 cm X-ray film (Scientific Laboratory Supplies, MOL7016).

2.5.2 Protein isolation and quantification

Cells for protein extraction were placed on ice, washed twice in ice cold PBS and lysed in RIPA buffer with protease inhibitors. Lysis was further aided by scraping cells from the growth surface with a cell scraper. The lysed cells were then transferred into a microcentrifuge tube. Small extracellular vesicles harvested for protein extraction were isolated as described in section 2.4.3.1. Following the final wash step, PBS was removed from and the pelleted vesicles were lysed in RIPA buffer with protease inhibitors on ice. The subsequent lysate was then then transferred into a microcentrifuge tube. Henceforth all protein samples were processed in the same manner. To facilitate further lysis, samples were sonicated on ice. The resultant protein lysates were then centrifuged at 10,000 x g for 30 minutes at 4°C to pellet cell debris. The supernatant containing the soluble protein was collected and used for further analysis. Where necessary protein samples were stored at -80°C.

The protein concentration of each sample was determined in a 96-well plate using the Bio-Rad Protein Assay, which is a colorimetric assay based on the Bradford protein analysis method. The concentrated Bio-Rad protein assay was diluted 1:4 in deionised water and 200 µl added per well to 2-4 µl of each sample. BSA standards ranging from 0-6 µg/ml were used each time. Absorbance at 595 nm was measured using a plate reader. Readings from the BSA standards, enabled a standard curve to be plotted and the equation of the line generated. Using the equation of the line, the protein concentration for each sample was calculated. Western blot loading samples were then generated ensuring each sample had 1 µg/µl of protein, Laemmli Buffer diluted to a 1X concentration and the appropriate amount of RIPA buffer to make up the final volume. Prior to electrophoresis, the samples were boiled on a heat block at 98°C for 5 minutes to denature the proteins.

2.5.3 Western blotting

Protein samples were resolved using the NuPAGE® Bis-Tris Electrophoresis System with NuPAGE™ 10% Bis-Tris Protein Gels (1.0 mm, 10-wells). The protein gels were inserted into an electrophoresis tank before the tank was filled with running buffer. 5 µl of PageRuler™ Plus Prestained Protein Ladder was added to the first well and 15-20 µl of each protein loading samples was added to the subsequent wells. The gel was then run at 80 V for 20 minutes to allow time for the proteins to stack and then subsequently resolved at 150 V for the remaining run time (roughly 1 hour or until blue sample buffer reached the base of the gel).

The resolved proteins were then transferred onto a PDVF membrane using the Mini Trans-Blot® wet transfer system. Prior to use, the PDVF membrane was equilibrated in methanol for 5 minutes. The gels and PDVF membrane were submerged in transfer buffer and tightly packaged into transfer cassettes, flanked either side with chromatography paper. These cassettes were then placed into the transfer tank and the tank was filled with transfer buffer. Additionally, to prevent over-heating, ice packs were added to the tank. The transfer was performed at 100 V for 1.25 hours.

2.5.4 Immunoblot detection

After transfer, the membranes were blocked in 10ml of blocking solution on a rocker at room temperature for 1 hour. Membranes were then incubated with primary antibody diluted in blocking buffer (See table 2.5.4 for primary antibodies and dilutions) on a gentle rocker at 4^{o}C overnight. 12-18 hours later, membranes were washed in TBS-T 3 times for 5 minutes each, on a rocker at room temperature. Membranes were then incubated with the appropriate secondary horseradish peroxidase (HRP)- conjugated antibody (See table 2.5.4 for secondary antibodies and dilutions) diluted in blocking buffer for 1 hour on a rocker at room temperature. Membranes were washed again with TBS-T 3 times for 5 minutes each, on a rocker at room temperature. Protein bands were the visualised by adding the Pierce™ enhanced chemiluminescence reagent (ECL) Western Blotting Substrate which acts as a substrate for HRP resulting in the emission

of low-intensity light. In a dark room, X-ray film is placed over the membranes for various exposure times and films were developed using a SRX-101A table top film processor.

Table 2.5.4 Antibodies for western blotting

Primary Antibodies	**Product number**	**Supplier**	**Species raised**	**Dilution**
Anti TSG101 (EPR7130(b))	ab125011	Abcam	Rabbit	1:1000
Anti CD63	ab68418	Abcam	Rabbit	1:1000
Anti CD81 (B-11)	sc-166029	Santa Cruz Biotechnology	Mouse	1:500
Anti ALIX (3A9)	2171	Cell signalling	Mouse	1:1000
Anti Flotillin-1 (18)	610821	Biosciences	Mouse	1:1000
Secondary Antibodies	**Product number**	**Supplier**	**Species**	**Dilution**
HRP- anti rabbit secondary	NA934V	GE Healthcare	Donkey	1:5000
HRP- anti mouse secondary	NA931V	GE Healthcare	Sheep	1:5000

2.6 $_s$EV uptake by recipient cells

To visualise $_s$EVs uptake by recipient cells, initially fluorescently labelled $_s$EVs were generated. To do this, $_s$EVs were harvested from PaTu-S cells using the ultracentrifugation protocol described in section 2.4.3.1 with the following alteration. Prior to the final PBS wash step, $_s$EVs were resuspended in 200 µl of PBS and fluorescently labelled with a 1/200 dilution of BODIPY. $_s$EVs were then incubated at room temperature for 5 minutes before being diluted in 31.5 ml of PBS to dilute out any unbound dye. The final 100,000 x g ultracentrifugation step was then performed and the subsequent $_s$EV pellet resuspended in 200 µl of PBS. The isolated $_s$EVs were then added

to the desired recipient cells (either PaTu-T or PS1 cells) that had been plated on glass coverslips 24 hours prior. 3 hours post addition of exosomes coverslips were fixed in 4% formaldehyde and stained with phalloidin and DAPI as described in section 2.3. Representative z-stack images were taken using a spinning disk confocal microscope as described in section 2.3.4.

2.7 $_s$EV-mediated PSC activation

PaTu-S.PLK4 cells were untreated or treated with 2 µg/ml doxycycline for 24 hours to induce over expression of the PLK4 transgene leading to centrosome amplification. The following day cells were plated into 14 T175 flasks at a density of $1x10^6$ cells per flask. Doxycycline (2 µg/ml) was again added to the cells being induced for centrosome amplification. 24 hours later, the cells were washed twice with PBS and 15 ml of fresh, vesicle depleted media (see section 2.4.2) was added to the cells. 48 hours later, $_s$EVs were harvested from the cells by ultracentrifugation alone, or in combination with SEC as described in section 2.4.3. The number of $_s$EVs present in each isolate was then quantified by ImageStream as described in section 2.4.4.1. PS1 cells were plated on glass coverslips at a density of $1x10^4$ cells 24 hours prior to $_s$EVs harvest. 24 hours after plating, PS1 cells were then left untreated (negative control), or treated with i) 5 ng/ml TGF-β (positive control), ii) 20 million $_s$EVs from cells without the induction of centrosome amplification, iii) 20 million $_s$EVs from cells with the induction of centrosome amplification. 48 hours later, a second dose of 20 million $_s$EVs was administered per condition. 24 hours post the final addition of $_s$EVs (72 hours post the initial addition of $_s$EVs), cells were fixed and stained for α-SMA and DAPI (as described in section 2.3). Representative images of the cells were taken using a spinning disk confocal microscope as described in section 2.3.4. PS1 activation was quantified based on α-SMA organisation, where the formation of α-SMA fibres was used as a measure of activation. Roughly 150 cells were quantified by eye per condition. All conditions were quantified blind.

2.8 SILAC based Proteomic Analysis

SILAC based proteomic analysis of exosomes was performed in collaboration with Dr Faraz Mardakheh. All amino acids (heavy and medium) and buffers were provided by our collaborator.

2.8.1 Reagents

Gibco ™ Foetal Bovine Serum, Dialyzed (FBS for SILAC): 50 ml aliquots were stored at -20^{o}C. Prior to use aliquots were thawed at 37^{o}C (Thermo Fisher Scientific, 26400044).

Dulbecco's modified Eagle's medium for SILAC (DMEM for SILAC): with L-glutamine, deficient in L-lysine and L-arginine. 0.2 µm Sterile filtered. Stored at 4^{o}C (Thermo Fisher Scientific, 88364).

Buffer A*: 2 ml acetonitrile, 0.1 ml trifluoroacetic acid, 0.5 ml acetic acid in 97.4 ml of H_2O.

Buffer A: 0.5 ml acetic acid in 99.5 ml H_2O.

Buffer B: 80 ml acetonitrile, 0.5 ml acetic acid in 19.5 ml H_2O.

STOP 5 Buffer: 4% acetonitrile, 1% trifluoroacetic acid in H_2O.

2.8.2 Generation of SILAC media

SILAC DMEM was supplemented with 10% dialyzed FBS that had been ultracentrifuged for 18 hours at 100,000 x g to removed naturally occurring EVs. Additionally, the media was supplemented with 600 mg/L Proline and 100 mg/L of heavy or medium Lysine and Arginine depending on the condition. Amino acids were dissolved in deionised and sterile filtered prior to media supplementation.

2.8.3 SILAC label incorporation tests

PaTu-S.PLK4 cells were grown in SILAC DMEM supplement with heavy or medium labelled amino acids, for 2 weeks before label incorporation tests were performed. Cells

were trypsinised and pelleted as previously described before being washed twice in PBS. Following the final PBS wash, residual PBS was removed from the cell pellet. Samples were then processed as described in section 2.8.5. For label incorporation tests, 3 µg of each sample was injected into the mass spectrometer for analysis. Upon confirmation that the PaTu-S.PLK4 cells had successfully incorporated the SILAC labels, these cells were used for further analysis.

2.8.4 Exosome harvest for SILAC based proteomic analysis

PaTu-S.PLK4 cells were grown in either heavy or medium SILAC in T175 flask. Cells grown in heavy growth medium were then induced to overexpress PLK4 with 2 µg/ml doxycycline and the cells grown in medium growth medium were left untreated. 24 hours later, cells were plated into 40 T175 flasks at a density of $1x10^6$ cells per flask, per condition. Doxycycline (2 µg/ml) was again added to each flask grown in heavy growth medium. The following day, media was removed from the flask, cells were washed twice with PBS and then 15 ml of fresh EV depleted medium supplemented with the correct amino acids (heavy or medium) was added to the cells. 48 hours later, the conditioned medium was harvested from the cells and pooled together. Additionally, a final cell count was performed to ensure that the same number of cells was present per condition. EVs were then isolated from the harvested cell culture medium using the ultracentrifugation protocol described in section 2.4.3.1. To further purify and separate the isolated $_s$EVs, SEC was then performed as described in section 2.4.3.2. Vesicles per ml were then quantified in each SEC fraction using ImageStream as described in section 2.4.4.1. Samples were then frozen at -80^{o}C prior to processing for mass spectrometry analysis. The whole experiment was then repeated using the reverse labelling, where cells grown in the medium labelled medium were induced with doxycycline and the heavy left untreated to replicate the experiment and account for any potential effects of the different labels.

2.8.5 Sample processing for mass spectrometry

Cells or extracellular vesicles were lysed in 8 M Urea dissolved on a rocker in 50 mM Ammonium bi-carbonate (ABC) (made up in deionised water, pH 8). Samples were then sonicated using a Diagenode Bioruptor sonicator at 4°C. Samples were sonicated at high power for 15 cycles of 30 seconds on and 30 seconds off. A reducing step was then performed by adding 1 M DTT to a final concentration of 10 mM for 20 minutes at room temperature. Next an alkylating step was performed by adding 550 mM Iodoacetamide to a final concentration of 55 mM incubated for 30 minutes in the dark. Samples were then centrifuged using a tabletop centrifuge at full speed to remove debris. Protein quantification was then performed as previously described. 15 µg of protein was then selected per sample for the label incorporation tests. Urea was then diluted out of the sample from 8 M to 2 M final concentration using 50 mM ABC. Digestion of the sample was then performed by incubating the sample with 0.1 µg of trypsin per µg of protein for 16-18 hours at room temperature. Digestion was then stopped by acidifying the sample using equal amounts of the STOP 5 buffer and sample. Additionally, 2% Acetonitrile (ACN) was added to the sample to enable sample binding to the filter for stagetipping. It was then ensured that the sample has a pH of less than 2. The sample is then cleaned up and desalted using a stagetipping approach. Stage tips were generated using 200 µl pipette tips (no filter) as the column. Then 3 layers of C18 were cut out using a plunger and then plunged into the bottom of the 200 µl tip. The filter was plunged gently and as far as possible to pack the filter down. Stagetips were then added to 2 ml collection tubes with a custom-made black holder added to the opening to hold stagetips in place. Optimally packed tips elute 200 µl in 3 minutes at 2000 x g and so stagetips were tested for this capability prior to use. To activate the filter, 100 µl of methanol was added to each stagetip. The stagetips were then centrifuged at 2000 x g for 3 minutes at room temperature to pass the methanol through the filter. Next 200 µl of buffer A* was added and the stage tips centrifuged as before. Once the flow through had been discarded the last step was repeated. The sample was then loaded onto the stage tip and centrifuged at 500 x g for 3 minutes at room temperature. 200 µl of buffer A was then added to the stage tip and centrifuged at 2000 x g for 3 minutes at room temperature. Stage tips were then transferred into RNase free micro-centrifuge collection tubes with Mass spectrometry (Mass spec) collection tubes placed inside,

ensuring that the stagetip tip was placed inside the Mass spec tube. 20 µl of the elution buffer, buffer B was then added to each stage tip. The stagetips were then centrifuged at 500 x g for 3 minutes. This step was then repeated resulting in the eluted peptides being present in 40 µl of buffer B. Peptides were then dried using a speed vac. Finally, the peptides were resuspended in 10 µl of buffer A*. Mass spec and subsequent analysis was performed by our collaborator Dr Faraz Mardakheh.

2.9 Statistical analysis

Graphs and statistics were generated using Prism 8 (GraphPad Software) where results are presented as mean ± standard deviation (SD) unless otherwise stated. Statistical analysis was performed using one-way ANOVA with Tukey's post hoc test unless otherwise stated. Significance is equal to *p<0.1, **p<0.01, ***p<0.001 and ***P<0.0001.

Chapter 3

Results I:

Centrosome amplification induces small extracellular vesicle secretion in pancreatic adenocarcinoma cell lines

3.1 Centrosome amplification in pancreatic cancer cell lines

Pancreatic ductal adenocarcinoma (PDAC) is one of the most lethal malignancies with a less than 2% 5 year survival rate (Siegel, Miller and Jemal, 2019). Currently surgical resection is the most successful treatment option, however upon diagnosis only 15-20% of patients are suitable for this potentially curative surgery (Kim, Ahmed and Hsueh, 2011). For patients where surgical resection is not an option, chemotherapy can be administered. However, current chemotherapeutics for PDAC patients offer limited responses and life expectancy in these patients is extended by mere months (Burris *et al.*, 1997; Berlin *et al.*, 2000; Conroy *et al.*, 2011; Vaccaro, Sperduti and Milella, 2011). Thus, there is an urgent need for further research into the development and progression of pancreatic cancer in the hopes of developing novel and more successful treatment options.

A study performed by Sato and colleagues (Sato *et al.*, 1999) identified centrosome amplification in ~85% of analysed pancreatic tumours. Therefore, understanding the role of centrosome amplification in the development of pancreatic cancer could lead to the identification of novel targets for new cancer therapeutics. Interestingly in our most recent publication (Arnandis *et al.*, 2018) we showed that cells with supernumerary centrosomes secrete an increased number of proteins associated with the extracellular compartment. In particular these proteins were found to be associated with extracellular vesicles (EVs), and more specifically, exosomes. Thus, we hypothesised that pancreatic cancer cells with extra centrosomes may secrete more EVs. Additionally, as exosomes have been shown to play roles in tumourigenesis (reviewed in Wortzel *et al.*, 2019), we speculated that an increase in EV secretion may contribute to the progression and spread of pancreatic cancer.

To investigate if pancreatic cancer cells with amplified centrosomes secrete more EVs, we first assessed centrosome amplification in a panel of 12 PDAC cell lines: PaTu-T, Capan-1, PANC-1, CFPAC-1, Hs766T, BxCP3, AsPC-1, Capan-2, Panc 04.03, PaTu-S, HPAF-II and MIA PaCa-2, and two immortalised cell lines generated from normal pancreas: HPDE and DEC hTERT. Cells were grown on glass coverslips for 48 hours before being fixed and labelled with antibodies directed against microtubules (α-tubulin) and centrioles (centrin). DNA was stained with Hoechst dye.

Using 2D immunofluorescence microscopy the percentage of cells with either normal or amplified centrosome number was quantified. Since centrosome number changes throughout the cell cycle, centrosome amplification was quantified specifically during metaphase (as evidenced by the presence of the mitotic spindle). During normal cell division, cells in metaphase have one centrosome (2 centrioles) present at each pole of the bipolar mitotic spindle (Figure 3.1.1 left panel). Cells with more than two centrosomes either in a pseudo-bipolar or multipolar spindle formation are considered to have amplified centrosomes (Figure 3.1.1 middle and right panels respectively).

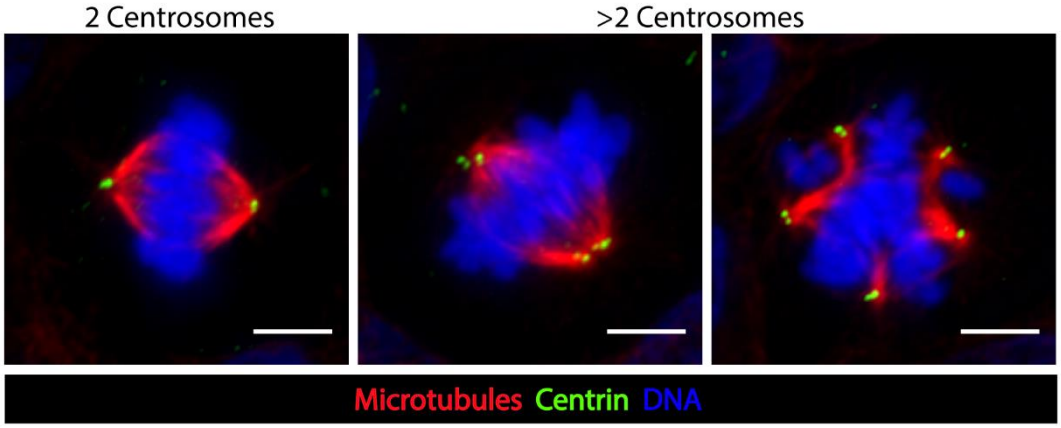

Figure 3.1.1 Representative images of cells in metaphase with normal or amplified centrosomes. Immunofluorescent staining of microtubules and centrioles in metaphase cells. Representative images of cells undergoing bipolar cell division (left), clustered pseudo bipolar division (middle) and multipolar cell division (right). Cells stained with centrin (green), α-tubulin (red) and DNA in Hoechst (blue). Cells are HPAF-II, scale bar represents 5μm.

Centrosome amplification levels are stratified in the current literature, where > 30% centrosome amplification is considered high and < 10% is considered low (Lopes *et al.*, 2018; Rhys *et al.*, 2018) . As expected, centrosome amplification was found to be low (<3%) in the pancreatic control cell lines HPDE and DEC-hTERT. The levels of centrosome amplification varied across the panel of PDAC cell lines (Figure 3.1.2), however, with 4 cell lines exhibiting particularly high levels of centrosome amplification (>30% of cells): PaTu-T, Capan-1, Panc-1 and CFPAC-1. In contrast, 3 cell lines emerged as having particularly low centrosome amplification (<7% of cells): PaTu-S, HPAF-II and MIA-PaCa-2. These 9 cell lines harbouring particularly high or low percentages of cells containing

centrosome amplification were selected to investigate the secretion of vesicles from pancreatic cells in relation to centrosome amplification.

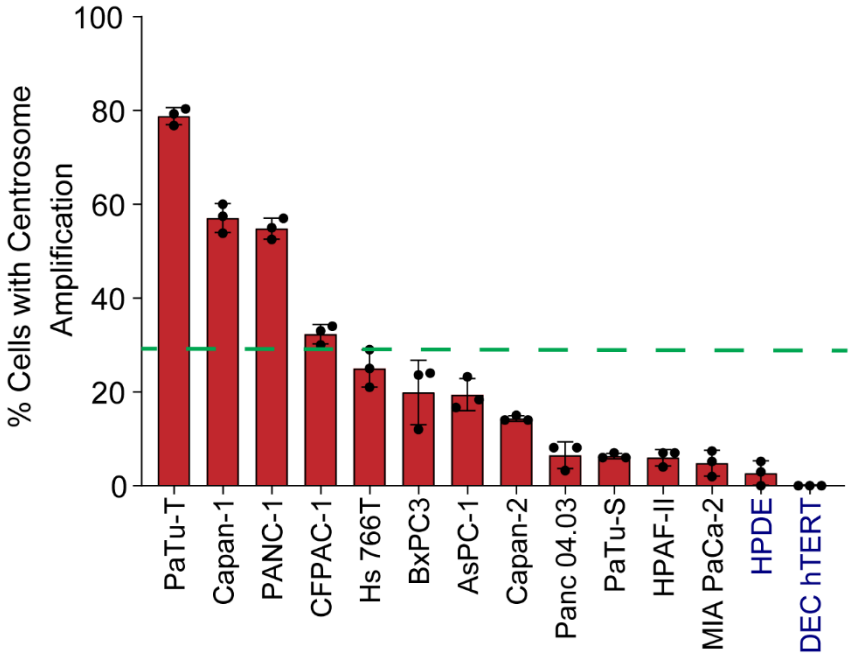

Figure 3.1.2 Quantification of centrosome amplification in PDAC cell lines. Average percentage of cells with amplified centrosomes in a panel of pancreatic cell lines. Total centrosome amplification (clustered and multipolar) was assessed in 12 pancreatic cancer cell lines (Black text) and 2 pancreatic control cell lines (Blue text). The dashed line represents 30% centrosome amplification. Centrosome amplification above this threshold is considered high. Error bars represent mean ± standard deviation (n=3).

3.2 Extraction of extracellular vesicles.

3.2.1 Isolation and quantification of extracellular vesicles from cell culture medium

Extracellular vesicles (EVs) including larger microvesicles (100-1000nm) and smaller exosomes (30-150nm) are secreted by cells into the extracellular space. In cultured cells, the secreted EVs can be isolated from the cell culture medium. As these two types of EVs somewhat differ in size/buoyant density (size of particle and density of cargo), we can crudely isolate the two populations based on their sedimentation rate using a serial ultracentrifugation protocol similar to that used by Costa-Silva *et al.*, 2015 (Figure 3.2.1.1 A). Initially, the cell culture medium is removed from cells and subjected to a low

speed centrifugation (500 x g for 10 minutes) to remove cell debris and apoptotic bodies from the supernatant. The supernatant is then centrifuged at 12,000 x g for 20 minutes to pellet the large EVs ($_{L}$EVs) which in theory should be >200nm in size (Théry *et al.*, 2018) and therefore likely to be microvesicles. The subsequent supernatant is then subjected to high speed ultracentrifugation (100,000 x g for 70 mins) to pellet the smaller EVs ($_{s}$EVs), which should be <200nm in size (Théry *et al.*, 2018) and thus enriched in exosomes. Non-EV contaminants are removed with a wash step and subsequent high speed ultracentrifugation (Théry *et al.*, 2006). Although this wash step is known to decrease EV yield it is important for increasing the purity of the EV pellet (Webber and Clayton, 2013). Finally, the isolated EV pellet is re-suspended in PBS for further analysis. Two parameters for ultracentrifugation are particularly important to ensure good separation of the vesicles. Duration of the ultracentrifugation is vital, as increasing the time of the spin will increase the presence of impurities in the pellet (Van Deun *et al.*, 2014). Ultracentrifugation speed is also critical as increasing the speed will elevate the formation of EV aggregates. Although re-suspension in PBS can separate most of the aggregates, the presence of residual EV aggregates may interfere with downstream analysis (Théry *et al.*, 2006).

To validate the serial ultracentrifugation protocol for isolation of EVs, we isolated $_{L}$EVs and $_{s}$EVs from the PDAC cell line PaTu-T. Cells were grown in vesicle-depleted media (see section 3.2.2) before the culture medium was removed and EVs were isolated. The size distribution of vesicles in each pellet was quantified by nanoparticle tracking analysis (NTA) using the NanoSight NS300. Analysis using the NTA 3.2 analysis software demonstrated that the $_{L}$EVs population had a mean size of 290.9 nm and a mode size of 158.7 nm, whereas the $_{s}$EV population had a mean size of 141.6 nm and a mode size of 113.3 nm (Figure.3.2.1.1 B). This analysis confirmed that the two populations were within the correct average size range to be considered large and small EVs respectively. As there is an overlap in the size of microvesicles (100-1000 nm) and exosomes (30-150 nm), size alone cannot distinguish the two vesicle types. However, the observed size ranges suggest an enrichment of microvesicles in the $_{L}$EV pellet and enrichment of exosomes in the $_{s}$EV pellet.

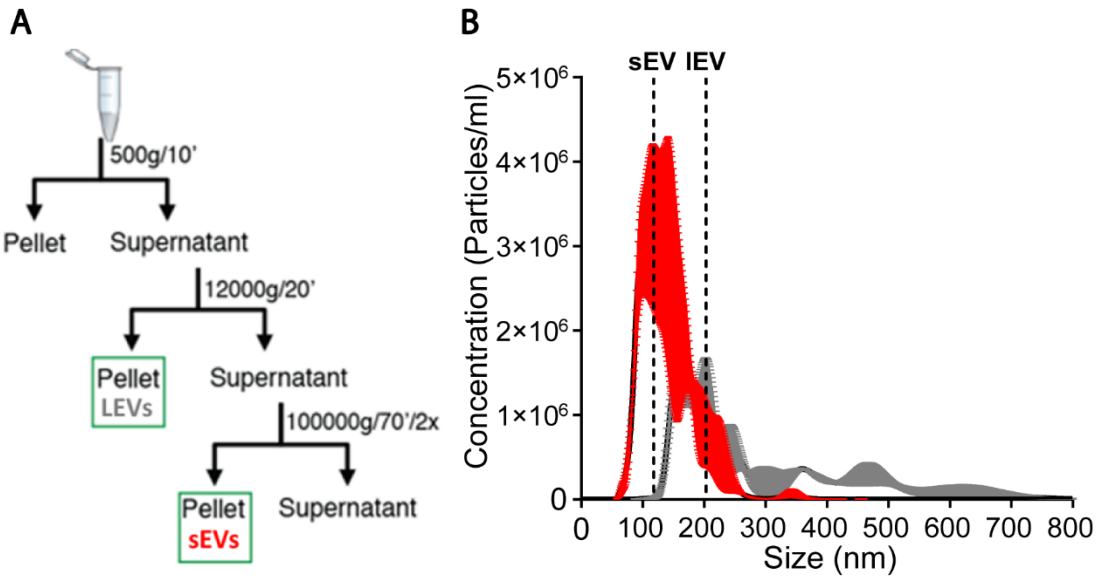

Figure 3.2.1.1 Extracellular vesicle isolation by ultracentrifugation and particle size distribution quantification by Nanosight NS300. A) Schematic of the serial ultracentrifugation protocol for isolation of Large EVs and Small EVs. **B)** Size distribution curves determined by Nanosight NS300 (Nano-particle tracking analysis) of $_{L}$EVs and $_{s}$EV isolates. $_{L}$EV isolates have a mean size of 290.9nm and a mode size of 158.7nm (grey distribution) whereas $_{s}$EV isolates have a mean size of 141.6nm and a mode size of 113.3nm (red distribution). Dotted line indicates the mode size of each EV population. Error bars (shown in red for $_{s}$EVs and grey for $_{L}$EVs) indicate standard error of the mean.

An Amnis ImageStream® Mark II Imaging Flow Cytometer (ImageStream) was used to quantify the number of EVs present in each pellet. Traditionally, NTA has been considered the gold standard for quantification of EV number and EV size. However, whilst the ImageStream does not have the capacity to quantify EV size, it offers certain advantages for the quantification of EV number. Unlike ImageStream, classical NTA is likely to over-estimate EV counts as the technique is not specific to EVs and analyses all particles regardless of their composition (reviewed in Théry *et al.*, 2018). The ImageStream, however, enables quantification of particles specifically containing lipids by virtue of fluorescent labelling, in this case using the lipid dye BODIPY-Maleimide. It should be noted that the ImageStream may underestimate vesicle numbers as vesicles smaller than 20nm may be below the fluorescence threshold (Headland *et al.*, 2014). The ImageStream calculates a BODIPY intensity value and side scatter value for each particle, and a graph of BODIPY intensity against side scatter intensity can be plotted. Extracellular vesicles are predicted to have low side scatter and mid to low BODIPY fluorescence distinguishing them from other particles and thus can be gated as shown

in Figure 3.2.1.2 A. Speed beads are used to internally calibrate the machine but can be excluded from the gating region as they have high side scatter and low BODIPY intensity. Contaminating cells and cell debris can also be removed from the gating region as they have high side scatter and high BODIPY intensities (See Figure 3.2.1.2 A)(Headland *et al.*, 2014). The ImageStream also provides an image gallery of all objects that pass through the stream permitting confirmation that the particles within the gated region are small and spherical, indicative of vesicles (representative images shown in Figure 3.2.1.2 B). We have therefore opted to use ImageStream to quantify vesicle number and NTA to quantify vesicle size.

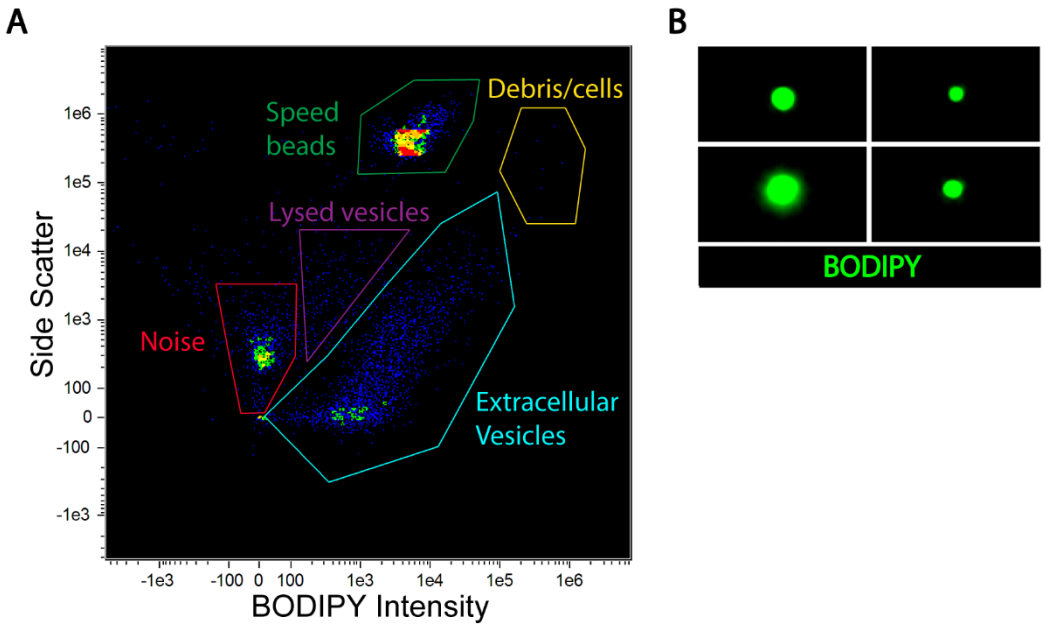

Figure 3.2.1.2 Extracellular vesicle quantification by Nanosight NS300 and Amnis ImageStream® Mark II Imaging Flow Cytometer. A) Example graph from the Amnis ImageStream, displaying side scatter plotted against BODIPY intensity. Representative gating regions are shown. Gating region for extracellular vesicles (in blue) at low side scatter and mid to low BODIPY intensity. Gating region for contaminating cells and cell debris (yellow) at high side scatter and high BODIPY. Gating region for speed beads (green) used to internally calibrate the ImageStream at high side scatter and low BODIPY. Gating region for lysed vesicles (purple) at low side scatter and low BODIPY **B)** Representative images of particles taken from the ImageStream image gallery that are present in the extracellular vesicles gating region, showing small spherical vesicles. Vesicles are labelled with BODIPY-Maleimide (green).

3.2.2 Depletion of extracellular vesicles from foetal bovine serum

Foetal bovine serum (FBS) which is used to supplement cell growth media contains a large number of bovine extracellular vesicles that may affect the quantitative and qualitative analyses of EVs secreted by cultured cells. Therefore, depletion of

contaminating EVs from the FBS prior to use in cell culture is crucial. Ultracentrifugation is used to remove bovine EVs from the FBS. During this process, the duration of the ultracentrifugation was found to be critical and had to be optimised for FBS from different providers. We tested vesicle depletion in both Gibco FBS (non-tetracycline screened) and GE Healthcare (tetracycline Screened) FBS which are used throughout this thesis. Post ultracentrifugation, the FBS was added to DMEM to a final concentration of 10% and the residual bovine vesicles present in this media were quantified (Figure 3.2.2). Two hours of ultracentrifugation was sufficient to deplete Gibco FBS of contaminating EVs (from a mean of ~1.3 $x10^8$ to ~3.8 $x10^7$ objects/ml), however, GE Healthcare FBS required ultracentrifugation for 18 hours to deplete EVs to acceptable levels (from a mean of ~7.1 $x10^8$ to ~2.8 $x10^7$ objects/ml).

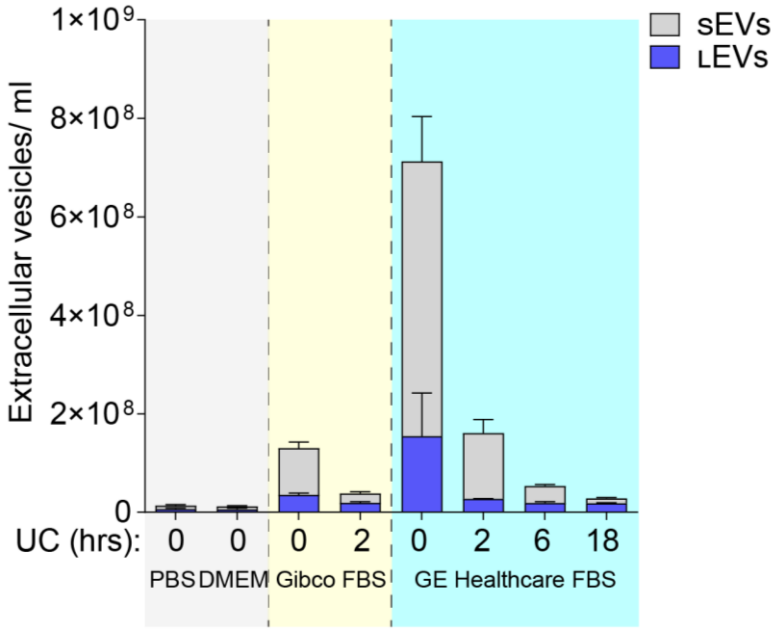

Figure 3.2.2 Optimisation of vesicle depletion in foetal bovine serum (FBS). Gibco (non-tetracycline screened) or GE Healthcare (tetracycline screened) FBS was ultracentrifuged at 100,000 x g for 0, 2, 6 or 18 hours to deplete bovine EVs. Following the addition of vesicle-depleted FBS to DMEM, residual vesicles ($_L$EVs and $_s$EVs) present in the media were isolated by ultracentrifugation and quantified by ImageStream. Error bars represent mean ± standard deviation (n=3).

3.3 Extracellular vesicle secretion in pancreatic cancer and pancreatic control cell lines

3.3.1 Pancreatic cancer cells with supernumerary centrosomes secrete more small extracellular vesicles

As previously shown in Figure 3.1 B, centrosome amplification levels vary between pancreatic cell lines. To investigate if pancreatic cell lines with amplified centrosomes secrete more EVs, $_{L}$EVs and $_{s}$EVs were isolated from the following pancreatic cell lines:

i) PaTu-T, Capan-1, Panc-1 and CFPAC-1 (PDAC cell lines with high centrosome amplification),

ii) PaTu-S, HPAF-II, MIA-PaCa-2 (PDAC cell lines with low centrosome amplification),

iii) HPDE, DEC-hTERT (pancreatic control cell lines which harbour low levels of centrosome amplification).

Cells were grown in vesicle-depleted media for 48 hours ensuring that at the 48-hour time point all cell lines had the same final cell count of ~$6x10^6$ cells/ml. The conditioned media was then harvested and EVs were isolated using serial ultracentrifugation. Quantification of the isolated vesicles showed an increased presence of $_{s}$EVs and $_{L}$EVs in the media of cells with extra centrosomes compared to cells with little or no centrosome amplification (Figure 3.3.1 A). Further analysis of these results revealed a strong significant correlation between $_{s}$EVs secretion and centrosome amplification where rSpearman=0.6863, compared to $_{L}$EV secretion and centrosome amplification where rSpearman = 0.2971 (Figure 3.3.1 B). These results demonstrate a robust correlation between centrosome amplification and the secretion of $_{s}$EVs, potentially indicating increased exosome secretion in cells with extra centrosomes. This result, however, is purely correlative and does not in itself indicate causation, prompting further analysis into whether centrosome amplification is sufficient to induce EV secretion in pancreatic cancer cell lines.

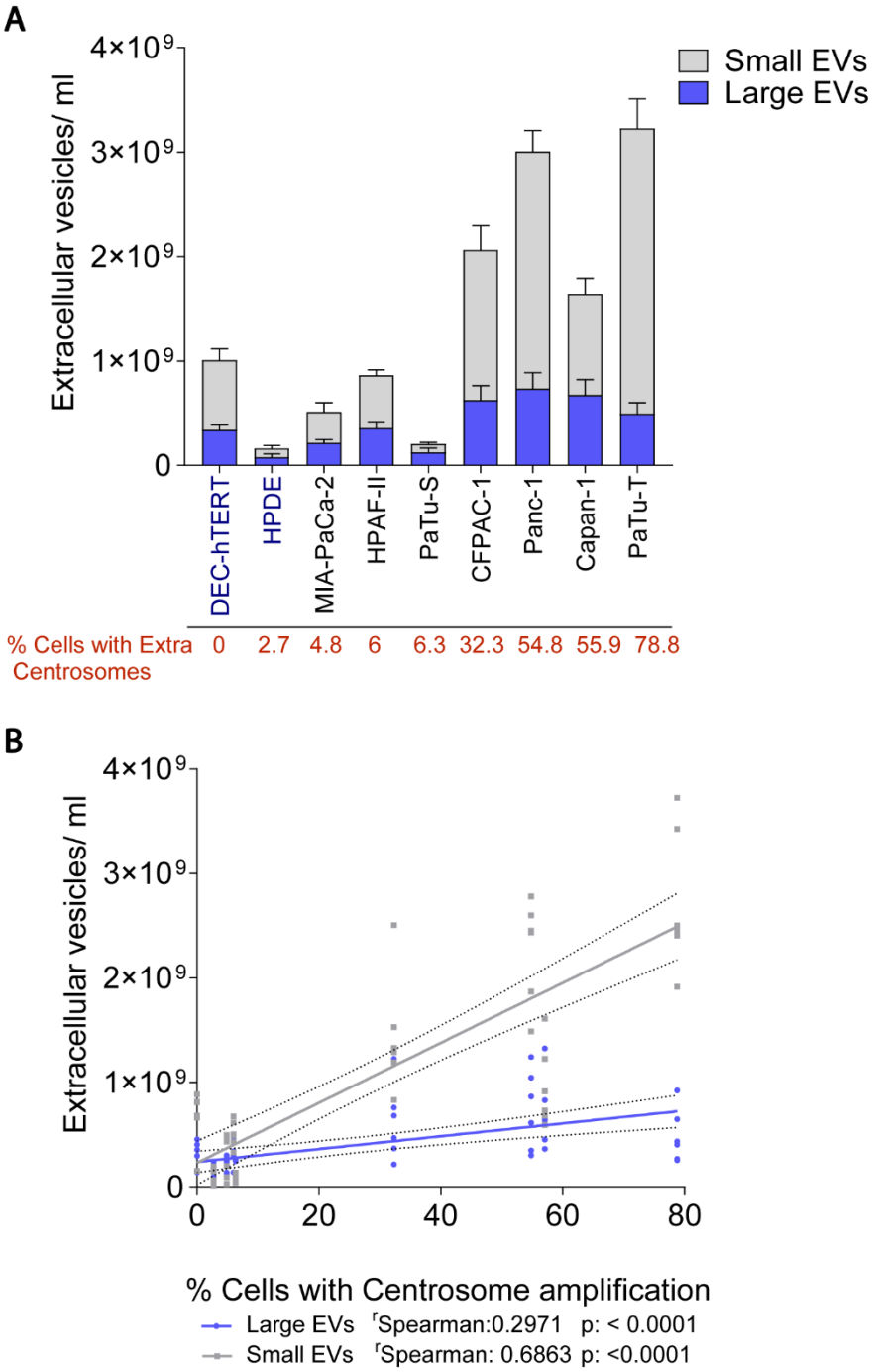

Figure 3.3.1 Extracellular vesicle secretion in pancreatic cells. A) Quantification of $_{L}$EVs and $_{s}$EVs secreted by pancreatic cancer cells (black text) and immortalised pancreatic cells (blue text) with high and low centrosome amplification. Error bars represent mean ± standard deviation (n=6). **B)** Linear regression graph of the data present in A and Spearman correlation coefficients (^{r}Spearman) showing a correlation between $_{L}$EVs (blue) or $_{s}$EV (grey) secretion in relation to centrosome amplification. Significant correlation is observed between both $_{L}$EVs and $_{s}$EV secretion and increased centrosome amplification ($_{L}$EVs ^{r}Spearman = 0.2971, $_{s}$EV ^{r}Spearman =0.6863 and p< 0.0001). Dashed lines = confidence intervals.

3.3.2 Small extracellular vesicle isolates contain canonical extracellular vesicle protein markers

To further validate the presence of EVs in our $_s$EV preparations we analysed the $_s$EV isolates for the presence of the canonical EV protein markers CD63, CD81 and flotillin. As expected, western blot analysis showed the $_s$EV pellet to be enriched in these EV protein markers compared to the cell lysate (Figure 3.3.2). To date, it is not possible to conclusively distinguish different types of extracellular vesicles by the presence of specific protein markers (Théry *et al.*, 2018). However, the presence of certain protein markers may indicate which biogenesis pathway the majority of the EVs in the sample originate from. Vesicles in the $_s$EV pellet were enriched in the endosomal sorting complex responsible for transport (ESCRT) machinery component TSG101 and ESCRT associated protein ALIX (Figure 3.3.2). The presence of these proteins may indicate that the vesicles originate from the endocytic compartment and are therefore likely to be exosomes. It should be noted however, that to date the only way to specifically determine the origin of an EV is through live cell imaging and tracking of the vesicles (Théry *et al.*, 2018).

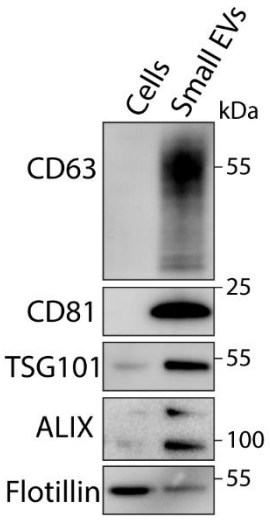

Figure 3.3.2 Western blot analysis of $_s$EVs lysates and total cell lysates from PaTu-T cells. The preparations were probed for EV/Exosomal protein markers using antibodies directed against CD63, CD81, TSG101 and ALIX and flotillin.

3.4 Transient overexpression of PLK4 results in centrosome amplification in PaTu-S and HPAF-II cell lines

Our data thus far suggest that cells with supernumerary centrosomes secrete more $_{s}$EVs, however, it is unclear whether centrosome amplification itself is sufficient to induce $_{s}$EV secretion, or if increased $_{s}$EV secretion is simply a result of other undefined cellular changes. To further explore this, we investigated whether the induction of centrosome amplification in cell lines that naturally harbour low levels of centrosome amplification would lead to increased $_{s}$EV secretion.

To generate supernumerary centrosomes, a previously established method was used whereby centrosome amplification can be achieved through transient overexpression of PLK4 (Godinho *et al.*, 2014), the master regulator of centriole duplication (Bettencourt-Dias *et al.*, 2005; Habedanck *et al.*, 2005; Kleylein-Sohn *et al.*, 2007; Basto *et al.*, 2008). PLK4 overexpression is controlled by the presence of a tetracycline repressor (TetR) which binds to the CMV/TO promoter inhibiting the expression of PLK4. The addition of doxycycline hyclate (DOX) supresses the tetracycline repressor allowing PLK4 overexpression and the subsequent induction of centrosome amplification.

We selected two PDAC cell lines which naturally harbour low levels of centrosome amplification (<7% of cells), PaTu-S and HPAF-II and transduced them with a tetracycline repressor using lentivirus. These cells were then subsequently transduced with lentivirus harbouring inducible PLK4, generating two cell lines, PaTu-S TetR PLK4 (henceforth referred to as PaTu-S.PLK4) and HPAF-II TetR PLK4 (hence forth referred to as HPAF-II.PLK4) in which centrosome amplification can be induced upon the addition of DOX. To generate extra centrosomes, DOX was added to the newly generated cell lines for 48 hours to ensure that sufficient time had passed for centrosome over duplication and subsequent maturation to occur (Godinho *et al.*, 2014) (Figure 3.4 A).

PLK4 overexpression for 48 hours in PaTu-S.PLK4 and HPAF-II.PLK4 cells upon the addition of DOX led to significantly increased centrosome amplification in both cell lines (Figure 3.4 B/C). With centrosome amplification increasing from average 26% to 92% in PaTu-S.PLK4 and from average 18% to 81% in HPAF-II.PLK4. It should be noted that even in the absence of DOX, both PLK4 inducible cell lines have higher centrosome

amplification than their parental cell lines (PaTu-S and HPAF-II). We attribute this observation to the TetR PLK4 system being "leaky" and resulting in low levels of recombinant PLK4 expression. However, the increase in centrosome amplification upon the induction of DOX is highly significant making these cell lines suitable for further study.

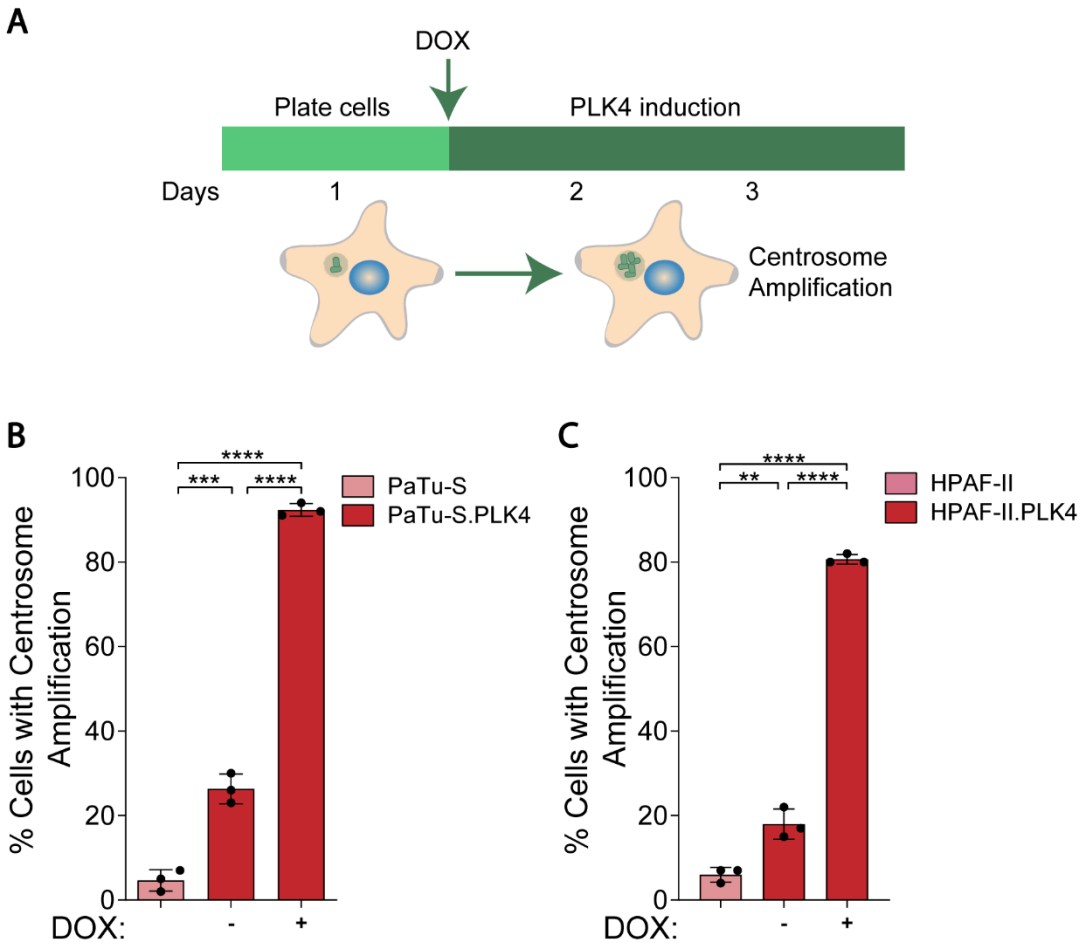

Figure 3.4 Centrosome amplification upon PLK4 overexpression in PaTu-S and HPAF-II cells. A) Schematic diagram illustrating method for inducing extra centrosomes via transient overexpression of PLK4. PLK4 overexpression is induced for 48 hours following the addition of DOX, resulting in cells with extra centrosomes. **B)** Centrosome amplification in PaTu-S.PLK4 cells treated with (+) and without (-) DOX and the parental PaTu-S cell line (no treatment). **C)** Centrosome amplification in HPAF-II.PLK4 cells treated with (+) and without (-) DOX and the parental HPAF-II cell line (no treatment). Error bars represent mean ± standard deviation (n=3, 300 cells). Data analysed using one-way ANOVA with Tukey's post hoc test (**** $p<0.0001$ *** $p<0.001$,** $p<0.01$). DOX=doxycycline hyclate.

3.5 Small extracellular vesicle secretion is elevated upon induction of centrosome amplification

To investigate whether centrosome amplification induces EV secretion in pancreatic cancer cell lines, we analysed EV secretion in the newly generated PaTu-S.PLK4 and HPAF-II.PLK4 cells with and without the induction of extra centrosomes. PaTu-S.PLK4 and HPAF-II.PLK4 cells were induced with DOX for 48 hours before the conditioned media was removed, the cells were washed and fresh vesicle-depleted media (see Figure 3.2.2) was added. Cells were subsequently cultured for 48 hours before the conditioned media was collected and secreted EVs were isolated and quantified.

A significant increase in the secretion of $_{s}$EVs was observed following induction of centrosome amplification in both PaTu-S.PLK4 (from a mean of ~2.8 x10^8 to ~5.6 x10^8 objects/ml) and HPAF-II.PLK4 cells (from a mean of ~8 x10^8 to ~1.9 x10^9 objects/ml) (Figure 3.5). However, no significant difference was observed in $_{L}$EVs secretion upon induction of centrosome amplification in either cell line. This result reflects the data shown in Figure 3.3 where a strong correlation was only observed between centrosome amplification and $_{s}$EV secretion in the panel of pancreatic cell lines. Thus, it appears that the induction of centrosome amplification preferentially increases the secretion of $_{s}$EVs.

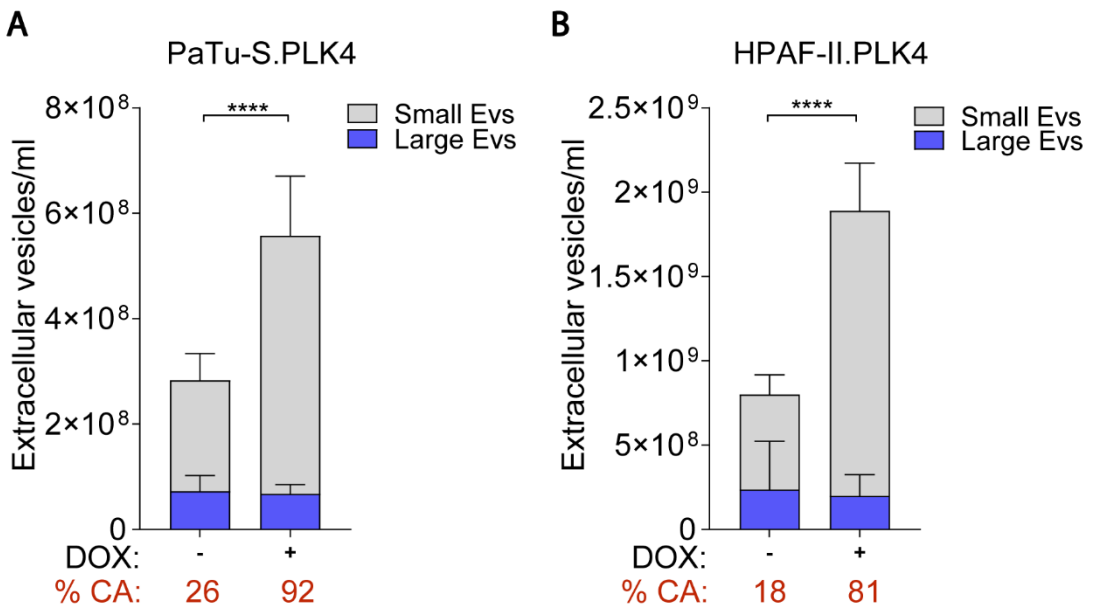

Figure 3.5 Extracellular vesicle secretion upon induction of centrosome amplification in PaTu-S.PLK4 and HPAF-II.PLK4 cells. A) Secretion of $_{L}$EVs and $_{s}$EVs from PaTu-S.PLK4 with (+DOX) and without (-DOX) the induction of centrosome amplification. **B)** Secretion of $_{L}$EVs and $_{s}$EVs from HPAF-II.PLK4 with (+DOX) and without (-DOX) the induction of centrosome amplification. Levels of centrosome amplification (%CA) are indicated in red. Error bars represent mean ± standard deviation (n=6). Data analysed using two-way ANOVA with Tukey's post hoc test (**** $p<0.0001$). Significance relates to $_{s}$EVs secretion only. No significant difference was observed in $_{L}$EVs secretion between conditions (DOX=doxycycline hyclate, %CA = % cells with centrosome amplification).

3.6 In the absence of centrosome amplification, PLK4 overexpression is not sufficient to induce extracellular vesicle secretion

To ensure that the increase in $_{s}$EV secretion observed upon induction of centrosome amplification in PaTu-S.PLK4 and HPAF-II.PLK4 is attributed to centrosome amplification alone and is not an artefact of the induction method, we controlled for unspecific affects caused by the addition of DOX and the overexpression of PLK4.

Previous studies have shown the centrosomal protein SAS-6 to be necessary for centriole duplication, and so depletion of SAS-6 has been shown to hamper the amplification of centrosomes induced by PLK4 overexpression (Arnandis *et al.*, 2018). Therefore, in order to analyse the effect of PLK4 overexpression on EV secretion in the

absence of centrosome amplification we performed siRNA mediated SAS-6 knockdown whilst inducing PLK4 overexpression with DOX.

As expected, quantification of centrosome amplification following siRNA knockdown of SAS-6 (siSAS-6) in PaTu-S.PLK4 and HPAF-II.PLK4 treated with DOX, resulted in significantly lower centrosome amplification levels compared to cells treated with the siRNA control (siCntrl) and DOX (Figure 3.6.1 A/B). SAS-6 depletion in HPAF-II.PLK4 cells +DOX resulted in levels of centrosome amplification that were similar to the untreated control cells, however, SAS-6 depletion in PaTu-S.PLK4 cells +DOX resulted in centrosome amplification levels that were significantly lower than the untreated control cells. Centriole number was therefore quantified to ensure that SAS-6 depletion did not cause high levels of centrosome loss in cells overexpressing PLK4. Quantification of centriole number revealed that SAS-6 depletion in PLK4 overexpressing cells leads to a relatively small percentage of metaphase cells containing less than three centrioles (Figure 3.6.1 C/D), 35% in PaTu-S.PLK4 cells and 28% in HPAF-II.PLK4 cells. As SAS-6 is important for centriole duplication, it is possible that these results arise as a consequence of SAS-6 depletion in cells that do not have amplified centrosomes, thus preventing centriole duplication in these cells and leading to the observed centriole losses. Despite these low levels of centrosome loss, most cells in both cell lines contained normal centriole numbers and were able to form a bipolar metaphase plate with either 3 or 4 centrioles present at each pole. These conditions were therefore used for further analysis.

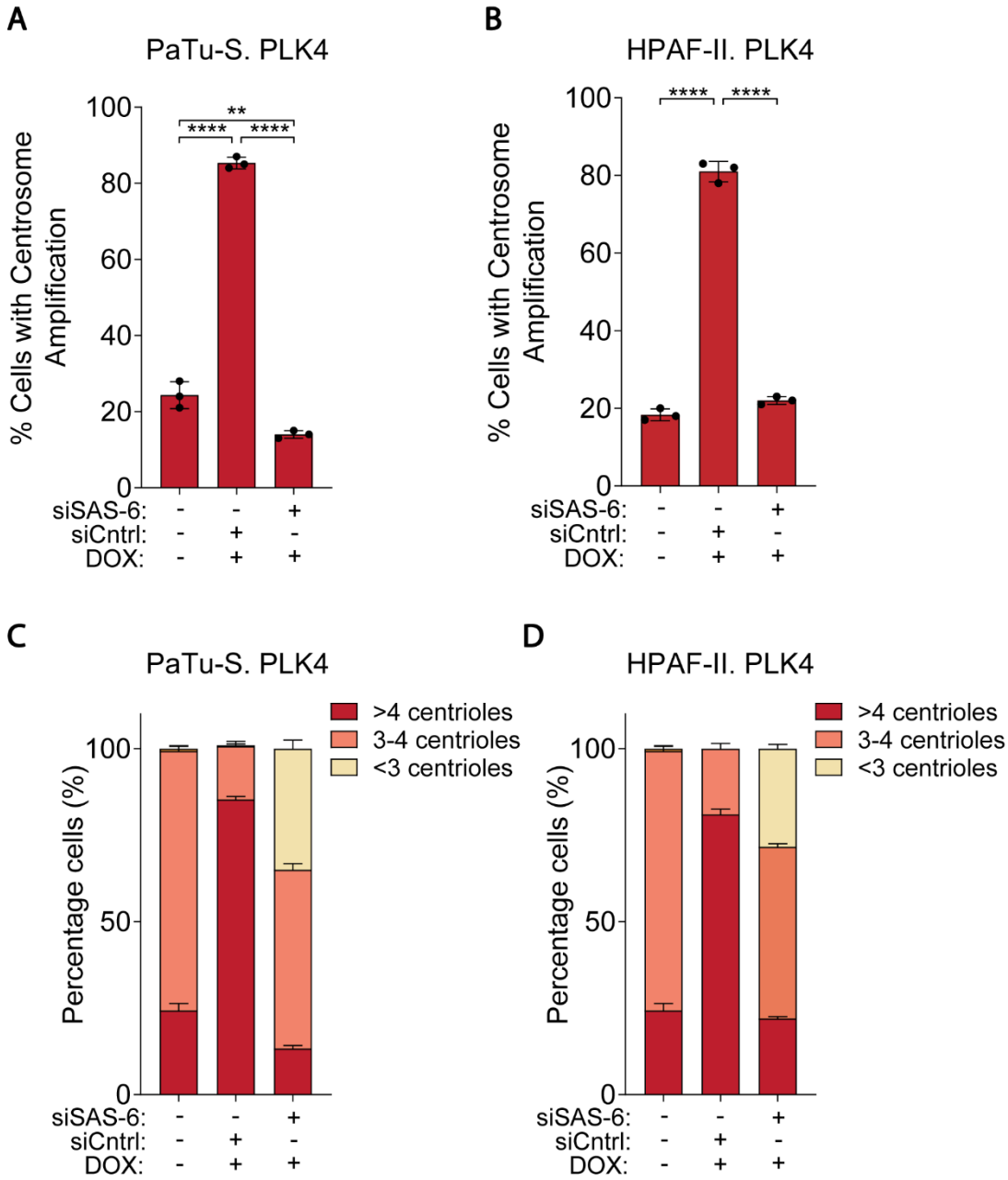

Figure 3.6.1 Centrosome amplification upon siRNA depletion of centrosomal protein SAS-6 in the presence of PLK4 overexpression. A) Quantification of the percentage of cells with centrosome amplification in PaTu-S.PLK4 cells untreated, or treated with DOX and siCntrl or DOX and siSAS-6. **B)** Quantification of the percentage of cells with centrosome amplification in HPAF-II.PLK4 cells untreated, or treated with DOX and siCntrl or DOX and siSAS-6. **C)** Quantification of the percentage cells with >4, 3-4 or <3 centrioles in PaTu-S.PLK4 cells untreated, or treated with DOX and siCntrl or DOX and siSAS-6. **D)** Quantification of the percentage cells with >4, 3-4 or <3 centrioles in HPAF-II.PLK4 cells untreated, or treated with DOX and siCntrl or DOX and siSAS-6. Error bars represent mean ± standard deviation (n=3, 300 cells). Data analysed using one-way ANOVA with Tukey's post hoc test (**** $p<0.0001$, ** $p<0.01$). DOX=doxycycline hyclate.

Extracellular vesicles were then harvested from the conditioned medium of cells treated in the same manner as above. It was found that, following SAS-6 depletion, $_{S}$EVs secretion is greatly decreased compared to the siCntrl treated cells, despite DOX treatment and over expression of PLK4 in both PaTu-S.PLK4 and HPAF-II.PLK4 cells (Figure 3.6.2). No significant difference was observed in $_{L}$EV secretion between conditions. These results indicate that the increased $_{S}$EV secretion observed upon the induction of centrosome amplification is not an artefact of PLK4 overexpression or DOX treatment but is instead due to the increased presence of extra centrosomes.

Taken together, these results indicate that centrosome amplification is sufficient to induce $_{S}$EV secretion in pancreatic cancer cells. In contrast, $_{L}$EV secretion remains largely unchanged following induction of supernumerary centrosomes.

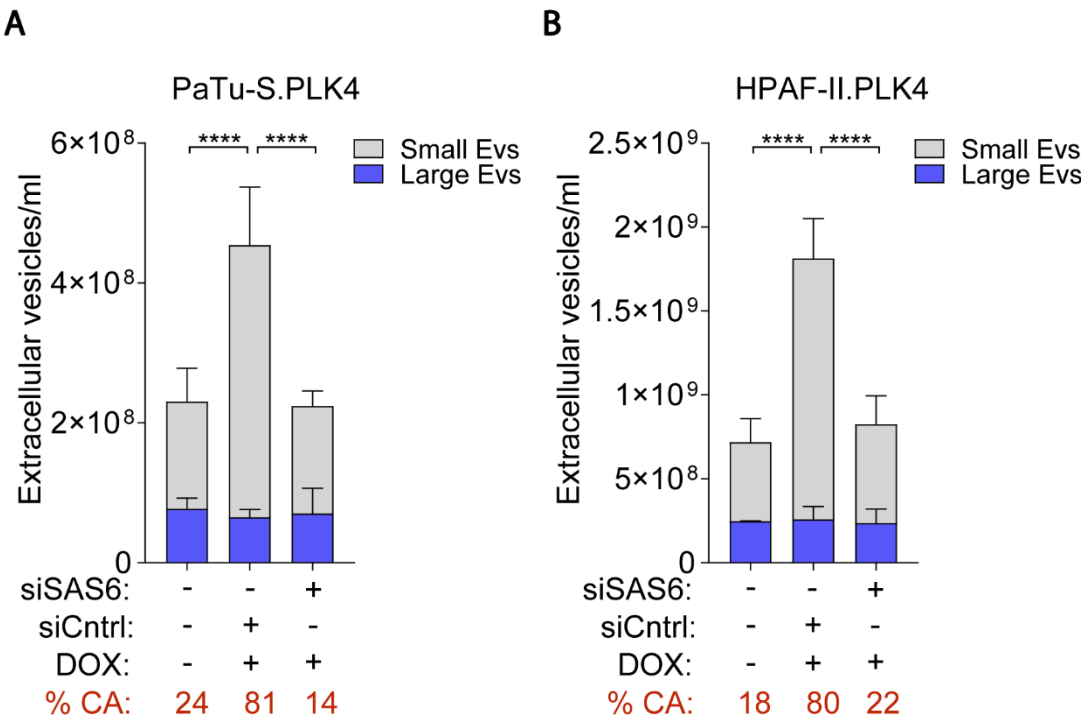

Figure 3.6.2 Extracellular vesicle secretion upon siRNA depletion of SAS-6 in the presence of PLK4 overexpression. A) Quantification of $_{L}$EVs and $_{S}$EVs secreted by PaTu-S.PLK4 cells untreated, or treated with DOX and siCntrl or DOX and siSAS-6. **B)** Quantification of $_{L}$EVs and $_{S}$EVs secreted by HPAF-II.PLK4 cells untreated or treated with DOX and siCntrl or DOX and siSAS-6. Levels of centrosome amplification denoted in red. Error bars represent mean ± standard deviation (n=3). Data analysed using two-way ANOVA with Tukey's post hoc test (**** $p<0.0001$). Significance relates to $_{S}$EV secretion only. No significant difference was observed in $_{L}$EVs secretion between conditions. DOX=doxycycline hyclate, % CA= % cells with centrosome amplification.

3.7 Discussion

In recent years centrosome amplification has been shown to play an active role in tumourigenesis *in vivo* (Coelho *et al.*, 2015; Serçin *et al.*, 2015; Levine *et al.*, 2017). Since pancreatic tumours have been shown to harbour up to 85% of cells with centrosome amplification (Sato *et al.*, 1999), further research into the role of centrosome amplification in the initiation and progression of pancreatic cancer may reveal new targets for the development of novel therapeutic strategies.

Recent work from our laboratory (Arnandis *et al.*, 2018), demonstrated that cells with extra centrosomes secrete an increased number of proteins associated with EVs. We therefore hypothesised, that cells with amplified centrosomes secrete more EVs than cells that do not contain supernumerary centrosomes.

Here we show that centrosome amplification positively correlates with the secretion of $_{L}$EVs and $_{s}$EVs in pancreatic cancer cell lines. Moreover, using two different cell lines in which we can induce centrosome amplification through transient overexpression of PLK4, we have demonstrated that centrosome amplification induces the secretion of $_{s}$EVs in PDAC cells. However, no change was observed in the ability of either cell line to secrete $_{L}$EVs upon induction of centrosome amplification. Furthermore, we have shown that in the absence of centrosome amplification, DOX treatment and PLK4 overexpression do not result in increased EV secretion. Taken together these results suggest that centrosome amplification itself is sufficient to induce $_{s}$EV secretion in PDAC cell lines.

Throughout this chapter, vesicle isolation was performed using a serial ultracentrifugation protocol which separated EVs into $_{L}$EVs and $_{s}$EVs based on differences in buoyant densities (particle size and density of cargo). Although the classical ultracentrifugation protocol is still widely used, it is not without its drawbacks and the purity of the isolated vesicles has been questioned, leading to the development of new methods for EV isolation. In recent years, a modification to the ultracentrifugation protocol utilising a density gradient has emerged as a better method of EV isolation from cell culture medium (Abramowicz, Widlak and Pietrowska, 2016). The presence of a density gradient results in further separation of the EVs due to their specific buoyant densities. This method is now believed to yield EVs with a higher purity

compared to the classical ultracentrifugation protocol (Théry *et al.*, 2006; Webber and Clayton, 2013; Abramowicz, Widlak and Pietrowska, 2016). Size exclusion chromatography (SEC), where samples are passed through a column containing porous resin particles, has also emerged as an effective method of EV isolation and purification. Vesicles pass through the SEC column largely unimpeded due to their size, whereas impurities including small molecules and contaminating proteins enter the pores and elute much later. As such, SEC has been shown to yield high purity EVs (Böing *et al.*, 2014; Muller *et al.*, 2014; Welton *et al.*, 2015; Benedikter *et al.*, 2017). Although the work described in this chapter was carried out using the classical serial ultracentrifugation approach for EV isolation, an additional SEC purification step was included in subsequent work to improve EV purity where necessary (see chapter 5). Although it is not possible to definitively identify the type of EV present in the $_{s}$EV pellet, our work provides evidence to suggest that the pellet may be enriched in exosomes. Nano-particle tracking analysis showed that the $_{s}$EV pellets have a size distribution curve with a mode particle size of 113.3nm. This particle size is within the accepted size range for exosomes ie 30-150nm. Furthermore, the presence of the protein markers TSG101 and ALIX in the $_{s}$EV pellet may give insight into the biogenesis pathway from which these vesicles originate. Since both TSG101 and ALIX are associated with the ESCRT machinery and thus the endocytic pathway, it is likely that the $_{s}$EV pellet is enriched in exosomes. In addition, proteomic analysis recently published by our laboratory (Arnandis *et al.*, 2018) revealed that cells with extra centrosomes secrete a number of proteins specifically associated with exosomes. Taken together these results suggest that the vesicles isolated in the $_{s}$EV pellet are likely to be enriched exosomes, thus indicating that centrosome amplification likely results in the increased secretion of exosomes. Further evidence corroborating the identification of these vesicles is detailed in Chapter 5.

Interestingly, current literature in the extracellular vesicle field has indicated that EV secretion is increased in cancer cells and that EV proteins are elevated in the sera of cancer patients (Szczepanski *et al.*, 2011; Huang and Deng, 2019). However, it is not known if all cancer cells or a subset of cancer cells are responsible for this increased secretion. Our results suggest that, a subset of cancer cells, those harbouring amplified centrosomes, may contribute to the increase in EV protein secretion that has been observed in cancer patients. Since cancer-associated EVs, including exosomes, are

known to contribute to the progression and spread of cancers (reviewed in Wortzel *et al.*, 2019) our findings may have much wider implications and raise the following questions (i) why do cells with extra centrosomes secrete high levels of $_{s}$EVs and (ii) do these vesicles contribute to tumourigenesis?

Chapter 4

Results II:

Centrosome amplification-induced oxidative stress impairs lysosome function, preventing lysosomal degradation of multivesicular bodies and resulting in increased small extracellular vesicle secretion

4.1 Cells with Centrosome amplification have increased levels of reactive oxygen species

To better understand the role of centrosome amplification in tumourigenesis we first investigated why cells with extra centrosomes secrete high levels of $_s$EVs. Recent work published by our laboratory demonstrated that centrosome amplification induces an early oxidative stress response through increased generation of reactive oxygen species (ROS) (Arnandis *et al.*, 2018). Interestingly, the increase in cellular ROS associated with centrosome amplification resulted in an altered secretory phenotype, an extra centrosome-associated secretory phenotype (ECASP), that lead to paracrine cell invasion. As this work also showed the ECASP included the increased secretion of exosomal proteins, we hypothesised that centrosome amplification-associated ROS may be responsible for the increased secretion of $_s$EVs. To investigate this, we first quantified ROS levels in our PaTu-S.PLK4 and HPAF-II.PLK4 cell lines following the induction of centrosome amplification. ROS levels were determined using the Promega GSH/GSSG-Glo™ Assay. Glutathione (GSH) is an important antioxidant/ ROS scavenger which exists mostly in its reduced form, however, following oxidative stress, GSH is converted into its oxidized form Glutathione disulfide (GSSG), which consists of two GSH molecules linked by a disulphide bond. Briefly, the Promega GSH/GSSG-Glo™ Assay is a linked assay utilising glutathione S-transferase and Luciferin-NT that generates a luminescent signal in response to levels of GSH present in the sample. The ratio of GSH to GSSG can then be calculated to give a read out of oxidative stress in the cells, where a decrease in the ratio indicates an increase in oxidative stress.

As expected, the induction of centrosome amplification (+DOX) in PaTu-S.PLK4 and HPAF-II.PLK4 cells results in a decreased ratio of GSH/GSSG indicating an increase in cellular oxidative stress/ROS (Figure 4.1.1 A/B). PaTu-S.PLK4 cells were found to exhibit ~1 fold increase in cellular ROS, whereas HPAF-II.PLK4 exhibited ~2 fold increase. Furthermore, it is possible to manipulate levels of cellular ROS using the ROS scavenger N-acetyl cysteine (NAC) and the ROS inducing reagent, hydrogen peroxide (H_2O_2). The addition of NAC to samples where centrosome amplification has been induced (+DOX +NAC) reverted the ratio of GSH/GSSG back to that of the control cells (no treatment) in both cell lines. Moreover, the addition H_2O_2 at low concentration was sufficient to

induce ROS independently of centrosome amplification in both cell lines and results in a ratio of GSH/GSSG similar to that observed upon the induction of centrosome amplification. Interestingly, PaTu-S.PLK4 cells were found to have higher basal levels of ROS compared to HPAF-II.PLK4 cells. Whilst HPAF-II.PLK4 cells exhibited the largest fold increase in ROS upon the induction of centrosome amplification, HPAF-II.PLK4 ROS levels were still lower than even the basal ROS levels observed in the PaTu-S.PLK4 cells (discussed in more detail later in this chapter).

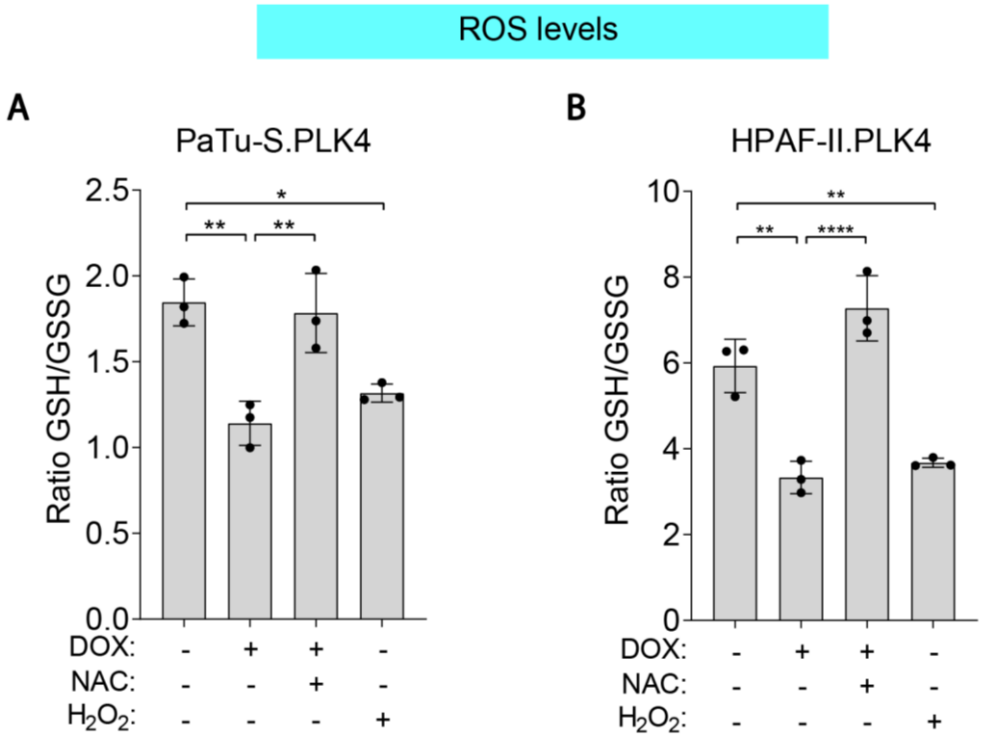

Figure 4.1.1 Levels of intracellular reactive oxygen species as measured by the ratio of GSH/GSSG. A) Ratio of GSH/GSSG in PaTu-S.PLK4 cells untreated or treated with +DOX, +DOX +NAC or + H_2O_2. **B)** Ratio of GSH/GSSG in HPAF-II.PLK4 cells untreated or treated with +DOX, +DOX +NAC or + H_2O_2. Error bars represent mean ± standard deviation (n=3). Data analysed using one-way ANOVA with Tukey's post hoc test (**** p<0.0001 , ** p<0.01, * p<0.05). DOX=doxycycline hyclate, NAC = N-acetyl cysteine, H_2O_2= hydrogen peroxide.

It has been previously demonstrated that changes in cellular ROS do not affect centrosome amplification (Arnandis *et al.*, 2018). To confirm this finding in our cell lines, we quantified centrosome amplification in each of the four conditions: i) no treatment, ii) +DOX, iii) +DOX +NAC and iv) +H_2O_2 (Figure 4.1.2 A/B). Centrosome amplification in cells treated with DOX and NAC yield similar levels of centrosome amplification (%) to

the cells treated with DOX alone. Thus, the reduction of cellular ROS does not prevent centrosome amplification in PaTu-S.PLK4 or HPAF-II.PLK4 cells treated with DOX. Moreover, centrosome amplification levels in cells treated with H_2O_2 remain similar to those of the untreated control cells, indicating that oxidative stress does not induce supernumerary centrosomes.

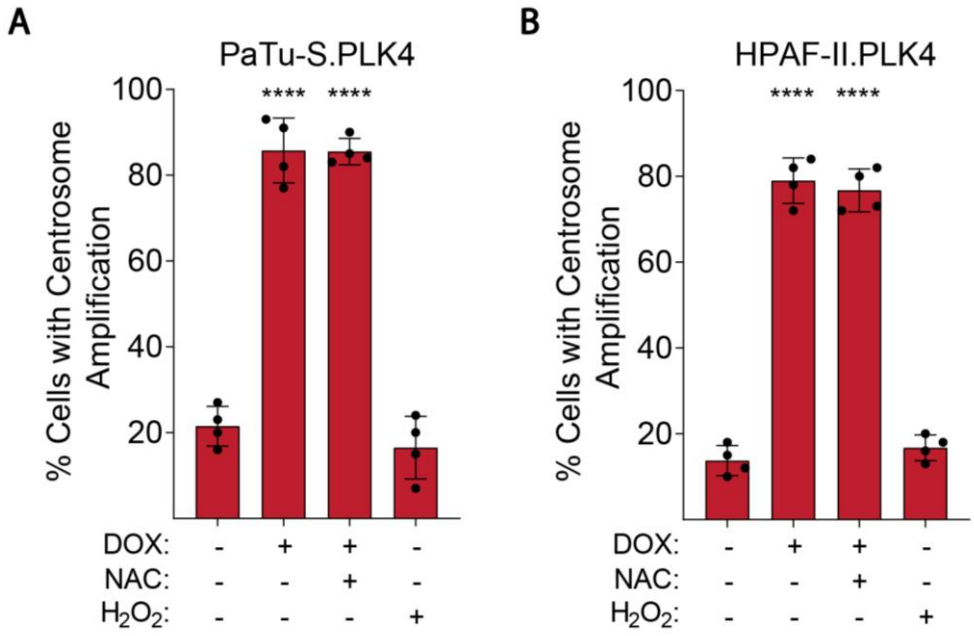

Figure 4.1.2 Intracellular reactive oxygen species do not affect centrosome amplification in PaTu-S.PLK4 or HPAF-II.PLK4 cells. A) Centrosome amplification in PaTu-S.PLK4 cells untreated or treated with +DOX, +DOX +NAC or + H_2O_2. **B)** Centrosome amplification in HPAF-II.PLK4 cells untreated or treated with +DOX, +DOX +NAC or + H_2O_2. Error bars represent mean ± standard deviation (n=3). Data analysed using one-way ANOVA with Tukey's post hoc test (**** $p<0.0001$). Significance stars shown where conditions are significantly different from the untreated control cells. DOX=doxycycline hyclate, NAC = N-acetyl cysteine, H_2O_2= hydrogen peroxide.

Taken together these results demonstrate that centrosome amplification leads to increased cellular ROS in PDAC cell lines. Importantly, however, changing ROS levels does not affect the percentage of cells with extra centrosomes.

4.2 Enhanced reactive oxygen species in cells with extra centrosomes drives small extracellular vesicle secretion

Thus far, our results have demonstrated that cells with extra centrosomes secrete significantly more $_{s}$EVs and have increased levels of cellular ROS. We therefore investigated whether centrosome amplification-induced changes in cellular ROS were responsible for the altered $_{s}$EV secretion observed. To test this, we harvested $_{L}$EV and $_{s}$EVs from PaTu-S.PLK4 and HPAF-II.PLK4 cells under the following conditions: i) no treatment, ii) +DOX, iii) +DOX +NAC and iv) +H_2O_2 (see Figure 4.2). Interestingly, whilst centrosome amplification induced $_{s}$EV secretion as expected, quenching ROS with NAC in these cells prevented this increase in $_{s}$EV secretion. This suggests that the increase in $_{s}$EV secretion observed from cells with extra centrosomes is caused by centrosome amplification-induced cellular ROS. Additionally, it was found that the induction of ROS with H_2O_2 resulted in a significant increase in $_{s}$EV secretion compared to the untreated control cells. This indicates that increased cellular ROS can induce $_{s}$EV secretion independently of centrosome amplification. No changes were observed in the secretion of $_{L}$EVs under any experimental condition, suggesting that changes in cellular ROS are only responsible for the secretion of $_{s}$EVs. Interestingly, whilst HPAF-II.PLK4 cells were found to have relatively less ROS than PaTu-S.PLK4 cells before and after the induction of centrosome amplification, these cells always exhibited higher $_{s}$EV secretion. As basal ROS levels do not appear to correlate to $_{s}$EV secretion, it is possible that centrosome amplification induces the production of a specific form of ROS that is capable of increasing the secretion of $_{s}$EV. Importantly, ROS can be produced in different sub-cellular compartments including the mitochondria, where the majority of cellular ROS is produced, and the cytosol (reviewed in Klionsky *et al.*, 2016). Our previous work demonstrated centrosome amplification to induce cytoplasmic ROS, where ROS was generated by the NADPH oxidases (NOXs) in the cytoplasm (Arnandis *et al.*, 2018). It is therefore possible that the generation of cytoplasmic ROS, induced by centrosome amplification, is required to induce $_{s}$EV secretion in PDAC cells.

Taken together, these results indicate that centrosome amplification-induced cellular ROS are responsible for the increase in $_{s}$EV secretion observed in cells with extra

centrosomes. Furthermore, the effect of increased ROS is specific to the secretion of $_{s}$EVs only, indicating that centrosome amplification-associated increases in ROS affects the biogenesis and/or the trafficking of $_{s}$EVs.

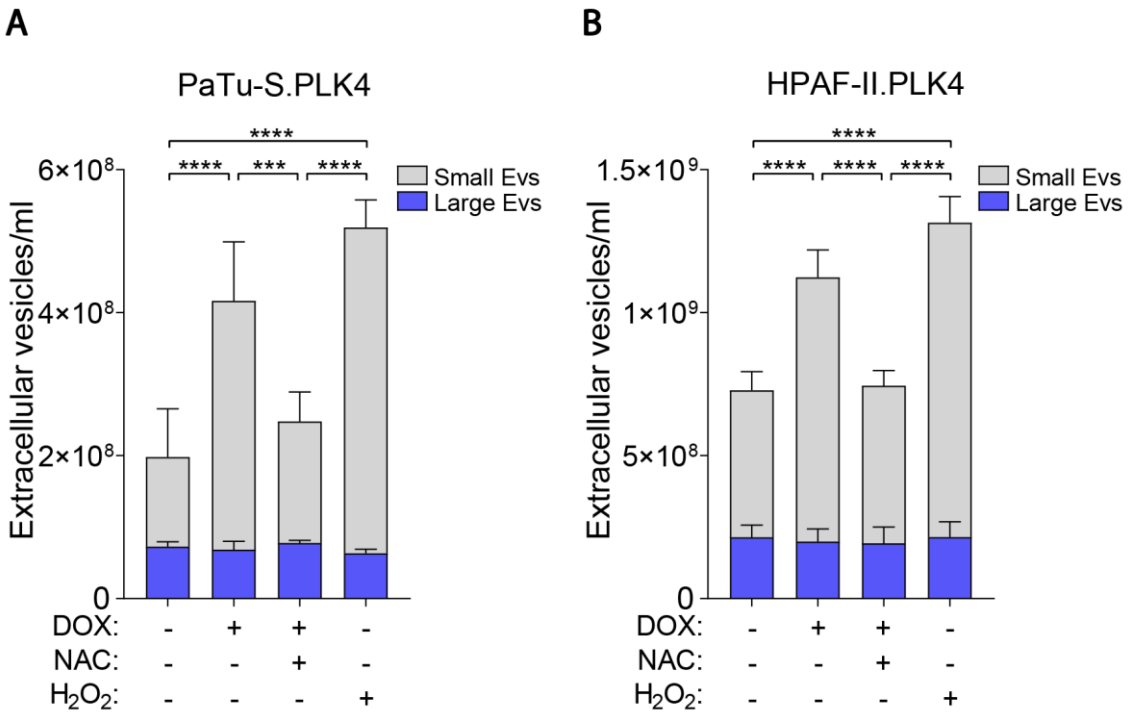

Figure 4.2 Extracellular vesicle secretion is affected by cellular reactive oxygen species in PaTu-S.PLK4 and HPAF-II.PLK4. A) Secretion of $_{L}$EVs and $_{s}$EVs from PaTu-S.PLK4 cells untreated or treated with +DOX, +DOX +NAC or + H_2O_2. **B)** Secretion of $_{L}$EVs and $_{s}$EVs from HPAF-II.PLK4 cells untreated or treated with +DOX, +DOX +NAC or + H_2O_2. Error bars represent mean ± standard deviation (n=3). Data analysed using two-way ANOVA with Tukey's post hoc test (**** p<0.0001, *** p<0.001). Significance relates to $_{s}$EVs secretion only. No significant difference was observed in $_{L}$EVs secretion between conditions. DOX=doxycycline hyclate, NAC = N-acetyl cysteine, H_2O_2= hydrogen peroxide.

4.3 Lysosomal deacidification by bafilomycin A1 leads to increased small extracellular vesicle secretion

To further investigate how centrosome amplification-induced ROS contributes to increased $_{s}$EV secretion in pancreatic cancer cells we looked into the likely origins of the secreted $_{s}$EVs. Previous analysis of the isolated $_{s}$EV by nanoparticle tracking analysis (NTA) (Chapter 3) indicated that these vesicles are within the size range associated with

exosomes. Moreover, western blot analysis revealed the presence of the ESCRT associated proteins TSG101 and ALIX in the $_s$EV isolates, indicating a possible endosomal origin for these vesicles. Furthermore, proteomic analysis of $_s$EVs isolated from PaTu-S.PLK4 cells revealed them to be significantly enriched in proteins associated with exosomes (see Chapter 5). This analysis also revealed a significant enrichment in proteins associated with recycling endosomes, the ESCRT, late endosomes and the endocytic vesicle, further supporting the notion that these vesicles are of endosomal origin and therefore likely to be exosomes. We therefore investigated the effects of ROS on exosome biogenesis and trafficking.

Exosomes form within the cell by inward budding into early and late endosomes, which are generally referred to as multivesicular endosomes, or multivesicular bodies (MVBs). These MVBs are usually destined for fusion with lysosomes, resulting in degradation of their contents. Alternatively, MVBs can be trafficked to the extremities of the cell, where fusion with the plasma membrane results in exosome secretion (C Harding, Heuser and Stahl, 1983; Pan and Johnstone, 1983; Johnstone *et al.*, 1987). Interestingly, it has recently been shown that lysosome dysfunction can shift the fate of MVBs targeted for degradation to fusion with the plasma membrane and exocytosis, leading to increased exosome secretion *(*Alvarez-Erviti *et al., 2011;* Miao *et al*., 2015; Latifkar *et al*., 2019). Since the functional capacity of lysosomes is dependent on an acidic luminal pH, lysosomes are particularly sensitive to membrane permeabilization and loss of acidity. Interestingly, cellular ROS has been shown to contribute to lysosome membrane permeabilization (LMP) through the generation of highly reactive hydroxyl radicals which compromise the integrity of lysosomal membranes by causing lipid peroxidation and damaging lysosomal membrane proteins (Nilsson, Ghassemifar and Brunk, 1997; Kurz, Terman, Gustafsson and Ulf T Brunk, 2008; Kurz, Terman, Gustafsson and Ulf T. Brunk, 2008; Johansson *et al.*, 2010; Aits and Jaattela, 2013). Other methods of ROS-mediated lysosome dysfunction have also been suggested, including constitute activation of lysosomal Ca^{2+} channels leading to LMP (Sumoza-Toledo and Penner, 2011) and ROS -linked changes in lysosomal enzyme activity (Aits and Jaattela, 2013). We therefore hypothesised that increased ROS in cells with centrosome amplification impairs lysosome function, preventing lysosomal degradation of MVBs and resulting in increased exosome secretion (Figure 4.3.1).

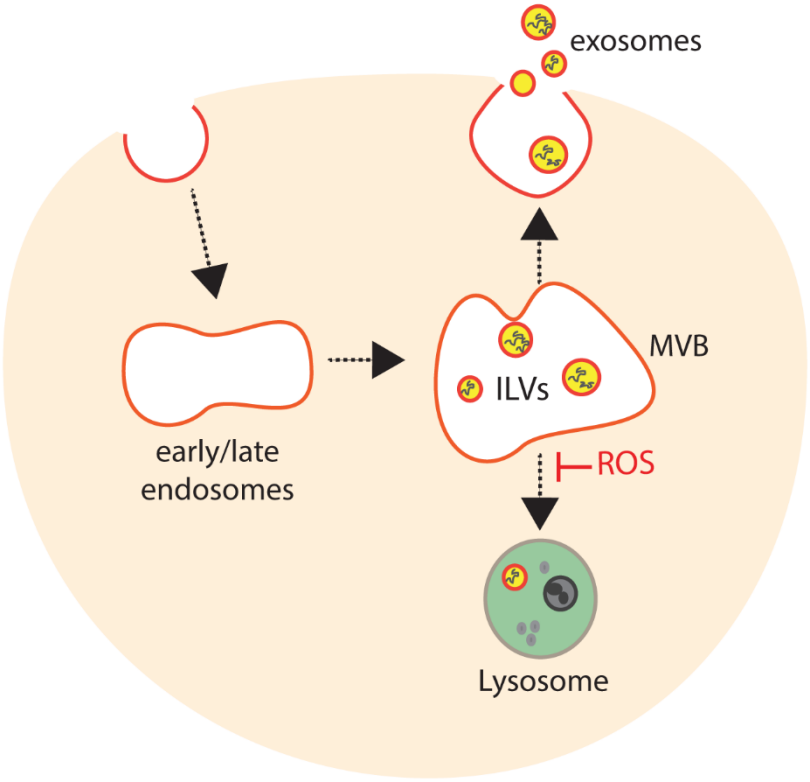

Figure 4.3.1 Hypothesis schematic: Increased intracellular reactive oxygen species blocks lysosomal/multivesicular body fusion, resulting in increased exosome secretion. ROS = reactive oxygen species, MVBs = multivesicular bodies, ILVs = intraluminal vesicles.

Initially, to confirm whether lysosome dysfunction induces the secretion of $_{s}$EV in our cells, we treated cells with low levels (20nM final concentration) of the macrolide antibiotic bafilomycin A1. Bafilomycin A1 is potent vacuolar proton pump inhibitor that prevents the acidification of lysosomes, thereby hampering their degradative capacity (Yoshimori *et al.*, 1991) and results in the increased release of exosomes (Savina *et al.*, 2003). Bafilomycin A1 has also been shown to inhibit autophagy by preventing autophagosome-lysosome fusion (Müller *et al.*, 2015). To confirm bafilomycin A1 activity in the PaTu-S.PLK4 cells, we immunofluorescently stained for autophagy marker light chain 3-II (LC3-II). LC3-II can be used as a quantitative marker for the presence of autophagosomes since it is recruited to the autophagosome membranes and degraded following fusion with lysosomes (Kabeya, 2000; Mizushima and Yoshimori, 2007; Tanida, Ueno and Kominami, 2008; Klionsky *et al.*, 2016; Redmann *et al.*, 2017). As expected, LC3-II accumulates following bafilomycin A1 treatment in PaTu-S.PLK4 cells (Figure 4.3.2 A), indicating an increase in autophagosomes at low antibiotic concentration. Large and small EVs were then harvested from the PaTu-S.PLK4 cell line treated with and without

bafilomycin A1 and quantified (Figure 4.3.2 B). As expected, Bafilomycin A1 treatment significantly increased the secretion of $_{s}$EVs in PaTu-S.PLK4 cells, from a mean of ~ 1.9 x10^{8} to ~ 6.75 x10^{8}. No significant difference was observed in the levels of $_{L}$EVs secretion. These results confirm that deacidification of lysosomes induces secretion of $_{s}$EVs in pancreatic cancer cells.

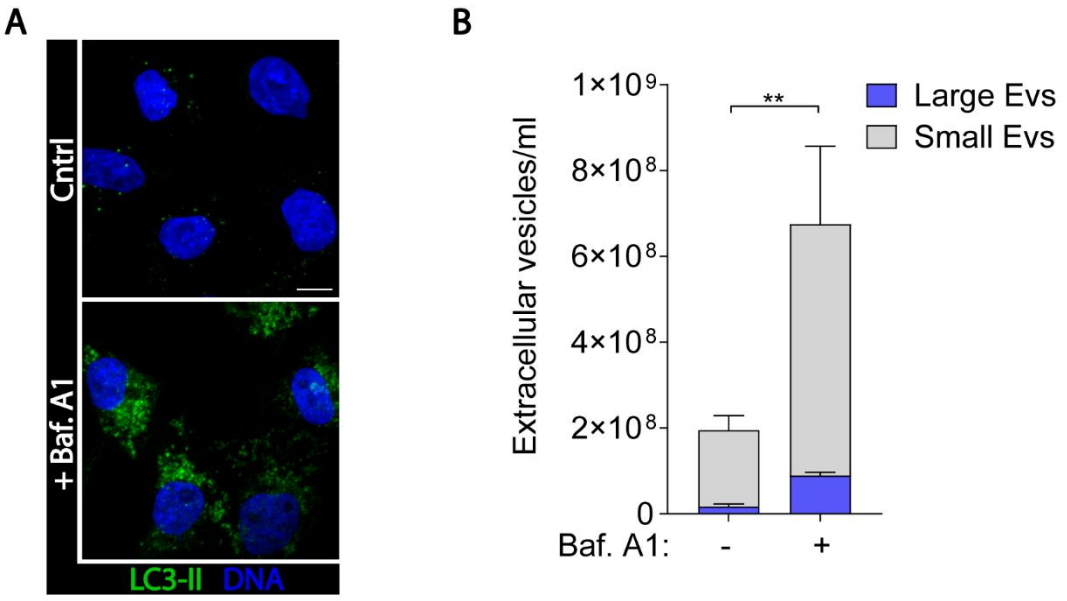

Figure 4.3.2 Extracellular vesicle secretion post treatment with Bafilomycin A1 in PaTu-S.PLK4 cells. A) Immunofluorescent staining of LC3-II in PaTu-S.PLK4 cells, showing an increase in LC3-II puncta upon treatment with 20nM Bafilomycin A1. LC3-II (LC3B (D11) XP) shown in green, DNA (Hoechst) in blue. Scale bar represents 10 µm. **B)** Secretion of $_{L}$EVs and $_{s}$EVs from PaTu-S.PLK4 cells treated without (-) and with (+) bafilomycin A1 (20nM final concentration). Error bars represent mean ± standard deviation (n=3). Data analysed using two-way ANOVA with Tukey's post hoc test (** $p<0.01$). Significance relates to $_{s}$EV secretion only. No significant difference was observed in $_{L}$EVs secretion between conditions. Baf.A1 = bafilomycin A1, LC3-II = Autophagy marker light chain 3-II.

4.4 Centrosome amplification-associated ROS compromises lysosomal protease activity

Our results thus far have demonstrated that centrosome amplification-associated ROS is responsible for the increased secretion of $_{s}$EVs in cells with extra centrosomes. Furthermore, we have demonstrated that lysosome dysfunction induces $_{s}$EVs secretion in PDAC cell lines. We therefore analysed whether centrosome amplification increased

in ROS may impair lysosome function, preventing MVB-lysosome fusion and shifting the fate of MVBs from degradation by the lysosome to secretion at the plasma membrane. To test our hypothesis, we first analysed the activity of the lysosomal hydrolase cathepsin B as a proxy to lysosome function in PaTu-S.PLK4 cells under the following conditions: i) untreated, ii) + DOX (to induce centrosome amplification), iii) +DOX +NAC (to quench the induction of ROS in cells with extra centrosomes), iv) + H_2O_2 (to induce ROS independently of centrosome amplification) and v) + bafilomycin A1 (to induce lysosome dysfunction through alkalinisation of the lysosomal lumen). Cathepsin B is a cysteine protease responsible for driving proteolytic degradation in the lysosome (Leung-Toung *et al.*, 2002). Initially synthesised as an inactive zymogen, cathepsin B becomes activated upon entry into the acidic environment of the lysosome (reviewed by Stoka, Turk and Turk, 2016), making it a good measure of lysosome function. To detect cathepsin B protease activity in live cells we used a Cathepsin B Magic Red ™ kit. Magic Red™ is a non-toxic and freely permeable substrate that is cleaved in the presence of active cathepsin B to produce a red (Cresyl Violet) fluorescent product. Thus, a strong Magic Red™ fluorescence intensity is indicative of functional lysosomes.

Spinning disk confocal microscopy was used to visualise changes in Magic Red™ fluorescence intensity between conditions (Figure 4.4 A). Using Image J the mean Magic Red™ fluorescence intensity per cell was quantified and normalised to cell area (Figure 4.4 B). To ensure that total Magic Red™ fluorescence intensity was analysed per cell, z-stack sum intensity projection images were used for quantification. Analysis revealed that Magic Red™ fluorescence intensity significantly decreased in cells with extra centrosomes (+DOX) compared to the untreated control cells (represented in grey). This demonstrates that cells with extra centrosomes have decreased lysosomal protease activity. Interestingly, quenching ROS accumulation in cells with extra centrosomes (+DOX +NAC) prevented this decrease in Magic Red™ fluorescence. Furthermore, when ROS was induced in the absence of centrosome amplification (+H_2O_2), Magic Red™ fluorescence intensity also significantly decreased. Together, these results indicate that lysosome dysfunction in cells with extra centrosomes is caused by increased cellular ROS. Moreover, preventing lysosome acidification with bafilomycin A1 also lead to a marked decrease in Magic Red™ fluorescence intensity (see Figure 4.4). We therefore asked the question, does centrosome amplification-induced ROS causes lysosome

dysfunction through the deacidification of the lysosomes or through another, as yet, unidentified mechanism?

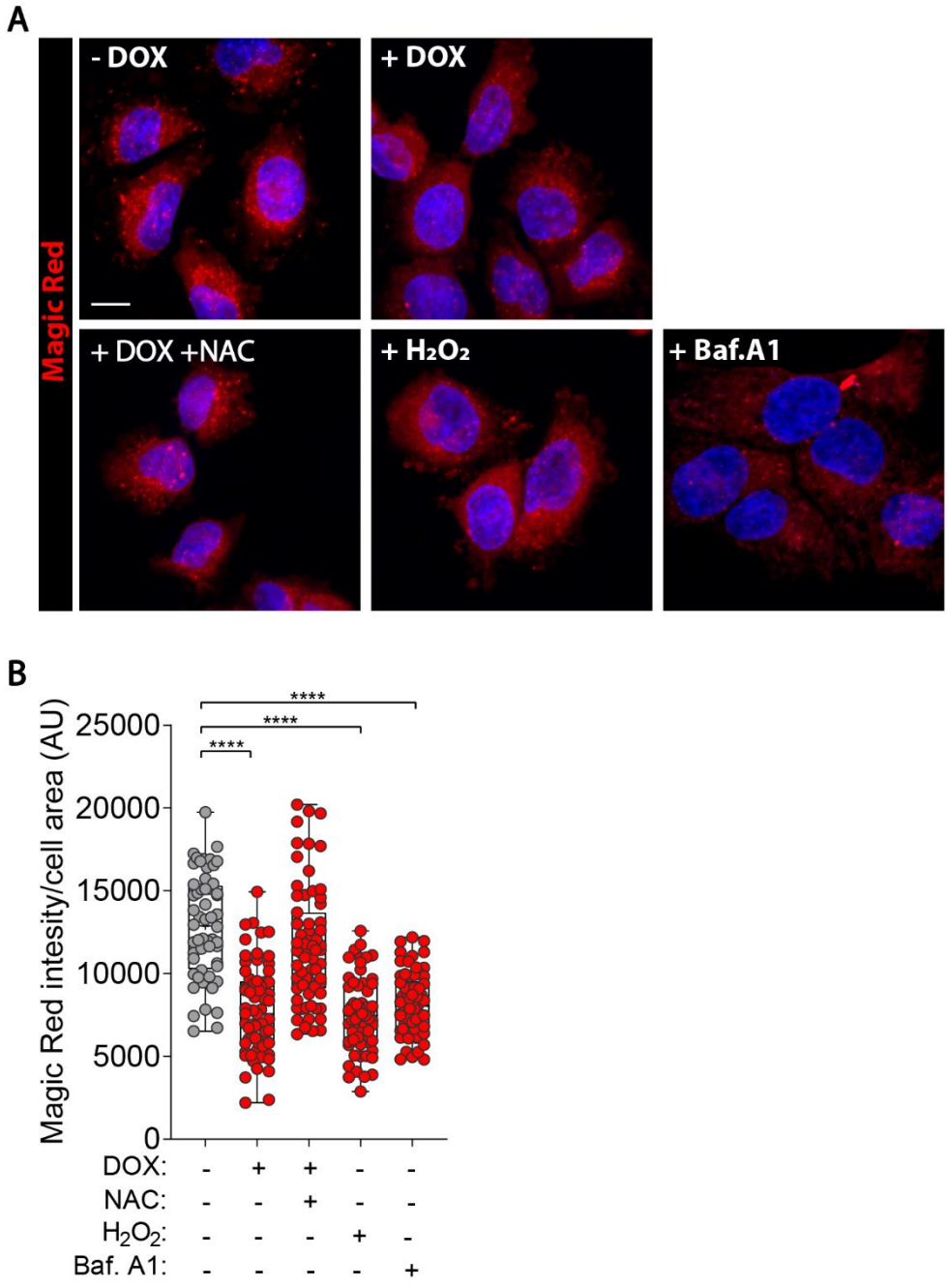

Figure 4.4 Cathepsin B activity as measured by Magic Red™ fluorescence intensity in PaTu-S.PLK4. A) Representative confocal z-stack projection images of Magic Red™ fluorescence (red) in PaTu-S.PLK4 cells, untreated or treated with DOX, DOX and NAC, H_2O_2, or Baf.A1. DNA was stained with Hoechst. Scale bar represents 10µm. **B)** Quantification of total Magic Red™ fluorescence intensity per cell in PaTu-S.PLK4 cells treated as described in A. Control represented in grey, treatment conditions in red. Error bars represent mean ± standard deviation (n=60 ± 5 cells). Data analysed using one-way ANOVA with Tukey's post hoc test (**** $p<0.0001$). DOX=doxycycline hyclate, NAC = N-acetyl cysteine, H_2O_2= hydrogen peroxide, Baf.A1 = bafilomycin. A1.

4.5 Oxidative stress in cells with centrosome amplification impairs lysosome and multivesicular body fusion

Since centrosome amplification-induced ROS was found to compromise lysosome function in pancreatic cancer cells (see Figure 4.4) and compromising lysosome function with bafilomycin A1 leads to increased $_s$EV secretion we postulated that lysosome impairment may prevent lysosomal degradation of MVBs leading to the increased $_s$EV secretion observed in cells with supernumerary centrosomes. Furthermore, we hypothesised that centrosome amplification-associated ROS may lead to lysosome dysfunction through deacidification of lysosomes. To investigate this, we analysed changes in lysosome number, MVB number and lysosome/MVB co-localisation in PaTu-S.PLK4 cells treated as detailed in Figure 4.4 above.

Lysosome number was quantified using the red fluorescent dye LysoTracker® Red DND-99 (LysoTracker). LysoTracker contains a fluorophore linked to a weak base which is partially protonated at neutral pH and can freely permeate cell and organelle membranes in live cells. Upon entry to the acidic environment of the lysosome, the lysotracker red probe becomes protonated and is sequestered in the lumen of the lysosome (Zhitomirsky, Farber and Assaraf, 2018). Thus, LysoTracker is highly selective for acidic organelles, and a strong LysoTracker fluorescent signal is indicative of lysosomes with a functional low pH. PaTu-S.PLK4 cells were incubated with LysoTracker Red for 1 hour before being fixed and subsequently stained for the presence of MVBs. To analyse MVBs, cells were labelled with an antibody directed against the MVB marker lyso-bisphosphatidic acid (LBPA). LBPA plays a role in the formation of intraluminal vesicles (Kobayashi *et al.*, 1998). Confocal fluorescence microscopy revealed the presence of red (LysoTracker) and green (LBPA) puncta as shown in Figure 4.5.1.

To ensure all endosomes were quantified, z-stack projection images were used for analysis. Lysosome number was analysed in Image J using the point maxima function to quantify LysoTracker positive puncta per cell (Figure 4.5.2 A). This analysis revealed a significant decrease in LysoTracker puncta in PaTu-S.PLK4 cells where centrosome amplification had been induced (+DOX) compared to the untreated control cells (represented in grey). This result suggests that cells with supernumerary centrosomes have significantly fewer acidic lysosomes. Furthermore, this result is consistent with our

magic red data, in demonstrating the reduced presence of functional lysosomes in cells with amplified centrosomes. Interestingly when ROS was quenched with NAC in cells with extra centrosomes, the number of LysoTracker positive puncta reverted back to that of the untreated control. Additionally, induction of ROS with H_2O_2 in control cells was sufficient to significantly decrease LysoTracker puncta independently of centrosome amplification. Together, these results indicate that centrosome amplification-associated increases in cellular ROS are responsible for the significant decrease in acidic lysosomes observed in cells with supernumerary centrosomes. As expected, treatment of PaTu-S.PLK4 cells with the lysosome alkalising agent bafilomycin A1 resulted in significantly fewer acidic lysosomes.

The number of LBPA positive MVBs was also quantified in ImageJ using the point maxima function (figure 4.5.2 B). Interestingly, no changes were observed in the number of LBPA puncta following the induction of centrosome amplification (+DOX) in PaTu-S.PLK4 compared to the untreated control (represented in grey). In addition, no changes in the number of LBPA puncta were observed following ROS quenching in cells with extra centrosomes (+DOX +NAC), or the induction of ROS in the absence of centrosome amplification (H_2O_2). These results indicate, that the number of $LBPA^{+ve}$ MVBs is unaffected by centrosome amplification or ROS. Interestingly, $LBPA^{+ve}$ MVBs were more disperse throughout the cytoplasm in cells with centrosome amplification and those treated with H_2O_2 compared to untreated control cells (-DOX). This result may indicate enhanced trafficking of MVBs in cells with centrosome amplification and treated with H_2O_2. A significant increase in LBPA positive puncta (MVBs) was observed, however, upon treatment with bafilomycin A1, indicating a different mechanism of action from increased ROS. Importantly, bafilomycin A1 has been shown to result in the accumulation and expansion of autophagic structures in addition to preventing lysosome acidification. It is therefore possible that in bafilomycin A1 treated cells, increased LBPA puncta are representative of an increased number of autophagosomes (Mauvezin and Neufeld, 2015).

Next, we investigated whether lysosome dysfunction caused by centrosome amplification-induced ROS could also prevent lysosome-MVB fusion in PDAC cells. Using the Image J threshold function, fluorescence intensity masks were generated for the LysoTracker channel (red) and LBPA channel (green) and overlaid to generate a co-

localisation mask (co-localisation observed in yellow) (representative images shown in Figure 4.5 A). Co-localisation events between LysoTracker and LBPA puncta were then quantified as a proxy to lysosome-MVB fusion. Points of co-localisation were manually analysed per cell and the percentage of LBPA co-localised with LysoTracker was calculated (Figure 4.5.2 C). Induced lysosome dysfunction with bafilomycin A1, resulted in a significant decrease in LysoTracker/LBPA co-localisation in PaTu-S.PLK4 cells compared to the control cells (represented in grey), confirming that lysosome dysfunction impairs lysosome-MVB fusion in PDAC cells. We then went on to analyse the effects of centrosome amplification on lysosome-MVB fusion in PaTu-S.PLK4 cells. This analysis revealed that cells with extra centrosomes (+DOX) have significantly fewer LysoTracker/LBPA co-localisation events compared to control cells indicating that centrosome amplification does in fact impair lysosome-MVB fusion. Interestingly, the decrease in LysoTracker/LBPA co-localisation in cells with extra centrosomes was reverted when centrosome amplification-associated ROS were prevented with NAC (+DOX +NAC). This effect of ROS was confirmed using H_2O_2 treatment in control cells (no centrosome amplification), where a significant decrease in LysoTracker/LBPA co-localisation was also observed (see Figure 4.5.1/4.5.2 C). Taken together, these results demonstrate that centrosome amplification-induced increases in cellular ROS are responsible for impairing lysosome-MVB fusion in PaTu-S.PLK4 cells.

In conclusion, these results demonstrate that centrosome amplification-associated increases in cellular ROS lead to a significant decrease in the levels of acidic functional lysosome and significantly fewer lysosome-MVB co-localisation events in PDAC cells. Thus, our results support our hypothesis that centrosome amplification-induced ROS impairs lysosome function, reducing MVB degradation by lysosomes and leading to increased $_s$EV secretion in pancreatic cancer cells.

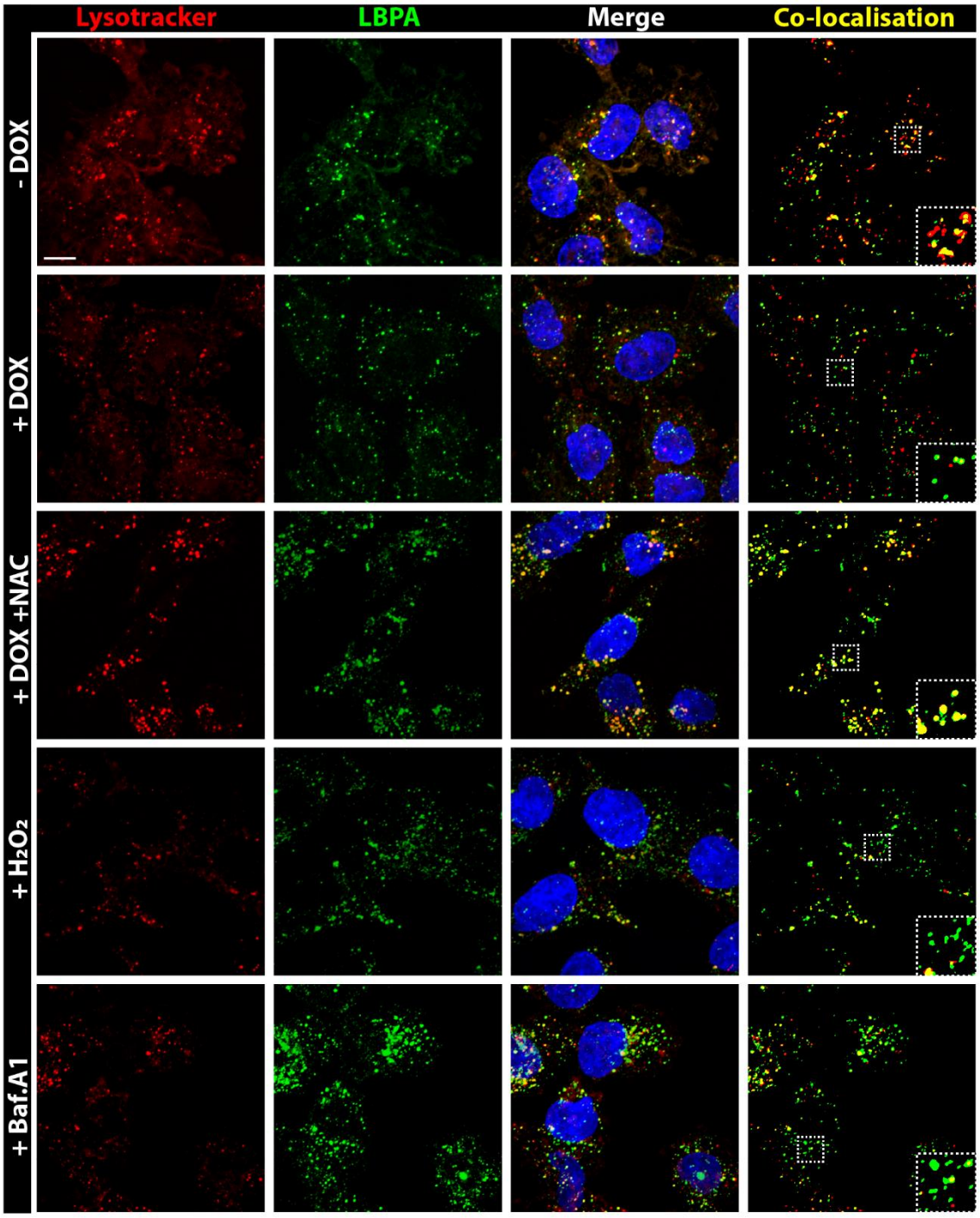

Figure 4.5.1 Representative images of LysoTracker and LBPA co-localisation events in PaTu-S.PLK4 cells. Representative confocal z-stack projection images of LysoTracker (red), LBPA (green), merged images and co-localization masks (col-localisation in yellow) in PaTu-S.PLK4 cells, untreated or treated with i)DOX, ii)DOX and NAC, iii)+ H_2O_2, iv) bafilomycin A1. DNA was stained with Hoechst. Scale bar represents 10 µm. DOX=doxycycline hyclate, NAC = N-acetyl cysteine, H_2O_2= hydrogen peroxide, Baf.A1 = bafilomycin. A1.

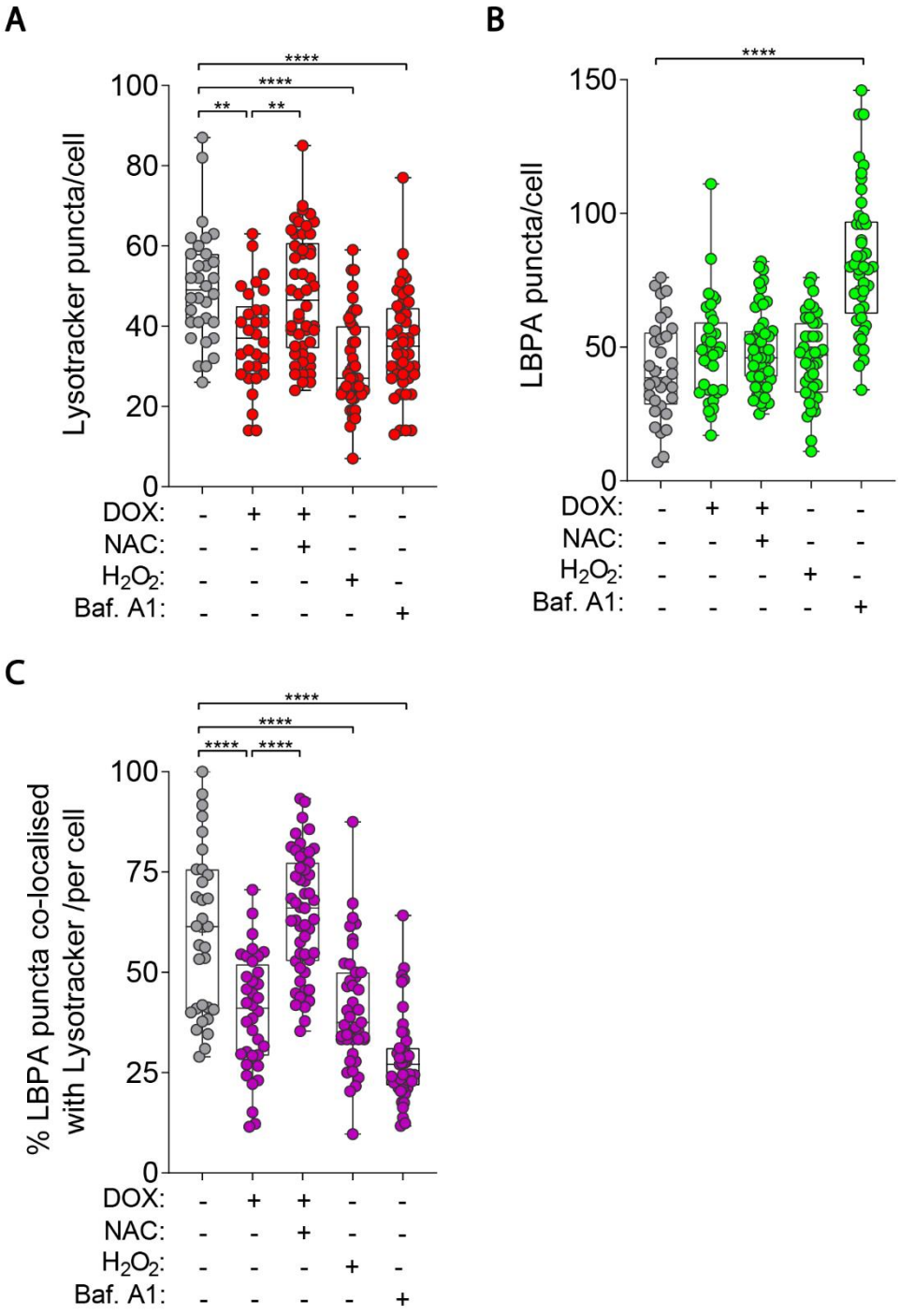

Figure 4.5.2 Quantification of LysoTracker and LBPA co-localisation events in PaTu-S.PLK4 cells. A) Quantification of LysoTracker puncta per cell in PaTu-S.PLK4 cells, untreated or treated with i)DOX, ii)DOX and NAC, iii)+ H_2O_2, iv) bafilomycin A1. Control cells (-DOX) are represented in grey, treatment conditions are shown in red. **B)** Quantification of LBPA puncta per cell in PaTu-S.PLK4 cells treated as described in A. Control cells (-DOX) are represented in grey, treatment conditions are shown in green. **C)** Quantification of LBPA puncta co-localised with LysoTracker per cell in PaTu-S.PLK4 cells treated as described in A. Control cells (-DOX) are represented in grey, treatment conditions are shown in purple. Error bars represent mean ± standard deviation (n= 45 ± 6 cells). Data analysed using one-way ANOVA with Tukey's post hoc test (**** $p<0.0001$, ** $p<0.01$). DOX=doxycycline hyclate, NAC = N-acetyl cysteine, H_2O_2= hydrogen peroxide, Baf.A1 = bafilomycin. A1.

4.6 Discussion

Our initial findings demonstrate that pancreatic cancer cells with extra centrosomes secrete an increased number of $_s$EVs (see Chapter 3). Since EVs secreted by cancer cells have been shown to play important roles in the development and spread of cancer (reviewed in Wortzel *et al.*, 2019), we asked two important questions, (i) why do cells with extra centrosomes secrete more $_s$EVs? and (ii) do $_s$EVs secreted by cells with supernumerary centrosomes contribute to tumourigenesis? We address the first of these questions in this chapter.

Previous work from our laboratory (Arnandis *et al.*, 2018) indicated that centrosome amplification-associated increases in cellular ROS were responsible for the altered secretory phenotype observed in cells with supernumerary centrosomes. We therefore hypothesised that centrosome amplification-associated changes in cellular ROS may lead to the increased $_s$EV secretion observed by cells with extra centrosomes. Here we show that the induction of centrosome amplification in PaTu-S.PLK4 and HPAF-II.PLK4 cells leads to an increase in cellular ROS in PDAC cells, confirming the findings of Arnandis *et al* in mammary cells and establishing that this effect is not tissue specific. Importantly, whilst centrosome amplification is sufficient to induce ROS in PDAC cells, changing ROS levels do not affect the levels of centrosome amplification. Furthermore, we demonstrate that centrosome amplification-associated increases in cellular ROS are in fact responsible for the increased $_s$EV secretion observed in cells with extra centrosomes, confirming our hypothesis.

To further elucidate the mechanisms behind ROS-mediated increases in $_s$EV secretion we first investigated the origin of these $_s$EVs. Within this study we have demonstrated that the secreted $_s$EVs harbour many characteristics of exosomes, we therefore investigated the possible effects of ROS on exosome biogenesis and trafficking. Exosomes are generated intracellularly through intraluminal budding into MVBs and are released upon MVB fusion with the plasma membrane (C Harding, Heuser and Stahl, 1983). However, a second fate exists for MVBs, whereby upon fusion with the lysosome the MVB contents are degraded and recycled, thus preventing exosome secretion (reviewed in Piper and Katzmann, 2007). Interestingly, lysosome dysfunction has been shown to prevent MVB-lysosome fusion *(*Alvarez-Erviti *et al., 2011;* Miao *et al*., 2015;

Latifkar *et al*., 2019) and high cellular ROS has been shown to elicit LMP, which leads to lysosome dysfunction (reviewed by Aits and Jaattela, 2013). We therefore hypothesised that centrosome amplification-associated ROS mediate lysosome dysfunction, ultimately reducing MVB degradation by lysosomes and shifting the fate of the MVBs to secretion at the plasma membrane. Our results demonstrate that centrosome amplification-associated increases in cellular ROS do in fact lead to decreased lysosomal activity (as measured by cathepsin B activity) in pancreatic cancer cells. In addition, we found that supernumerary centrosome-associated increases in ROS lead to a significant decrease in the number of acidic lysosomes. Taken together, these results indicate that high levels of cellular ROS, induced by cells with extra centrosomes, results in lysosome dysfunction in PDAC cells. Interestingly, centrosome amplification did not induce changes in MVB number in pancreatic cancer cells. This indicates that the increase in $_{s}$EV secretion observed from cells with extra centrosomes is not caused by increased MVB biogenesis but is a result of altered MVB trafficking. Furthermore, analysis of lysosome-MVB fusion events through co-localisation of lysosome (LysoTracker) and MVB (LBPA) markers demonstrate that centrosome amplification leads to significantly reduced lysosome-MVB fusion in the cells. Additionally, it was shown that quenching ROS (+NAC) in cells with extra centrosomes prevented this decrease in lysosome-MVB fusion. Taken together, our results suggest that oxidative stress in cells with supernumerary centrosomes mediates lysosome dysfunction, subsequently impairing MVB-lysosome fusion and resulting in the increased secretion of $_{s}$EVs.

The exact mechanisms behind centrosome amplification-associated ROS-induced lysosome dysfunction remain elusive. Currently, our results cannot distinguish whether increases in cellular ROS affect lysosome biogenesis, or lysosomes functionality. Current literature indicates that high cellular ROS can lead to LMP, resulting in lysosome dysfunction (reviewed by Aits and Jaattela, 2013). Our results demonstrate that increased cellular ROS depletes lysosomal protease activity and decreases the number of acidic, and therefore, functional lysosomes. Thus, centrosome amplification-induced increases in ROS may cause lysosome dysfunction through deacidification of the lysosomal lumen. To confirm this, we plan to quantify total lysosome number in each cell using additional markers for lysosomes that are not dependent on an acidic pH, such as LAMP1. Comparison between total lysosome number and acidic lysosome number

should give an indication of whether centrosome amplification-associated increases in cellular ROS cause lysosome dysfunction/deacidification or if lysosome biogenesis is affected.

It is important to note that the complexity of the endocytic pathways within a cell make the identification of specific endosomes very difficult and most markers will identify multiple endosomes. For example, whilst LysoTracker has a high affinity for lysosomes, due to their acidic nature, it is also possible that other acidic organelles will be identified using this fluorescent probe. Therefore, it is possible that some lysosomes and lysosome co-localisation events have been over-estimated. Moreover, the MVB marker LBPA has been shown to be present in late endosomes as well as multivesicular bodies, thus it is not possible to distinguish which endosomal type is being identified in our cells. It is also possible that $LBPA^{+ve}$ MVBs only account for only a subset of the total MVBs present within a cell, which may also account for the differences in MVB number we observed upon Bafilomycin A1 treatment. It is possible that whilst Bafilomycin A1 results in the increased presence of $LBPA^{+ve}$ MVBs, centrosome amplification may affect other subsets of MVBs. Thus, analysis with additional MVB markers may reveal previously undetected changes in MVB number or size. Additionally, to overcome the limitations of endosomal markers, we plan to analyse changes in lysosomes, MVBs and lysosome-MVB fusion events in PDAC cells using electron microscopy to visually identify the different endosomal types. Furthermore, as analysis of lysosomes, MVBs and lysosome-MVB co-localisation was performed on z-stack projection images, it is possible that endosomes from different plans will project together. Thus, it is possible that the number of lysosomes and MVBs have been underestimated and co-localisation events have been over estimated. However, these inaccuracies are predicted to be infrequent and consistent between treatments.

Whilst our results to date provide evidence to support our hypothesis, it is possible that this mechanism only accounts in part for the increase in $_{s}$EV secretion observed in cells with extra centrosomes. Endosomes, including MVBs are trafficked along microtubules within the cell to reach their destination. Interestingly, increased microtubule nucleation has been observed in cells with supernumerary centrosomes (Godinho *et al.*, 2014). It is therefore possible that cells with extra centrosome do have elevated numbers of MVBs but they are trafficked for secretion faster than in cells with normal

centrosome number and so numerical differences are not observed. We therefore plan to investigate the effect of centrosome amplification-induced microtubule nucleation on exosome secretion in PDAC cells. To do this, PaTu-S.PLK4 cells induced to have centrosome amplification will be treated with siRNA targeted against the centrosomal protein CEP192. Depletion of this centrosomal protein has previously been shown to revert the level of microtubule nucleation back to that of normal cells without extra centrosomes (Godinho *et al.*, 2014). Extracellular vesicles will be harvested from cells with extra centrosomes following treatment with siRNA (siCEP192) and the number of secreted EVs will be quantified to determine if increased microtubule nucleation promotes increased $_s$EV secretion. If microtubule nucleation is found to affect $_s$EV secretion, we will analyse the effects of ROS on microtubule nucleation in cells with extra centrosomes. Recent literature has shown that high cellular ROS can lead to changes in the post-translational modification (PTM) of microtubules including detyrosination (Kerr *et al.*, 2015). Interestingly, detyrosination of microtubules has been shown to favour microtubule plus end directed transport via kinesin-1 (Janke and Chloë Bulinski, 2011). Thus, ROS-linked changes in microtubule PTMs may facilitate MVB trafficking to the plasma membrane, potentially resulting in increased $_s$EV secretion. To test this, we plan to quantify the levels of microtubule detyrosination via immunofluorescence staining and microscopy in PaTu-S.PLK4 cells under the following conditions: i) untreated, ii) + DOX, iii) +DOX +NAC and iv) + H_2O_2. If detyrosination is observed in cells with extra centrosomes, it may be possible to analyse the effects on $_s$EV secretion. To do this, levels of detyrosination may be reduced in cells with extra centrosomes using Parthenolide, an inhibitor of the tubulin carboxypeptidase (Chen *et al*., 2018), and sEV secretion quantified.

In conclusion, whilst further work is necessary to determine the exact mechanism of action, our results suggest that centrosome amplification-induced changes in cellular ROS causes reduced lysosome functionality and results in increased $_s$EVs secretion.

Chapter 5

Results III:

Small extracellular vesicles derived from cells with supernumerary centrosomes induce pancreatic stellate cell activation

5.1 Extracellular vesicles secreted by PDAC cells are naturally taken up by recipient cells

Our results thus far have demonstrated that cells with supernumerary centrosomes secrete more $_s$EVs. Since cancer-derived $_s$EVs are known to contribute to tumour progression and metastasis (Tai *et al.*, 2018; Tung *et al.*, 2019; Wortzel *et al.*, 2019), and centrosome amplification has recently been shown to play an active role in tumourigenesis (Coelho *et al.*, 2015; Serçin *et al.*, 2015; Levine *et al.*, 2017), we hypothesised that $_s$EVs secreted by cells with extra centrosomes may have pro-tumourigenic properties. We therefore decided to investigate functional roles for these vesicles in tumourigenesis. In order to do this, we analysed cellular changes in response to treatment with $_s$EVs from cells with and without the induction of centrosome amplification.

Importantly, to elicit biological changes in recipient cells, $_s$EV cargo must be transferred to the target cell. Therefore, we first had to determine if $_s$EVs secreted by PDAC cells could be naturally taken up by recipient cells to facilitate transfer of their biological cargo. As cancer-$_s$EVs have been shown to affect the behaviour of both cancer cells and fibroblast/stellate cells, we initially investigated the ability of both the PDAC cell line PaTu-T and the pancreatic stellate cell (PSC) line PS1 to engulf $_s$EVs secreted by cancer cells. To do this we isolated pancreatic cancer $_s$EVs from the conditioned media of PaTu-S cells using the previously described ultracentrifugation method (Section 2.4) with one modification: prior to the final PBS wash step, the isolated $_s$EVs were fluorescently labelled by incubation with the lipid dye BODIPY for 5 minutes. The $_s$EVs were then re-suspended in 31.5 mls of PBS to dilute out any unbound dye and the final 100,000 x g ultracentrifugation step was performed. The isolated fluorescent vesicles were then added to the growth media of the recipient cells. Cells were incubated with fluorescent $_s$EVs over a time course (data not shown) and it was determined that 3 hours of incubation with BODPIY labelled $_s$EVs was optimal to visualise uptake. The cells were then fixed and stained with phalloidin (F-actin) and Hoescht. Spinning disk confocal z-stack images were taken of the cells and maximum intensity projection images generated using image J. This revealed the presence of BODPIY labelled $_s$EVs (green) inside both the cancer cells (PaTu-T) and the PSCs (PS1) as shown in Figure 5.1. The

presence of the BODPIY labelled $_s$EVs inside both cell types demonstrates that $_s$EVs from PaTu-S cells are naturally taken up by recipient cells.

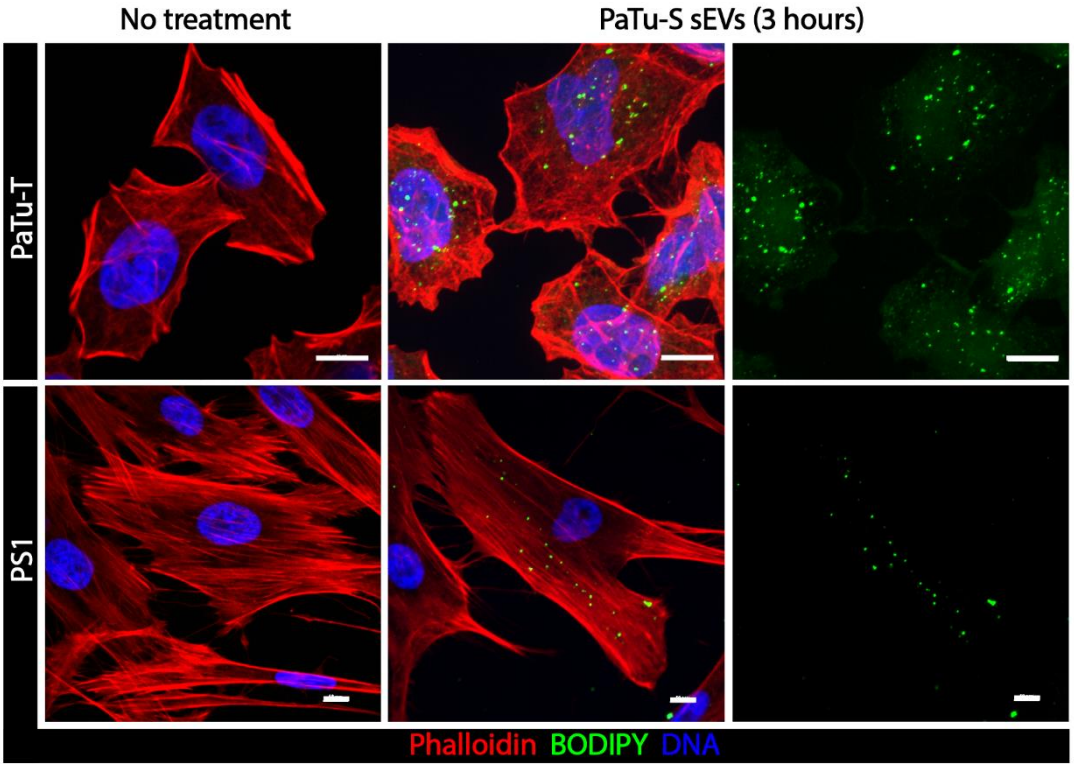

Figure 5.1 Cancer sEVs uptake in PaTu-T and PS1 cells. Top row, PaTu-T cells untreated (left) and treated with BODIPY labelled sEVs (middle = merge, right = sEVs only). Bottom row, PS1 cells untreated (left) and treated with BODIPY labelled sEVs (middle = merge, right = sEVs only). Cells stained with Phalloidin (F-actin) in red, BODIPY (sEVs) in green and Hoechst (DNA) in blue. Cells were fixed for 3 hours after the addition of sEVs. Scale bar represents 10 µm.

5.2. $_s$EVs secreted by PDAC cells with supernumerary centrosomes significantly enhance PSC activation

Having confirmed that PaTu-S $_s$EVs can be transferred to recipient cells and thus have the potential to transfer their biological cargo to target cells, we investigated whether $_s$EVs secreted by cells with and without extra centrosomes are functionally different from one another. Initially, we decided to investigate possible tumourigenic roles for these EVs in the cells of the tumour microenvironment.

Pancreatic cancer is characterised by the presence of a dense desmoplastic stroma that consists of numerous extracellular matrix (ECM) proteins, and stromal cells including cancer associated fibroblasts (CAFs) and pancreatic stellate cells (PSCs) (Erkan, Hausmann, *et al.*, 2012). In recent years, the desmoplastic stromal reaction/ fibrosis that is characteristic of PDAC has been attributed to chronic and sustained activation of PSCs during tumour progression (Erkan, Adler, *et al.*, 2012). Additionally, once activated, the PSCs promote fibrosis and facilitate tumour growth progression through extensive bidirectional interplay between the PSCs and PDAC cells (Apte *et al.*, 2004; Bachem *et al.*, 2005; Rosa F Hwang *et al.*, 2008; Vonlaufen *et al.*, 2008; Xu *et al.*, 2010). Notably, it has been demonstrated, that during tumourigenesis, PSCs can become activated in response to paracrine signalling from neighbouring cancer cells (Apte *et al*., 1999; Mews *et al*., 2002; Gao and Brigstock, 2005; Kordes *et al*., 2005; Vonlaufen *et al.*, 2010). Furthermore, recent studies have identified a role for cancer-derived $_{s}$EVs (e.g. exosomes) in the activation of fibroblasts and pancreatic stellate cells (Webber *et al.*, 2010a; Masamune *et al.*, 2018). We therefore, decided to investigate changes in PSC activation in response to treatment with $_{s}$EVs derived from cells with and without the induction of centrosome amplification.

5.2.1. Design of EV-mediated PSC activation experiments

To analyse differences in the activating capacity of EVs from cells with and without extra centrosomes the following experimental procedure was used: PaTu-S.PLK4 cells were plated in T175 cell culture flasks and either left untreated or treated with DOX (to induce centrosome amplification) for 48 hours. Cells were then washed in PBS before EV-depleted growth medium was added to each flask. 48 hours later, the conditioned medium was harvested and EVs were isolated by serial ultracentrifugation as previously described (section 2.4). As we have previously shown that cells with extra centrosomes secrete more EVs, EV quantities were normalised between conditions, either by EV protein or EV number. Equal amounts (protein or number) of EVs from cells with (+ DOX) and without (- DOX) induction of centrosome amplification were then added to PS1 cells. If required, a second dose of the EVs was added 48 hours after the first. A schematic of the experimental procedure is detailed in Figure 5.2.1 A. In addition to EV treatments,

two control conditions were also included with each experiment: a negative control in which no treatment was issued to the PS1 cells to ensure basal activation levels remained low and a positive control in which TGF-β was used to strongly activate the PS1 cells to ensure the stellate cells were sensitive to activation stimuli.

Activated PSCs are characterised by an increase in expression and change in the organisation of the cytoskeletal protein α-SMA. Upon activation α-SMA shifts from diffuse throughout the cell to organised stress fibres, therefore, to analyse PSC activation, we performed immunofluorescent staining of α-SMA on PSCs 72 hours after the addition of EVs and quantified stress fibre formation per cell. Activation was stratified into three categories; i) basal activation, where α-SMA is predominantly diffuse throughout the cell ii) activation, where thin α-SMA stress fibres have formed but some α-SMA still remains diffuse throughout the cell and iii) strong activation, where α-SMA is no longer diffuse and full α-SMA fibres have formed throughout the cell. Representative images of these three activation categories are shown in Figure 5.2.1 B. Activation was quantified per cell, based on α-SMA fibre formation in roughly 150 cells per condition.

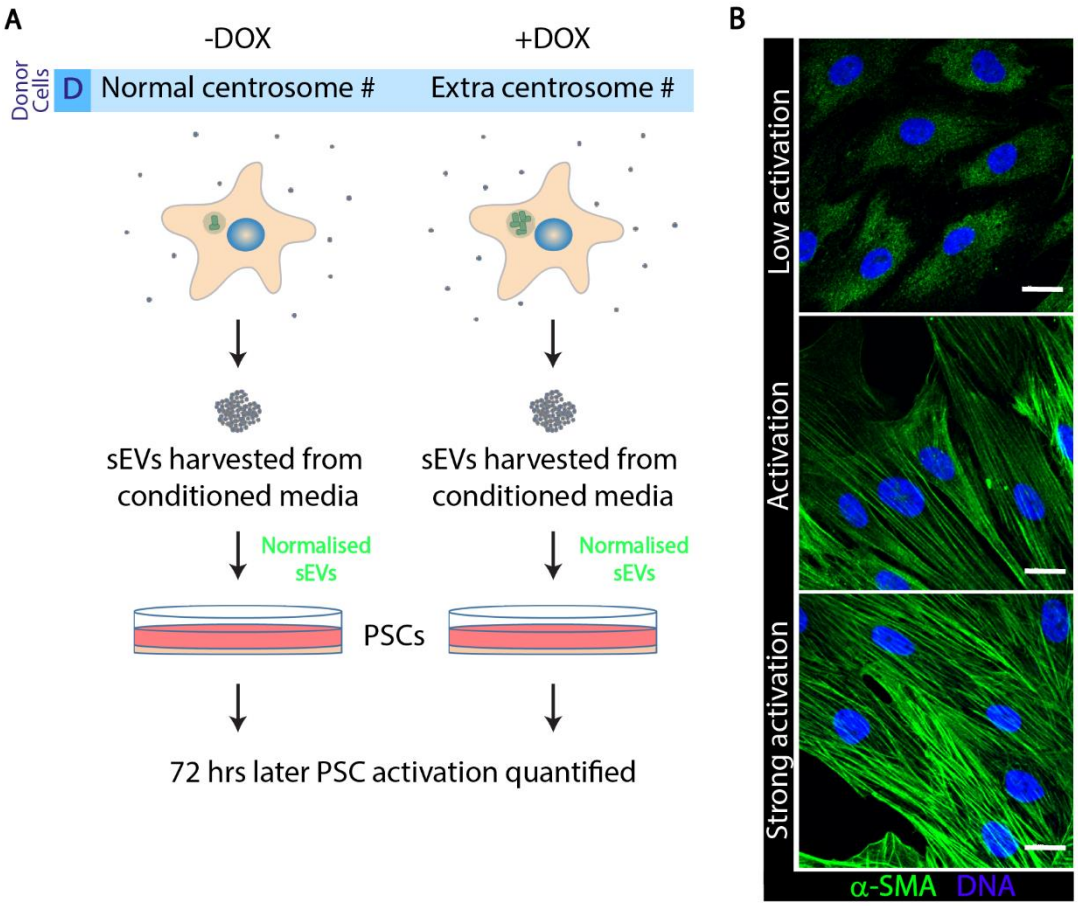

Figure 5.2.1 Experimental design for analysing EV-mediated PSC activation. A) Schematic of the experimental procedure. EVs were harvested from donor cells (PaTu-S.PLK4) with (+ DOX) or without (- DOX) centrosome amplification. EVs were normalised either to EV protein or EV number. Equal amounts of the isolated EVs was added to the growth media of PS1 cells. 72 hours later PS1 activation was quantified based on α-SMA fibre formation. D= donor cells **B)** Representative confocal images of PS1 activation levels based on α-SMA organisation showing low activation, activation and strong activation. α-SMA is depicted in green, DNA in blue. Scale bar represents 20 µm.

5.2.2. Optimising experimental conditions for analysing EV-mediated PSC activation

Whilst EVs have been used in functional assays for the past few decades, no standard protocols are currently in place specifically for $_{s}$EVs. Initial experiments were therefore performed using different quantities and doses of $_{s}$EV exosomes to optimise the experimental conditions. EV quantities were used at 5-30 µg, similar to that used in a selection of recent publications (Costa-Silva *et al.*, 2015; Wei *et al.*, 2017).

Prior to the addition of EVs to PS1 cells, a number of important controls were performed and used throughout subsequent experiments (see Figure 5.2.2.1 A). Here we show that basal levels of PS1 activation remain consistently at around 5% (ctr; see Figure 5.2.2.1) and we demonstrate that the PS1 cells have a high capacity for activation in response to recombinant TGF-β, our positive control, which resulted in activation in ~98-99% of cells. Furthermore, we tested the activating capacity of the conditioned media harvested from PaTu-S.PLK4 cells with (+) and without (-) DOX both before and after EV removal by ultracentrifugation (After UC; see Figure 5.2.2.1). To do this, conditioned medium was added directly onto PS1 cells for 72 hours and PS1 activation was quantified (see Figure 5.2.2.1). This analysis showed that conditioned media alone was not sufficient to induce PS1 activation above basal levels.

To analyse the effect of concentrated EVs on PS1 activation, $_{L}$EVs and $_{s}$EVs were harvested from PaTu-S.PLK4 cells as described in section 5.2.1 and the protein content of each sample quantified using the BioRad protein assay. EV protein concentration was then normalised between conditions and incremental concentrations of EVs were added to the stellate cells, ranging from 5 µg -30 µg (see Figure 5.2.2.1 A). As $_{L}$EV harvests always resulted in a much lower yield than $_{s}$EVs harvests, $_{L}$EVs were used at 20 µg only. From these initial experiments, it was found that in all cases, stellate cells incubated with EVs from + DOX cells always resulted in increased total PS1 activation (strong activation and activation combined) as determined by α-SMA fibre formation, indicating for the first time that EVs from cells with supernumerary centrosomes can enhance PSC activation. Furthermore, in most cases, a clear increase was also observed in % strong activation after treatment with EVs from + DOX cells. As conditioned media alone is not sufficient to elicit PS1 activation, this result indicates that a higher concentration of EVs

is necessary to induce PSC activation and indicates that it is the EVs and not other secreted factors that are causing PSC activation. These initial experiments also demonstrate that increasing the $_{S}$EV protein concentration from 5 µg to 10 µg more than doubled the % total PS1 activation, where activation with $_{S}$EVs from - DOX cells rose from 9.7 - 21.1% and activation with $_{S}$EVs from +DOX cells rose from 16.2 - 38.3%. Interestingly, the % of PS1 activation after treatment with 20 µg and 30 µg of $_{S}$EVs, resulted in only modest increases in activation (~5-6%) compared to those achieved with 10 µg for both types of $_{S}$EV. As TGF- β has the capacity to strongly activate almost all the PS1 cells present in the sample (~95%), this result may indicate that a threshold exists for PS1 activation by $_{S}$EVs. Whether increased incubation time or further increases in $_{S}$EV protein could overcome this remains to be tested. These experiments also revealed that treatment of PS1 cells with 20 µg of $_{L}$EVs resulted in very minor levels of PS1 activation, <9% with $_{L}$EVs from + DOX cells and < 5% with $_{L}$EVs from - DOX cells. Thus, as $_{S}$EVs are secreted more and $_{L}$EVs do not activate PSCs, $_{S}$EVs became the focus of the subsequent work.

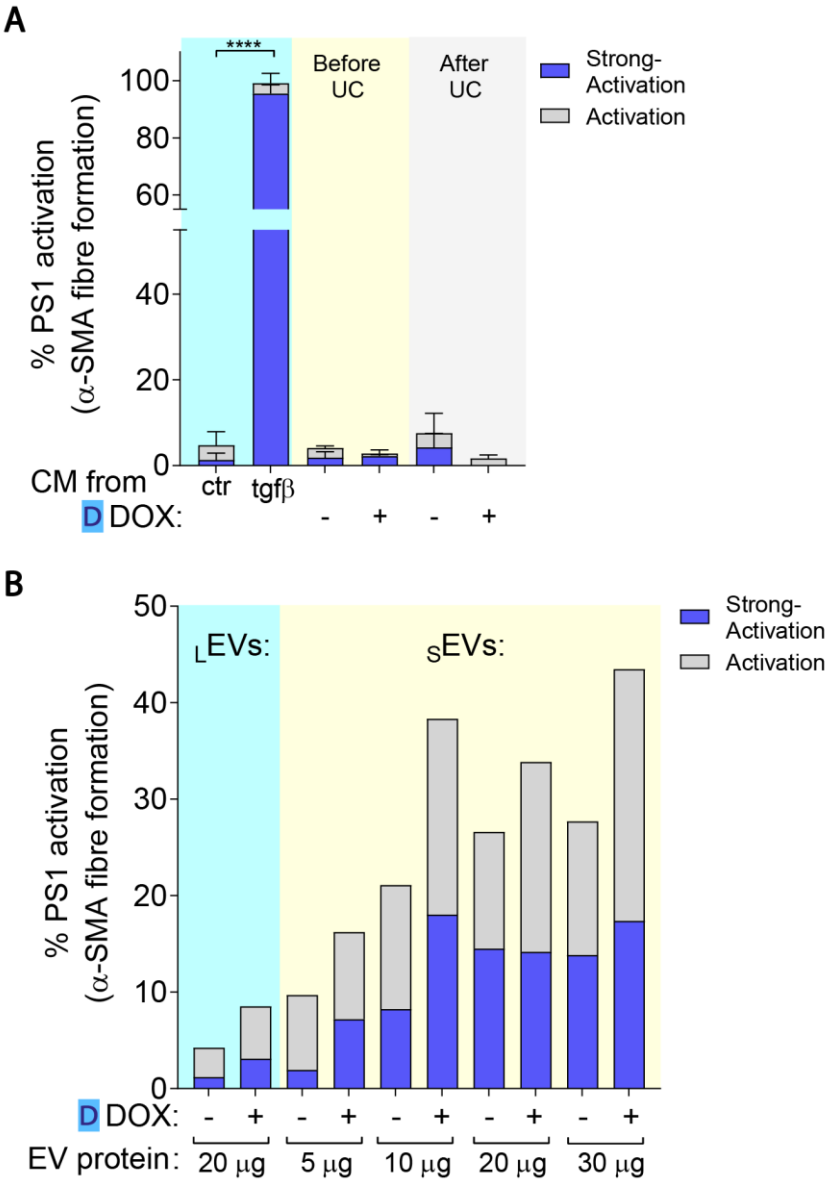

Figure 5.2.2.1 Initial PS1 activation tests. A) Quantification of % PS1 activation as determined by α-SMA fibre formation in control conditions. PS1 cells were treated as follows for 72 hours: i) untreated (ctr), ii) TGF-β, iii) CM from donor cells - DOX, iv) CM from donor cells + DOX, v) CM from donor cells – DOX after UC, vi) CM from donor cells + DOX after UC. Error bars represent mean ± standard deviation, N=3. Data analysed using one-way ANOVA with Tukey's post hoc test (**** $p<0.0001$). Significant difference to the control is highlighted with ****. **B)** Quantification of % PS1 activation as determined by α-SMA fibre formation after 72 hour treatment with 5- 30 µg of $_{s}$EVs and 20 µg of $_{L}$EVs from donor cells – or + DOX. N=1.
Activation levels stratified into two categories: strong activation and activation. Ctr=control, CM= conditioned media, UC = ultracentrifugation, DOX=doxycycline hyclate. D = donor cells. Donor cells were PaTu-S.PLK4.

To determine if the % PS1 activation achieved with 10 µg of $_s$EV protein could be improved, similar experiments were set up with an additional $_s$EV dosing step. Here, two doses of $_s$EVs at either 10 µg or 20 µg were added to the PS1 cells, the first at 0 hours and the second at 48 hours. As can be seen in Figure 5.2.2.2 A, a clear increase in PS1 activation can be seen upon treatment with 2 doses of $_s$EVs from + DOX cells compared to 2 doses of $_s$EVs from – DOX cells both at 10 µg and 20 µg of sEV protein. The addition of a second dose of $_s$EVs resulted in around 10% higher PS1 activation in cells treated with $_s$EVs from +DOX cells compared to an increase of merely 4% in $_s$EVs from – DOX cells. All subsequent experiments were therefore performed using a double dose of $_s$EVs. Whilst two doses of $_s$EVs at 20 µg resulted in visibly higher levels of PSC activation, $_s$EV preparation is a limiting step. Consequently, for practical reasons, two doses of $_s$EVs at 10 µg were used for future experiments.

While normalising $_s$EVs to protein content has long been the norm for functional assays, it is conceivable that the induction of centrosome amplification may alter the protein content of the $_s$EVs. As our initial results, (outlined in Chapter 3), show that centrosome amplification induces $_s$EV secretion, it was decided that normalising to $_s$EV number may be more prudent. Using ImageStream to analyse EV number and BioRad protein assay to quantify protein, it was determined that there were roughly 20 million $_s$EVs present in 10 µg of the PaTu-S.PLK4 – DOX $_s$EVs. We therefore investigated whether two doses of 20 million $_s$EVs would elicit similar results to those observed with 10 µg of $_s$EVs protein. As can be seen in Figure 5.2.2.2 B, when $_s$EVs were normalised to number, a clear increase in % total PS1 activation (similar to when normalising to EV protein) could still be observed in PS1 cells treated with $_s$EVs from + DOX cells compared to $_s$EVs from - DOX cells. Notably, however, PSC activation post treatment with 20 million $_s$EVs resulted in lower levels of PSC activation compared to treatment with 10 µg of EV protein. It is therefore likely that 20 million $_s$EVs does not equate exactly to 10 µg of EV protein. However, as 20 million $_s$EVs still resulted in a clear increase in PSC activation, henceforth, all further PS1 activation experiments were performed using two doses of 20 million $_s$EVs.

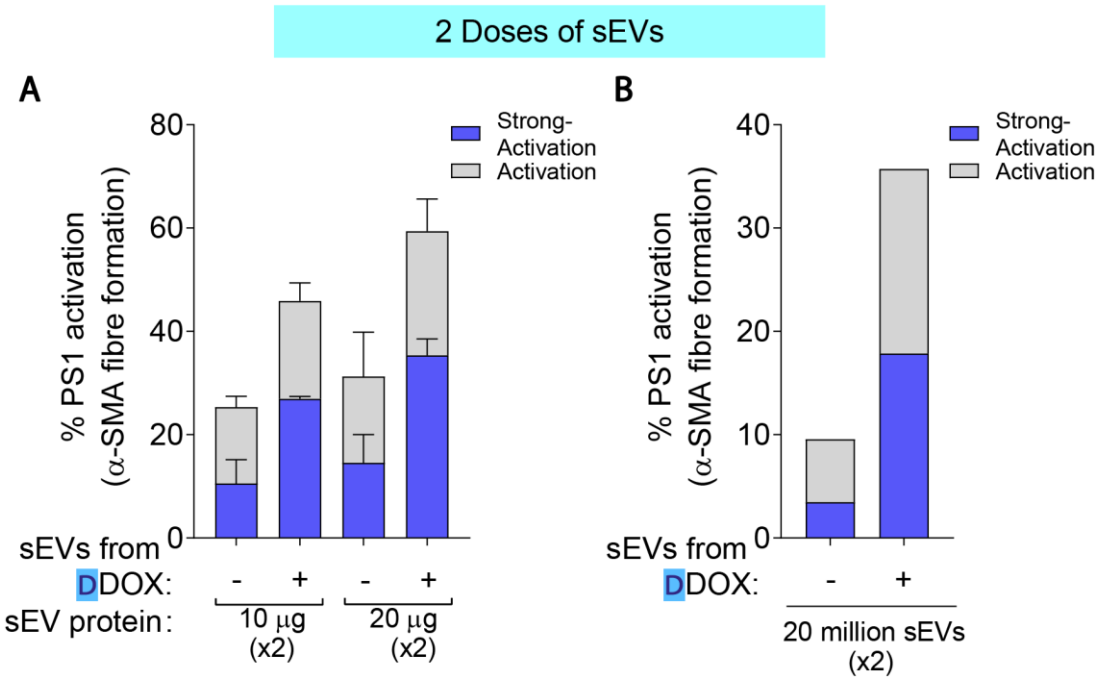

Figure 5.2.2.2 PS1 activation following 2 doses of ₛEVs normalised to protein or ₛEVs number. **A)** Quantification of % PS1 activation as determined by α-SMA fibre formation after 72 hour treatment with 2 doses of ₛEVs from donor cells – /+ DOX normalised to ₛEV protein (10 µg or 20 µg) N=2. **B)** Quantification of % PS1 activation as determined by α-SMA fibre formation after 72 hour treatment with 2 doses of ₛEVs from donor cells – /+ DOX normalised to ₛEV number (20 million ₛEVs). N=1.
Activation levels stratified into two categories: strong activation and activation. Error bars represent mean ± standard deviation. DOX=doxycycline hyclate. D = donor cells. Donor cells were PaTu-S.PLK4.

5.2.3. ₛEVs secreted by cells with supernumerary centrosomes significantly enhance PS1 cell activation

Using the experimental conditions outlined in section 5.2.2, we investigated the ability of ₛEVs secreted by PATu-S.PLK4 cells with (+DOX) and without (-DOX) the induction of centrosome amplification to activate PS1 cells. Analysis revealed that ₛEVs secreted by cells with supernumerary centrosomes significantly enhanced PS1 activation (Figure 5.2.3). An average of 30% total PS1 activation (strong activation and activation) was observed in samples treated with ₛEVs from + DOX donor cells compared to 6.8% total PS1 activation in samples treated with ₛEVs from - DOX donor cells. In fact, significant increases could be observed in strong activation alone, where strong activation reached ~ 13.9% in PS1 cells treated with ₛEVs from + DOX donor cells compared to 1.6% in PS1

cells treated with sEVs from - DOX donor cells, indicating that sEVs secreted by cells with extra centrosomes have a much stronger effect on the activation of PSCs.

Taken together, the work presented here demonstrates for the first time that sEVs derived from cells with amplified centrosomes elicit a stronger activation of PSCs compared to sEVs from cells with normal centrosome number. As sEV number was normalised between conditions, our results suggest that sEVs secreted by cells with extra centrosomes may have an altered biological cargo. This in turn suggests that centrosome amplification may not only induce overall secretion of sEVs but also induce secretion of a specific subset of sEVs which have enhanced PSC activating potential. Furthermore, these results have since been replicated by another member of the Godihno laboratory using sEVs secreted by the HPAF-II.PLK4 cell line, providing further evidence to support the findings presented here.

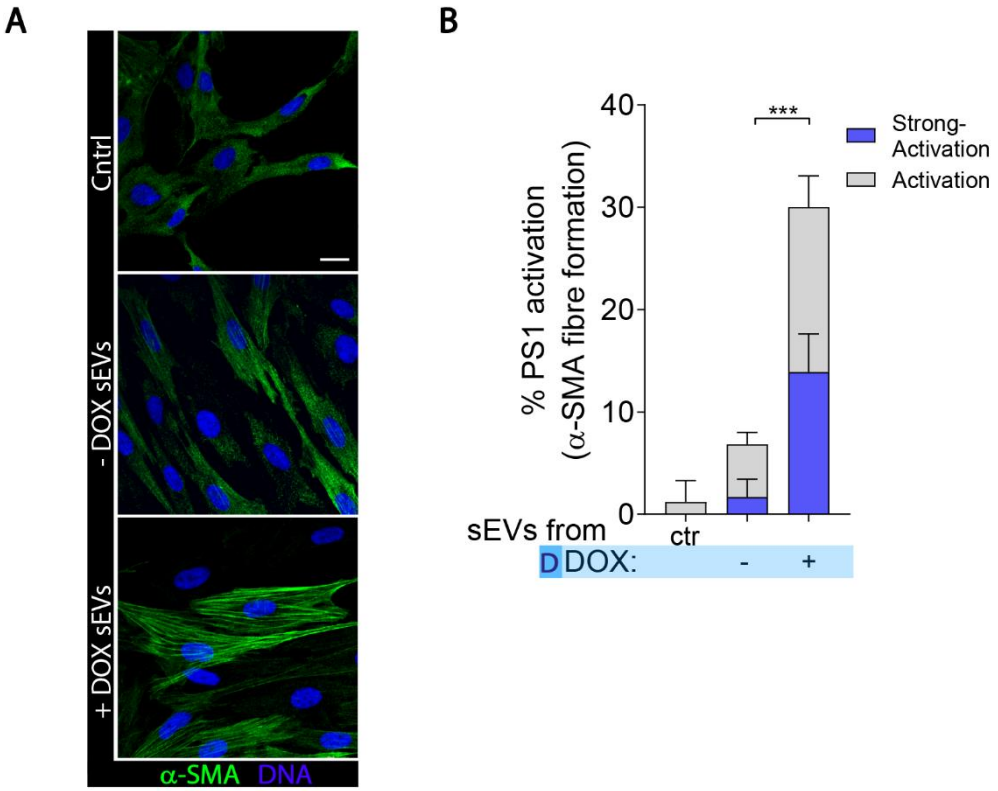

Figure 5.2.3 sEVs from PDAC cells with supernumerary centrosomes significantly enhance PS1 cell activation. A) Representative confocal images of α-SMA organisation in PS1 cells 72 hours post treatment with i) untreated control (ctr) ii) 20 million sEVs (2 doses) from – DOX donor cells iii) 20 million sEVs (2 doses) from + DOX donor cells. α-SMA is depicted in green, DNA in blue. Scale bar represents 20 µm. **B)** Quantification of % PS1 activation as determined by α-SMA fibre formation in PS1 cells treated as described in (A). Activation levels stratified into two categories: strong activation and activation. Error bars represent mean ± standard deviation, N=3. Data analysed using one-way ANOVA with Tukey's post hoc test (*** p<0.001).
DOX=doxycycline hyclate. D = donor cells. Donor cells were PaTu-S.PLK4.

5.2.4. Centrosome amplification-associated ROS is required for PSC activation by $_s$EVs from cells with amplified centrosomes

Our results demonstrate that $_s$EVs secreted by cells with supernumerary centrosomes have enhanced PSC activating capabilities, suggesting that centrosome amplification induces not only an increase in total $_s$EV secretion but also in the secretion of a subset of $_s$EVs. Since our previous work (Chapter 4) found centrosome amplification-linked ROS to be responsible for the increased secretion of $_s$EVs by cells with extra centrosomes, we hypothesised that these changes in cellular ROS may also play a role in the secretion of $_s$EVs that harbour the heightened PSC activation capacity. To test this, we analysed the PS1 activating capacity of $_s$EVs secreted by PaTu-S.PLK4 donor cells that had been treated as follows: i) – DOX, ii) + DOX and iii) +DOX +NAC. Interestingly, whilst $_s$EVs derived from + DOX cells increased PS1 activation as expected, quenching centrosome amplification–associated ROS with NAC in these cells prevented the secreted $_s$EVs from eliciting the same increase in PS1 activation. Whilst a third replicate is still required for this experiment, these results indicate that centrosome amplification-associated ROS is likely responsible for the increased secretion of a subset of $_s$EVs which contain an altered biological cargo that confers a heightened capacity for $_s$EV-mediated PSC activation. The experiments performed here, however, cannot determine whether the observed effect is specific to increased cellular ROS alone, or specific to centrosome amplification-associated ROS. It would therefore be interesting to perform the same analysis using $_s$EVs harvested from cells where ROS is induced independently of centrosome amplification with H_2O_2. These additional experiments would provide a clearer view on whether this result is specific to centrosome amplification-associated ROS or if it is a more global mechanism relating to generalised increases in cellular ROS.

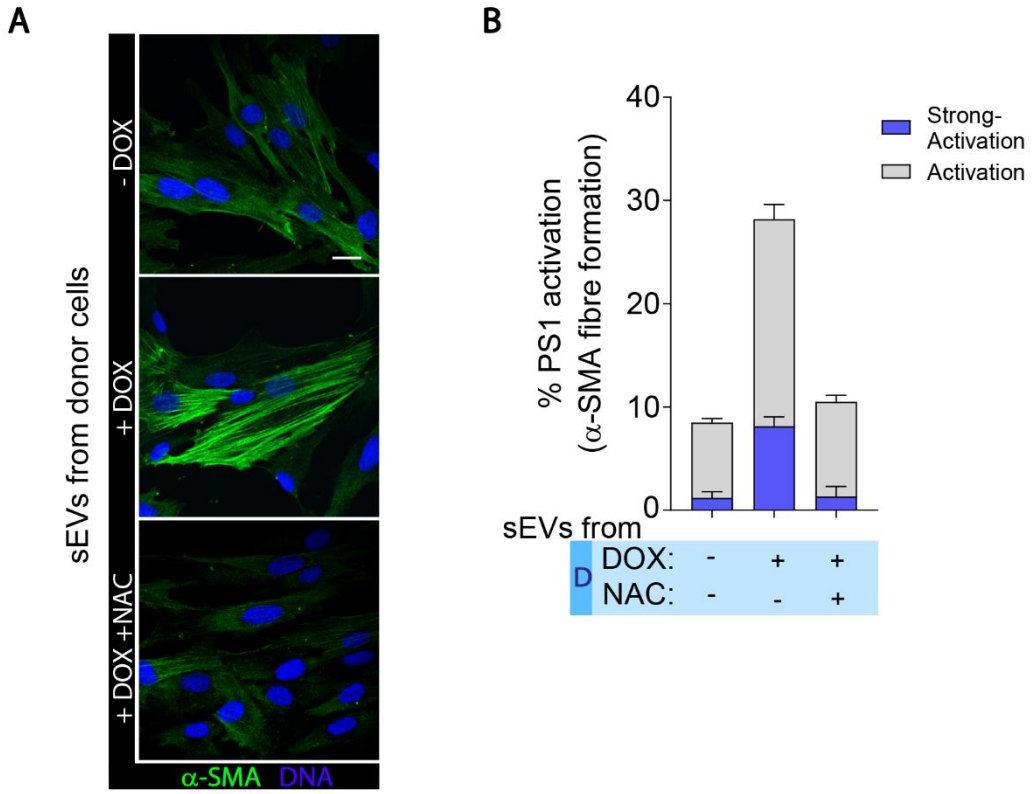

Figure 5.2.4 Centrosome amplification-associated ROS is required for PSC activation by $_s$EVs from cells with amplified centrosomes. A) Representative confocal images of α-SMA organisation in PS1 cells 72 hours post treatment with: i) 20 million $_s$EVs (2 doses) from – DOX donor cells ii) 20 million $_s$EVs (2 doses) from + DOX donor cells, iii) 20 million $_s$EVs (2 doses) from donor cells treated with DOX and NAC. α-SMA is depicted in green, DNA in blue. Scale bar represents 20 µm. **B)** Quantification of % PS1 activation as determined by α-SMA fibre formation in PS1 cells treated as described in A. Activation levels stratified into two categories: strong activation and activation. Error bars represent mean ± standard deviation, N=2.
DOX=doxycycline hyclate, NAC = N-acetyl cysteine, D = donor cells. Donor cells were PaTu-S.PLK4.

5.3 $_s$EVs capable of activating PSCs elute specifically in Size Exclusion Chromatography fraction 8.

Whilst classical ultracentrifugation (UC) is still one of the most widely used methods for EV isolation it has a number of drawbacks. Crucially, the purity of the isolated vesicles has been questioned and a number of studies have revealed EVs isolated by UC to co-pellet with larger contaminating proteins. Thus, we cannot be certain if the PSC activation we observed with $_s$EVs pelleted by UC is truly due to the EVs themselves or contaminating proteins/ other aggregates. To address this, the PSC experiments were performed using vesicles prepared with an additional EV purification step, whereby EVs isolated by UC were then subjected to size exclusion chromatography (SEC). This process

involves passing the UC sample through a column containing porous resin particles. Due to their size, EVs themselves pass through the column largely unimpeded, however, impurities including proteins, protein complexes and other small molecules enter the pores of the resin particles. This impedes their passing through the column and results in them eluting in much later fractions (see schematic in Figure 5.3.1 A). SEC columns such as the qEV original izon science SEC columns used for these experiments, have previously been shown to yield high purity EVs (Böing *et al.*, 2014; Muller *et al.*, 2014; Welton *et al.*, 2015; Benedikter *et al.*, 2017). To perform SEC, 500 µl of $_{s}$EVs isolated by UC were applied to the column. Once the sample had passed into the top filter, the column was topped up with PBS buffer that had been twice filtered using 0.22 µm syringe filters. Immediately after the sample had passed into the column, 500 µl fractions were taken. Fractions 1-12 were collected, (EVs are expected to elute in fractions 7-10 using this column), with contaminating proteins eluting in fractions 11 onwards (as described in izon science technical note). The number of $_{s}$EVs present in each fraction was then quantified using ImageStream (Figure 5.3.1 B). As expected, $_{s}$EVs were found to elute in fractions 7-10, with the majority eluting in fractions 8 and 9. Whilst some vesicles were observed in fraction 7 and 10, the yield is very low. The primary eluting fractions (8 and 9) did not change with sample type i.e $_{s}$EVs isolated from donor cells treated with and without DOX eluted in similar fractions. It is important to note that whilst purity of these $_{s}$EVs is improved, the yield is clearly decreased. It was found that only around 55-60% of the $_{s}$EVs present in the UC samples were recovered in the SEC fractions (sum fractions 7-10). Additionally, these fractions are significantly diluted as they are split over 4 x 500 µl fractions. Therefore, to obtain vesicles after SEC at a high enough concentration to perform PSC activation experiments, a much larger initial UC harvest of EVs is required. To perform these experiments, we therefore harvest EVs from the conditioned media of at least 12 x T175 flasks per condition.

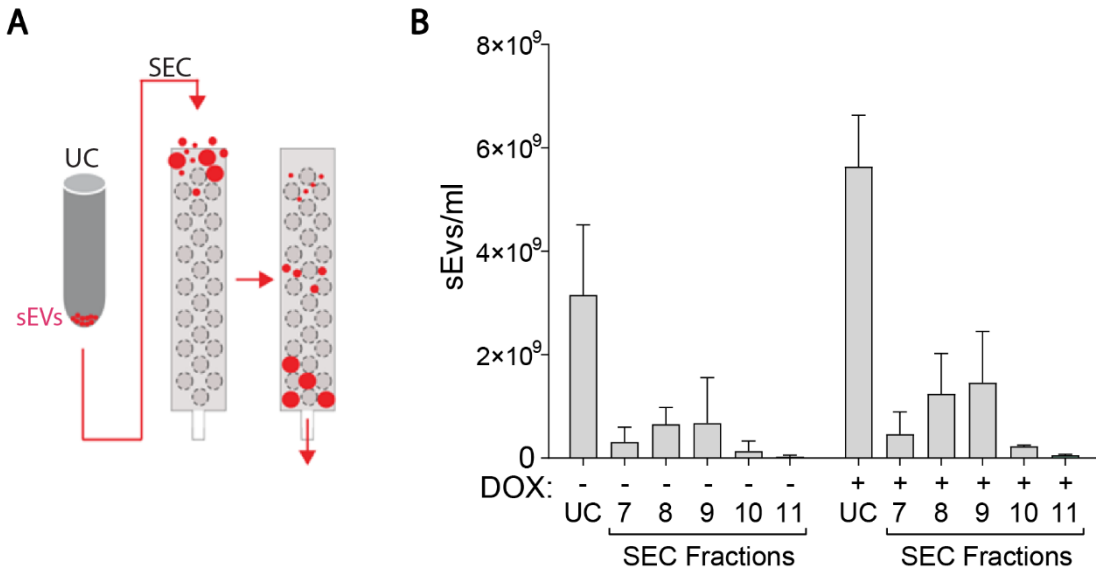

Figure 5.3.1 $_s$EV purification and separation by size exclusion chromatography. A) Schematic diagram depicting size exclusion chromatography. Larger particles including EVs pass largely unimpeded through the column, whereas small molecules including contaminating proteins enter the pores of the resin beads, impeding their progress and resulting in their elution in much later fractions. **B)** Quantification of $_s$EVs isolated from donor cells treated without (-) and with (+) DOX, after UC and then subsequently after SEC as measured by ImageStream® Mark II Imaging Flow Cytometer. Error bars represent mean ± standard deviation, N=3.
DOX=doxycycline hyclate, UC=ultracentrifugation, SEC=size exclusion chromatography. Donor cells were PaTu-S.PLK4.

In addition to vesicle concentration, the size distribution of $_s$EVs present in each sample was also quantified (Figure 5.3.2). As before, size was measured using NanoSight particle tracking analysis (NTA) with a NanoSight NS300. Analysis revealed that $_s$EVs isolated by UC only, from PaTu-S.PLK4 cells without centrosome amplification had a mean particle size of 96 nm. Interestingly, upon induction of centrosome amplification in these cells, the mean particle $_s$EV size increased slightly to 101 nm. Furthermore, NTA analysis revealed slight differences in the mean $_s$EVs populations in the two main SEC fractions (fraction 8 and fraction 9). It was found that $_s$EVs from – DOX cells that eluted in SEC fraction 8 had a mean size of 97 nm whereas those that eluted in fraction 9 had a mean size of 95 nm. Similarly, $_s$EVs isolated from + DOX cells, that eluted in SEC fraction 8 had a mean size of 104 nm compared to a mean size of 101 nm in SEC fraction 9. Therefore, in addition to suggesting that $_s$EVs secreted by cells with extra centrosomes may be slightly larger than those secreted by cells with normal centrosome number, this result also indicates that the vesicles present in each SEC fraction may differ in size.

Importantly, the observed particle sizes all fall within the correct size range to be considered exosomes. However, whilst size alone is not sufficient to distinguish exosomes from MVs or other EV types, this result indicates that there is likely an enrichment of exosomes in the isolated $_s$EV pellets. Due to the small volume of vesicles collected in Fraction 7, the size of these vesicles could not be analysed.

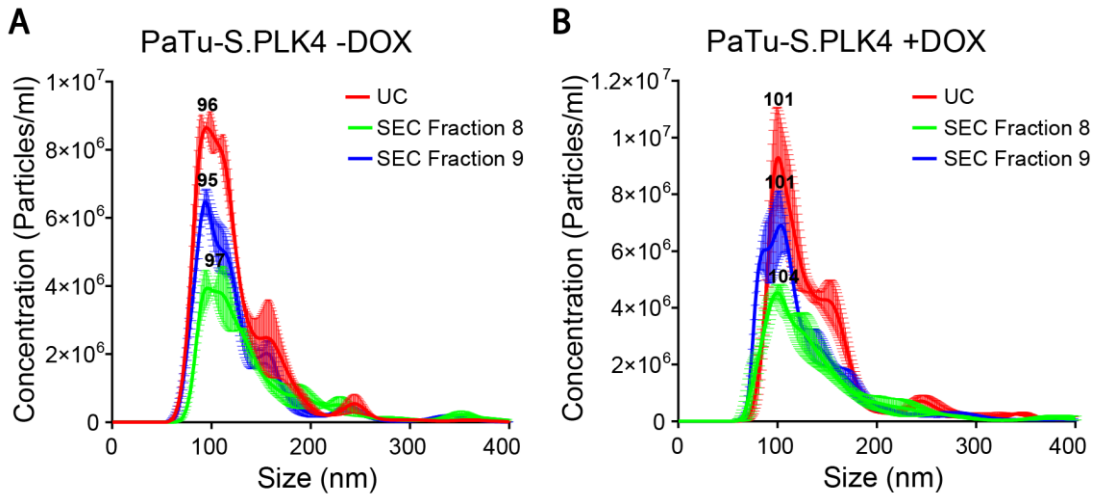

Figure 5.3.2 Particle size distribution quantification of UC and SEC samples. A) Size distribution curves determined by Nanosight NS300 (Nano-particle tracking analysis) of $_s$EVs isolated from donor cells treated without (-) DOX after UC alone and post SEC. The primary EV elution fractions, SEC fraction 8 and SEC fraction 9 were analysed. Mean particle size was determined as 96 nm for UC isolates (red distribution), 97 nm for SEC 8 isolates (green distribution) and 95 nm for SEC 9 isolates (blue distribution). **B)** Size distribution curves determined by Nanosight NS300 (Nano-particle tracking analysis) of $_s$EVs isolated from donor cells treated with (+) DOX after UC alone and post SEC. The primary EV elution fractions, SEC fraction 8 and SEC fraction 9 were analysed. Mean particle size was determined as 101 nm for UC isolates (red distribution), 104 nm for SEC 8 isolates (green distribution) and 101 nm for SEC 9 isolates (blue distribution). Error bars (shown in red for UC isolates, green for SEC 8 isolates and blue for SEC 9 isolates) indicate standard error of the mean. DOX=doxycycline hyclate, UC=ultracentrifugation, SEC=size exclusion chromatography. Donor cells were PaTu-S.PLK4.

The $_s$EVs isolated by SEC were then used for subsequent PS1 activation experiments (Figure 5.3.3). Additionally, where possible $_s$EVs that eluted in SEC fraction 7 were also used, however low yields resulted in only one replicate to be generated with these $_s$EVs.

Analysis revealed that $_s$EVs derived from cells without the induction of centrosome amplification (- DOX) induced only low levels of total activation (<10%) regardless of SEC fraction. As expected $_s$EVs isolated from cells with extra centrosomes (+ DOX) were

found to activate PS1 cells as previously demonstrated. Interestingly however, the $_{s}$EVs that retain these activating capabilities were found to elute specifically in SEC fraction 8, where these vesicles resulted in an average of ~36% PS1 activation. Furthermore, $_{s}$EVs from + DOX donor cells that eluted in this fraction were also found to significantly induce strong activation of PSCs compared to controls and all other SEC fractions.

In conclusion, after the removal of contaminating small molecules by SEC, these results provide strong evidence to support the hypothesis that the $_{s}$EVs in the samples are responsible for the observed increases in PS1 activation. Moreover, these experiments revealed that the $_{s}$EVs from + DOX cells that confer PS1 activating capabilities specifically elute in one SEC fraction (fraction 8). This result suggests that cells with centrosome amplification may secrete a specific subset of $_{s}$EVs that have heightened PSC activating abilities.

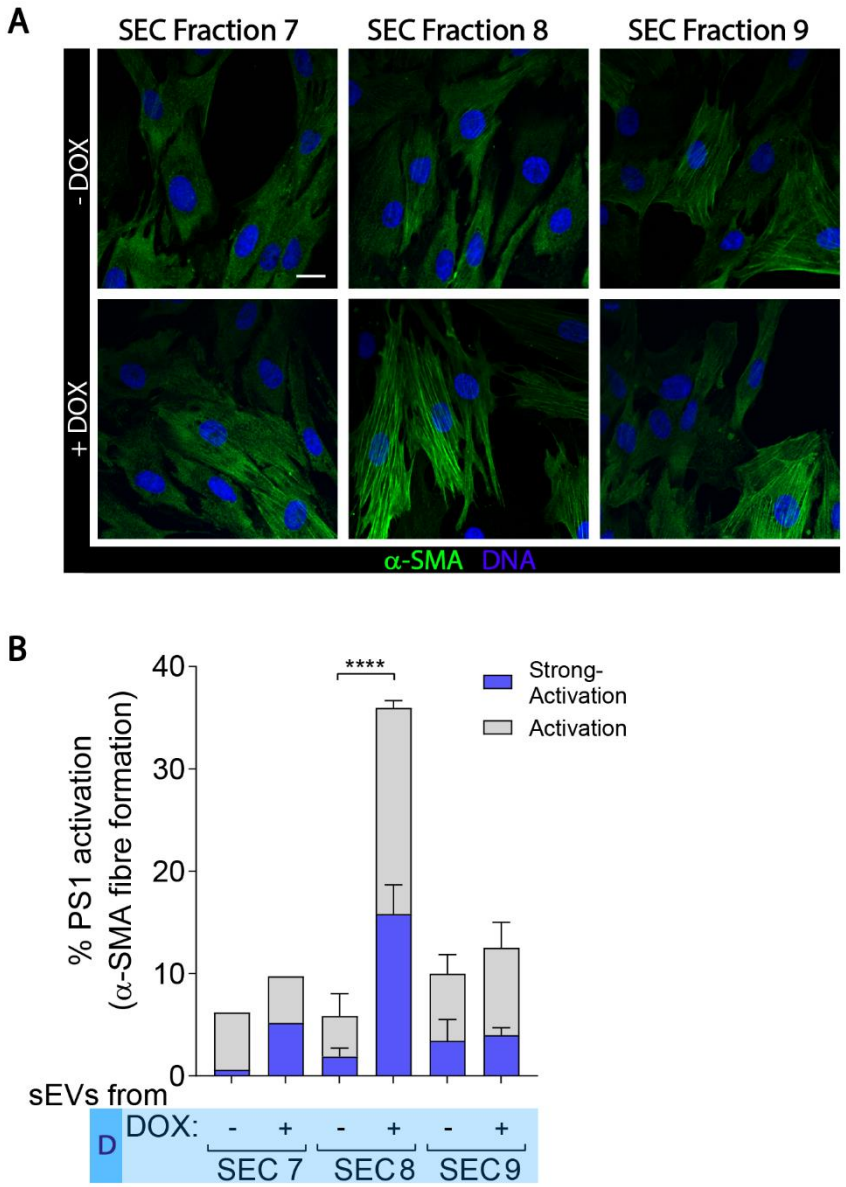

Figure 5.3.3 $_s$EVs from PDAC cells with supernumerary centrosomes that elute in SEC fraction 8 significantly enhance PS1 cell activation. A) Representative confocal images of α-SMA organisation in PS1 cells 72 hours post treatment with $_s$EVs derived from – DOX or + DOX donor cells that have eluted in SEC fractions 7-9. PS1 cells were treated with 2 doses of 20 million $_s$EVs per condition. α-SMA is depicted in green, DNA in blue. Scale bar represents 20 µm. **B)** Quantification of % PS1 activation as determined by α-SMA fibre formation in PS1 cells treated as described in A. Activation levels stratified into two categories: strong activation and activation. For SEC fraction 8 and 9 N=3, for SEC fraction 7 N=1. Error bars represent mean ± standard deviation. Data analysed using one-way ANOVA with Tukey's post hoc test (**** $p<0.0001$).
DOX=doxycycline hyclate, SEC=size exclusion chromatography, D = donor cells. Donor cells were PaTu-S.PLK4.

5.4. Proteomic analysis of $_s$EVs with stable isotope labelling of amino acids in culture

5.4.1 $_s$EVs sample preparation for SILAC-based proteomic analysis

The difference in PSC activating potential between exosomes from cells with and without supernumerary centrosomes suggests that they harbour a different biological cargo. We therefore planned to analyse changes in the cargoes of these vesicles, in the hopes of identifying the factor/s contributing to PSC activation. Whilst EVs contain a number of different biological cargos, including proteins, RNA, DNA and lipid rafts, a number of studies looking at the EV-mediated activation of PSCs had previously identified EV proteins such as TGF-β to have key roles in this process (Webber *et al.*, 2010b; Charrier *et al.*, 2014; Masamune *et al.*, 2018). We therefore began our analysis on the biological cargo of the isolated $_s$EVs by performing proteomic analysis. To analyse protein changes in $_s$EVs upon the induction of centrosome amplification, we used a stable isotope labelling by amino acids in cell culture (SILAC) based proteomic technique in collaboration with Faraz Mardakheh at the BCI. SILAC is a powerful method of quantitative proteomics that involves metabolic labelling of the samples with normal, medium and heavy labelled amino acids prior to mass spectrometry (MS). Typically, SILAC labelling involves labelling of lysine and arginine residues with normal/light, heavy [$^{15}N_2{}^{13}C_6$-lysine (Lys8) and $^{15}N_4{}^{13}C_6$-arginine (Arg10)] or medium [$^{2}H_4$-lysine (Lys4) and $^{13}C_6$-arginine (Arg6)] labels, which in combination with trypsin digest, ensures that all peptides in the sample will retain a label. Label incorporation followed by Liquid Chromatography with tandem mass spectrometry (LC-MS-MS) enables the identification and quantitation of the proteins present in each sample. As this method relies on efficient incorporation of the labels, cells are grown in media supplement with dialysed serum. This ensures that the amino acids added to the cell culture are the exclusive source of amino acids. Proline is also added to the medium to prevent metabolic conversion of the labelled arginine to proline. Whilst other proteomic methods require labelling post processing, SILAC-based differential labelling of cells allows samples to be combined early on during sample preparation. Thus, SILAC samples can be processed together, eliminating variability that could result from separate sample preparations. Additionally, the samples can be analysed together by LC-MS/MS,

enabling the relative peaks of the differentially labelled proteins to be accurately quantified in relation to each other and a ratio of the two labels to be generated.

SILAC based proteomic analysis of cells is fairly straightforward, light and heavy labels are usually sufficient. SILAC proteomic analysis of EVs however proved more complex. As EVs contain a relatively small number of proteins compared to total cell lysates, contaminating proteins can become an issue. Therefore, as EVs are isolated from the conditioned growth medium, it is possible that media proteins will be present in the samples and may cloud the analysis. As naturally occurring amino acids, such as those present in the media are labelled light, proteomic analysis of exosomes was performed using medium and heavy amino acid labels. This enabled any light labelled amino acids present in the samples to be disregarded as media/ other contaminants.

Prior to vesicle harvest for SILAC based proteomic analysis, PaTu-S.PLK4 cells were grown in SILAC DMEM supplemented with 10% dialysed FBS (that had been ultracentrifuged at 100,000 x g for 18 hours to deplete EVs), 1% penicillin/streptomycin and heavy or medium labelled amino acids for 2 weeks. The efficiency of heavy and medium label incorporation into cells was then analysed. To do this, a small aliquot of cells was lysed and digested as described in section 2.8 and analysed by Mass spec. MaxQuant analysis performed by our collaborator Faraz Mardakheh identified over 99% label incorporation in both cell lines. Once label incorporation had been confirmed, cells were plated for $_{s}$EV harvest. 40 x T175 flask containing heavy labelled cells were induced to amplify centrosomes (+DOX) and 40 x T175 flasks containing medium labelled cells were left untreated (-DOX). A schematic representation of the experimental workflow is depicted in Figure 5.4.1.1. Importantly, the experiment was replicated twice, the second time with reverse labelling i.e where medium labelled cells were induced with DOX and the heavy labelled cells left untreated. Reverse labelling was used to eliminate potential protein changes that result from the differentially labelled amino acids.

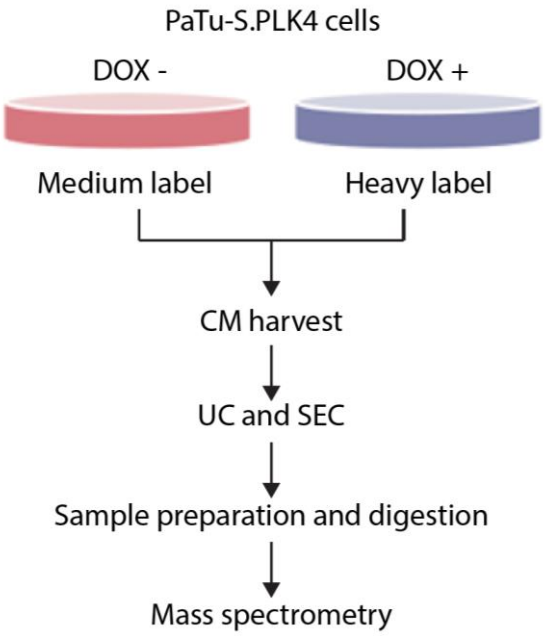

Figure 5.4.1.1 Schematic representation of SILAC proteomic analysis protocol. PaTu-S.PLK4 cells were grown in SILAC DMEM supplemented with heavy or medium labelled amino acids. Conditioned medium was harvested from untreated (- DOX) medium labelled cells and centrosome amplification induced (+DOX) heavy labelled cells. CM was harvested from all cells and pooled prior to $_{s}$EV isolation by UC and purification by SEC. SEC fractions 7, 8 and 9 were then prepared from mass spec analysis and mass spec was performed by our collaborator Faraz Mardakheh.
DOX=doxycycline hyclate, UC=ultracentrifugation, SEC=size exclusion chromatography, CM = conditioned media.

To ensure that the vesicles harvested were suitable for MS analysis, the conditioned media from two flasks per condition were collected and the $_{s}$EVs were isolated by ultracentrifugation for use in PS1 activation experiments. Analysis revealed that $_{s}$EVs secreted by + DOX cells for both the forward and reverse experiments were able to activate PS1 cells as expected (see Figure 5.4.1.2). Therefore, the $_{s}$EVs were deemed suitable for mass spec analysis. The conditioned media from the remaining flasks was then harvested to be processed for MS. Henceforth the conditioned media from the heavy labelled and medium labelled cells was pooled together and the samples were processed as one, eliminating potential variations associated with separate sample preparation. $_{s}$EVs were then isolated from the pooled conditioned media by ultracentrifugation and then purified further by SEC.

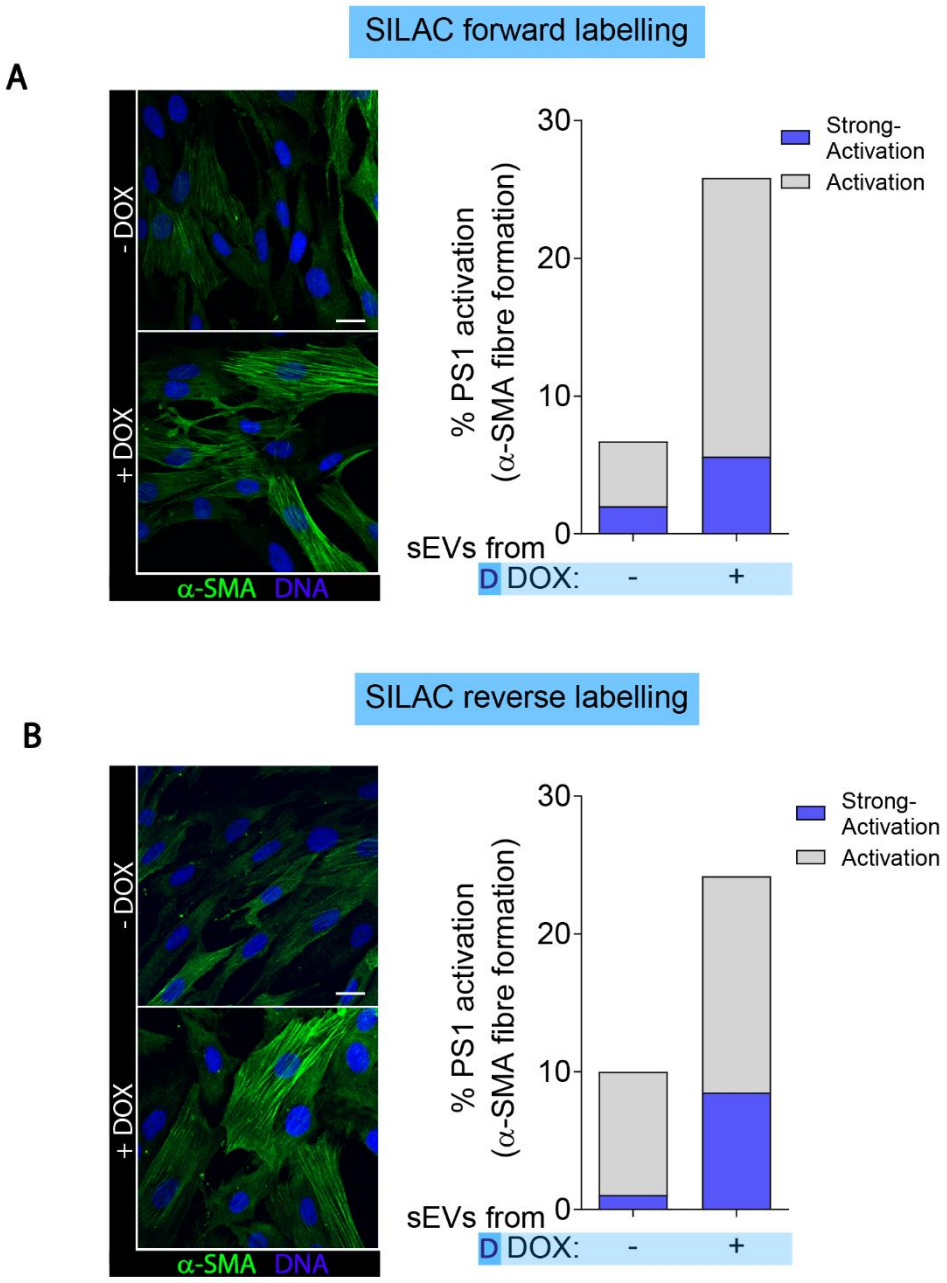

Figure 5.4.1.2 ₛEVs isolated for SILAC based proteomic analysis activate PS1 cells. A) PS1 activation after the addition of ₛEVs from the SILAC forward labelling experiment. Representative confocal images of α-SMA organisation and quantification of activation as determined by α-SMA fibre formation in PS1 cells 72 hours post treatment with i) 20 million ₛEVs (2 doses) from – DOX medium labelled donor cells iii) 20 million ₛEVs (2 doses) from + DOX heavy labelled donor cells. α-SMA is depicted in green, DNA in blue. Scale bar represents 20 µm. **B)** PS1 activation post the addition of ₛEVs from the SILAC reverse labelling experiment. Representative confocal images of α-SMA organisation and quantification of activation as determined by α-SMA fibre formation in PS1 cells 72 hours post treatment with i) 20 million ₛEVs (2 doses) from – DOX heavy labelled donor cells iii) 20 million ₛEVs (2 doses) from + DOX medium labelled donor cells. α-SMA is depicted in green, DNA in blue. Scale bar represents 20 µm.
Activation levels stratified into two categories: strong activation and activation. N=1.
DOX=doxycycline hyclate. D = donor cells. Donor cells were PaTu-S.PLK4.

The number of ₛEVs present in each SEC fraction for both the forward and reverse experiments was quantified by ImageStream (see Figure 5.4.1.3). Analysis revealed similar distributions of ₛEVs post SEC as had been previously observed. A slightly higher yield of ₛEVs was recovered, however, in the reverse labelled experiment. SEC fractions 7, 8 and 9 were then prepared for MS analysis as described in section 2.8. MS and MaxQuant analysis was performed by our collaborator Faraz Mardakheh.

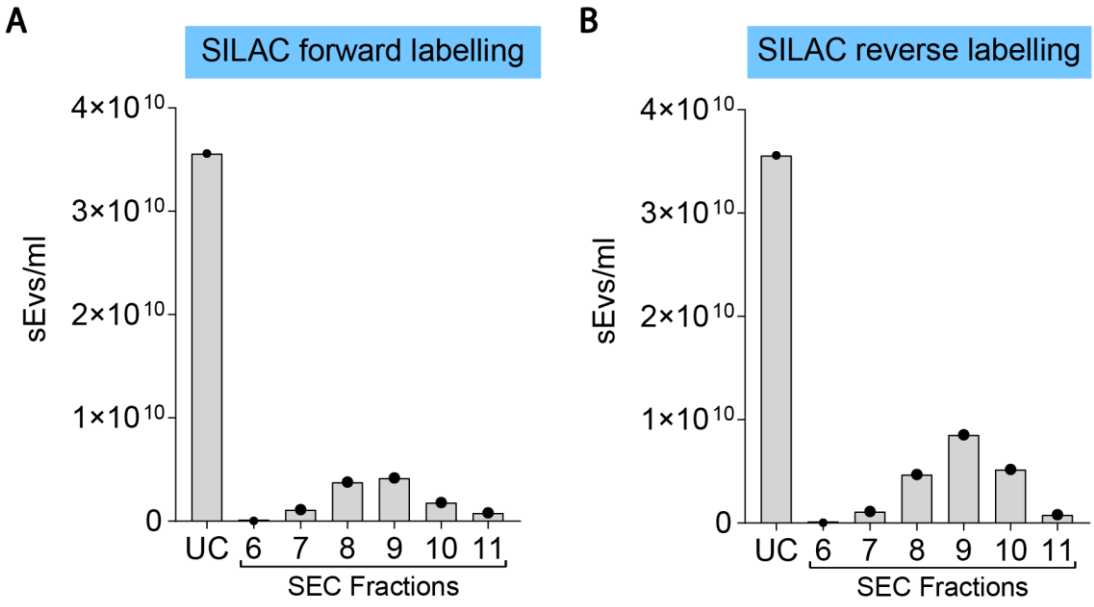

Figure 5.4.1.3 Purification and separation of ₛEVs for proteomic analysis by size exclusion chromatography. A) Quantification of ₛEVs isolated from the SILAC forward labelling experiment after UC and then subsequently after SEC, as measured by ImageStream® Mark II Imaging Flow Cytometer N=1. **B)** Quantification of ₛEVs isolated from the SILAC reverse labelling experiment after UC and then subsequently after SEC, as measured by ImageStream® Mark II Imaging Flow Cytometer. N=1.
UC=ultracentrifugation, SEC=size exclusion chromatography. Donor cells were PaTu-S.PLK4.

5.4.2 SILAC-based proteomic analysis of $_s$EVs derived from cells with and without the induction of centrosome amplification

MaxQuant analysis of the proteomic data provided a comprehensive list of all the proteins (heavy and medium labelled) detected in each SEC fraction. A total of 486 proteins were detected in SEC fraction 7, 825 in SEC fraction 8 and 836 in SEC fraction 9 (Figure 5.4.2.1 A). Of the proteins identified, 464 were found to be common to all fractions, including the key exosomal markers including CD81, CD9, TSG101 and ALIX, providing further evidence to suggest that analysed vesicles are likely to be enriched in exosomes. CD63, however, could not be detected in any of the 3 fractions. Interestingly, other EV studies have found CD63 expression to be low or restricted in comparison to the other tetraspanins including CD81 and CD9 (Kowal *et al.*, 2016b; Barranco *et al.*, 2019). Therefore, levels of CD63 in our samples may simply be too low for detection. Comparison of our $_s$EV proteomics data with the extracellular vesicle database Vesiclepedia (Kalra *et al.*, 2012) revealed that the majority of the proteins observed in our screen have previously been identified in other EV proteomic studies, with only 14 emerging as specific to our data set (Figure 5.4.2.1 B). The significant overlap between our data set and the Vesiclepedia data set provides further evidence that our samples are enriched in extracellular vesicles.

Initial analysis our SILAC screen also revealed that TGF-β was not present in any of the samples. Exosomal TGF-β has previously been shown to trigger fibroblast to myofibroblast differentiation (Webber *et al.*, 2010b). The absence of TGF-β in our samples therefore indicates that PSC activation is likely achieved through an ulterior mechanism. Furthermore, proteins that have previously been linked to oncogenic transformation and tumourigenesis were also identified within the samples, including CEP55 and CTGF.

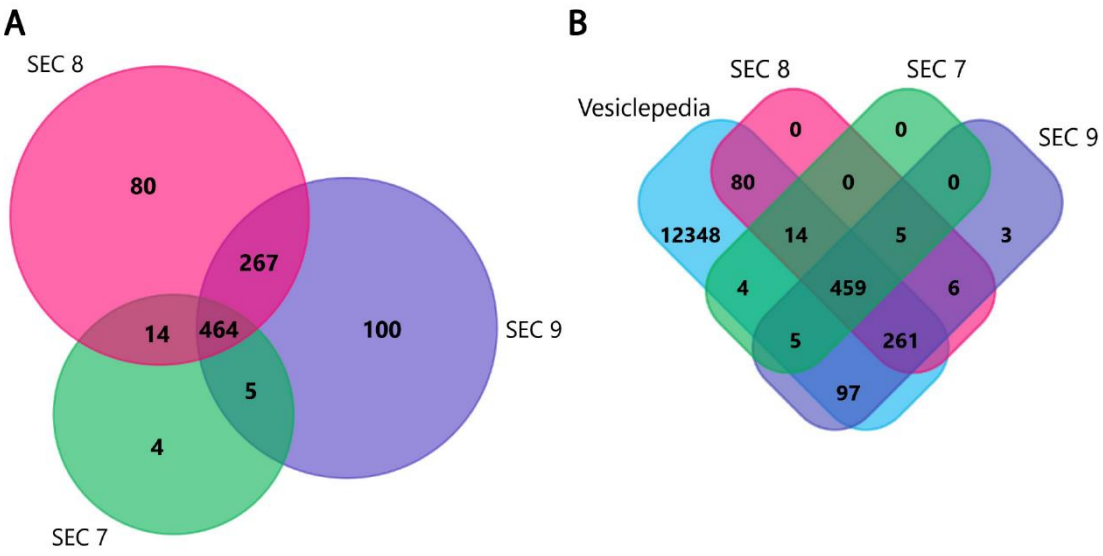

Figure 5.4.2.1 Venn diagrams comparing extracellular vesicle proteomes. A) Venn diagram comparing the $_{s}$EV proteomes of SEC fractions 7,8 and 9. **B)** Venn diagram comparing the EV proteomes of SEC fractions 7, 8 and 9 with the Vesiclepedia database (Kalra *et al.*, 2012). SEC=size exclusion chromatography.

To identify the most commonly upregulated protein pathways in each fraction, enrichment analysis was performed by our collaborator Faraz Mardakheh using a Fishers exact test (see Figure 5.4.2.2). This analysis calculates an enrichment score which reflects the degree to which proteins associated with a specific category are overrepresented in the sample compared to proteins outside of the pathway. We found that in all three SEC fractions, the top 3 most significantly enriched categories consisted of vesicles, membrane-bound vesicles and exosomes. Furthermore, all three fractions were found to also be significantly enriched in pathways unique to exosome biogenesis including; ESCRT I, Recycling endosomes, endocytic vesicles and late endosomes. The results of this analysis therefore highlight that our samples are significantly enriched in protein associated with exosomes.

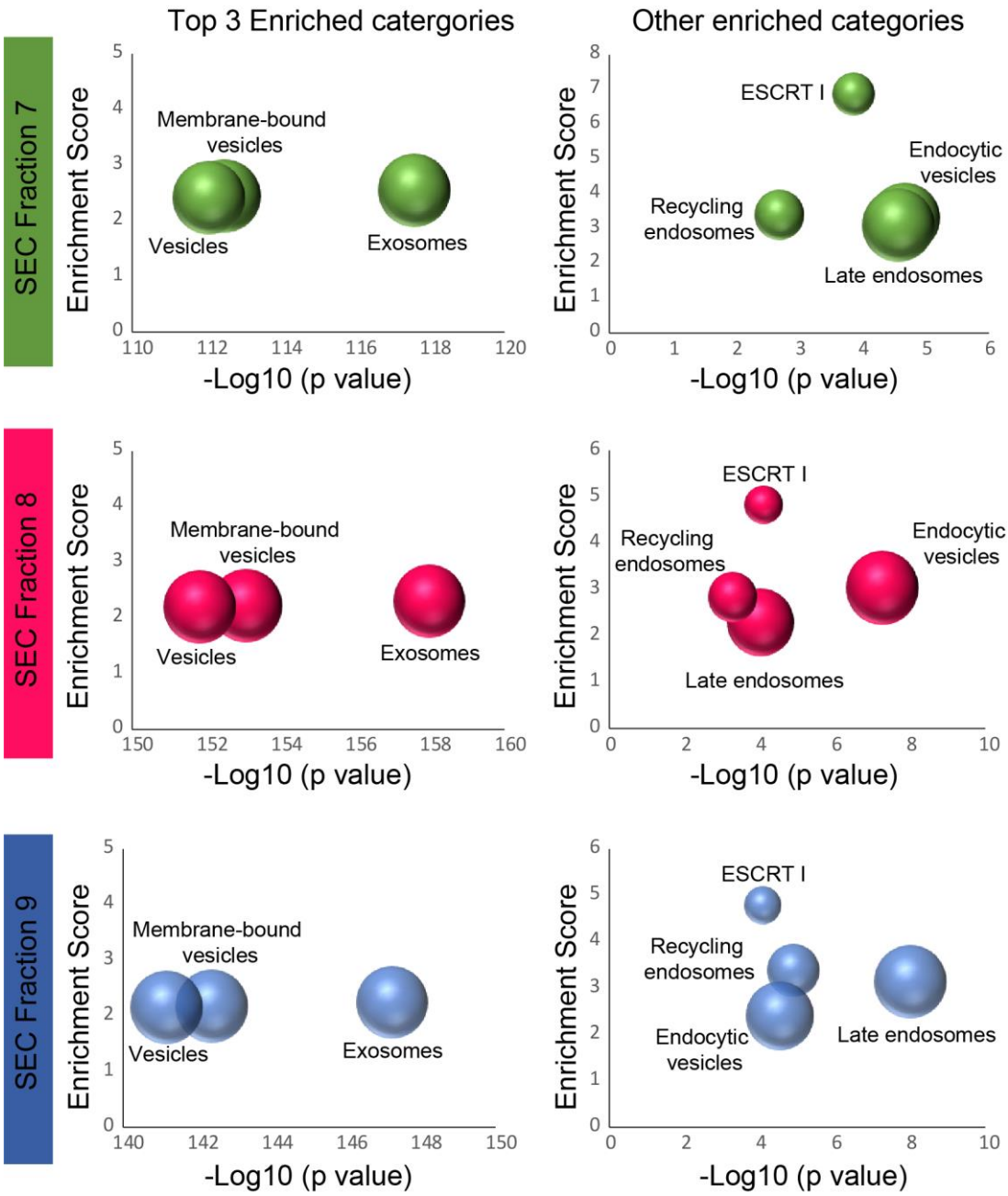

Figure 5.4.2.2 Pathway enrichment analysis of sEV proteins identified using SILAC-based proteomics. Bubble graphs depicting pathway enrichment per SEC fraction (7, 8 &9), where bubble size is indicative of the number of enriched proteins per pathway. Enrichment analysis was performed using a Fishers exact test. Results for SEC fraction 7 shown in green, SEC fraction 8 in pink and SEC fraction 9 in blue. Left graphs show the top 3 most significantly enriched categories per fraction. Right graphs show other highly significantly enriched categories per fraction. SEC=size exclusion chromatography.

To analyse changes in the ratio of proteins present in the heavy labelled and medium labelled $_s$EVs, normalisation was first performed. As samples were mixed at an early stage, results were auto normalised to ensure that heavy and medium intensities in each sample were equivalent. Subsequently, SILAC ratios of the proteins present in each sample were calculated. A fold change of 1.5 or above, that could be replicated in the forward and reverse experiments, were considered significant hits . Log_2 fold change of heavy to medium labels, for the forward and reverse experiments were plotted on correlation graphs for each SEC fraction (figure 5.4.2.3). The dashed diagonal line indicates where identical M and H values would be plotted. The closer the proteins are plotted to this line, the more consistent the values are for the forward and reverse experiment. Interestingly, SILAC ratios did not significantly change in any fraction and the fold change per protein largely remained below 1. Where fold changes above 1.5 were observed, they were only present in one repeat and so not deemed reliable. The analysis of these results indicates that the induction of centrosome amplification in PDAC cells does not change the relative ratios of the proteins identified inside the secreted $_s$EVs. Crucially however, alteration in the protein content of $_s$EVs may not be restricted to changes in the ratios of proteins but also total changes in the presence or absence of specific protein which SILAC ratios do not reflect. Therefore, whilst analysis of SILAC ratios is prudent for whole cell lysates, it may miss key protein changes in EV proteins. We therefore also analysed the original intensity files provided by MaxQuant analysis to determine if total changes in protein were observed between the SILAC labelled samples in each condition per SEC fraction. Interestingly, this new analysis revealed total loss/gain of 8 new proteins in Fraction 7 (see Table 5.4.2.1) and 6 proteins in fraction 8 (see Table 5.4.2.2). No differences were observed in fraction 9. As fraction 8 contains the $_s$EVs that activate PSCs, protein changes in this fraction were considered our hits. These hits were the tetraspanin CD81 which was lost in $_s$EVs from + DOX cells and phosphoglucomutase 3 (PGM3), carbamoyl-phosphate synthetase 2 aspartate transcarbamylase and dihydroorotase (CAD), mitochondrially encoded cytochrome C oxidase II (MT-CO2), FAM129A (NIBAN) and coiled-coil domain containing 124 (CCDC214) which were all gained in $_s$EVs from + DOX cells. These findings confirmed that $_s$EVs secreted by cells with extra centrosomes, do have an altered protein cargo and it is therefore possible that one or more of these 6 proteins may be responsible for the

heightened capacity of sEVs from cells with extra centrosomes to activate pancreatic stellate cells.

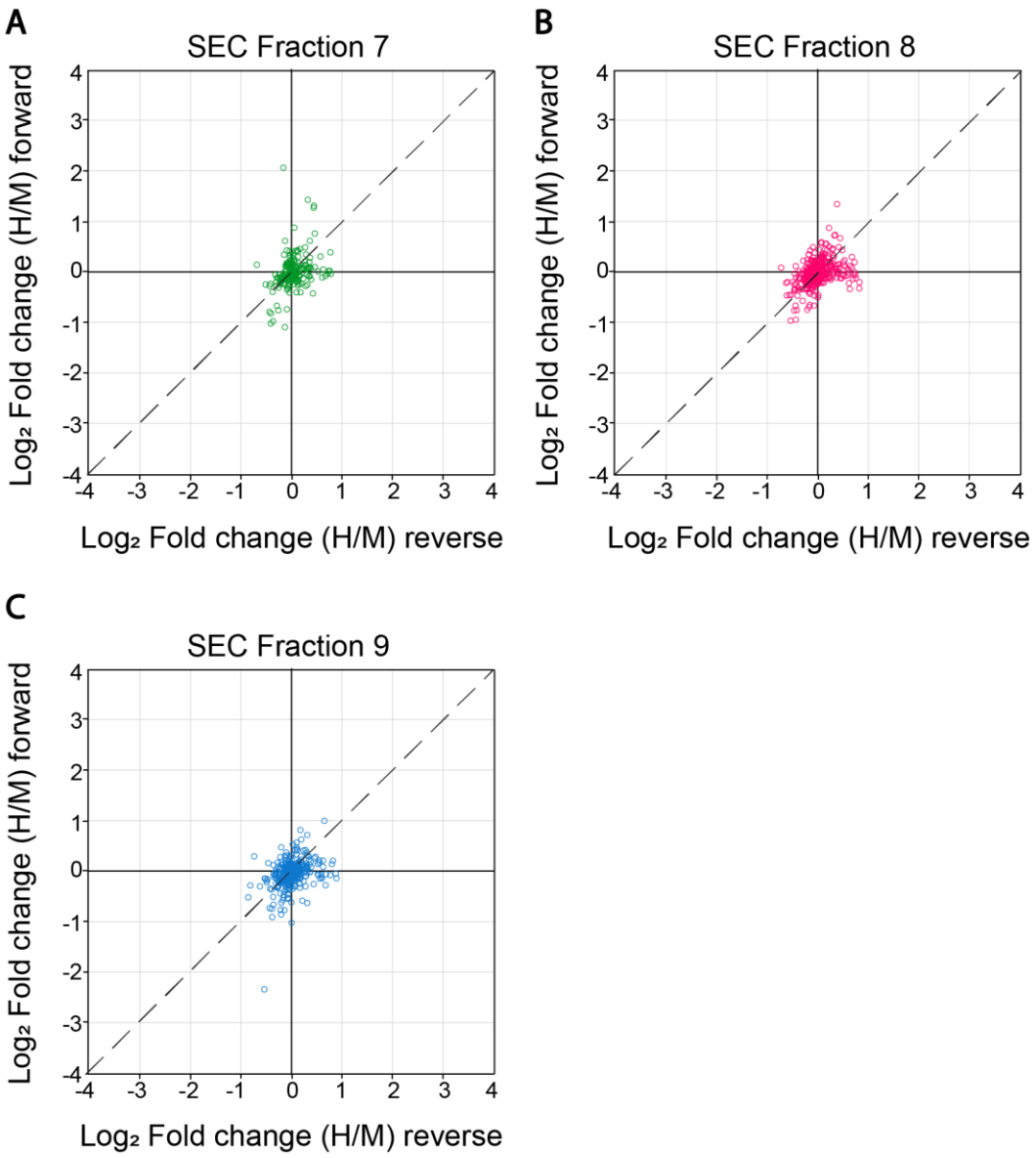

Figure 5.4.2.3 Correlation graphs of sEV protein expression ratios in forward and reverse SILAC experiments. A) Correlation graphs plotting Log_2 fold change in the ratio of heavy and medium labelled proteins of the forward and reverse experiments from SEC fraction 7 (green). **B)** Correlation graphs plotting Log_2 fold change in the ratio of heavy and medium labelled proteins of the forward and reverse experiments from SEC fraction 8 (pink). **C)** Correlation graphs plotting Log_2 fold change in the ratio of heavy and medium labelled proteins of the forward and reverse experiments from SEC fraction 9 (blue).
Dashed diagonal line characterises where identical M and H values would lie. SEC= size exclusion chromatography.

Table 5.4.2.1 SILAC protein hits SEC fraction 7

Gene name	- DOX $_s$EVs	+ DOX $_s$EVs	Peptide number
KIF5B	×	✓	42
B2M	×	✓	3
CYBRD1	×	✓	1
ERLIN2	×	✓	13
SLC25A3	×	✓	14
OCLN	×	✓	5
ANXA3	×	✓	19
MAPK1IP1L	✓	×	1

Table 5.4.2.2 SILAC protein hits SEC fraction 8

Gene name	- DOX $_s$EVs	+ DOX $_s$EVs	Peptide number
CD81	✓	×	3
PGM3	×	✓	8
CAD	×	✓	48
MT-CO2	×	✓	3
NIBAN	×	✓	9
CCDC124	×	✓	8

To help narrow down which proteins may be playing a role in PSC activation we checked whether or not the proteins identified in SEC fraction 8 were also present in the $_{s}$EVs isolated in fraction 7 and 9 which did not activate PSCs (see Table 5.4.2.3). Importantly, whilst the same protein hits were found in both the forward and reverse experiment in SEC fraction 8, the presence or absence of these proteins was not robustly established across replicates in the other two fractions, making interpretation difficult. CD81 was found to be present in at least one replicate of $_{s}$EVs isolated from donor cells with (+ DOX) and without (-DOX) the induction of centrosome amplification that eluted in both SEC fractions 7 and 9. This result may indicate that CD81 is only completely lost in $_{s}$EVs isolated from + DOX cells that elute in fraction 8, making it a strong candidate for further investigation (see Table5.4.2.3). Interestingly, CAD was only identified in $_{s}$EVs isolated from + DOX cells that eluted in fraction 8, thus CAD is also a strong candidate for further investigation. CCDC124 and MT-CO2, which were identified in SEC fraction 8 +DOX $_{s}$EVs only, were also both identified in SEC fraction 9. However, these proteins were only found in one replicate of SEC fraction 9 (CCDC124 in one -DOX replicate and MT-CO2 in one +DOX replicate of SEC fraction 9) (see Table 5.4.2.3). It is therefore possible that these are false positives and so further validation is required to confirm the presence/absence of these proteins under these conditions. Furthermore, NIBAN1 and PGM3 were also identified in SEC fraction 9. These proteins were identified in two replicates , one +DOX and one – DOX, making interpretation difficult (see Table 5.4.2.3). Therefore, until these results are validated, it is unclear what, if any, potential role these proteins may play in PSC activation.

In conclusion, SILAC-based proteomic analysis demonstrated that upon the induction of centrosome amplification, cells secrete $_{s}$EVs with an altered protein cargo. In particular, $_{s}$EVs that retain the PSC activating potential were found to have alterations in the loss or gain of 6 proteins. Of these 6 proteins, CD81 and CAD appear to be strong candidates for further analysis due to their pattern of presence/absence in various protein fractions from treated and untreated cells. Furthermore, enrichment analysis revealed all samples to be significantly enriched in proteins associated with exosomes and exosome biogenesis, providing further evidence that our $_{s}$EVs preparations are enriched in exosomes.

Table 5.4.2.3 Presence of SEC fraction 8 SILAC $_s$EV protein hits (from cells in the presence of DOX) in SEC fraction 7, 8 and 9

	SEC Fraction 7				**SEC Fraction 8**				**SEC Fraction 9**			
	- DOX		**+ DOX**		**- DOX**		**+ DOX**		**- DOX**		**+ DOX**	
Gene name	**Rep 1**	**Rep 2**	**Rep 1**	**Rep 2**	**Rep 1**	**Rep 2**	**Rep 1**	**Rep 2**	**Rep 1**	**Rep 2**	**Rep 1**	**Rep 2**
CD81	✓	×	✓	×	✓	✓	×	×	✓	×	✓	✓
PGM3	×	×	✓	×	×	×	✓	✓	✓	×	×	✓
CAD	×	×	×	×	×	×	✓	✓	×	×	×	×
MT-CO2	×	×	×	×	×	×	✓	✓	×	×	✓	×
NIBAN	×	×	✓	×	×	×	✓	✓	✓	×	✓	×
CCDC124	×	×	✓	×	×	×	✓	✓	✓	×	×	×

5.5 Discussion

Our previous results had demonstrated that PDAC cells with amplified centrosomes secrete an increased number of $_{s}$EVs (Chapter 3). Since $_{s}$EVs are known to contribute to tumourigenesis, we hypothesised that $_{s}$EVs from cells with extra centrosomes may have pro-tumourigenic properties. As $_{s}$EVs have been shown to promote tumour growth and metastasis through activation of cancer-associated fibroblasts and stellate cells we decided to investigate the PSC activating capabilities of $_{s}$EVs derived from cells with and without the induction of centrosome amplification.

Here we report for the first time that $_{s}$EVs from PDAC cells with supernumerary centrosomes significantly enhance PSC activation compared to $_{s}$EVs from cells with normal centrosome number. We also demonstrate that $_{s}$EVs from cells with amplified centrosomes have an altered biological cargo. Interestingly, conditioned medium from these cells was not sufficient to induce PSC activation, and we found it necessary to concentrate the $_{s}$EVs to elicit an effect. Importantly, the design of these experiments dictated that PS1 cells be treated with equal numbers of $_{s}$EVs from cells with and without the induction of centrosome amplification (to exclude any differential vesicle concentration effects). Despite normalisation, $_{s}$EVs from cells with extra centrosomes significantly activated the PSCs whereas those from cells without centrosome amplification did not. As our previous work has shown that cells with extra centrosomes secrete more $_{s}$EVs than normal cells, normalisation of the $_{s}$EV numbers may in fact be minimising the true effects of centrosome amplification derived $_{s}$EVs on PSC activation. Additionally, in a tumour setting where cells with extra centrosomes are present, the PSCs would likely be in proximity to a more concentrated population of $_{s}$EVs with heightened capacity for PSC activation. Whilst the concentration of EVs present in the conditioned media was not sufficient to induce PSC activation over 3 days, it would be interesting to analyse activation over a longer time period to determine if an extended exposure would be sufficient to elicit a response. Additionally, it would be interesting to analyse PSC activation upon co-culture with cells with and without the induction of centrosome amplification. This would determine if proximity to a constant supply of $_{s}$EVs would increase PSC activation without the need to concentrate the vesicles. Although the results we present here are robust, it will be important to analyse PSC activation

using a second PSC cell line to confirm the theory. To rule out experimental artefacts, alternative methods of measuring PSC activation may be employed. For example, PSC cells become highly contractile once they are activated. It would therefore be interesting to analyse the contractility of the PSCs after treatment with $_{s}$EVs using gel contraction assays similar to those performed by Calvo *et al.*, 2013.

Interestingly, $_{s}$EVs that conferred heightened PSC activating capabilities were shown to elute in one specific fraction following SEC. NanoSight analysis revealed that the $_{s}$EVs present in SEC fraction 8 were slightly larger than those present in SEC fraction 9. Together these results indicate that the $_{s}$EVs that harbour enhanced PSC activating capabilities may be a specific subset of $_{s}$EVs. SILAC-based proteomic analysis of $_{s}$EVs isolated from cells with and without centrosome amplification revealed 6 proteins changes in SEC fraction 8, confirming that $_{s}$EVs from cells with supernumerary centrosomes have an altered protein cargo compared to those secreted by cells with a normal centrosome number. Importantly, TGF-β was not detected in the any of the samples, indicating that the mechanism of PSC activation is TGF-β independent and is therefore due to some other factor(s)/mechanism yet to be identified. Candidate proteins involved in a TGF-β independent mechanism of activation have been identified (CD81, CAD, MT-CO2, NIBAN1, CCDC124 and PGM3), but confirmation of their identities is required before further experimentation is carried out. To achieve this, the presence or absence of the identified proteins will be analysed in $_{s}$EVs from PaTu-S.PLK4 and HPAF-II.PLK4 cells with and without the induction of centrosome amplification by dot blot. Once the protein identities have been confirmed, siRNA knock down of the SILAC hits may be performed and the ability of the secreted vesicles to activate PSCs analysed. These experiments should confirm whether or not the targeted proteins play a role in this TGF-β independent mechanism of activation.

Thus far, our work has demonstrated that cells with amplified centrosomes not only induce $_{s}$EV secretion (Chapter 3) but also induce secretion of $_{s}$EVs with an altered biological cargo. Importantly, we have previously demonstrated that this increased $_{s}$EV secretion is associated with centrosome amplification-induced ROS (Chapter 4). We therefore hypothesised that centrosome amplification-associated ROS may also be responsible for secretion of $_{s}$EVs containing a cargo that confers heightened PSC activation capabilities. ROS was therefore quenched in cells with extra centrosomes and

the ability of the secreted $_s$EVs to activate PSCs quantified. Analysis revealed that when centrosome amplification- associated ROS was diminished, the $_s$EVs no longer retained enhanced PSC activating capabilities, indicating that centrosome amplification-associated ROS is responsible for the secretion of $_s$EVs with an altered biological cargo. As our SILAC screen identified a number of EV proteins that change in response to centrosome amplification it would be interesting to see if depletion of ROS in cells with centrosome amplification reverts the cargo of these EVs back to those of – DOX cells or results in a completely different protein cargo. Our initial experiments indicate that centrosome amplification-associated ROS is responsible for the secretion of $_s$EVs which contain factors that activate PSCs. Whether this ROS related change in secretion is specific to centrosome amplification or a more global mechanism remains to be seen. It would be interesting to test the ability of $_s$EVs harvested from cells where ROS is induced independently of centrosome amplification with H_2O_2 to activate PSC. Subsequent analysis of protein changes in these $_s$EVs may provide insight into whether centrosome amplification-associated ROS or ROS in general is responsible for the changes in EV protein cargoes.

In conclusion, the work presented here demonstrates for the first time that $_s$EVs secreted by cells with extra centrosomes have an altered biological cargo that enhances PSC activation compared to $_s$EVs from cells with normal centrosome number. SILAC-based proteomic analysis identified 6 factors present in the $_s$EVs secreted by cells with amplified centrosomes that may be involved in PSC activation. Furthermore, our results indicate that the changes in $_s$EV protein cargo observed in cells with extra centrosomes may be influenced by centrosome amplification-associated increases in cellular ROS levels.

Chapter 6

Discussion

6.1 Overview

In recent years, centrosome amplification has emerged as a hallmark of human malignancies including pancreatic cancer (Chan, 2011), with up to 85% of PDAC tumours harbouring amplified centrosomes (Sato *et al.*, 1999). In fact, despite offering no proliferative advantage to the cancer cells in which the supernumerary centrosomes reside, centrosome amplification has been shown to play a role in both the development and progression of cancer. Indeed, amplified centrosomes have now been associated with tumourigenic properties such as elevated CIN, altered signalling, changes in cell polarity and heightened invasive capabilities (reviewed in Godinho and Pellman, 2014). For example, a recent study from our laboratory demonstrated that amplified centrosomes drive non-cell-autonomous invasion in 3D mammary organoids through the secretion of the ECASP (Arnandis *et al.*, 2018). This altered secretion was attributed to centrosome amplification-driven changes in cellular ROS (Arnandis *et al.*, 2018). Proteomic analysis of the altered secretome revealed that cells with extra centrosomes also secrete a number of proteins associated with EVs. As numerous studies have now identified clear roles for cancer-derived EVs in the development and progression of cancer (reviewed in Xu *et al.*, 2018), we hypothesised that cells with supernumerary centrosomes may contribute to cancer progression through the secretion of tumour promoting EVs. Here, we show for the first time, that cells harbouring supernumerary centrosomes secrete an increased number of $_{s}$EVs. We identify a role for centrosome amplification-associated ROS in the induction of this increased EV release and reveal that $_{s}$EVs secreted by cells with extra centrosomes have an altered protein cargo. We also demonstrate that $_{s}$EVs from cells with amplified centrosomes have heightened PSC activating capabilities and are therefore likely to contribute to PSC-mediated fibrosis and PDAC progression (see Figure 6.1).

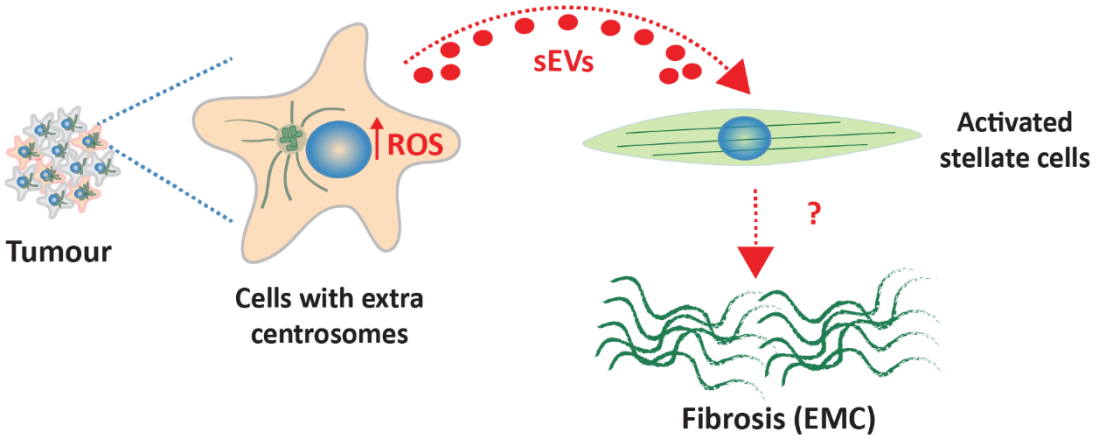

Figure 6.1 Working model of tumour progression driven by sEV secretion. Tumour cells harbouring extra centrosomes have increased cellular ROS which leads to the elevated secretion of sEVs with an altered protein cargo. These secreted sEVs enhance activation of pancreatic stellate cells, which may in theory lead to increased ECM deposition/fibrosis and promote tumour progression.

6.2 The secretion and packaging of $_{s}$EVs in cells with extra centrosomes

The work presented here demonstrates a positive correlation between centrosome amplification and EV secretion in pancreatic cancer cell lines. In fact, using two cell lines in which centrosome amplification can be induced through overexpression of PLK4, we reveal that centrosome amplification is sufficient to drive the secretion of elevated levels of $_{s}$EVs in PDAC cells, but not $_{L}$EVs. Interestingly, increased EV secretion has already been observed in a number of tumour-derived cell lines compared to non-transformed cells, and exosomes are often elevated in the plasma and bodily fluids of cancer patients (Dabitao *et al.*, 2011; Szczepanski *et al.*, 2011; Keustermans *et al.*, 2013). It is not currently known, however, if all tumour cells or a subset of tumour cells are responsible for the increased EV secretion. Our results suggest that a subset of tumour cells harbouring extra centrosomes secrete more EVs than other tumour cells and non-malignant cells and may be responsible for the elevated presence of EVs in patient fluids.

Whilst our results provide strong evidence to suggest centrosome amplification induces $_{s}$EV secretion in pancreatic cancer cells, the driving mechanism behind increased vesicle release has been elusive. Recent work from our laboratory, however, has revealed that centrosome amplification induces an early stress response though increased generation of ROS. Moreover, this centrosome amplification linked increase in cellular ROS was

found to result in an altered secretion profile, the ECASP (Arnandis *et al.*, 2018). We therefore hypothesised that centrosome-amplification induced ROS may also be the driving force behind increased $_s$EV secretion in cells with supernumerary centrosomes. Here, we confirm the findings of Arnandis *et al.,* that cells with supernumerary centrosomes have increased cellular ROS. Furthermore, we demonstrate that this increase in ROS is required for the elevated $_s$EV release observed by cells with extra centrosomes. Interestingly, however, despite having higher basal levels of ROS, PaTu-S.PLK4 cells were found to secrete less $_s$EVs than HPAF-II.PLK4 cells. ROS can be produced in different sub-cellular compartments including the mitochondria, where the majority of cellular ROS is produced, and the cytosol, where ROS is largely produced by NADPH-oxidases (NOXs) (reviewed in Klionsky *et al.*, 2016). Recent work from our laboratory demonstrated that centrosome amplification-associated ROS is cytoplasmic in origin and generated by NOXs (Arnandis *et al.*, 2018). It is therefore possible that the relatively high basal levels of ROS in PaTu-S.PLK4 cells are the result of increased production of a different type of ROS (ROS from a different subcellular compartment) that does not induce $_s$EV secretion.

In support of our findings, similar mechanisms of stress driven EV secretion have been described in the literature. For example, heat stress and ER stress have been shown to induce EV release (Kanemoto *et al.*, 2016; Bewicke-Copley *et al.*, 2017). In other work, metabolic stress in pancreatic cancer cells was shown to induce autophagy and increase EV secretion (Bhattacharya *et al.*, 2014) and a number of studies have now revealed increases in EV secretion in response to chemotherapy and radiation-induced cell stress (reviewed in O'Neill, Gilligan and Dwyer, 2019). Furthermore, hypoxia has been shown to lead to the release of EVs in multiple different cancer types (reviewed in O'Neill, Gilligan and Dwyer, 2019). Hypoxia, or low oxygen tension, is a common feature of tumours and is caused by the high oxygen demand of proliferating cancer cells coupled with the low supply of oxygen due to irregular vascularisation and distance from the supporting blood supply (reviewed in Eales, Hollinshead and Tennant, 2016; Ayob and Ramasamy, 2018). Hypoxia has been shown to alter the expression of numerous plasma membrane receptors including EGFR and GLUT-1 which can result in increased internalisation of these receptors via endocytosis and result in the increased production of MVBs and exosomes (Huber, Kraut and Beug, 2005). Moreover, hypoxia is known to

induce production of cellular ROS in the cytosol through NOX activation (Jiang, Zhang and Dusting, 2011), thus, it is possible that cytoplasmic ROS is also the driving force behind EV secretion in hypoxic cells. It is conceivable that cellular stress-induced ROS generation may alter the expression of plasma membrane proteins influencing the exosome biogenesis pathway, leading to increases in exosome secretion.

To further understand how centrosome amplification-associated ROS contributes to increased $_s$EV secretion in pancreatic cancer cells, we first identified the likely origins of these vesicles. Here we demonstrate that the vesicles in our $_s$EV isolates exhibit many characteristics of exosomes. Initially, we performed nanoparticle tracking analysis on the isolated vesicles which confirmed that these $_s$EVs were within the correct size range for exosomes (30-150 nm). Furthermore, subsequent full proteomic profiling of the vesicles using a SILAC-based proteomic method revealed the $_s$EVs to be significantly enriched in proteins associated with exosomes, and exosome biogenesis. Whilst it is not possible to definitively define the vesicles based on these characteristics, our analysis provides significant evidence to suggest that our $_s$EV isolates are heavily enriched in exosomes. We therefore decided to analyse the effects of centrosome-amplification associated ROS on exosome biogenesis and trafficking.

Using a SILAC-based proteomic approach, our analysis revealed that $_s$EVs secreted by cells with and without the induction of centrosome amplification have different protein cargos. Interestingly, a number of these differentially expressed proteins, CD81, CAD, NIBAN and CCDC124 have been shown to localise, at least in part, to cellular membranes (Sigoillot *et al.*, 2005; Sato *et al.*, 2015; Thul *et al.*, 2017). Changes in the presence or absence of these proteins at the plasma membrane may therefore influence MVB and ILV formation. As the enhanced $_s$EV secretion observed in cells with supernumerary centrosomes is driven by centrosome-associated ROS, it will be important to determine if the changes in $_s$EV protein cargo associated with centrosome amplification, can be reverted back to those observed in the control conditions upon treatment with the ROS quenching agent NAC.

Whilst the results reported here do not indicate changes in MVB formation upon centrosome amplification or ROS induction, only LBPA^{+ve} MVBs were analysed due to time constraints. It is possible that LBPA^{+ve} MVBs only account for a subset of the total

MVBs present within a cell, therefore analysis with additional MVB markers may reveal previously undetected changes in MVB number or size. Our analysis did reveal however, that in cells with centrosome amplification, the cellular localisation of LBPA^{+ve} MVBs is more disperse throughout the cytoplasm compared to cells with normal centrosome number where LBPA^{+ve} MVBs are localised closer to the perinuclear region. These observations may indicate that more MVBs are trafficked to the plasma membrane of cells harbouring supernumerary centrosomes, enabling the expulsion of more exosomes. In our current work we were not able to analyse cellular MVBs in real time, so we cannot discount the possibility that cells with extra centrosomes generate elevated levels of LBPA^{+ve} MVBs but they are trafficked for secretion faster than in cells with normal centrosome number and so numerical differences are not observed.

MVBs are believed to be trafficked along microtubules and it is now well established that centrosome amplification induces increased microtubule nucleation resulting in larger microtubule networks (Godinho *et al* 2014; Monteiro and Godinho, unpublished). Interestingly, current work being performed in our laboratory suggests that centrosome amplification induces a change in the balance of microtubule motors that favour the + end directed motor kinesin-1 (Monteiro and Godinho, unpublished). It is therefore possible that centrosome amplification may result in increased trafficking of MVBs to the plasma membrane through the induction of larger microtubule networks and the increased activity of kinesin-1. Furthermore, recent studies have shown increased cellular ROS to lead to post-translational modifications (PTM) of microtubules, including detyrosination which has been shown to favour microtubule + end directed transport by kinesin-1 (Janke and Chloë Bulinski, 2011; Kerr *et al.*, 2015). It is therefore also possible that centrosome amplification-linked changes in ROS alter microtubule PTMs and facilitate increased MVB trafficking to the plasma membrane, resulting in increased $_{s}$EV secretion. In order to provide a comprehensive view of MVB formation and trafficking upon the induction of centrosome amplification and ROS treatments, a live cell imaging approach should be used.

The MVBs formed within a cell have two fates, either they are trafficked to the plasma membrane, where fusion results in release of their ILVs as exosomes, or they are targeted to the lysosome for degradation. Recent work has shown that lysosome dysfunction shifts the fate of MVBs targeted for degradation, to instead fuse with the

plasma membrane *(*Alvarez-Erviti *et al., 2011;* Miao *et al*., 2015; Latifkar *et al*., 2019). The degradative activities of lysosomes are dependent on the presence of an acidic intraluminal pH and so it has been suggested that preventing the acidification of exosomes would result in increased $_s$EV secretion (Yoshimori *et al.*, 1991; Savina *et al.*, 2003). We therefore quantified $_s$EV secretion in our cells following treatment with the vacuolar proton pump inhibitor bafilomycin A1 which prevents the acidification of lysosomes (Yoshimori *et al.*, 1991). As expected, bafilomycin A1 treatment significantly increased the secretion of $_s$EVs in PaTu-S.PLK4 cells confirming what has previously been described in the literature. We therefore hypothesised that lysosome function may be compromised in cells with amplified centrosomes leading to the observed increase in $_s$EV secretion.

Lipids are one of the most significant targets of cellular ROS. These free radicals steal electrons from lipids in cell membranes in a process termed lipid peroxidation which substantially impacts the structure and permeability of the targeted membranes (reviewed in Tafani *et al.*, 2016). As lysosomal function is dependent on an acidic intraluminal pH, lysosomes are particularly sensitive to lipid peroxidation and subsequent membrane permeabilisation. We therefore hypothesised that centrosome amplification-associated ROS may induce lysosome peroxidation, raising the intraluminal pH and impairing lysosome function. Using LysoTracker as a marker for lysosomes with a functional low pH and Magic Red as a readout of lysosome activity, we showed that cells with centrosome amplification have significantly fewer acidic lysosomes and lower lysosomal activity compared to cells with normal centrosome number. Taken together, these results indicate that centrosome amplification initiates lysosome dysfunction in PDAC cells. Furthermore, we demonstrated that centrosome amplification-associated changes in cellular ROS are responsible for this observed lysosome dysfunction. Whilst the exact mechanisms leading to this dysfunction remain elusive we hypothesis that lysosomal lipid peroxidation may be involved. Analysing lysosomal lipid peroxidation could be achieved using a newly generated Foam-LPO fluorescent probe, which specifically targets lysosomes and contains a fluorophore that degrades in response to lipid peroxidation, resulting in a fluorescence shift (X. Zhang *et al.*, 2015; Ahmad and Leake, 2019). Using this technique, lysosomal lipid peroxidation could be monitored over time, in response to centrosome amplification. To analyse the

effects of centrosome amplification induced lysosome dysfunction on MVBs and their degradation, we analysed co-localisation events between the lysosome marker LysoTracker and the MVB marker LBPA as a proxy for lysosome/MVB fusion. Here we demonstrate that centrosome amplification, and more specifically, centrosome amplification- associated ROS, significantly reduces the incidence of lysosome/MVB co-localisation in PDAC cells. These observations indicate that centrosome amplification linked ROS may prevent lysosomal degradation of MVBs, shifting the fate of these MVBs to fusion with the plasma membrane and resulting in increased $_s$EV secretion. These results again highlight the need to analyse MVB trafficking in cells with and without the induction of centrosome amplification by live cell imaging. Additionally, it is important to note, that the induction of ROS with H_2O_2 in the absence of centrosome amplification, recapitulated the effects of centrosome amplification on lysosomal function and lysosome/MVB co-localisation. These findings indicate that the effects are not specific to centrosome amplification-associated ROS and may represent a more globalised response to certain types of ROS.

Our results to date indicate that centrosome amplification-associated ROS may change the fate of MVBs, directing them away from lysosomal degradation and instead to the cell surface where they fuse with the plasma membrane and expel their ILVs as exosomes. Since some MVBs within a cell are targeted for degradation and others for transport to the plasma membrane, trafficking regulators must be in place to direct MVB fate. Evidence now suggests a role for ubiquitination, a reversible PTM, in the sorting of protein cargo into ILVs and the targeting of MVBs to the lysosome (reviewed in Davies *et al.*, 2009). Similarly, ISGylation, a ubiquitin-like PTM, was also recently shown to trigger MVB co-localisation with lysosomes, promoting degradation of the MVBs and impairing exosome secretion (Villarroya-Beltri *et al.*, 2016). Moreover, a recent study performed by Latifkar *et al.*, revealed that upon the SIRT1-mediated induction of lysosome dysfunction, cells secrete an increased numbers of exosomes with significantly higher levels of protein ubiquitination (Latifkar *et al.*, 2019), providing further evidence to suggest a role for PTMs in directing MVB trafficking. It is therefore possible that currently unknown centrosome amplification associated PTMs could influence the packaging and trafficking of ILVs and MVBs. Crucially, an increasing number of studies suggest that ubiquitination and other PTMs including SUMOylation can be regulated by

ROS during oxidative stress (reviewed in Stankovic-Valentin and Melchior, 2018). It is therefore possible that centrosome amplification-associated ROS plays a role in both the packaging and trafficking of ILVs and MVBs through regulation of PTMs. It would therefore be interesting to analyse changes in EV protein cargo PTMs, particularly ubiquitination, in response to centrosome amplification and ROS treatments.

Whilst the PTM status of the protein cargos in $_s$EV secreted by cells with supernumerary centrosome is currently unknown, SILAC-based proteomic analysis revealed changes in the protein cargo. Six proteins were identified as being differentially present or absent upon the induction of centrosome amplification, these were CD81, PGM3, CAD, MT-CO2, NIBAN and CCDC214. Importantly, CD81, a key membrane tetraspanin, was the only protein found to be lost in $_s$EVs secreted by cells with extra centrosomes. Interestingly, Latifkar *et al.*, reported similar loses of CD81 in exosomes upon the induction of lysosome dysfunction by SIRT1 down regulation (Latifkar *et al.*, 2019). As we have shown that centrosome amplification also leads to lysosomal dysfunction, it is possible that similar mechanisms of CD81 loss are present in both systems. It has been previously demonstrated that ubiquitination of tetraspanins, including CD81 and CD151, downregulate their expression at the cell surface (Lineberry *et al.*, 2008). Thus, cellular stresses (such as ROS) leading to, or resulting from lysosome dysfunction, may result in the PTM of CD81, thereby signalling for its downregulation or preventing its incorporation into ILVS. To gain further understanding as to why CD81 is lost in $_s$EVs secreted by cells with supernumerary centrosomes, it will be important to analyse the PTM status of CD81 following the induction of centrosome amplification, or H_2O_2 treatment. A similar investigation into the PTMs on the other 5 proteins identified in the SILAC-based proteomic analysis may provide insight into the mechanisms behind their packaging into ILVs and their trafficking to the plasma membrane.

6.3 The activation of PSC by $_s$EVs derived from cells with amplified centrosomes

Since our results show that cells with supernumerary centrosomes secrete more $_s$EVs and amplified centrosomes have been associated with tumourigenesis, we hypothesised

that $_s$EVs secreted by cells with extra centrosomes may have pro-tumourigenic properties in PDAC. In recent years it has been established that activated pancreatic stellate cells have key roles in PDAC tumourigenesis, including facilitating fibrosis, tumour growth and metastasis. Since PSCs can be activated through paracrine signalling from cancer cells, including through transfer of cancer-derived exosomes, we decided to investigate changes in PSC activation in response to treatment with $_s$EVs derived from cells with and without the induction of centrosome amplification. Here we report for the first time that $_s$EVs derived from PDAC cells with supernumerary centrosomes significantly enhance PSC activation compared to $_s$EVs from cells with normal centrosome number. PSCs were treated with equal numbers of $_s$EVs or equal $_s$EVs protein from cells with and without the induction of centrosome amplification. In all cases, $_s$EVs from cells with extra centrosomes significantly activated the PSCs whereas those from cells without centrosome amplification did not. Interestingly, we found that the conditioned media generated by cells with extra centrosomes, was not sufficient to significantly induce PSC activation, and that concentration of the $_s$EVs was required to elicit an effect. Since these experiments were only performed over 72 hours, it would be interesting to determine if long term exposure to the conditioned media (where $_s$EV concentration is low) would result in enhanced PSC activation, or if $_s$EV concentration is absolute required to elicit the effect. In a tumour setting, PSCs are in close proximity to large numbers of tumour cells, which could harbour extra centrosomes. Since we have already demonstrated that cells with amplified centrosomes secrete significantly more $_s$EVs, PSCs may therefore, be in close proximity to a constant supply of elevated levels of $_s$EVs from these cells. Therefore, it is conceivable that the close proximity and prolonged exposure to these $_s$EVs in tumours tissues would elicit PSC activation. It would therefore be interesting to analyse PSC activation following co-culture with PDAC cells with and without the induction of centrosome amplification.

Interestingly, the $_s$EVs harbouring a heightened capacity for PSC activation were found to elute in one specific fraction, SEC fraction 8, following size exclusion chromatography. Whilst large numbers of $_s$EVs were also present in SEC fraction 9, these vesicles did not significantly activate PSCs, indicating that the $_s$EVs conferring heightened PSC activating capabilities may be a specific subset of vesicles.

The work presented here demonstrates that lysosome function becomes impaired following the induction of centrosome amplification due to the presence of centrosome amplification associated ROS. Furthermore, we have shown that this lysosome dysfunction results in decreased MVB/lysosome fusion and increased $_s$EV secretion. It is therefore possible that the MVBs carrying the $_s$EVs capable of inducing PSC activation are normally targeted for degradation within the cell by lysosomes. However, upon the induction of lysosome dysfunction by centrosome amplification associated ROS, these MVBs are instead targeted for secretion resulting in the secretion of $_s$EVs that can activate PSCs. Thus, centrosome amplification may play a role in PDAC tumourigenesis, by inducing the secretion of a subset of $_s$EVs that contain pro-tumourigenic factors.

Our results demonstrate that $_s$EVs secreted by cells with supernumerary centrosomes have an altered biological cargo and that the changes to the protein complement are dependent on centrosome amplification-associated ROS. In fact, $_s$EVs secreted by cells with supernumerary centrosomes where ROS has been depleted through treatment with NAC, were found to no longer retain enhanced PSC activating capabilities. A number of studies have also identified exosomal cargo changes in response to insult/cellular stress that confer pro-tumourigenic properties (reviewed in O'Neill, Gilligan and Dwyer, 2019). For example, hypoxia in glioblastoma multiforme (GBM) cells results in the secretion of exosomes elevated in protein-lysine 6-oxidase (LOX), thrombospondin 1 (TSP1) and VEGF which were shown to enhance tumour progression, metastasis and angiogenesis in recipient cells (Kore *et al.*, 2018). Similarly, chemotherapeutic stresses have been shown to induce the increased secretion of exosomes with an altered cargo that confer drug resistance upon uptake by recipient cells (reviewed in O'Neill, Gilligan and Dwyer, 2019). For instance, breast cancer cells have been shown to secrete exosomes containing the multi drug resistance related gene MDR-1 and P-glycoprotein upon chemotherapeutic insult, that induce a drug resistant phenotype in recipient cells (X. Wang *et al.*, 2016). Additionally, upon exposure to the microtubule stabilising agent paclitaxel, breast cancer cells were shown to secrete exosomes enriched in survivin, which promotes drug resistance and cell survival in recipient cells (Kreger *et al.*, 2016). Furthermore, oxidative stress itself has been shown to induce changes in the exosomal cargoes of mouse mast cells which can communicate a protective message to surrounding cells upon their uptake, conferring resistance to

subsequent oxidative insult (Eldh *et al.*, 2010). Thus, cellular stress induced changes in exosomal cargoes are a well-established means of communicating important information to surrounding cells to increase cell survival under otherwise detrimental stimuli.

6.3.1 Proteomic analysis of $_s$EVs derived from cells with extra centrosomes

To determine the factors influencing PSC activation, we first analysed changes in the $_s$EV protein cargo upon the induction of centrosome amplification. SILAC-based proteomic analysis was performed on $_s$EVs from cells with (+DOX) and without (-DOX) the induction of centrosome amplification that had been separated into three SEC fraction, fractions, 7,8 and 9. Crucially, $_s$EVs that contained the enhanced PSC activating potential were found to elute specifically in SEC fraction 8. Analysis revealed differential gains or losses of six proteins in the $_s$EVs isolated from +DOX compared to – DOX cells that eluted in SEC fraction 8. These consisted of gains in CAD, MT-CO2, NIBAN1, CCDC124 and PGM3 and loss of CD81. Interestingly, CD81 was identified in at least one replicate of all fractions except $_s$EVs from + DOX cells that eluted in SEC fraction 8 (see Table 5.4.2.3). Thus, CD81 was identified as a strong candidate for further analysis. Additionally, CAD was only observed in $_s$EVs from + DOX cells that eluted in SEC fraction 8 and so was also selected as a strong candidate for further analysis. Whilst CCDC124 and MT-CO2 were identified in $_s$EVs isolated from +DOX cells and not – DOX cells that eluted in SEC fraction 8, these proteins were also identified in $_s$EVs that eluted in fraction 9 (see Table 5.4.2.3). Crucially however, these proteins were each present in only one sample replicate (CCDC124 in one -DOX replicate and MT-CO2 in one +DOX replicate of SEC fraction 9) leading to the possibility that these are false positives. Validation of these hits by Western blot should determine whether or not these are true findings. NIBAN1 and PGM3 were also identified in SEC fraction 9(see Table 5.4.2.3). Both proteins were identified in two replicates, one +DOX and one – DOX, making interpretation difficult. Until this result is confirmed (for example by validation by Western blot) it is unclear what, if any, potential role these proteins may play in PSC activation.

As discussed above, CD81 and CAD were selected as strong candidates for further analysis due to their presence/absence in specific $_s$EV samples and the effects of these

samples on PSC activation. CD81 is a cell surface glycoprotein that is a member of the transmembrane 4 superfamily known as the tetraspanins. Interestingly, the tetraspanins have been shown to influence cell proliferation and migration and tumour cell invasion (Hemler, Mannion and Berditchevski, 1996; Raimondo *et al.*, 2011). In addition to appearing on cell surface membranes, the tetraspanins have been identified on the surface of EVs including exosomes (Berditchevski and Odintsova, 1999; Sincock *et al.*, 1999; Witwer *et al.*, 2018). A mounting body of evidence now suggests that interplay between tetraspanins, integrins and other adhesion molecules on the surface of EVs are crucial for regulating targeting and uptake of EVs (reviewed in Willms *et al.*, 2018). In fact, a recent publication has demonstrated that neuroblastoma cells secrete different subsets of exosomes which have altered protein cargoes, where one subset was CD63 positive and the other negative for CD63 but positive for amyloid precursor protein (APP) (Laulagnier *et al.*, 2018). Crucially, whilst the CD63 positive exosomes were able to bind to multiple target cells, the APP positive subset were found to be specifically endocytosed by neurons (Laulagnier *et al.*, 2018). It is therefore possible that changes in the expression of CD81 on the surface of the $_{s}$EVs could alter targeting and uptake of the vesicles. Thus, loss of CD81 in $_{s}$EVs secreted by cells with extra centrosomes may facilitate increased EV uptake. Proteomic analysis identified the presence of numerous proteins inside the isolated $_{s}$EVs that have previously been associated with tumourigenesis. Increased delivery of these EVs would therefore potentially result in the increased transfer of a number of oncogenic proteins.

The second protein identified as a strong candidate for PSC activation, CAD, is a multifunctional protein that catalyses the first three steps of de novo pyrimidine biosynthesis. Pyrimidine nucleotide biosynthesis is essential for DNA synthesis and so upon phosphorylation by its activator mitogen-activated protein (MAP) kinase, CAD plays an important role in regulating the cell cycle and proliferation (Sigoillot *et al.*, 2005). CAD has also been shown to regulate notch signalling (Coxam *et al.*, 2015) which is known to mediate cell proliferation and differentiation as well as cell fate. Furthermore, Notch signalling has been shown to play a role in the activation of hepatic stellate cells (HSCs) (Bansal *et al.*, 2015). Therefore, delivery of CAD to PSCs by $_{s}$EVs may initiate PSC activation by inducing Notch. Additionally, whilst CAD is usually located in the cytoplasm, it has also been shown to accumulate at the membranes of LAMP2

positive late endosomes (Sigoillot *et al.*, 2005; Sato *et al.*, 2015), thus CAD may be present on the surface of $_s$EVs. Similar to CD81, it is therefore possible that CAD could affect the behaviours of PSCs by facilitating increased delivery of the $_s$EVs.

Proteomic analysis also revealed MT-CO2 to be gained in $_s$EVs derived from cells with extra centrosomes. MT-CO2 is the second subunit of the mitochondrially encoded cytochrome C oxidase (COX) enzyme. COX is a large transmembrane protein that plays a key role in the final stages of the respiratory electron transport chain by catalysing the reduction of oxygen to water. Importantly , the biogenesis and activities of COX appear to prevent oxidative stress (Bourens *et al.*, 2013). Down regulation of MT-CO2 has been shown to decrease the activity of COX and initiate the differential expression of genes involved in cell cycle, signalling, apoptosis and angiogenesis (Nuha M, Hiba S and Christina Wasunna, 2015). Additionally, MT-CO2 is highly prevalent in the plasma of cancer patients, including sufferers of breast cancer, ovarian cancer and melanoma (Jang *et al.*, 2019). Thus, it is hypothesised that MT-CO2 may play a role in tumourigenesis. Therefore, whilst a link between MT-CO2 and PSC activation is not immediately apparent, it is possible that exosomal delivery of MT-CO2 to PSCs may induce pro-tumourigenic changes in these cells resulting in their activation. Furthermore, Jang *et al*., described MT-CO2 as being present within the membranes of cancer-derived EVs (Jang *et al.*, 2019). As EV membrane proteins can affect the uptake of $_s$EVs by their target cells, this protein could also play a role in delivery of $_s$EVs to PSCs.

CCDC124 was also found to be gained in $_s$EVs secreted upon the induction of centrosome amplification. CCDC124 is a novel centrosomal protein that co-localises with ϒ-tubulin at the centrosome until telophase where it relocates to the midbody, where it is required for the progression of the late cytokinesis stage (Telkoparan *et al.*, 2013). Whilst little is known about this protein, it has been identified as an unfavourable prognostic marker in liver cancer (Uhlen *et al.*, 2017) and its presence in EVs has been confirmed in Vesiclepedia data sets (Kalra *et al.*, 2012). Additionally, CCDC124 has been identified as enriched in both the cytoplasm and in the plasma membrane (Thul *et al.*, 2017). It is therefore possible that CCDC124 could affect PSC activation itself, or by mediating delivery of the $_s$EVs to PSCs. As the activity and function of this protein remain relatively unstudied, it is not clear exactly how transfer of CCDC124 would mediate PSC activation.

Although not considered a strong hit, PGM3 was also identified as gained in $_{s}$EVs secreted by cells with amplified centrosomes. Whilst this protein is not one of the strongest candidates for inducing tumourigenesis due to its presence in multiple SEC fractions, a role for this protein in PSC activation cannot be ruled out. PGM3 plays an important role in carbohydrate metabolism by mediating glycogen formation and utilization. Interestingly, inhibition of PGM3 by the inhibitor FR054 has been shown to decrease the proliferation, survival, adhesion and migration of breast cancer cells, highlighting a potential role for PGM3 in promoting cancer growth and spread (Ricciardiello *et al.,* 2018). Additionally, the presence of PGM3 has been identified as an unfavourable marker for breast cancer and prostate cancer (Munkley *et al.*, 2016; Uhlen *et al.*, 2017). Whilst studies describing the presence of PGM3 in EVs are currently lacking, its appearance in the Vesiclepedia database indicates its presence in vesicles (Kalra *et al.*, 2012). Furthermore, PGM3 is a cytoplasmic protein that has not been identified in cell membranes (Thul *et al.*, 2017) and is therefore not likely to be involved in the delivery of EVs to target cells. Therefore, any PGM3 mediated PSC activation is likely to de due to the transfer of PGM3 itself. Exactly how PGM3 could activate PSCs, however, is unclear and would require further experimental investigation.

The last protein that we identified as potentially gained in our sEVs is NIBAN1, although further validation is required to confirm this finding. NIBAN1, also known as FAM129A, is believed to have a role in the endoplasmic reticulum stress response and modulates apoptosis by regulating translation (Sun *et al.*, 2007). NIBAN1 has also been shown to promote prostate cancer cell growth and survival through regulation of ATF4 (Pällmann *et al.*, 2019). In fact, NIBAN1 is highly expressed in a number of cancers including prostate, thyroid, renal and head and neck cancers (Adachi *et al.*, 2004; Matsumoto *et al.*, 2006; Ito *et al.*, 2010; Pällmann *et al.*, 2019). Crucially, NIBAN1 was found to be overexpressed in HSCs upon activation (Kannangai *et al.*, 2005). Moreover, NIBAN1 has been identified in EVs as reported by Vesiclepedia (Kalra *et al.*, 2012). It is therefore possible that $_{s}$EV directed transfer of NIBAN1 to pancreatic stellate cells may induce their activation, making NIBAN1 a promising candidate for future analysis if presence in the activating fraction alone is confirmed. Furthermore, NIBAN1 has also been shown to localise to the plasma membrane. Thus, as with CD81, CAD, MT-CO2 and CCDC124,

NIBAN1 may play a role in enhancing the delivery of $_s$EVs to target PSCs, thereby promoting PSC activation.

To investigate roles for these proteins in $_s$EV-mediated PCS activation, a small siRNA screen will be performed to deplete each protein from $_s$EVs secreted by cells with amplified centrosomes and the PSC activating potential of the vesicles will be quantified. If proteins involved in the activation are identified, these will be selected for further analysis. It is possible, however, that the PSC activation observed is not mediated by $_s$EV protein but by other $_s$EV cargoes, such as RNA. In fact, a number of studies have now identified specific miRNAs as having a role in PSC activation and inducing PSC-mediated fibrosis. For example, exosomal transfer of miRNA from hepatitis C virus replicating cells has been shown to induce HSC differentiation (Kim, Lee and Lee, 2019), whilst cancer-derived exosomes harbouring miR-214 promoted HSC activation and liver fibrosis (Ma *et al.*, 2018). Additionally, exosomes derived from pancreatic cancer cells that were enriched in mir-1246 and mir-1290 were shown to upregulate fibrosis related genes in PSC (Masamune *et al.*, 2018). Therefore, if $_s$EV protein proves not to be responsible for the observed PSC activation, additional $_s$EV cargos should be analysed. Furthermore, it has recently been demonstrated that ROS can be transferred to recipient cells via exosomes or other EVs (reviewed in Tafani *et al.*, 2016). As cells with extra centrosomes have increased cytoplasmic ROS, it is possible that the $_s$EVs secreted by these cells harbour ROS that can be transferred to target cells upon uptake by the recipient cells. Importantly, ROS has been shown to activate stellate cells by elevating NF-κB activation (reviewed in Gandhi, 2012), therefore direct transfer of ROS via $_s$EVs may induce PSC activation.

6.3.2 Delivery of $_s$EVs derived from cells with supernumerary centrosomes to PSCs

As the proteins identified in our SILAC screen may be affecting $_s$EV delivery, it will be necessary to quantify the uptake of $_s$EVs from cells with and without centrosome amplification in PS1 cells. To analyse vesicle uptake, PS1 cells are currently generating a Cre-LoxP reporter system which will result in a cell colour change due to a switch from dsRed to EGFP expression upon Cre-mediated recombinase incorporation. In parallel we are generating PaTu-S.PLK4 cells to overexpress (OE) Cre, leading to Cre incorporation

into secreted EVs. As demonstrated by Zomer *et al.*, 2015, encapsulation of Cre inside EVs is sufficient to drive the dsRed- EGFP switch (see Figure 6.3.2). Once the system is generated, $_{s}$EVs secreted by Cre OE in PaTu-S.PLK4 cells with and without the induction of centrosome amplification will be isolated and added to the conditioned media of PS1 dsRed-EGFP cells. $_{s}$EV uptake will then be quantified based on the number of GFP positive cells. If uptake of $_{s}$EV differs between $_{s}$EVs secreted by cells with amplified and normal centrosome number, we will analyse the ability of $_{s}$EVs secreted by cells with extra centrosomes to enter PSCs following-depletion of each of the previously identified candidate proteins in an attempt to identify factor(s) responsible for increased $_{s}$EV uptake. Should $_{s}$EV uptake be found to be affected, $_{s}$EV cargos that do not change between the activating and non-activating $_{s}$EVs could be influencing the activation of PSC.

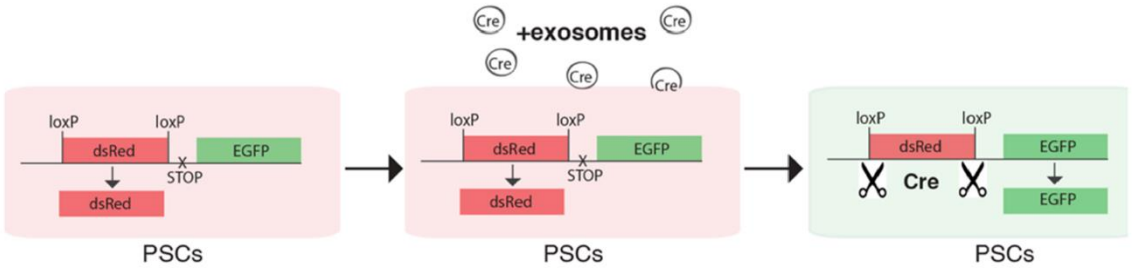

Figure 6.3.2 Schematic diagram of Cre-loxP reporter system for dsRed to EGFP switch upon delivery of Cre enriched exosomes. Cre-LoxP reporter system results in a cell colour change from dsRed to EGFP expression upon Cre-mediated recombinase. sEVs secreted by PaTu-S.PLK4 cells over-expressing Cre will be enriched in Cre and drive a dsRed- EGFP switch-following their incorporation.

Our SILAC-based proteomic analysis revealed a large number of additional proteins present in the isolated $_{s}$EVs, however, a few are particularly noteworthy including connecting tissue growth factor (CTGF/CCN2) and Cep55. CTGF is known to be a central mediator of tissue remodelling through the activation of HSCs resulting in increased ECM deposition and liver fibrosis (Huang and Brigstock, 2012; Lipson *et al.*, 2012; Hao *et al.*, 2014). Furthermore, it is has been demonstrated that CTGF can be transferred between HSCs in exosomes (Charrier *et al.*, 2014). Thus, it is possible that $_{s}$EVs derived from PDAC cells with centrosome amplification activate PSCs due to increased uptake and

subsequent heightened transfer of the pro-fibrotic CTGF. Additionally, whilst not yet shown to play a role in stellate cell activation directly, the centrosomal protein CEP55 has been shown to promote pancreatic cancer progression and aggressiveness (Peng *et al.*, 2017). CEP55 promotes progression through the activation of NF-κB signalling (Peng *et al.*, 2017) and since activated PSCs are known to have elevated NF-κB activation (Masamune *et al.*, 2002; Masamune and Shimosegawa, 2009), it is possible that CEP55 could induce PSC activation through activation of NF-κB (Peng *et al.*, 2017). Hence, the increased delivery of $_s$EVs derived from cells with extra centrosomes could result in PSC activation through CEP55 mediated NF-κB activation.

Therefore, although the identity of $_s$EVs factor(s) mediating PSC activation remains to be confirmed, a number of candidate factors have been identified for further analysis.

6.4 Future directions

Here we report the increased secretion of $_s$EVs from cells harbouring supernumerary centrosomes. We also demonstrate that these sEVs have an altered protein cargo compared to sEVs secreted from cells with a normal centrosome number. Furthermore, we have shown that $_s$EVs secreted specifically by cells with extra centrosomes are able to activate the main fibrosis promoting cells of the pancreas, the pancreatic stellate cells. The mechanisms leading to this PSC activation however remain elusive. Initially, we plan to perform a small siRNA screen based on our SILAC proteomic analysis, to deplete the identified protein in $_s$EVs. The PSC activating potential of the $_s$EVs will then be analysed to determine if these proteins play a role in $_s$EV-mediated PSC activation. Additionally, as ROS can be transferred to recipient cells directly through exosomes (reviewed in Tafani *et al.*, 2016), we plan to assess the potential role of ROS transfer. To do this we will quantify PSC activation upon treatment with $_s$EVs in the presence of the ROS scavenger NAC. Furthermore, whilst our proteomics data rule out TGF-β as the direct activator of the PSCs (since TGF-β was not identified in the $_s$EVs), a role for the TGF-β pathway could initially not be ruled out. Recent work performed in our laboratory however found that $_s$EV-mediated PSC activation did not result in the accumulation of nuclear SMAD4 (Csere and Godinho, unpublished) which is a hallmark of TGF-β activation (Dennler *et al.*, 1998). Thus, indicating that $_s$EVs from cells with extra

centrosomes activate PSCs in a TGF- β independent manner. We therefore plan to perform RNA-seq and phosphoproteomics analysis to determine the signalling pathways activated upon $_s$EV-mediated PSC activation.

Although we have identified a role for $_s$EVs in the activation of PSCs, the direct cellular consequences of this activation remain to be analysed. Future work will therefore focus on determining the physiological effects of PSC activation by $_s$EVs from cells with extra centrosomes, looking in particular at ECM deposition/fibrosis and PSC mediated PDAC cell invasion. Initially, centrosome amplification-induced fibrosis will be analysed *in vitro* by performing matrisome proteomic analysis of PSC derived ECM upon treatment with $_s$EVs from cells with and without the induction of centrosome amplification. If a centrosome amplification-associated fibrotic signature is identified, this signature will be subsequently analysed in 3-D using a recently establish 3-D spheroid model (in collaboration with Richard Grose and Ed Carter at the BCI). Prior to co-culture, PSCs will be pre-educated with $_s$EVs derived from PaTu-S.PLK4 and HPAF-II.PLK4 cells with and without the induction of centrosome amplification. The resultant PSCs will then be co-cultured with PaTu-S or HPAF-II cells and the presence or absence of a centrosome amplification-associated fibrotic signature will be analysed. As activated pancreatic cells have been shown to induce PDAC cell invasion, we will also utilise this model to analyse the role of centrosome amplification associated PSC activation on PDAC cell invasion. Again, PSCs will be pre-educated by $_s$EVs derived by PDAC cells with and without centrosome amplification before being co-cultured with PDAC cells. PSC led PDAC invasion out from the 3D sphere will then be analysed by quantifying the total percentage invasive area after 2-5 days.

If centrosome amplification associated activation of PSCs results in fibrosis, the role of PSC activation will be analysed *in vivo.* In collaboration with Professor Hemant Kocher at the BCI we plan to use orthotopic xenograft models to assess the role of cells with centrosome amplification in the recruitment and activation of PSCs, development of fibrosis and metastasis. PDAC cells with and without the induction of centrosome amplification will be injected orthotopically into the pancreases of immunocompromised mice (Hotz *et al.*, 2003) and 10 weeks later, the mice will be sacrificed and the tumours analysed. Paraffin embedded tumour sections will be used to perform immunofluorescence staining of α-SMA to enable PSC

recruitment/activation to be quantified. Frozen tumour sections will be analysed for the fibrotic signature developed *in vitro*, and mRNA and protein analysis will be performed (see Figure 6.1.4). MRI will be used throughout the experiment to monitor tumour burden and metastasis to the liver (the main metastasis site for pancreatic cancer). Furthermore, to analyse the effects of $_{s}$EVs secreted by cells with supernumerary centrosomes in PDAC fibrosis, we are currently developing a synergistic mouse model to enable us to track cells that incorporate $_{s}$EVs. To do this we will use the mT/mG mouse model which constitutively expresses membrane targeted tdTomato until Cre recombination switches expression to membrane targeted GFP (Muzumdar *et al.*, 2007) and the mouse KPC-derived cell line TB32048, that we are currently generating to express our PLK4 inducible construct (enabling the induction of centrosome amplification) and constitutive Cre. As has been previously described by Zomer *et al.*, 2015, overexpression of Cre results in its incorporation into exosomes/ $_{s}$EVs (Zomer *et al.*, 2015). Therefore, mT/mG mouse cells that incorporate $_{s}$EVs from TB32048.PLK4.CRE cells will result in a cre recombination mediated switch from membrane targeted tdTomato to membrane targeted GFP, permitting us to determine which of the surrounding tumour cells incorporate $_{s}$EVs from the tumour. The mT/mG mouse will be injected with TB32048.PLK4.CRE cells with and without the induction of centrosome amplification. After 4 weeks, mice will be sacrificed and tumours will be analysed. Analysis of the GFP^{+ve} cells will enable us to determine differences in the uptake of $_{s}$EVs from cells with and without centrosome amplification. Furthermore, we will quantify the percentage of activated fibroblasts using an α-SMA^{+ve} GFP^{+ve} cell analysis, to determine if cells with extra centrosomes enhance PSC activation via exosomal cargo transfer *in vivo* compared to cells with normal centrosome number. Subsequently, fibrosis and metastasis will be analysed again as previously described. If changes in PSC activation and fibrosis are observed upon injection of TB32048.PLK4.CRE cells induced for centrosome amplification, we will analyse the response of these tumours to the PDAC chemotherapeutic agent gemcitabine. As fibrosis is known to provide a barrier to therapeutic intervention, we hypothesise that increased fibrosis induced by cells with centrosome amplification will hamper treatment.

In addition to analysing the effects of centrosome amplification derived $_{s}$EVs on tumourigenesis, we also aim to determine whether or not these $_{s}$EVs may be used as a

centrosome amplification associated prognostic biomarker for PDAC. As our proteomic analysis revealed gains and losses in 6 key proteins, we plan to determine if these changes in $_{s}$EV protein can be used as a signature for centrosome amplification. We therefore plan to isolate $_{s}$EVs from the blood of mice taken at multiple time points following injection with PDAC cells with and without the induction of centrosome amplification. $_{s}$EVs in the blood will be harvested and analysed for our centrosome amplification signature (see Figure 6.4). This mouse model will enable us to quantify centrosome amplification at various stages of PDAC progression and blood biopsies taken from the same mice will enable us to identify the stage of PDAC progression in which our marker presents. Furthermore, in collaboration with Professor Hemant Kocher at the BCI we also plan to analyse matching blood and tumour samples from PDAC patients to determine whether or not centrosome amplification in human tumours correlates with our centrosome amplification signature in liquid biopsies (see Figure 6.4).

The dense fibrosis associated with PDAC is now understood to be a significant barrier to therapeutic intervention. Thus, therapeutics were designed to ablate the tumour stroma in the hopes of improving drug delivery and reducing metastasis (Provenzano *et al.*, 2012; Chauhan *et al.*, 2013; Jacobetz *et al.*, 2013). Mounting evidence now indicates, however, that ablating the tumour stroma is actually detrimental to survival and promotes tumour cell proliferation and invasion (Özdemir *et al.*, 2014; Rhim *et al.*, 2014). Subsequent efforts have therefore been focused on modulating the tumour microenvironment rather than completely ablating it. Clearly it is necessary to increase our understanding of stroma dynamics in PDAC. The future work presented here aims to identify a centrosome amplification associated stromal signature that could help us identify novel targets to modulate the PDAC stroma. Furthermore, we aim to identify a centrosome amplification associated $_{s}$EV signature that could potentially be used as a biomarker for PDAC patients with tumours harbouring extra centrosomes. In this way, we hope to be able to identify patients who may benefit from centrosome amplification targeting or associated therapies.

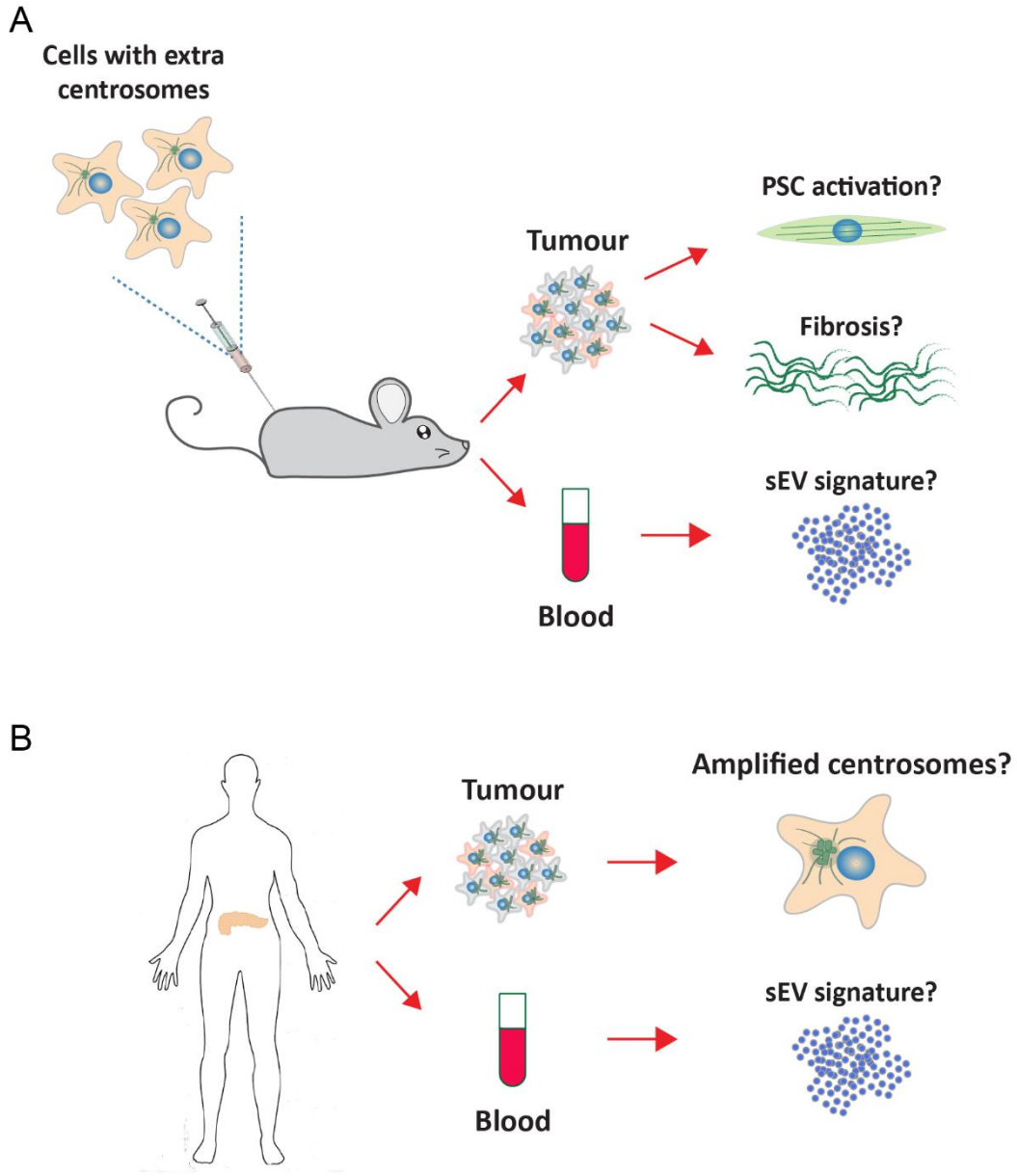

Figure 6.4 Schematic diagrams of future *in vivo* work. A) Mouse xenograft model. Immunocompromised mice will be injected with cells harbouring supernumerary or normal centrosomes. Tumours will be analysed for PSC activation and fibrosis. $_{s}$EVs from the blood of the mice will be isolated and analysed for the presence of the centrosome amplification-associated $_{s}$EV signature. **B)** Human validation model. Matching human tumour and blood biopsies will be used to determine whether a centrosome amplification marker can be detected in $_{s}$EVs isolated from the blood of patients with tumours harbouring supernumerary centrosomes.

Bibliography

Abrami, L., Brandi, L., Moayeri, M., Brown, M. J., Krantz, B. A., Leppla, S. H. and VanderGoot, F. G. (2013) 'Hijacking Multivesicular Bodies Enables Long-Term and Exosome-Mediated Long-Distance Action of Anthrax Toxin', *Cell Rep.*, 5(4), pp. 986–996.

Abramowicz, A., Widlak, P. and Pietrowska, M. (2016) 'Proteomic analysis of exosomal cargo: The challenge of high purity vesicle isolation', *Mol. Biosyst.*, 12(5), pp. 1407–1419.

Adachi, H., Majima, S., Kon, S., Kobayashi, T., Kajino, K., Mitani, H., Hirayama, Y., *et al.* (2004) 'Niban gene is commonly expressed in the renal tumors: A new candidate marker for renal carcinogenesis', *Oncogene*, 23(19), pp. 3495–3500.

Adamska, A., Domenichini, A. and Falasca, M. (2017) 'Pancreatic ductal adenocarcinoma: Current and evolving therapies', *Int. J. Mol. Sci.* MDPI AG.

Ahmad, F. and Leake, D. S. (2019) 'Lysosomal oxidation of LDL alters lysosomal pH, induces senescence, and increases secretion of pro-inflammatory cytokines in human macrophages', *J. Lipid Res.*, 60(1), pp. 98–110.

Ahmed, S., Bradshaw, A.-D., Gera, S., Dewan, M. and Xu, R. (2017) 'The TGF-β/Smad4 Signaling Pathway in Pancreatic Carcinogenesis and Its Clinical Significance', *J. Clin. Med.*, 6(1), p. 5.

Aits, S. and Jaattela, M. (2013) 'Lysosomal cell death at a glance', *J. Cell Sci.*, 126(9), pp. 1905–1912.

Al-Nedawi, K., Meehan, B., Micallef, J., Lhotak, V., May, L., Guha, A. and Rak, J. (2008) 'Intercellular transfer of the oncogenic receptor EGFRvIII by microvesicles derived from tumour cells', *Nat. Cell Biol.*, 10(5), pp. 619–624.

Alderton, G. K. (2014) 'Microenvironment: An exercise in restraint.', *Nat. Rev. Cancer*, 14(7), p. 449.

Alegre, E., Sanmamed, M. F., Rodriguez, C., Carranza, O., Martín-Algarra, S. and González, Á. (2014) 'Study of circulating MicroRNA-125b levels in serum exosomes

in advanced melanoma', *Arch. Pathol. Lab. Med.*, 138(6), pp. 828–832.

Allan, V. J. (2011) 'Cytoplasmic dynein.', *Biochem. Soc. Trans.*, 39(5), pp. 1169–78.

Alvarez-Erviti, L., Seow, Y., Schapira, A. H., Gardiner, C., Sargent, I. L., Wood, M. J. A. and Cooper, J. M. (2011) 'Lysosomal dysfunction increases exosome-mediated alpha-synuclein release and transmission', *Neurobiol. Dis.*, 42(3), pp. 360–367.

Amrutkar, M., Aasrum, M., Verbeke, C. S. and Gladhaug, I. P. (2019) 'Secretion of fibronectin by human pancreatic stellate cells promotes chemoresistance to gemcitabine in pancreatic cancer cells', *BMC Cancer*, 19(1).

Andersen, J. S., Wilkinson, C. J., Mayor, T., Mortensen, P., Nigg, E. A. and Mann, M. (2003) 'Proteomic characterization of the human centrosome by protein correlation profiling', *Nature*.

Andoh, A., Takaya, H., Saotome, T., Shimada, M., Hata, K., Araki, Y., Nakamura, F., *et al.* (2000) 'Cytokine regulation of chemokine (IL-8, MCP-1, and RANTES) gene expression in human pancreatic periacinar myofibroblasts.', *Gastroenterology*, 119(1), pp. 211–9.

Andreassen, P. R., Lohez, O. D., Lacroix, F. B. and Margolis, R. L. (2001) 'Tetraploid State Induces p53-dependent Arrest of Nontransformed Mammalian Cells in G1', *Mol. Biol. Cell*.

Ansari, D., Del Pino Bellido, C., Bauden, M. and Andersson, R. (2018) 'Centrosomal Abnormalities in Pancreatic Cancer: Molecular Mechanisms and Clinical Implications', *Anticancer Res.*, 38(3), pp. 1241–1245.

Antonyak, M. A., Wilson, K. F. and Cerione, R. A. (2012) 'R(h)oads to microvesicles', *Small GTPases*. Taylor and Francis Inc.

Aoki, H., Ohnishi, H., Hama, K., Ishijima, T., Satoh, Y., Hanatsuka, K., Ohashi, A., *et al.* (2005) 'Autocrine loop between TGF-β 1 and IL-1β through Smad3- and ERK-dependent pathways in rat pancreatic stellate cells', *Am. J. Physiol. Physiol.*, 290(4), pp. C1100–C1108.

Apte, M. V., Wilson, J. S., Lugea, A. and Pandol, S. J. (2013) 'A starring role for stellate cells in the pancreatic cancer microenvironment', *Gastroenterology*, 144(6), pp.

1210–1219.

Apte, M. V, Haber, P. S., Applegate, T. L., Norton, I. D., McCaughan, G. W., Korsten, M. A., Pirola, R. C., *et al.* (1998) 'Periacinar stellate shaped cells in rat pancreas: identification, isolation, and culture.', *Gut*, 43(1), pp. 128–33.

Apte, M. V, Haber, P. S., Darby, S. J., Rodgers, S. C., McCaughan, G. W., Korsten, M. A., Pirola, R. C., *et al.* (1999) 'Pancreatic stellate cells are activated by proinflammatory cytokines: implications for pancreatic fibrogenesis.', *Gut*, 44(4), pp. 534–41.

Apte, M. V, Phillips, P. A., Fahmy, R. G., Darby, S. J., Rodgers, S. C., McCaughan, G. W., Korsten, M. A., *et al.* (2000) 'Does alcohol directly stimulate pancreatic fibrogenesis? Studies with rat pancreatic stellate cells.', *Gastroenterology*, 118(4), pp. 780–94.

Apte, M. V, Park, S., Phillips, P. A., Santucci, N., Goldstein, D., Kumar, R. K., Ramm, G. A., *et al.* (2004) 'Desmoplastic reaction in pancreatic cancer: role of pancreatic stellate cells.', *Pancreas*, 29(3), pp. 179–87.

Apte, M. V and Wilson, J. S. (2012) 'Dangerous liaisons: Pancreatic stellate cells and pancreatic cancer cells', *J. Gastroenterol. Hepatol.*, 27(SUPPL.2), pp. 69–74.

Arnandis, T., Monteiro, P., Adams, S. D., Bridgeman, V. L., Rajeeve, V., Gadaleta, E., Marzec, J., *et al.* (2018) 'Oxidative Stress in Cells with Extra Centrosomes Drives Non-Cell-Autonomous Invasion', *Dev. Cell*, 47(4), pp. 409-424.e9.

Arquint, C. and Nigg, E. A. (2016) 'The PLK4-STIL-SAS-6 module at the core of centriole duplication', *Biochem. Soc. Trans.* Portland Press Ltd, pp. 1253–1263.

Arumugam, T., Brandt, W., Ramachandran, V., Moore, T. T., Wang, H., May, F. E., Westley, B. R., *et al.* (2011) 'Trefoil factor 1 stimulates both pancreatic cancer and stellate cells and increases metastasis', *Pancreas*, 40(6), pp. 815–822.

Ayob, A. Z. and Ramasamy, T. S. (2018) 'Cancer stem cells as key drivers of tumour progression.', *J. Biomed. Sci.*, 25(1), p. 20.

Bachem, M. G., Schneider, E., Gross, H., Weidenbach, H., Schmid, R. M., Menke, A., Siech, M., *et al.* (1998) 'Identification, culture, and characterization of pancreatic

stellate cells in rats and humans.', *Gastroenterology*, 115(2), pp. 421–32.

Bachem, M. G., Schünemann, M., Ramadani, M., Siech, M., Beger, H., Buck, A., Zhou, S., *et al.* (2005) 'Pancreatic carcinoma cells induce fibrosis by stimulating proliferation and matrix synthesis of stellate cells.', *Gastroenterology*, 128(4), pp. 907–21.

Bahe, S., Stierhof, Y.-D., Wilkinson, C. J., Leiss, F. and Nigg, E. A. (2005) 'Rootletin forms centriole-associated filaments and functions in centrosome cohesion.', *J. Cell Biol.*, 171(1), pp. 27–33.

Baietti, M. F., Zhang, Z., Mortier, E., Melchior, A., Degeest, G., Geeraerts, A., Ivarsson, Y., *et al.* (2012) 'Syndecan-syntenin-ALIX regulates the biogenesis of exosomes', *Nat. Cell Biol.*, 14(7), pp. 677–685.

Bailey, J. M., Swanson, B. J., Hamada, T., Eggers, J. P., Singh, P. K., Caffery, T., Ouellette, M. M., *et al.* (2008) 'Sonic hedgehog promotes desmoplasia in pancreatic cancer', *Clin. Cancer Res.*, 14(19), pp. 5995–6004.

Balderhaar, H. J. kleine and Ungermann, C. (2013) 'CORVET and HOPS tethering complexes - coordinators of endosome and lysosome fusion.', *J. Cell Sci.*, 126(Pt 6), pp. 1307–16.

Bansal, R., Van Baarlen, J., Storm, G. and Prakash, J. (2015) 'The interplay of the Notch signaling in hepatic stellate cells and macrophages determines the fate of liver fibrogenesis', *Sci. Rep.*, 5.

Bardeesy, N. and DePinho, R. A. (2002) 'Pancreatic cancer biology and genetics', *Nat. Rev. Cancer*, pp. 897–909.

Barranco, I., Padilla, L., Parrilla, I., Álvarez-Barrientos, A., Pérez-Patiño, C., Peña, F. J., Martínez, E. A., *et al.* (2019) 'Extracellular vesicles isolated from porcine seminal plasma exhibit different tetraspanin expression profiles', *Sci. Rep.*, 9(1), p. 11584.

Barrès, C., Blanc, L., Bette-Bobillo, P., André, S., Mamoun, R., Gabius, H. J. and Vidal, M. (2010) 'Galectin-5 is bound onto the surface of rat reticulocyte exosomes and modulates vesicle uptake by macrophages', *Blood*, 115(3), pp. 696–705.

Barros, T. P., Kinoshita, K., Hyman, A. A. and Raff, J. W. (2005) 'Aurora A activates D-

TACC-Msps complexes exclusively at centrosomes to stabilize centrosomal microtubules.', *J. Cell Biol.*, 170(7), pp. 1039–46.

Basto, R., Lau, J., Vinogradova, T., Gardiol, A., Woods, C. G., Khodjakov, A. and Raff, J. W. (2006) 'Flies without Centrioles', *Cell*, 125(7), pp. 1375–1386.

Basto, R., Brunk, K., Vinadogrova, T., Peel, N., Franz, A., Khodjakov, A. and Raff, J. W. (2008) 'Centrosome Amplification Can Initiate Tumorigenesis in Flies', *Cell*, 133(6), pp. 1032–1042.

Batagov, A. O., Kuznetsov, V. A. and Kurochkin, I. V. (2011) 'Identification of nucleotide patterns enriched in secreted RNAs as putative cis-acting elements targeting them to exosome nano-vesicles', in *10th Int. Conf. Bioinforma. - 1st ISCB Asia Jt. Conf. 2011, InCoB 2011/ISCB-Asia 2011 Comput. Biol. - Proc. from Asia Pacific Bioinforma. Netw.*

Baumbach, J., Novak, Z. A., Raff, J. W. and Wainman, A. (2015) 'Dissecting the function and assembly of acentriolar microtubule organizing centers in Drosophila cells in vivo.', *PLoS Genet.*, 11(5), p. e1005261.

Bazzi, H. and Anderson, K. V (2014) 'Acentriolar mitosis activates a p53-dependent apoptosis pathway in the mouse embryo.', *Proc. Natl. Acad. Sci. U. S. A.*, 111(15), pp. E1491-500.

Becker, A., Thakur, B. K., Weiss, J. M., Kim, H. S., Peinado, H. and Lyden, D. (2016) 'Extracellular Vesicles in Cancer: Cell-to-Cell Mediators of Metastasis', *Cancer Cell*, pp. 836–848.

Behrens, G., Jochem, C., Schmid, D., Keimling, M., Ricci, C. and Leitzmann, M. F. (2015) 'Physical activity and risk of pancreatic cancer: a systematic review and meta-analysis.', *Eur. J. Epidemiol.*, 30(4), pp. 279–98.

Belham, C., Roig, J., Caldwell, J. A., Aoyama, Y., Kemp, B. E., Comb, M. and Avruch, J. (2003) 'A Mitotic Cascade of NIMA Family Kinases', *J. Biol. Chem.*, 278(37), pp. 34897–34909.

Benedikter, B. J., Bouwman, F. G., Vajen, T., Heinzmann, A. C. A., Grauls, G., Mariman, E. C., Wouters, E. F. M., *et al.* (2017) 'Ultrafiltration combined with size exclusion

chromatography efficiently isolates extracellular vesicles from cell culture media for compositional and functional studies', *Sci. Rep.*, 7(1).

Berditchevski, F. and Odintsova, E. (1999) 'Characterization of Integrin–Tetraspanin Adhesion Complexes: Role of Tetraspanins in Integrin Signaling', *J. Cell Biol.*, 146(2), p. 477.

Berlin, J. D., Adak, S., Vaughn, D. J., Flinker, D., Blaszkowsky, L., Harris, J. E. and Benson IIIAB, A. B. A. B. B. (2000) 'A phase II study of gemcitabine and 5-fluorouracil in metastatic pancreatic cancer: an Eastern Cooperative Oncology Group Study (E3296).', *Oncology*, 58(3), pp. 215–8.

Bertran, M. T., Sdelci, S., Regué, L., Avruch, J., Caelles, C. and Roig, J. (2011) 'Nek9 is a Plk1-activated kinase that controls early centrosome separation through Nek6/7 and Eg5.', *EMBO J.*, 30(13), pp. 2634–47.

Bettencourt-Dias, M., Rodrigues-Martins, A., Carpenter, L., Riparbelli, M., Lehmann, L., Gatt, M. K., Carmo, N., *et al.* (2005) 'SAK/PLK4 is required for centriole duplication and flagella development', *Curr. Biol.*, 15(24), pp. 2199–2207.

Bettencourt-Dias, M. and Glover, D. M. (2007) 'Centrosome biogenesis and function: centrosomics brings new understanding.', *Nat. Rev. Mol. Cell Biol.*, 8(6), pp. 451–63.

Bewicke-Copley, F., Mulcahy, L. A., Jacobs, L. A., Samuel, P., Akbar, N., Pink, R. C. and Carter, D. R. F. (2017) 'Extracellular vesicles released following heat stress induce bystander effect in unstressed populations.', *J. Extracell. vesicles*, 6(1), p. 1340746.

Bhattacharya, S., Pal, K., Sharma, A. K., Dutta, S. K., Lau, J. S., Yan, I. K., Wang, E., *et al.* (2014) 'GAIP interacting protein C-Terminus regulates autophagy and exosome biogenesis of pancreatic cancer through metabolic pathways', *PLoS One*, 9(12).

Bianco, F, Perrotta, C, Novellino, L, Francolini, M, Riganti, L, Menna, E, Saglietti, L, *et al.* (2009) 'Acid sphingomyelinase activity triggers microparticle release from glial cells.[Erratum appears in EMBO J. 2009 May 6;28(9):1374]', *EMBO J.*, 28(8), pp. 1043–1054.

Bignold, L. P., Coghlan, B. L. D. and Jersmann, H. P. A. (2006) 'Hansemann, Boveri, chromosomes and the gametogenesis-related theories of tumours', *Cell Biol. Int.*, 30(7), pp. 640–644.

Bilimoria, K. Y., Talamonti, M. S., Tomlinson, J. S., Stewart, A. K., Winchester, D. P., Ko, C. Y. and Bentrem, D. J. (2008) 'Prognostic score predicting survival after resection of pancreatic neuroendocrine tumors: analysis of 3851 patients.', *Ann. Surg.*, 247(3), pp. 490–500.

Binenbaum, Y., Na'ara, S. and Gil, Z. (2015) 'Gemcitabine resistance in pancreatic ductal adenocarcinoma.', *Drug Resist. Updat.*, 23, pp. 55–68.

Blachon, S., Gopalakrishnan, J., Omori, Y., Polyanovsky, A., Church, A., Nicastro, D., Malicki, J., *et al.* (2008) 'Drosophila asterless and vertebrate Cep152 Are orthologs essential for centriole duplication.', *Genetics*, 180(4), pp. 2081–94.

Blangy, A., Lane, H. A., d'Hérin, P., Harper, M., Kress, M. and Nigg, E. A. (1995) 'Phosphorylation by p34cdc2 regulates spindle association of human Eg5, a kinesin-related motor essential for bipolar spindle formation in vivo.', *Cell*, 83(7), pp. 1159–69.

Böing, A., van der Pol, E., Grootemaat, A., Coumans, F., Sturk, A. and Nieuwland, R. (2014) 'Single-step isolation of extracellular vesicles by size-exclusion chromatography', *J. Extracell. Vesicles*, 3(1).

Bonifacino, J. S. and Glick, B. S. (2004) 'The Mechanisms of Vesicle Budding and Fusion', *Cell*. Cell Press, pp. 153–166.

Bornens, M. (2012) 'The centrosome in cells and organisms', *Science (80-.).*, 335(6067), pp. 422–426.

Bosetti, C., Lucenteforte, E., Silverman, D. T., Petersen, G., Bracci, P. M., Ji, B. T., Negri, E., *et al.* (2012) 'Cigarette smoking and pancreatic cancer: An analysis from the International Pancreatic Cancer Case-Control Consortium (PANC4)', *Ann. Oncol.*, 23(7), pp. 1880–1888.

Bosetti, C., Bravi, F., Turati, F., Edefonti, V., Polesel, J., Decarli, A., Negri, E., *et al.* (2013) 'Nutrient-based dietary patterns and pancreatic cancer risk.', *Ann. Epidemiol.*,

23(3), pp. 124–8.

Bosetti, C., Rosato, V., Li, D., Silverman, D., Petersen, G. M., Bracci, P. M., Neale, R. E., *et al.* (2014) 'Diabetes, antidiabetic medications, and pancreatic cancer risk: an analysis from the International Pancreatic Cancer Case-Control Consortium.', *Ann. Oncol. Off. J. Eur. Soc. Med. Oncol.*, 25(10), pp. 2065–72.

Bourens, M., Fontanesi, F., Soto, I. C., Liu, J. and Barrientos, A. (2013) 'Redox and reactive oxygen species regulation of mitochondrial cytochrome C oxidase biogenesis', *Antioxidants Redox Signal.*, pp. 1940–1952.

Boveri, T. (1887) 'Uber Die Befunchtung Der Eier von Ascaris Megalocephala.tle', *SitzBer. Ges. Morph. Phys. Munchen*, 3, pp. 71–80.

Boveri, T. (1888) 'Zellen-Studien 2: Die Befrunchtung Und Telung Des Eies von Ascaris Megalocephala', *Jenaische Zeitschr. Med. Naturw*, 22, pp. 685–882.

Boveri, T. (2008) 'Concerning the Origin of Malignant Tumours by Theodor Boveri. Translated and annotated by Henry Harris', *J. Cell Sci.*, 121(Supplement 1), pp. 1–84.

van Breugel, M., Hirono, M., Andreeva, A., Yanagisawa, H. -a., Yamaguchi, S., Nakazawa, Y., Morgner, N., *et al.* (2011) 'Structures of SAS-6 Suggest Its Organization in Centrioles', *Science (80-.).*, 331(6021), pp. 1196–1199.

van Breugel, M., Wilcken, R., McLaughlin, S. H., Rutherford, T. J. and Johnson, C. M. (2014) 'Structure of the SAS-6 cartwheel hub from Leishmania major', *Elife*, 3, p. e01812.

Brinkley, B. R. (2001) 'Managing the centrosome numbers game: from chaos to stability in cancer cell division.', *Trends Cell Biol.*, 11(1), pp. 18–21.

Brown, K. F., Rumgay, H., Dunlop, C., Ryan, M., Quartly, F., Cox, A., Deas, A., *et al.* (2018) 'The fraction of cancer attributable to modifiable risk factors in England, Wales, Scotland, Northern Ireland, and the United Kingdom in 2015.', *Br. J. Cancer*, 118(8), pp. 1130–1141.

Brownlee, C. W., Klebba, J. E., Buster, D. W. and Rogers, G. C. (2011) 'The Protein Phosphatase 2A regulatory subunit Twins stabilizes Plk4 to induce centriole

amplification', *J. Cell Biol.*, 195(2), p. 231.

Brownlee, C. W. and Rogers, G. C. (2013) 'Show me your license, please: deregulation of centriole duplication mechanisms that promote amplification', *Cell. Mol. Life Sci.*, 70(6), pp. 1021–1034.

Bryant, R. J., Pawlowski, T., Catto, J. W. F., Marsden, G., Vessella, R. L., Rhees, B., Kuslich, C., *et al.* (2012) 'Changes in circulating microRNA levels associated with prostate cancer', *Br. J. Cancer*, 106(4), pp. 768–774.

Burris, H. A., Moore, M. J., Andersen, J., Green, M. R., Rothenberg, M. L., Modiano, M. R., Cripps, M. C., *et al.* (1997) 'Improvements in survival and clinical benefit with gemcitabine as first- line therapy for patients with advanced pancreas cancer: A randomized trial', *J. Clin. Oncol.*, 15(6), pp. 2403–2413.

Bynigeri, R. R., Jakkampudi, A., Jangala, R., Subramanyam, C., Sasikala, M., Rao, G. V., Reddy, D. N., *et al.* (2017) 'Pancreatic stellate cell: Pandora's box for pancreatic disease biology', *World J. Gastroenterol.*, 23(3), p. 382.

Cai, S., Weaver, L. N., Ems-McClung, S. C. and Walczak, C. E. (2008) 'Kinesin-14 Family Proteins HSET/XCTK2 Control Spindle Length by Cross-Linking and Sliding Microtubules', *Mol. Biol. Cell*, 20(5), pp. 1348–1359.

Caldas, C., Hahn, S. A., da Costa, L. T., Redston, M. S., Schutte, M., Seymour, A. B., Weinstein, C. L., *et al.* (1994) 'Frequent somatic mutations and homozygous deletions of the p16 (MTS1) gene in pancreatic adenocarcinoma.', *Nat. Genet.*, 8(1), pp. 27–32.

Calvo, F., Ege, N., Grande-Garcia, A., Hooper, S., Jenkins, R. P., Chaudhry, S. I., Harrington, K., *et al.* (2013) 'Mechanotransduction and YAP-dependent matrix remodelling is required for the generation and maintenance of cancer-associated fibroblasts', *Nat. Cell Biol.*, 15(6), pp. 637–646.

Cancer Research UK (2019) *Cancer Statistics for the UK*. Available at: https://www.cancerresearchuk.org/health-professional/cancer-statistics-for-the-uk.

Canto, M. I., Hruban, R. H., Fishman, E. K., Kamel, I. R., Zhang, Z., Topazian, M.,

Takahashi, N., *et al.* (2012) 'Frequent detection of pancreatic lesions in asymptomatic high-risk individuals: screening for early pancreatic neoplasia (CAPS 3 Study)', *Gastroenterology*, 142(4), pp. 796–804.

Carapuça, E. F., Gemenetzidis, E., Feig, C., Bapiro, T. E., Williams, M. D., Wilson, A. S., Delvecchio, F. R., *et al.* (2016) 'Anti-stromal treatment together with chemotherapy targets multiple signalling pathways in pancreatic adenocarcinoma.', *J. Pathol.*, 239(3), pp. 286–96.

Carelli, S., Ceriotti, A., Cabibbo, A., Fassina, G., Ruvo, M. and Sitia, R. (1997) 'Cysteine and glutathione secretion in response to protein disulfide bond formation in the ER.', *Science*, 277(5332), pp. 1681–4.

Carvalho-Santos, Z., Azimzadeh, J., Pereira-Leal, J. B. and Bettencourt-Dias, M. (2011) 'Evolution: Tracing the origins of centrioles, cilia, and flagella.', *J. Cell Biol.*, 194(2), pp. 165–75.

Chan, J. Y. (2011) 'A clinical overview of centrosome amplification in human cancers', *Int. J. Biol. Sci.*, 7(8), pp. 1122–1144.

Chari, S. T., Leibson, C. L., Rabe, K. G., Timmons, L. J., Ransom, J., de Andrade, M. and Petersen, G. M. (2008) 'Pancreatic cancer-associated diabetes mellitus: prevalence and temporal association with diagnosis of cancer.', *Gastroenterology*, 134(1), pp. 95–101.

Charrier, A., Chen, R., Chen, L., Kemper, S., Hattori, T., Takigawa, M. and Brigstock, D. R. (2014) 'Exosomes mediate intercellular transfer of pro-fibrogenic connective tissue growth factor (CCN2) between hepatic stellate cells, the principal fibrotic cells in the liver', *Surg. (United States)*, 156(3), pp. 548–555.

Chaudhary, P. (2015) 'Acinar Cell Carcinoma of the Pancreas: A Literature Review and Update', *Indian J. Surg.* Springer India, pp. 226–231.

Chauhan, V. P., Martin, J. D., Liu, H., Lacorre, D. A., Jain, S. R., Kozin, S. V, Stylianopoulos, T., *et al.* (2013) 'Angiotensin inhibition enhances drug delivery and potentiates chemotherapy by decompressing tumour blood vessels.', *Nat. Commun.*, 4, p. 2516.

Chen, C. Y., Caporizzo, M. A., Bedi, K., Vite, A., Bogush, A. I., Robison, P., Heffler, J. G., *et al.* (2018) 'Suppression of detyrosinated microtubules improves cardiomyocyte function in human heart failure', *Nat. Med.*, 24(8), pp. 1225–1233.

Chen, W. X., Liu, X. M., Lv, M. M., Chen, L., Zhao, J. H., Zhong, S. L., Ji, M. H., *et al.* (2014) 'Exosomes from drug-resistant breast cancer cells transmit chemoresistance by a horizontal transfer of microrna', *PLoS One*. Edited by M. Tan, 9(4), p. e95240.

Chen, Y. W., Hsiao, P. J., Weng, C. C., Kuo, K. K., Kuo, T. L., Wu, D. C., Hung, W. C., *et al.* (2014) 'SMAD4 Loss triggers the phenotypic changes of pancreatic ductal adenocarcinoma cells', *BMC Cancer*, 14(1).

Chivet, M., Javalet, C., Laulagnier, K., Blot, B., Hemming, F. J. and Sadoul, R. (2014) 'Exosomes secreted by cortical neurons upon glutamatergic synapse activation specifically interact with neurons.', *J. Extracell. vesicles*, 3, p. 24722.

Cho, J. A., Park, H., Lim, E. H. and Lee, K. W. (2012) 'Exosomes from breast cancer cells can convert adipose tissue-derived mesenchymal stem cells into myofibroblast-like cells', *Int. J. Oncol.*, 40(1), pp. 130–138.

Cimini, D. (2008) 'Merotelic kinetochore orientation, aneuploidy, and cancer', *Biochim. Biophys. Acta - Rev. Cancer*.

Coelho, P. A., Bury, L., Shahbazi, M. N., Liakath-Ali, K., Tate, P. H., Wormald, S., Hindley, C. J., *et al.* (2015) 'Over-expression of Plk4 induces centrosome amplification, loss of primary cilia and associated tissue hyperplasia in the mouse.', *Open Biol.*, 5(12), pp. 150209-.

Colin, E., Zala, D., Liot, G., Rangone, H., Borrell-Pagès, M., Li, X. J., Saudou, F., *et al.* (2008) 'Huntingtin phosphorylation acts as a molecular switch for anterograde/retrograde transport in neurons', *EMBO J.*, 27(15), pp. 2124–2134.

Collins, A., Warrington, A., Taylor, K. A. and Svitkina, T. (2011) 'Structural organization of the actin cytoskeleton at sites of clathrin-mediated endocytosis.', *Curr. Biol.*, 21(14), pp. 1167–75.

Colombo, M., Moita, C., van Niel, G., Kowal, J., Vigneron, J., Benaroch, P., Manel, N., *et*

al. (2013) ‘Analysis of ESCRT functions in exosome biogenesis, composition and secretion highlights the heterogeneity of extracellular vesicles.’, *J. Cell Sci.*, 126(Pt 24), pp. 5553–65.

Colombo, M., Raposo, G. and Théry, C. (2014) ‘Biogenesis, Secretion, and Intercellular Interactions of Exosomes and Other Extracellular Vesicles’, *Annu. Rev. Cell Dev. Biol.*, 30(1), pp. 255–289.

Conduit, P. T., Wainman, A. and Raff, J. W. (2015) ‘Centrosome function and assembly in animal cells’, *Nat. Rev. Mol. Cell Biol.*, 16(10), pp. 611–624.

Conroy, T., Desseigne, F., Ychou, M., Bouché, O., Guimbaud, R., Bécouarn, Y., Adenis, A., *et al.* (2011) ‘FOLFIRINOX versus gemcitabine for metastatic pancreatic cancer.’, *N. Engl. J. Med.*, 364(19), pp. 1817–25.

Costa-Silva, B., Aiello, N. M., Ocean, A. J., Singh, S., Zhang, H., Thakur, B. K., Becker, A., *et al.* (2015) ‘Pancreatic cancer exosomes initiate pre-metastatic niche formation in the liver.’, *Nat. Cell Biol.*, 17(6), pp. 1–7.

Costa Verdera, H., Gitz-Francois, J. J., Schiffelers, R. M. and Vader, P. (2017) ‘Cellular uptake of extracellular vesicles is mediated by clathrin-independent endocytosis and macropinocytosis.’, *J. Control. Release*, 266, pp. 100–108.

Couch, F. J., Johnson, M. R., Rabe, K. G., Brune, K., de Andrade, M., Goggins, M., Rothenmund, H., *et al.* (2007) ‘The prevalence of BRCA2 mutations in familial pancreatic cancer.’, *Cancer Epidemiol. Biomarkers Prev.*, 16(2), pp. 342–6.

Coxam, B., Neyt, C., Grassini, D. R., Le Guen, L., Smith, K. A., Schulte-Merker, S. and Hogan, B. M. (2015) ‘carbamoyl-phosphate synthetase 2, aspartate transcarbamylase, and dihydroorotase (cad) regulates Notch signaling and vascular development in zebrafish’, *Dev. Dyn.*, 244(1), pp. 1–9.

Crasta, K., Ganem, N. J., Dagher, R., Lantermann, A. B., Ivanova, E. V., Pan, Y., Nezi, L., *et al.* (2012) ‘DNA breaks and chromosome pulverization from errors in mitosis’, *Nature*.

Crawford, N. (1971) ‘The presence of contractile proteins in platelet microparticles isolated from human and animal platelet-free plasma.’, *Br. J. Haematol.*, 21(1),

pp. 53–69.

Cunha-Ferreira, I., Rodrigues-Martins, A., Bento, I., Riparbelli, M., Zhang, W., Laue, E., Callaini, G., *et al.* (2009) 'The SCF/Slimb Ubiquitin Ligase Limits Centrosome Amplification through Degradation of SAK/PLK4', *Curr. Biol.*, 19(1), pp. 43–49.

D'Assoro, A. B., Barrett, S. L., Folk, C., Negron, V. C., Boeneman, K., Busby, R., Whitehead, C., *et al.* (2002a) 'Amplified centrosomes in breast cancer: a potential indicator of tumor aggressiveness.', *Breast Cancer Res. Treat.*, 75(1), pp. 25–34.

D'Assoro, A. B., Barrett, S. L., Folk, C., Negron, V. C., Boeneman, K., Busby, R., Whitehead, C., *et al.* (2002b) 'Amplified centrosomes in breast cancer: a potential indicator of tumor aggressiveness.', *Breast Cancer Res. Treat.*, 75(1), pp. 25–34.

Dabitao, D., Margolick, J. B., Lopez, J. and Bream, J. H. (2011) 'Multiplex measurement of proinflammatory cytokines in human serum: comparison of the Meso Scale Discovery electrochemiluminescence assay and the Cytometric Bead Array.', *J. Immunol. Methods*, 372(1–2), pp. 71–7.

Davies, B. A., Lee, J. R. E., Oestreich, A. J. and Katzmann, D. J. (2009) 'Membrane protein targeting to the MVB/lysosome', *Chem. Rev.*, pp. 1575–1586.

Debec, A. (1978) 'Haploid cell cultures of Drosophila melanogaster [19]', *Nature*, pp. 255–256.

Dennler, S., Itoh, S., Vivien, D., Dijke, P. Ten, Huet, S. and Gauthier, J. M. (1998) 'Direct binding of Smad3 and Smad4 to critical TGFβ-inducible elements in the promoter of human plasminogen activator inhibitor-type 1 gene', *EMBO J.*, 17(11), pp. 3091–3100.

Denzer, K., Kleijmeer, M. J., Heijnen, H. F., Stoorvogel, W. and Geuze, H. J. (2000) 'Exosome: from internal vesicle of the multivesicular body to intercellular signaling device.', *J. Cell Sci.*, 113 Pt 19, pp. 3365–74.

Van Deun, J., Mestdagh, P., Sormunen, R., Cocquyt, V., Vermaelen, K., Vandesompele, J., Bracke, M., *et al.* (2014) 'The impact of disparate isolation methods for extracellular vesicles on downstream RNA profiling', *J. Extracell. Vesicles*, 3(1), p. 24858.

Dinarvand, P. and Lai, J. (2017) 'Solid pseudopapillary neoplasm of the pancreas a rare entity with unique features', *Arch. Pathol. Lab. Med.* College of American Pathologists, pp. 990–995.

DuFort, Christopher. C DelGiorno, K. E. and Hingorani, S. R. (2016) 'Mounting Pressure in the Microenvironment: Fluids, Solids, and Cells in Pancreatic Ductal Adenocarcinoma', *Rev. BASIC Clin. Gastroenterol. Hepatol.*, 150, pp. 1545–1557.

Dumont, J. and Desai, A. (2012) 'Acentrosomal spindle assembly and chromosome segregation during oocyte meiosis.', *Trends Cell Biol.*, 22(5), pp. 241–9.

Dzhindzhev, N. S., Tzolovsky, G., Lipinszki, Z., Schneider, S., Lattao, R., Fu, J., Debski, J., *et al.* (2014) 'Plk4 phosphorylates Ana2 to trigger Sas6 recruitment and procentriole formation.', *Curr. Biol.*, 24(21), pp. 2526–32.

Eales, K. L., Hollinshead, K. E. R. and Tennant, D. A. (2016) 'Hypoxia and metabolic adaptation of cancer cells.', *Oncogenesis*, 5, p. e190.

Edgar, J. R., Manna, P. T., Nishimura, S., Banting, G. and Robinson, M. S. (2016) 'Tetherin is an exosomal tether.', *Elife*, 5.

Eguchi, D., Ikenaga, N., Ohuchida, K., Kozono, S., Cui, L., Fujiwara, K., Fujino, M., *et al.* (2013) 'Hypoxia enhances the interaction between pancreatic stellate cells and cancer cells via increased secretion of connective tissue growth factor', *J. Surg. Res.*, 181(2), pp. 225–233.

Eichelser, C., Stückrath, I., Müller, V., Milde-Langosch, K., Wikman, H., Pantel, K. and Schwarzenbach, H. (2014) 'Increased serum levels of circulating exosomal microRNA-373 in receptor-negative breast cancer patients', *Oncotarget*, 5(20), pp. 9650–63.

Eldh, M., Ekström, K., Valadi, H., Sjöstrand, M., Olsson, B., Jernås, M. and Lötvall, J. (2010) 'Exosomes Communicate Protective Messages during Oxidative Stress; Possible Role of Exosomal Shuttle RNA', *PLoS One*, 5(12), pp. 1–8.

Emmanouilidi, A., Paladin, D., Greening, D. W. and Falasca, M. (2019) 'Oncogenic and Non-Malignant Pancreatic Exosome Cargo Reveal Distinct Expression of Oncogenic and Prognostic Factors Involved in Tumor Invasion and Metastasis.',

Proteomics, 19(8), p. e1800158.

Erkan, M., Michalski, C. W., Rieder, S., Reiser-Erkan, C., Abiatari, I., Kolb, A., Giese, N. A., *et al.* (2008) 'The activated stroma index is a novel and independent prognostic marker in pancreatic ductal adenocarcinoma.', *Clin. Gastroenterol. Hepatol.*, 6(10), pp. 1155–61.

Erkan, M., Adler, G., Apte, M. V, Bachem, M. G., Buchholz, M., Detlefsen, S., Esposito, I., *et al.* (2012) 'StellaTUM: current consensus and discussion on pancreatic stellate cell research', *Gut*, 61(2), pp. 172–178.

Erkan, M., Hausmann, S., Michalski, C. W., Fingerle, A. A., Dobritz, M., Kleeff, J. and Friess, H. (2012) 'The role of stroma in pancreatic cancer: Diagnostic and therapeutic implications', *Nat. Rev. Gastroenterol. Hepatol.*, pp. 454–467.

Fava, L. L., Schuler, F., Sladky, V., Haschka, M. D., Soratroi, C., Eiterer, L., Demetz, E., *et al.* (2017) 'The PIDDosome activates p53 in response to supernumerary centrosomes', *Genes Dev.*

Feldmann, G., Karikari, C., Dal Molin, M., Duringer, S., Volkmann, P., Bartsch, D. K., Bisht, S., *et al.* (2011) 'Inactivation of Brca2 cooperates with Trp53R172H to induce invasive pancreatic ductal adenocarcinomas in mice: A mouse model of familial pancreatic cancer', *Cancer Biol. Ther.*, 11(11), pp. 959–968.

Fendrich, V., Oh, E., Bisht Bang, S., Karikari, C., Ottenhof, N., Bisht Bang, S., Lauth, M., *et al.* (2011) 'Ectopic overexpression of Sonic Hedgehog (Shh) induces stromal expansion and metaplasia in the adult murine pancreas', *Neoplasia*, 13(10), pp. 923–930.

Ferdek, P. E. and Jakubowska, M. A. (2017) 'Biology of pancreatic stellate cells—more than just pancreatic cancer', *Pflugers Arch. Eur. J. Physiol.* Springer Verlag, pp. 1039–1050.

Fielding, A. B., Dobreva, I., McDonald, P. C., Foster, L. J. and Dedhar, S. (2008) 'Integrin-linked kinase localizes to the centrosome and regulates mitotic spindle organization', *J. Cell Biol.*

Fitzner, D., Schnaars, M., Van Rossum, D., Krishnamoorthy, G., Dibaj, P., Bakhti, M.,

Regen, T., *et al.* (2011) 'Selective transfer of exosomes from oligodendrocytes to microglia by macropinocytosis', *J. Cell Sci.*, 124(3), pp. 447–458.

Frampton, A. E., Prado, M. M., López-Jiménez, E., Fajardo-Puerta, A. B., Jawad, Z. A. R., Lawton, P., Giovannetti, E., *et al.* (2018) 'Glypican-1 is enriched in circulating-exosomes in pancreatic cancer and correlates with tumor burden', *Oncotarget*, 9(27), pp. 19006–19013.

Friedman, S. L. (2008) 'Hepatic stellate cells: protean, multifunctional, and enigmatic cells of the liver.', *Physiol. Rev.*, 88(1), pp. 125–72.

Froeling, F. E. M., Feig, C., Chelala, C., Dobson, R., Mein, C. E., Tuveson, D. A., Clevers, H., *et al.* (2011) 'Retinoic acid-induced pancreatic stellate cell quiescence reduces paracrine Wnt-β-catenin signaling to slow tumor progression.', *Gastroenterology*, 141(4), pp. 1486–97, 1497.e1–14.

Frühbeis, C., Fröhlich, D., Kuo, W. P., Amphornrat, J., Thilemann, S., Saab, A. S., Kirchhoff, F., *et al.* (2013) 'Neurotransmitter-Triggered Transfer of Exosomes Mediates Oligodendrocyte-Neuron Communication', *PLoS Biol.* Edited by B. A. Barres, 11(7), p. e1001604.

Fu, J. and Glover, D. M. (2012) 'Structured illumination of the interface between centriole and peri-centriolar material', *Open Biol.*, 2(AUG), p. 120104.

Fu, J., Hagan, I. M. and Glover, D. M. (2015) 'The centrosome and its duplication cycle', *Cold Spring Harb. Perspect. Med.*, 5(1), p. a015800.

Fu, Y., Liu, S., Zeng, S. and Shen, H. (2018) 'The critical roles of activated stellate cells-mediated paracrine signaling, metabolism and onco-immunology in pancreatic ductal adenocarcinoma', *Mol. Cancer*. BioMed Central Ltd.

Fuentealba, L. C., Eivers, E., Ikeda, A., Hurtado, C., Kuroda, H., Pera, E. M. and De Robertis, E. M. (2007) 'Integrating Patterning Signals: Wnt/GSK3 Regulates the Duration of the BMP/Smad1 Signal', *Cell*.

Fujiwara, T., Bandi, M., Nitta, M., Ivanova, E. V., Bronson, R. T. and Pellman, D. (2005) 'Cytokinesis failure generating tetraploids promotes tumorigenesis in p53-null cells', *Nature*.

Fukasawa, K., Choi, T., Kuriyama, R., Rulong, S. and Vande Woude, G. F. (1996) 'Abnormal Centrosome Amplification in the Absence of p53', *Science (80-.).*, 271(5256), pp. 1744–1747.

Galeotti, G. (1893) 'Beitrag zum Studium des Chromatins in den Epithelzellen der Carcinome', *Beitr. Pathol. Anat. Allg. Pathol*, 14, pp. 249–271.

Gallo, A., Tandon, M., Alevizos, I. and Illei, G. G. (2012) 'The majority of microRNAs detectable in serum and saliva is concentrated in exosomes', *PLoS One*. Edited by K. Afarinkia, 7(3), p. e30679.

Gandhi, C. R. (2012) 'Oxidative Stress and Hepatic Stellate Cells: A PARADOXICAL RELATIONSHIP.', *Trends cell Mol. Biol.*, 7(4), pp. 1–10.

Ganem, N. J., Cornils, H., Chiu, S. Y., O'Rourke, K. P., Arnaud, J., Yimlamai, D., Théry, M., *et al.* (2014) 'Cytokinesis failure triggers hippo tumor suppressor pathway activation', *Cell*.

Ganem, N. J., Godinho, S. A. and Pellman, D. (2009) 'A mechanism linking extra centrosomes to chromosomal instability', *Nature*, 460(7252), pp. 278–282.

Ganier, O., Schnerch, D. and Nigg, E. A. (2018) 'Structural centrosome aberrations sensitize polarized epithelia to basal cell extrusion', *Open Biol.*, 8(6).

Gao, R. and Brigstock, D. R. (2005) 'Connective tissue growth factor (CCN2) in rat pancreatic stellate cell function: Integrin α5β1 as a novel CCN2 receptor', *Gastroenterology*, 129(3), pp. 1019–1030.

Ge, Q., Zhou, Y., Lu, J., Bai, Y., Xie, X. and Lu, Z. (2014) 'MiRNA in plasma exosome is stable under different storage conditions', *Molecules*, 19(2), pp. 1568–1575.

Ge, R., Tan, E., Sharghi-Namini, S. and Asada, H. H. (2012) 'Exosomes in cancer microenvironment and beyond: Have we overlooked these extracellular messengers?', *Cancer Microenviron.*, 5(3), pp. 323–332.

Géminard, C., De Gassart, A., Blanc, L. and Vidal, M. (2004) 'Degradation of AP2 during reticulocyte maturation enhances binding of hsc70 and Alix to a common site on TFR for sorting into exosomes.', *Traffic*, 5(3), pp. 181–93.

Genkinger, J. M., Kitahara, C. M., Bernstein, L., Berrington de Gonzalez, A., Brotzman,

M., Elena, J. W., Giles, G. G., *et al.* (2015) 'Central adiposity, obesity during early adulthood, and pancreatic cancer mortality in a pooled analysis of cohort studies', *Ann. Oncol.* Oxford University Press, pp. 2257–2266.

Giardiello, F. M., Welsh, S. B., Hamilton, S. R., Offerhaus, G. J., Gittelsohn, A. M., Booker, S. V, Krush, A. J., *et al.* (1987) 'Increased risk of cancer in the Peutz-Jeghers syndrome.', *N. Engl. J. Med.*, 316(24), pp. 1511–4.

Giehl, M., Fabarius, A., Frank, O., Hochhaus, A., Hafner, M., Hehlmann, R. and Seifarth, W. (2005) 'Centrosome aberrations in chronic myeloid leukemia correlate with stage of disease and chromosomal instability', *Leukemia*, 19(7), pp. 1192–1197.

Giet, R., McLean, D., Descamps, S., Lee, M. J., Raff, J. W., Prigent, C. and Glover, D. M. (2002) 'Drosophila Aurora A kinase is required to localize D-TACC to centrosomes and to regulate astral microtubules', *J. Cell Biol.*, 156(3), pp. 437–451.

Godinho, S. A., Picone, R., Burute, M., Dagher, R., Su, Y., Leung, C. T., Polyak, K., *et al.* (2014) 'Oncogene-like induction of cellular invasion from centrosome amplification', *Nature*, 510(7503), pp. 167–171.

Godinho, S. A. and Pellman, D. (2014) 'Causes and consequences of centrosome abnormalities in cancer.', *Philos. Trans. R. Soc. Lond. B. Biol. Sci.*, 369(1650).

Gogendeau, D., Guichard, P. and Tassin, A. M. (2015) 'Purification of centrosomes from mammalian cell lines', *Methods Cell Biol.*, 129, pp. 171–189.

Goldstein, D., El-Maraghi, R. H., Hammel, P., Heinemann, V., Kunzmann, V., Sastre, J., Scheithauer, W., *et al.* (2015) 'nab-Paclitaxel plus gemcitabine for metastatic pancreatic cancer: long-term survival from a phase III trial.', *J. Natl. Cancer Inst.*, 107(2).

Gönczy, P. (2012) 'Towards a molecular architecture of centriole assembly', *Nat. Rev. Mol. Cell Biol.* Nature Publishing Group, pp. 425–435.

Gönczy, P. (2015) 'Centrosomes and cancer: Revisiting a long-standing relationship', *Nat. Rev. Cancer*, pp. 639–652.

Gopalakrishnan, J., Guichard, P., Smith, A. H., Schwarz, H., Agard, D. A., Marco, S. and Avidor-Reiss, T. (2010) 'Self-assembling SAS-6 multimer is a core centriole building

block.', *J. Biol. Chem.*, 285(12), pp. 8759–70.

Goshima, G., Mayer, M., Zhang, N., Stuurman, N. and Vale, R. D. (2008) 'Augmin: a protein complex required for centrosome-independent microtubule generation within the spindle.', *J. Cell Biol.*, 181(3), pp. 421–9.

Goshima, G. and Kimura, A. (2010) 'New look inside the spindle: microtubule-dependent microtubule generation within the spindle', *Curr. Opin. Cell Biol.*, 22(1), pp. 44–49.

Granger, E., McNee, G., Allan, V. and Woodman, P. (2014) 'The role of the cytoskeleton and molecular motors in endosomal dynamics.', *Semin. Cell Dev. Biol.*, 31, pp. 20–9.

Graser, S., Stierhof, Y.-D., Nigg, E. A. and Rattner, J. B. (2007) 'Cep68 and Cep215 (Cdk5rap2) are required for centrosome cohesion.', *J. Cell Sci.*, 120(Pt 24), pp. 4321–31.

Grieve, A. G. and Rabouille, C. (2011) 'Golgi bypass: Skirting around the heart of classical secretion', *Cold Spring Harb. Perspect. Biol.*, 3(4), pp. 1–15.

Gross, J. C., Chaudhary, V., Bartscherer, K. and Boutros, M. (2012) 'Active Wnt proteins are secreted on exosomes', *Nat. Cell Biol.*, 14(10), pp. 1036–1045.

Gruss, O. J. and Vernos, I. (2004) 'The mechanism of spindle assembly: functions of Ran and its target TPX2.', *J. Cell Biol.*, 166(7), pp. 949–55.

Guardavaccaro, D., Kudo, Y., Boulaire, J., Barchi, M., Busino, L., Donzelli, M., Margottin-Goguet, F., *et al.* (2003) 'Control of meiotic and mitotic progression by the F box protein beta-Trcp1 in vivo.', *Dev. Cell*, 4(6), pp. 799–812.

Guderian, G., Westendorf, J., Uldschmid, A. and Nigg, E. A. (2010) 'Plk4 trans-autophosphorylation regulates centriole number by controlling TrCP-mediated degradation', *J. Cell Sci.*, 123(13), pp. 2163–2169.

Guichard, P., Desfosses, A., Maheshwari, A., Hachet, V., Dietrich, C., Brune, A., Ishikawa, T., *et al.* (2012) 'Cartwheel Architecture of Trichonympha Basal Body', *Science (80-.).*, 337(6094), pp. 553–553.

Guo, H., Gao, M., Ma, J., Xiao, T., Zhao, L., Gao, Y. and Pan, Q. (2007) 'Analysis of the

cellular centrosome in fine-needle aspirations of the breast.', *Breast Cancer Res.*, 9(4), p. R48.

György, B., Szabó, T. G., Pásztói, M., Pál, Z., Misják, P., Aradi, B., László, V., *et al.* (2011) 'Membrane vesicles, current state-of-the-art: Emerging role of extracellular vesicles', *Cell. Mol. Life Sci.*, pp. 2667–2688.

Habedanck, R., Stierhof, Y. D., Wilkinson, C. J. and Nigg, E. A. (2005) 'The Polo kinase Plk4 functions in centriole duplication', *Nat. Cell Biol.*, 7(11), pp. 1140–1146.

Hagan, I. M. and Grallert, A. (2013) 'Spatial control of mitotic commitment in fission yeast.', *Biochem. Soc. Trans.*, 41(6), pp. 1766–71.

Hahn, S. A., Schutte, M., Hoque, A. T., Moskaluk, C. A., da Costa, L. T., Rozenblum, E., Weinstein, C. L., *et al.* (1996) 'DPC4, a candidate tumor suppressor gene at human chromosome 18q21.1', *Science (80-.).*, 271(5247), pp. 350–353.

Hamada, S., Masamune, A., Takikawa, T., Suzuki, N., Kikuta, K., Hirota, M., Hamada, H., *et al.* (2012) 'Pancreatic stellate cells enhance stem cell-like phenotypes in pancreatic cancer cells.', *Biochem. Biophys. Res. Commun.*, 421(2), pp. 349–54.

Hansemann, D. (1890) 'Ueber asymmetrische Zelltheilung in Epithelkrebsen und deren biologische Bedeutung', *Arch. für Pathol. Anat. und Physiol. und für Klin. Med.*, 119, pp. 299–326.

Hanson, P. I. and Cashikar, A. (2012) 'Multivesicular Body Morphogenesis', *Annu. Rev. Cell Dev. Biol.*, 28(1), pp. 337–362.

Hao, C., Xie, Y., Peng, M., Ma, L., Zhou, Y., Zhang, Y., Kang, W., *et al.* (2014) 'Inhibition of connective tissue growth factor suppresses hepatic stellate cell activation in vitro and prevents liver fibrosis in vivo.', *Clin. Exp. Med.*, 14(2), pp. 141–50.

Haqq, J., Howells, L. M., Garcea, G., Metcalfe, M. S., Steward, W. P. and Dennison, A. R. (2014) 'Pancreatic stellate cells and pancreas cancer: Current perspectives and future strategies', *Eur. J. Cancer*, pp. 2570–2582.

Harding, Clifford, Heuser, J. and Stahl, P. (1983) 'Receptor-mediated endocytosis of transferrin and recycling of the transferrin receptor in rat reticulocytes.', *J. Cell Biol.*, 97(2), pp. 329–39.

Harding, C, Heuser, J. and Stahl, P. (1983) 'Receptor-mediated endocytosis of transferrin and recycling of the transferrin receptor in rat reticulocytes.', *J. Cell Biol.*, 97(2), pp. 329–39.

Hardy, P. and Zacharias, H. (2005) 'Reappraisal of the Hansemann–Boveri hypothesis on the origin of tumors', *Cell Biol. Int.*, 29(12), pp. 983–992.

Haren, L., Stearns, T. and Lüders, J. (2009) 'Plk1-Dependent Recruitment of γ-Tubulin Complexes to Mitotic Centrosomes Involves Multiple PCM Components', *PLoS One*. Edited by N. Hotchin, 4(6), p. e5976.

He, R., Huang, N., Bao, Y., Zhou, H., Teng, J. and Chen, J. (2013) 'LRRC45 is a centrosome linker component required for centrosome cohesion.', *Cell Rep.*, 4(6), pp. 1100–7.

Headland, S. E., Jones, H. R., D'Sa, A. S. V., Perretti, M. and Norling, L. V. (2014) 'Cutting-edge analysis of extracellular microparticles using imagestreamx imaging flow cytometry', *Sci. Rep.*, 4, pp. 469–486.

Hemler, M. E., Mannion, B. A. and Berditchevski, F. (1996) 'Association of TM4SF proteins with integrins: Relevance to cancer', *Biochim. Biophys. Acta - Rev. Cancer*. Elsevier B.V., pp. 67–71.

Hendrix, A., Maynard, D., Pauwels, P., Braems, G., Denys, H., Van Den Broecke, R., Lambert, J., *et al.* (2010) 'Effect of the secretory small GTPase Rab27B on breast cancer growth, invasion, and metastasis', *J. Natl. Cancer Inst.*, 102(12), pp. 866–880.

Henne, W. M., Stenmark, H. and Emr, S. D. (2013) 'Molecular mechanisms of the membrane sculpting ESCRT pathway', *Cold Spring Harb. Perspect. Med.*, 3(10), pp. a016766–a016766.

Hervera, A., De Virgiliis, F., Palmisano, I., Zhou, L., Tantardini, E., Kong, G., Hutson, T., *et al.* (2018) 'Reactive oxygen species regulate axonal regeneration through the release of exosomal NADPH oxidase 2 complexes into injured axons', *Nat. Cell Biol.*, 20(3), pp. 307–319.

Hinchcliffe, E. H., Li, C., Thompson, E. A., Maller, J. L. and Sluder, G. (1999)

'Requirement of Cdk2-cyclin E activity for repeated centrosome reproduction in Xenopus egg extracts.', *Science*, 283(5403), pp. 851–4.

Von Hoff, D. D., Ervin, T., Arena, F. P., Chiorean, E. G., Infante, J., Moore, M., Seay, T., *et al.* (2013) 'Increased survival in pancreatic cancer with nab-paclitaxel plus gemcitabine.', *N. Engl. J. Med.*, 369(18), pp. 1691–703.

Holland, A. J., Lan, W., Niessen, S., Hoover, H. and Cleveland, D. W. (2010) 'Polo-like kinase 4 kinase activity limits centrosome overduplication by autoregulating its own stability.', *J. Cell Biol.*, 188(2), pp. 191–8.

Holland, A. J., Fachinetti, D., Zhu, Q., Bauer, M., Verma, I. M., Nigg, E. A. and Cleveland, D. W. (2012) 'The autoregulated instability of Polo-like kinase 4 limits centrosome duplication to once per cell cycle', *Genes Dev.*, 26(24), pp. 2684–2689.

Holland, A. J. and Cleveland, D. W. (2012) 'Losing balance: The origin and impact of aneuploidy in cancer', *EMBO Rep.* European Molecular Biology Organization, pp. 501–514.

Horibe, S., Tanahashi, T., Kawauchi, S., Murakami, Y. and Rikitake, Y. (2018) 'Mechanism of recipient cell-dependent differences in exosome uptake.', *BMC Cancer*, 18(1), p. 47.

Hoshino, A., Costa-Silva, B., Shen, T. L., Rodrigues, G., Hashimoto, A., Tesic Mark, M., Molina, H., *et al.* (2015a) 'Tumour exosome integrins determine organotropic metastasis', *Nature*, 527(7578), pp. 329–335.

Hoshino, A., Costa-Silva, B., Shen, T. L., Rodrigues, G., Hashimoto, A., Tesic Mark, M., Molina, H., *et al.* (2015b) 'Tumour exosome integrins determine organotropic metastasis', *Nature*, 527(7578), pp. 329–335.

Hoshino, D., Kirkbride, K. C., Costello, K., Clark, E. S., Sinha, S., Grega-Larson, N., Tyska, M. J., *et al.* (2013) 'Exosome secretion is enhanced by invadopodia and drives invasive behavior', *Cell Rep.*, 5(5), pp. 1159–1168.

Hotz, H. G., Reber, H. A., Hotz, B., Yu, T., Foitzik, T., Buhr, H. J., Cortina, G., *et al.* (2003) 'An orthotopic nude mouse model for evaluating pathophysiology and therapy of pancreatic cancer.', *Pancreas*, 26(4), pp. e89-98.

Hruban, R. H., Goggins, M., Parsons, J. and Kern, S. E. (2000) 'Progression model for pancreatic cancer.', *Clin. Cancer Res.*, 6(8), pp. 2969–72.

Hruban, R. H., Canto, M. I., Goggins, M., Schulick, R. and Klein, A. P. (2010) 'Update on familial pancreatic cancer.', *Adv. Surg.*, 44, pp. 293–311.

Hruban, R. H., Maitra, A. and Goggins, M. (2008) 'Update on pancreatic intraepithelial neoplasia.', *Int. J. Clin. Exp. Pathol.*, 1(4), pp. 306–16.

Hsu, C., Morohashi, Y., Yoshimura, S. I., Manrique-Hoyos, N., Jung, S. Y., Lauterbach, M. A., Bakhti, M., *et al.* (2010) 'Regulation of exosome secretion by Rab35 and its GTPase-activating proteins TBC1D10A-C', *J. Cell Biol.*, 189(2), pp. 223–232.

Hsu, L. C., Kapali, M., DeLoia, J. A. and Gallion, H. H. (2005) 'Centrosome abnormalities in ovarian cancer', *Int. J. Cancer*, 113(5), pp. 746–751.

Huang, G. and Brigstock, D. R. (2012) 'Regulation of hepatic stellate cells by connective tissue growth factor.', *Front. Biosci. (Landmark Ed.*, 17, pp. 2495–507.

Huang, T. and Deng, C. X. (2019) 'Current progresses of exosomes as cancer diagnostic and prognostic biomarkers', *Int. J. Biol. Sci.* Ivyspring International Publisher, pp. 1–11.

Huber, M. A., Kraut, N. and Beug, H. (2005) 'Molecular requirements for epithelial-mesenchymal transition during tumor progression S0955-0674(05)00104-3 [pii] 10.1016/j.ceb.2005.08.001', *Curr Opin Cell Biol*. 2005/08/16, 17(5), pp. 548–558.

Hui, L. and Chen, Y. (2015) 'Tumor microenvironment: Sanctuary of the devil.', *Cancer Lett.*, 368(1), pp. 7–13.

Hurley, J. H. (2015) 'ESCRTs are everywhere.', *EMBO J.*, 34(19), pp. 2398–407.

Hurwitz, S. N., Rider, M. A., Bundy, J. L., Liu, X., Singh, R. K. and Meckes, D. G. (2016) 'Proteomic profiling of NCI-60 extracellular vesicles uncovers common protein cargo and cancer type-specific biomarkers.', *Oncotarget*, 7(52), pp. 86999–87015.

Hwang, Rosa F, Moore, T., Arumugam, T., Ramachandran, V., Amos, K. D., Rivera, A., Ji, B., *et al.* (2008) 'Cancer-associated stromal fibroblasts promote pancreatic tumor progression', *Cancer Res.*, 68(3), pp. 918–926.

Hwang, Rosa F., Moore, T., Arumugam, T., Ramachandran, V., Amos, K. D., Rivera, A., Ji, B., *et al.* (2008) 'Cancer-associated stromal fibroblasts promote pancreatic tumor progression', *Cancer Res.*, 68(3), pp. 918–926.

Hyenne, V., Apaydin, A., Rodriguez, D., Spiegelhalter, C., Hoff-Yoessle, S., Diem, M., Tak, S., *et al.* (2015) 'RAL-1 controls multivesicular body biogenesis and exosome secretion.', *J. Cell Biol.*, 211(1), pp. 27–37.

Ilic, M. and Ilic, I. (2016) 'Epidemiology of pancreatic cancer.', *World J. Gastroenterol.*, 22(44), pp. 9694–9705.

Insolera, R., Bazzi, H., Shao, W., Anderson, K. V and Shi, S.-H. (2014) 'Cortical neurogenesis in the absence of centrioles.', *Nat. Neurosci.*, 17(11), pp. 1528–35.

Iodice, S., Gandini, S., Maisonneuve, P. and Lowenfels, A. B. (2008) 'Tobacco and the risk of pancreatic cancer: a review and meta-analysis.', *Langenbeck's Arch. Surg.*, 393(4), pp. 535–45.

Iqbal, Nida and Iqbal, Naveed (2014) 'Human Epidermal Growth Factor Receptor 2 (HER2) in Cancers: Overexpression and Therapeutic Implications.', *Mol. Biol. Int.*, 2014, p. 852748.

Ireland, L., Santos, A., Ahmed, M. S., Rainer, C., Nielsen, S. R., Quaranta, V., Weyer-Czernilofsky, U., *et al.* (2016) 'Chemoresistance in Pancreatic Cancer Is Driven by Stroma-Derived Insulin-Like Growth Factors.', *Cancer Res.*, 76(23), pp. 6851–6863.

Ito, D. and Bettencourt-Dias, M. (2018) 'Centrosome Remodelling in Evolution.', *Cells*, 7(7).

Ito, S., Fujii, H., Matsumoto, T., Abe, M., Ikeda, K. and Hino, O. (2010) 'Frequent expression of Niban in head and neck squamous cell carcinoma and squamous dysplasia', *Head Neck*, 32(1), pp. 96–103.

Itoh, K., Jenny, A., Mlodzik, M. and Sokol, S. Y. (2009) 'Centrosomal localization of Diversin and its relevance to Wnt signaling', *J. Cell Sci.*

Jackson, C. E., Scruggs, B. S., Schaffer, J. E. and Hanson, P. I. (2017) 'Effects of Inhibiting VPS4 Support a General Role for ESCRTs in Extracellular Vesicle Biogenesis.', *Biophys. J.*, 113(6), pp. 1342–1352.

Jacobetz, M. A., Chan, D. S., Neesse, A., Bapiro, T. E., Cook, N., Frese, K. K., Feig, C., *et al.* (2013) 'Hyaluronan impairs vascular function and drug delivery in a mouse model of pancreatic cancer', *Gut*, 62(1), pp. 112–120.

Jakobsen, L., Vanselow, K., Skogs, M., Toyoda, Y., Lundberg, E., Poser, I., Falkenby, L. G., *et al.* (2011) 'Novel asymmetrically localizing components of human centrosomes identified by complementary proteomics methods', *EMBO J.*

Jang, S. C., Crescitelli, R., Cvjetkovic, A., Belgrano, V., Olofsson Bagge, R., Sundfeldt, K., Ochiya, T., *et al.* (2019) 'Mitochondrial protein enriched extracellular vesicles discovered in human melanoma tissues can be detected in patient plasma', *J. Extracell. Vesicles*, 8(1), p. 1635420.

Janke, C. and Chloë Bulinski, J. (2011) 'Post-translational regulation of the microtubule cytoskeleton: mechanisms and functions', *Nat. Rev. Mol. Cell Biol.*, 12(12), pp. 773–786.

Janssen, A., Van Der Burg, M., Szuhai, K., Kops, G. J. P. L. and Medema, R. H. (2011) 'Chromosome segregation errors as a cause of DNA damage and structural chromosome aberrations', *Science (80-.).*

Janvier, K., Pelchen-Matthews, A., Renaud, J. B., Caillet, M., Marsh, M. and Berlioz-Torrent, C. (2011) 'The ESCRT-0 component HRS is required for HIV-1 Vpu-mediated BST-2/tetherin down-regulation', *PLoS Pathog.*, 7(2).

Jiang, F., Zhang, Y. and Dusting, G. J. (2011) 'NADPH oxidase-mediated redox signaling: Roles in cellular stress response, stress tolerance, and tissue repair', *Pharmacol. Rev.*, pp. 218–242.

Jiang, X., Abiatari, I., Kong, B., Erkan, M., De Oliveira, T., Giese, N. A., Michalski, C. W., *et al.* (2009) 'Pancreatic islet and stellate cells are the main sources of endocrine gland-derived vascular endothelial growth factor/prokineticin-1 in pancreatic cancer', *Pancreatology*, 9(1–2), pp. 165–172.

Johansson, A. C., Appelqvist, H., Nilsson, C., Kågedal, K., Roberg, K. and Öllinger, K. (2010) 'Regulation of apoptosis-associated lysosomal membrane permeabilization', *Apoptosis*, pp. 527–540.

Johnstone, R. M., Adam, M., Hammond, J. R., Orr, L. and Turbide, C. (1987) 'Vesicle formation during reticulocyte maturation. Association of plasma membrane activities with released vesicles (exosomes).', *J. Biol. Chem.*, 262(19), pp. 9412–9420.

Jon Kull, F. and Endow, S. A. (2013) 'Force generation by kinesin and myosin cytoskeletal motor proteins', *J. Cell Sci.*, pp. 9–19.

Jones, S., Hruban, R. H., Kamiyama, M., Borges, M., Zhang, X., Parsons, D. W., Lin, J. C.-H., *et al.* (2009) 'Exomic sequencing identifies PALB2 as a pancreatic cancer susceptibility gene.', *Science*, 324(5924), p. 217.

Jung, T., Castellana, D., Klingbeil, P., Cuesta Hernández, I., Vitacolonna, M., Orlicky, D. J., Roffler, S. R., *et al.* (2009) 'CD44v6 dependence of premetastatic niche preparation by exosomes.', *Neoplasia*, 11(10), pp. 1093–105.

Kabeya, Y. (2000) 'LC3, a mammalian homologue of yeast Apg8p, is localized in autophagosome membranes after processing', *EMBO J.*, 19(21), pp. 5720–5728.

Kahlert, C., Melo, S. A., Protopopov, A., Tang, J., Seth, S., Koch, O., Zhang, J., *et al.* (2014) 'Identification of doublestranded genomic dna spanning all chromosomes with mutated KRAS and P53 DNA in the serum exosomes of patients with pancreatic cancer', *J. Biol. Chem.*, 289(7), pp. 3869–3875.

Kalra, H., Simpson, R. J., Ji, H., Aikawa, E., Altevogt, P., Askenase, P., Bond, V. C., *et al.* (2012) 'Vesiclepedia: A Compendium for Extracellular Vesicles with Continuous Community Annotation', *PLoS Biol.*, 10(12), p. e1001450.

Kamerkar, S., Lebleu, V. S., Sugimoto, H., Yang, S., Ruivo, C. F., Melo, S. A., Lee, J. J., *et al.* (2017) 'Exosomes facilitate therapeutic targeting of oncogenic KRAS in pancreatic cancer', *Nature*, 546(7659), pp. 498–503.

Kamisawa, T., Isawa, T., Koike, M., Tsuruta, K. and Okamoto, A. (1995) 'Hematogenous metastases of pancreatic ductal carcinoma.', *Pancreas*, 11(4), pp. 345–9.

Kamisawa, T., Wood, L. D., Itoi, T. and Takaori, K. (2016) 'Pancreatic cancer Seminar', *Lancet*, 388(10039), pp. 73–85.

Kanada, M., Bachmann, M. H., Hardy, J. W., Frimannson, D. O., Bronsart, L., Wang, A.,

Sylvester, M. D., *et al.* (2015) 'Differential fates of biomolecules delivered to target cells via extracellular vesicles.', *Proc. Natl. Acad. Sci. U. S. A.*, 112(12), pp. E1433-42.

Kanemoto, S., Nitani, R., Murakami, T., Kaneko, M., Asada, R., Matsuhisa, K., Saito, A., *et al.* (2016) 'Multivesicular body formation enhancement and exosome release during endoplasmic reticulum stress.', *Biochem. Biophys. Res. Commun.*, 480(2), pp. 166–172.

Kannangai, R., Diehl, A. M., Sicklick, J., Rojkind, M., Thomas, D. and Torbenson, M. (2005) 'Hepatic angiomyolipoma and hepatic stellate cells share a similar gene expression profile', *Hum. Pathol.*, 36(4), pp. 341–347.

van der Kant, R., Fish, A., Janssen, L., Janssen, H., Krom, S., Ho, N., Brummelkamp, T., *et al.* (2013) 'Late endosomal transport and tethering are coupled processes controlled by RILP and the cholesterol sensor ORP1L.', *J. Cell Sci.*, 126(Pt 15), pp. 3462–74.

Kapoor, T. M., Mayer, T. U., Coughlin, M. L. and Mitchison, T. J. (2000) 'Probing spindle assembly mechanisms with monastrol, a small molecule inhibitor of the mitotic kinesin, Eg5.', *J. Cell Biol.*, 150(5), pp. 975–88.

Karimi, N., Cvjetkovic, A., Jang, S. C., Crescitelli, R., Hosseinpour Feizi, M. A., Nieuwland, R., Lötvall, J., *et al.* (2018) 'Detailed analysis of the plasma extracellular vesicle proteome after separation from lipoproteins.', *Cell. Mol. Life Sci.*, 75(15), pp. 2873–2886.

Karsenti, E. and Vernos, I. (2001) 'The mitotic spindle: a self-made machine.', *Science*, 294(5542), pp. 543–7.

Keerthikumar, S., Gangoda, L., Liem, M., Fonseka, P., Atukorala, I., Ozcitti, C., Mechler, A., *et al.* (2015) 'Proteogenomic analysis reveals exosomes are more oncogenic than ectosomes', *Oncotarget*, 6(17), pp. 15375–15396.

Keogh, G. W., Wilson, J. S., Moran, C. S., Crawford, D. H. G., Ramm, G. A., McCaughan, G. W., Apte, M. V, *et al.* (2011) 'Activation of Pancreatic Stellate Cells in Human and Experimental Pancreatic Fibrosis', *Am. J. Pathol.*, 155(4), pp. 1087–1095.

Kerr, J. P., Robison, P., Shi, G., Bogush, A. I., Kempema, A. M., Hexum, J. K., Becerra, N., *et al.* (2015) 'Detyrosinated microtubules modulate mechanotransduction in heart and skeletal muscle', *Nat. Commun.*, 6(1), p. 8526.

Keustermans, G. C. E., Hoeks, S. B. E., Meerding, J. M., Prakken, B. J. and de Jager, W. (2013) 'Cytokine assays: An assessment of the preparation and treatment of blood and tissue samples', *Methods*, 61(1), pp. 10–17.

Kfoury, Y., Nasr, R., Favre-Bonvin, A., El-Sabban, M., Renault, N., Giron, M.-L., Setterblad, N., *et al.* (2008) 'Ubiquitylated Tax targets and binds the IKK signalosome at the centrosome.', *Oncogene*, 27(12), pp. 1665–76.

Kikuta, K., Masamune, A., Watanabe, T., Ariga, H., Itoh, H., Hamada, S., Satoh, K., *et al.* (2010) 'Pancreatic stellate cells promote epithelial-mesenchymal transition in pancreatic cancer cells.', *Biochem. Biophys. Res. Commun.*, 403(3–4), pp. 380–4.

Kim, C. B., Ahmed, S. and Hsueh, E. C. (2011) 'Current surgical management of pancreatic cancer', *Society*, 2(21), pp. 126–135.

Kim, J., Gee, Y. and Lee, M. G. (2018) 'Unconventional protein secretion-new insights into the pathogenesis and therapeutic targets of human diseases'.

Kim, J. H., Lee, C. H. and Lee, S. W. (2019) 'Exosomal Transmission of MicroRNA from HCV Replicating Cells Stimulates Transdifferentiation in Hepatic Stellate Cells', *Mol. Ther. - Nucleic Acids*, 14, pp. 483–497.

Kim, J. Y. and Hong, S.-M. (2018) 'Precursor Lesions of Pancreatic Cancer.', *Oncol. Res. Treat.*, 41(10), pp. 603–610.

Kim, S. and Dynlacht, B. D. (2013) 'Assembling a primary cilium.', *Curr. Opin. Cell Biol.*, 25(4), pp. 506–11.

Kim, T.-S., Park, J.-E., Shukla, A., Choi, S., Murugan, R. N., Lee, J. H., Ahn, M., *et al.* (2013) 'Hierarchical recruitment of Plk4 and regulation of centriole biogenesis by two centrosomal scaffolds, Cep192 and Cep152', *Proc. Natl. Acad. Sci.*, 110(50), pp. E4849–E4857.

Kimura, H., Ohtsuka, T., Matsunaga, T., Watanabe, Y., Tamura, K., Ideno, N., Aso, T., *et al.* (2015) 'Predictors and Diagnostic Strategies for Early-Stage Pancreatic Ductal

Adenocarcinoma: A Retrospective Study.', *Pancreas*, 44(7), pp. 1148–54.

Kinoshita, K., Noetzel, T. L., Pelletier, L., Mechtler, K., Drechsel, D. N., Schwager, A., Lee, M., *et al.* (2005) 'Aurora A phosphorylation of TACC3/maskin is required for centrosome-dependent microtubule assembly in mitosis.', *J. Cell Biol.*, 170(7), pp. 1047–55.

Kitagawa, D., Vakonakis, I., Olieric, N., Hilbert, M., Keller, D., Olieric, V., Bortfeld, M., *et al.* (2011) 'Structural Basis of the 9-Fold Symmetry of Centrioles', *Cell*, 144(3), pp. 364–375.

Kleeff, J., Korc, M., Apte, M., La Vecchia, C., Johnson, C. D., Biankin, A. V, Neale, R. E., *et al.* (2016) 'Pancreatic cancer.', *Nat. Rev. Dis. Prim.*, 2, p. 16022.

Klein, A. P., Brune, K. A., Petersen, G. M., Goggins, M., Tersmette, A. C., Offerhaus, G. J. A., Griffin, C., *et al.* (2004) 'Prospective Risk of Pancreatic Cancer in Familial Pancreatic Cancer Kindreds', *Cancer Res.*, 64(7), pp. 2634–2638.

Kleylein-Sohn, J., Westendorf, J., Le Clech, M., Habedanck, R., Stierhof, Y. D. and Nigg, E. A. (2007) 'Plk4-Induced Centriole Biogenesis in Human Cells', *Dev. Cell*, 13(2), pp. 190–202.

Kleylein-Sohn, J., Pöllinger, B., Ohmer, M., Hofmann, F., Nigg, E. A., Hemmings, B. A. and Wartmann, M. (2012) 'Acentrosomal spindle organization renders cancer cells dependent on the kinesin HSET', *J. Cell Sci.*, 125(22), pp. 5391–5402.

Klionsky, D. J., Abdelmohsen, K., Abe, A., Abedin, M. J., Abeliovich, H., Acevedo Arozena, A., Adachi, H., *et al.* (2016) 'Guidelines for the use and interpretation of assays for monitoring autophagy (3rd edition)', *Autophagy*, 12(1), pp. 1–222.

Kobayashi, T., Stang, E., Fang, K. S., De Moerloose, P., Parton, R. G. and Gruenberg, J. (1998) 'A lipid associated with the antiphospholipid syndrome regulates endosome structure and function', *Nature*, 392(6672), pp. 193–197.

Kogure, T., Lin, W. L., Yan, I. K., Braconi, C. and Patel, T. (2011) 'Intercellular nanovesicle-mediated microRNA transfer: A mechanism of environmental modulation of hepatocellular cancer cell growth', *Hepatology*, 54(4), pp. 1237–1248.

Kohlmaier, G., Loncarek, J., Meng, X., McEwen, B. F., Mogensen, M. M., Spektor, A., Dynlacht, B. D., *et al.* (2009) 'Overly long centrioles and defective cell division upon excess of the SAS-4-related protein CPAP.', *Curr. Biol.*, 19(12), pp. 1012–8.

Koles, K., Nunnari, J., Korkut, C., Barria, R., Brewer, C., Li, Y., Leszyk, J., *et al.* (2012) 'Mechanism of evenness interrupted (Evi)-exosome release at synaptic boutons', *J. Biol. Chem.*, 287(20), pp. 16820–16834.

Kong, D., Farmer, V., Shukla, A., James, J., Gruskin, R., Kiriyama, S. and Loncarek, J. (2014) 'Centriole maturation requires regulated Plk1 activity during two consecutive cell cycles', *J. Cell Biol.*, 206(7), pp. 855–865.

Koppers-Lalic, D., Hackenberg, M., Bijnsdorp, I. V, van Eijndhoven, M. A. J., Sadek, P., Sie, D., Zini, N., *et al.* (2014) 'Nontemplated nucleotide additions distinguish the small RNA composition in cells from exosomes.', *Cell Rep.*, 8(6), pp. 1649–1658.

Kordes, C., Brookmann, S., Häussinger, D. and Klonowski-Stumpe, H. (2005) 'Differential and synergistic effects of platelet-derived growth factor-BB and transforming growth factor-beta1 on activated pancreatic stellate cells.', *Pancreas*, 31(2), pp. 156–67.

Kore, R. A., Edmondson, J. L., Jenkins, S. V, Jamshidi-Parsian, A., Dings, R. P. M., Reyna, N. S. and Griffin, R. J. (2018) 'Hypoxia-derived exosomes induce putative altered pathways in biosynthesis and ion regulatory channels in glioblastoma cells.', *Biochem. Biophys. reports*, 14, pp. 104–113.

Korzeniewski, N., Treat, B. and Duensing, S. (2011) 'The HPV-16 E7 oncoprotein induces centriole multiplication through deregulation of Polo-like kinase 4 expression', *Mol. Cancer*, 10(1), p. 61.

Kosaka, N., Iguchi, H., Yoshioka, Y., Takeshita, F., Matsuki, Y. and Ochiya, T. (2010) 'Secretory mechanisms and intercellular transfer of microRNAs in living cells', *J. Biol. Chem.*, 285(23), pp. 17442–17452.

Kota, J., Hancock, J., Kwon, J. and Korc, M. (2017) 'Pancreatic cancer: Stroma and its current and emerging targeted therapies', *Cancer Lett.* Elsevier Ireland Ltd, pp. 38–49.

Kowal, J., Arras, G., Colombo, M., Jouve, M., Morath, J. P., Primdal-Bengtson, B., Dingli, F., *et al.* (2016a) 'Proteomic comparison defines novel markers to characterize heterogeneous populations of extracellular vesicle subtypes', *Proc. Natl. Acad. Sci. U. S. A.*, 113(8), pp. E968–E977.

Kowal, J., Arras, G., Colombo, M., Jouve, M., Morath, J. P., Primdal-Bengtson, B., Dingli, F., *et al.* (2016b) 'Proteomic comparison defines novel markers to characterize heterogeneous populations of extracellular vesicle subtypes', *Proc. Natl. Acad. Sci.*, 113(8), pp. E968–E977.

Krämer, A., Neben, K. and Ho, A. D. (2005) 'Centrosome aberrations in hematological malignancies', *Cell Biol. Int.*, pp. 375–383.

Kratz, A.-S., Bärenz, F., Richter, K. T. and Hoffmann, I. (2015) 'Plk4-dependent phosphorylation of STIL is required for centriole duplication.', *Biol. Open*, 4(3), pp. 370–7.

Kreger, B. T., Johansen, E. R., Cerione, R. A. and Antonyak, M. A. (2016) 'The Enrichment of Survivin in Exosomes from Breast Cancer Cells Treated with Paclitaxel Promotes Cell Survival and Chemoresistance.', *Cancers (Basel).*, 8(12).

Kruger, S., Elmageed, Z. Y. A., Hawke, D. H., Wörner, P. M., Jansen, D. A., Abdel-Mageed, A. B., Alt, E. U., *et al.* (2014) 'Molecular characterization of exosome-like vesicles from breast cancer cells', *BMC Cancer*, 14(1), p. 44.

Kurz, T., Terman, A., Gustafsson, B. and Brunk, Ulf T (2008) 'Lysosomes and oxidative stress in aging and apoptosis', *Biochim. Biophys. Acta - Gen. Subj.*, pp. 1291–1303.

Kurz, T., Terman, A., Gustafsson, B. and Brunk, Ulf T. (2008) 'Lysosomes in iron metabolism, ageing and apoptosis', *Histochem. Cell Biol.*, pp. 389–406.

Kwon, M., Godinho, S. A., Chandhok, N. S., Ganem, N. J., Azioune, A., Thery, M. and Pellman, D. (2008) 'Mechanisms to suppress multipolar divisions in cancer cells with extra centrosomes', *Genes Dev.*, 22(16), pp. 2189–2203.

Lacey, K. R., Jackson, P. K. and Stearns, T. (1999) *Cyclin-dependent kinase control of centrosome duplication*, *Cell Biol.*

Larsson, S. C. and Wolk, A. (2012) 'Red and processed meat consumption and risk of

pancreatic cancer: meta-analysis of prospective studies.', *Br. J. Cancer*, 106(3), pp. 603–7.

Latifkar, A., Ling, L., Hingorani, A., Johansen, E., Clement, A., Zhang, X., Hartman, J., *et al.* (2019) 'Loss of Sirtuin 1 Alters the Secretome of Breast Cancer Cells by Impairing Lysosomal Integrity', *Dev. Cell*, 49(3), pp. 393-408.e7.

Laulagnier, K., Javalet, C., Hemming, F. J., Chivet, M., Lachenal, G., Blot, B., Chatellard, C., *et al.* (2018) 'Amyloid precursor protein products concentrate in a subset of exosomes specifically endocytosed by neurons', *Cell. Mol. Life Sci.*, 75(4), pp. 757–773.

Lawo, S., Bashkurov, M., Mullin, M., Ferreria, M. G., Kittler, R., Habermann, B., Tagliaferro, A., *et al.* (2009) 'HAUS, the 8-subunit human Augmin complex, regulates centrosome and spindle integrity.', *Curr. Biol.*, 19(10), pp. 816–26.

Lawo, S., Hasegan, M., Gupta, G. D. and Pelletier, L. (2012) 'Subdiffraction imaging of centrosomes reveals higher-order organizational features of pericentriolar material', *Nat. Cell Biol.*, 14(11), pp. 1148–1158.

Lee, K. and Rhee, K. (2011) 'PLK1 phosphorylation of pericentrin initiates centrosome maturation at the onset of mitosis.', *J. Cell Biol.*, 195(7), pp. 1093–101.

Lee, K. and Rhee, K. (2012) 'Separase-dependent cleavage of pericentrin B is necessary and sufficient for centriole disengagement during mitosis', *Cell Cycle*, 11(13), pp. 2476–2485.

Lee, M., Seo, M. Y., Chang, J., Hwang, D. S. and Rhee, K. (2017) 'PLK4 phosphorylation of CP110 is required for efficient centriole assembly.', *Cell Cycle*, 16(12), pp. 1225–1234.

Lerit, D. A., Jordan, H. A., Poulton, J. S., Fagerstrom, C. J., Galletta, B. J., Peifer, M. and Rusan, N. M. (2015) 'Interphase centrosome organization by the PLP-Cnn scaffold is required for centrosome function.', *J. Cell Biol.*, 210(1), pp. 79–97.

Lerit, D. A. and Poulton, J. S. (2016) 'Centrosomes are multifunctional regulators of genome stability', *Chromosom. Res.*, 24(1), pp. 5–17.

Leung-Toung, R., Li, W., Tam, T. F. and Karimian, K. (2002) 'Thiol-dependent enzymes

and their inhibitors: a review.', *Curr. Med. Chem.*, 9(9), pp. 979–1002.

Levine, M. S., Bakker, B., Boeckx, B., Moyett, J., Lu, J., Vitre, B., Spierings, D. C., *et al.* (2017) 'Centrosome Amplification Is Sufficient to Promote Spontaneous Tumorigenesis in Mammals', *Dev. Cell*, 40(3), pp. 313-322.e5.

Li, J., Tan, M., Li, L., Pamarthy, D., Lawrence, T. S. and Sun, Y. (2005) 'SAK, A New Polo-Like Kinase, Is Transcriptionally Repressed by p53 and Induces Apoptosis upon RNAi Silencing', *Neoplasia*, 7(4), pp. 312–323.

Li, J., D'Angiolella, V., Seeley, E. S., Kim, S., Kobayashi, T., Fu, W., Campos, E. I., *et al.* (2013) 'USP33 regulates centrosome biogenesis via deubiquitination of the centriolar protein CP110', *Nature*, 495(7440), pp. 255–259.

Li, Q., Shao, Y., Zhang, X., Zheng, T., Miao, M., Qin, L., Wang, B., *et al.* (2015) 'Plasma long noncoding RNA protected by exosomes as a potential stable biomarker for gastric cancer', *Tumor Biol.*, 36(3), pp. 2007–2012.

Li, Z., Ma, Y. Y., Wang, J., Zeng, X. F., Li, R., Kang, W. and Hao, X. K. (2015) 'Exosomal microRNA-141 is upregulated in the serum of prostate cancer patients', *Onco. Targets. Ther.*, 9, pp. 139–148.

Liang, B., Peng, P., Chen, S., Li, L., Zhang, M., Cao, D., Yang, J., *et al.* (2013) 'Characterization and proteomic analysis of ovarian cancer-derived exosomes', *J. Proteomics*, 80, pp. 171–182.

Lin, Y.-C., Chang, C.-W., Hsu, W.-B., Tang, C.-J. C., Lin, Y.-N., Chou, E.-J., Wu, C.-T., *et al.* (2013) 'Human microcephaly protein CEP135 binds to hSAS-6 and CPAP, and is required for centriole assembly.', *EMBO J.*, 32(8), pp. 1141–54.

Lineberry, N., Su, L., Soares, L. and Fathman, C. G. (2008) 'The single subunit transmembrane E3 ligase gene related to anergy in lymphocytes (GRAIL) captures and then ubiquitinates transmembrane proteins across the cell membrane.', *J. Biol. Chem.*, 283(42), pp. 28497–505.

Lingle, W. L., Lutz, W. H., Ingle, J. N., Maihle, N. J. and Salisbury, J. L. (1998) 'Centrosome hypertrophy in human breast tumors: implications for genomic stability and cell polarity.', *Proc. Natl. Acad. Sci. U. S. A.*, 95(6), pp. 2950–5.

Lingle, W. L., Barrett, S. L., Negron, V. C., D'Assoro, A. B., Boeneman, K., Liu, W., Whitehead, C. M., *et al.* (2002) 'Centrosome amplification drives chromosomal instability in breast tumor development.', *Proc. Natl. Acad. Sci. U. S. A.*, 99(4), pp. 1978–83.

Lipson, K. E., Wong, C., Teng, Y. and Spong, S. (2012) 'CTGF is a central mediator of tissue remodeling and fibrosis and its inhibition can reverse the process of fibrosis', *Fibrogenesis Tissue Repair*, 5(S1), p. S24.

Liszka, Ł., Zielińska-Pajak, E., Pajak, J. and Gołka, D. (2008) 'Colloid carcinoma of the pancreas: Review of selected pathological and clinical aspects', *Pathology*, 40(7), pp. 655–663.

Liu, P., Wang, Y. and Li, X. (2019) 'Targeting the untargetable KRAS in cancer therapy', *Acta Pharm. Sin. B*. Chinese Academy of Medical Sciences.

Liu, Y., Gu, Y., Han, Y., Zhang, Q., Jiang, Z., Zhang, X., Huang, B., *et al.* (2016) 'Tumor Exosomal RNAs Promote Lung Pre-metastatic Niche Formation by Activating Alveolar Epithelial TLR3 to Recruit Neutrophils', *Cancer Cell*, 30(2), pp. 243–256.

Locigno, R. and Castronovo, V. (2001) 'Reduced glutathione system: role in cancer development, prevention and treatment (review).', *Int. J. Oncol.*, 19(2), pp. 221–36.

Logozzi, M., De Milito, A., Lugini, L., Borghi, M., Calabrò, L., Spada, M., Perdicchio, M., *et al.* (2009) 'High levels of exosomes expressing CD63 and caveolin-1 in plasma of melanoma patients', *PLoS One*. Edited by Y. Cao, 4(4), p. e5219.

Löhr, M., Schmidt, C., Ringel, J., Kluth, M., Müller, P., Nizze, H. and Jesnowski, R. (2001) 'Transforming growth factor-beta1 induces desmoplasia in an experimental model of human pancreatic carcinoma.', *Cancer Res.*, 61(2), pp. 550–5.

Löhr, M., Klöppel, G., Maisonneuve, P., Lowenfels, A. B. and Lüttges, J. (2005) 'Frequency of K-ras mutations in pancreatic intraductal neoplasias associated with pancreatic ductal adenocarcinoma and chronic pancreatitis: a meta-analysis.', *Neoplasia*, 7(1), pp. 17–23.

Lonardo, E., Frias-Aldeguer, J., Hermann, P. C. and Heeschen, C. (2012) 'Pancreatic

stellate cells form a niche for cancer stem cells and promote their self-renewal and invasiveness.', *Cell Cycle*, 11(7), pp. 1282–90.

Loncarek, J., Hergert, P., Magidson, V. and Khodjakov, A. (2008) 'Control of daughter centriole formation by the pericentriolar material.', *Nat. Cell Biol.*, 10(3), pp. 322–8.

Lončarek, J., Hergert, P. and Khodjakov, A. (2010) 'Centriole Reduplication during Prolonged Interphase Requires Procentriole Maturation Governed by Plk1', *Curr. Biol.*, 20(14), pp. 1277–1282.

Lopes, C. A. M., Mesquita, M., Cunha, A. I., Cardoso, J., Carapeta, S., Laranjeira, C., Pinto, A. E., *et al.* (2018) 'Centrosome amplification arises before neoplasia and increases upon p53 loss in tumorigenesis', *J. Cell Biol.*, 217(7), pp. 2353–2363.

Lowenfels, A. B., Maisonneuve, P., DiMagno, E. P., Elitsur, Y., Gates, L. K., Perrault, J. and Whitcomb, D. C. (1997) 'Hereditary pancreatitis and the risk of pancreatic cancer. International Hereditary Pancreatitis Study Group.', *J. Natl. Cancer Inst.*, 89(6), pp. 442–6.

Lozano, E., Betson, M. and Braga, V. M. M. (2003) 'Tumor progression: Small GTpases and loss of cell-cell adhesion', *BioEssays*.

Lucenteforte, E., La Vecchia, C., Silverman, D., Petersen, G. M., Bracci, P. M., Ji, B. T., Bosetti, C., *et al.* (2012) 'Alcohol consumption and pancreatic cancer: a pooled analysis in the International Pancreatic Cancer Case-Control Consortium (PanC4).', *Ann. Oncol. Off. J. Eur. Soc. Med. Oncol.*, 23(2), pp. 374–82.

Ma, L., Yang, X., Wei, R., Ye, T., Zhou, J. K., Wen, M., Men, R., *et al.* (2018) 'MicroRNA-214 promotes hepatic stellate cell activation and liver fibrosis by suppressing Sufu expression article', *Cell Death Dis.*, 9(7).

Macůrek, L., Lindqvist, A., Lim, D., Lampson, M. A., Klompmaker, R., Freire, R., Clouin, C., *et al.* (2008) 'Polo-like kinase-1 is activated by aurora A to promote checkpoint recovery', *Nature*, 455(7209), pp. 119–123.

Maitra, A., Fukushima, N., Takaori, K. and Hruban, R. H. (2005) 'Precursors to invasive pancreatic cancer.', *Adv. Anat. Pathol.*, 12(2), pp. 81–91.

Maitra, A. and Hruban, R. H. (2008) 'Pancreatic Cancer', *Annu. Rev. Pathol. Mech. Dis.*, 3(1), pp. 157–188.

Mantoni, T. S., Lunardi, S., Al-Assar, O., Masamune, A. and Brunner, T. B. (2011) 'Pancreatic stellate cells radioprotect pancreatic cancer cells through β1-integrin signaling', *Cancer Res.*, 71(10), pp. 3453–3458.

Mardin, B. R., Lange, C., Baxter, J. E., Hardy, T., Scholz, S. R., Fry, A. M. and Schiebel, E. (2010) 'Components of the Hippo pathway cooperate with Nek2 kinase to regulate centrosome disjunction', *Nat. Cell Biol.*, 12(12), pp. 1166–1176.

Mardin, B. R., Agircan, F. G., Lange, C. and Schiebel, E. (2011) 'Plk1 Controls the Nek2A-PP1γ Antagonism in Centrosome Disjunction', *Curr. Biol.*, 21(13), pp. 1145–1151.

Mardin, B. R. (2014) 'Separate to operate: control of centrosome positioning and separation', *Philos. Trans. R. Soc. Lond. B. Biol. Sci.*, pp. 20130461–20130461.

Mardin, B. R. and Schiebel, E. (2012) 'Breaking the ties that bind: new advances in centrosome biology.', *J. Cell Biol.*, 197(1), pp. 11–8.

Marteil, G., Guerrero, A., Vieira, A. F., De Almeida, B. P., Machado, P., Mendonça, S., Mesquita, M., *et al.* (2018) 'Over-elongation of centrioles in cancer promotes centriole amplification and chromosome missegregation', *Nat. Commun.*, 9(1).

Marteil, G., Dias Louro, M. A. and Bettencourt-Dias, M. (2017) 'Centrosome Assembly: Reconstructing the Core Cartwheel Structure In Vitro', *Curr. Biol.* Cell Press, pp. R606–R609.

Marthiens, V., Rujano, M. A., Pennetier, C., Tessier, S., Paul-Gilloteaux, P. and Basto, R. (2013) 'Centrosome amplification causes microcephaly', *Nat. Cell Biol.*, 15(7), pp. 731–740.

Martinez-Useros, J., Li, W., Cabeza-Morales, M. and Garcia-Foncillas, J. (2017) 'Oxidative Stress: A New Target for Pancreatic Cancer Prognosis and Treatment', *J. Clin. Med.*, 6(3), p. 29.

Marzec, J., Dayem Ullah, A. Z., Pirrò, S., Gadaleta, E., Crnogorac-Jurcevic, T., Lemoine, N. R., Kocher, H. M., *et al.* (2018) 'The Pancreatic Expression Database: 2018 update', *Nucleic Acids Res.*, 46(D1), pp. D1107–D1110.

Marzoq, A. J., Mustafa, S. A., Heidrich, L., Hoheisel, J. D. and Alhamdani, M. S. S. (2019) 'Impact of the secretome of activated pancreatic stellate cells on growth and differentiation of pancreatic tumour cells', *Sci. Rep.*, 9(1).

Masamune, A., Sakai, Y., Kikuta, K., Satoh, M., Satoh, A. and Shimosegawa, T. (2002) 'Activated rat pancreatic stellate cells express intercellular adhesion molecule-1 (ICAM-1) in vitro.', *Pancreas*, 25(1), pp. 78–85.

Masamune, A., Yoshida, N., Hamada, S., Takikawa, T., Nabeshima, T. and Shimosegawa, T. (2018) 'Exosomes derived from pancreatic cancer cells induce activation and profibrogenic activities in pancreatic stellate cells', *Biochem. Biophys. Res. Commun.*, 495(1), pp. 71–77.

Masamune, A. and Shimosegawa, T. (2009) 'Signal transduction in pancreatic stellate cells.', *J. Gastroenterol.*, 44(4), pp. 249–60.

Masoud, K., Herzog, E., Chabouté, M.-E. and Schmit, A.-C. (2013) 'Microtubule nucleation and establishment of the mitotic spindle in vascular plant cells', *Plant J.*, 75(2), pp. 245–257.

Mathieu, M., Martin-Jaular, L., Lavieu, G. and Théry, C. (2019) 'Specificities of secretion and uptake of exosomes and other extracellular vesicles for cell-to-cell communication', *Nat. Cell Biol.*, 21(1), pp. 9–17.

Mathivanan, S., Fahner, C. J., Reid, G. E. and Simpson, R. J. (2012) 'ExoCarta 2012: Database of exosomal proteins, RNA and lipids', *Nucleic Acids Res.*, 40(D1), pp. D1241-4.

Mathivanan, S., Ji, H. and Simpson, R. J. (2010) 'Exosomes: Extracellular organelles important in intercellular communication', *J. Proteomics*, pp. 1907–1920.

Matsumoto, F., Fujii, H., Abe, M., Kajino, K., Kobayashi, T., Matsumoto, T., Ikeda, K., *et al.* (2006) 'A novel tumor marker, Niban, is expressed in subsets of thyroid tumors and Hashimoto's thyroiditis', *Hum. Pathol.*, 37(12), pp. 1592–1600.

Matsumura, T., Sugimachi, K., Iinuma, H., Takahashi, Y., Kurashige, J., Sawada, G., Ueda, M., *et al.* (2015) 'Exosomal microRNA in serum is a novel biomarker of recurrence in human colorectal cancer', *Br. J. Cancer*, 113(2), pp. 275–281.

Matsuo, K., Ohsumi, K., Iwabuchi, M., Kawamata, T., Ono, Y. and Takahashi, M. (2012) 'Kendrin is a novel substrate for separase involved in the licensing of centriole duplication.', *Curr. Biol.*, 22(10), pp. 915–21.

Mauvezin, C. and Neufeld, T. P. (2015) 'Bafilomycin A1 disrupts autophagic flux by inhibiting both V-ATPase-dependent acidification and Ca-P60A/SERCA-dependent autophagosome-lysosome fusion', *Autophagy*, 11(8), pp. 1437–1438.

Mayor, T., Stierhof, Y. D., Tanaka, K., Fry, A. M. and Nigg, E. A. (2000) 'The centrosomal protein C-Nap1 is required for cell cycle-regulated centrosome cohesion.', *J. Cell Biol.*, 151(4), pp. 837–46.

Meckes, D. G. and Raab-Traub, N. (2011) 'Microvesicles and Viral Infection', *J. Virol.*, 85(24), pp. 12844–12854.

Megraw, T. L., Li, K., Kao, L. R. and Kaufman, T. C. (1999) 'The centrosomin protein is required for centrosome assembly and function during cleavage in Drosophila.', *Development*, 126(13), pp. 2829–39.

Megraw, T. L., Kao, L. R. and Kaufman, T. C. (2001) 'Zygotic development without functional mitotic centrosomes.', *Curr. Biol.*, 11(2), pp. 116–20.

Melo, S. A., Sugimoto, H., O'Connell, J. T., Kato, N., Villanueva, A., Vidal, A., Qiu, L., *et al.* (2014) 'Cancer Exosomes Perform Cell-Independent MicroRNA Biogenesis and Promote Tumorigenesis', *Cancer Cell*, 26(5), pp. 707–721.

Melo, S. A., Luecke, L. B., Kahlert, C., Fernandez, A. F., Gammon, S. T., Kaye, J., Lebleu, V. S., *et al.* (2015) 'Glypican-1 identifies cancer exosomes and detects early pancreatic cancer', *Nature*, 523(7559), pp. 177–182.

Mennella, V., Keszthelyi, B., Mcdonald, K. L., Chhun, B., Kan, F., Rogers, G. C., Huang, B., *et al.* (2012) 'Subdiffraction-resolution fluorescence microscopy reveals a domain of the centrosome critical for pericentriolar material organization', *Nat. Cell Biol.*, 14(11), pp. 1159–1168.

Mews, P., Phillips, P., Fahmy, R., Korsten, M., Pirola, R., Wilson, J. and Apte, M. (2002) 'Pancreatic stellate cells respond to inflammatory cytokines: potential role in chronic pancreatitis.', *Gut*, 50(4), pp. 535–41.

Miao, Y., Li, G., Zhang, X., Xu, H. and Abraham, S. N. (2015) 'A TRP channel senses lysosome neutralization by pathogens to trigger their expulsion', *Cell*, 161(6), pp. 1306–1319.

Mincheva-Nilsson, L. and Baranov, V. (2010) 'The Role of Placental Exosomes in Reproduction', *Am. J. Reprod. Immunol.*, 63(6), pp. 520–533.

Mirus, J. E., Zhang, Y., Li, C. I., Lokshin, A. E., Prentice, R. L., Hingorani, S. R. and Lampe, P. D. (2015) 'Cross-species antibody microarray interrogation identifies a 3-protein panel of plasma biomarkers for early diagnosis of pancreas cancer', *Clin. Cancer Res.*, 21(7), pp. 1764–1771.

Mittal, K., Ogden, A., Reid, M. D., Rida, P. C. G., Varambally, S. and Aneja, R. (2015) 'Amplified centrosomes may underlie aggressive disease course in pancreatic ductal adenocarcinoma', *Cell Cycle*, 14(17), pp. 2798–2809.

Mizushima, N. and Yoshimori, T. (2007) 'How to interpret LC3 immunoblotting', *Autophagy*, pp. 542–545.

Montecalvo, A., Larregina, A. T., Shufesky, W. J., Stolz, D. B., Sullivan, M. L. G., Karlsson, J. M., Baty, C. J., *et al.* (2012) 'Mechanism of transfer of functional microRNAs between mouse dendritic cells via exosomes', *Blood*, 119(3), pp. 756–766.

Mooren, O. L., Galletta, B. J. and Cooper, J. A. (2012) 'Roles for Actin Assembly in Endocytosis', *Annu. Rev. Biochem.*, 81(1), pp. 661–686.

Morelli, A. E. (2006) 'The immune regulatory effect of apoptotic cells and exosomes on dendritic cells: Its impact on transplantation', *Am. J. Transplant.*, pp. 254–261.

Mountain, V., Simerly, C., Howard, L., Ando, A., Schatten, G. and Compton, D. A. (1999) 'The kinesin-related protein, HSET, opposes the activity of Eg5 and cross-links microtubules in the mammalian mitotic spindle.', *J. Cell Biol.*, 147(2), pp. 351–66.

Moutinho-Pereira, S., Debec, A. and Maiato, H. (2009) 'Microtubule cytoskeleton remodeling by acentriolar microtubule-organizing centers at the entry and exit from mitosis in Drosophila somatic cells.', *Mol. Biol. Cell*, 20(11), pp. 2796–808.

Moyer, T. C., Clutario, K. M., Lambrus, B. G., Daggubati, V. and Holland, A. J. (2015) 'Binding of STIL to Plk4 activates kinase activity to promote centriole assembly.', *J.*

Cell Biol., 209(6), pp. 863–78.

Mulcahy, L. A., Pink, R. C. and Carter, D. R. F. (2014) 'Routes and mechanisms of extracellular vesicle uptake.', *J. Extracell. vesicles*, 3.

Muller, L., Hong, C. S., Stolz, D. B., Watkins, S. C. and Whiteside, T. L. (2014) 'Isolation of biologically-active exosomes from human plasma', *J. Immunol. Methods*, 411, pp. 55–65.

Müller, M., Schmidt, O., Angelova, M., Faserl, K., Weys, S., Kremser, L., Pfaffenwimmer, T., *et al.* (2015) 'The coordinated action of the MVB pathway and autophagy ensures cell survival during starvation', *Elife*, 4, p. e07736.

Munkley, J., Vodak, D., Livermore, K. E., James, K., Wilson, B. T., Knight, B., Mccullagh, P., *et al.* (2016) 'Glycosylation is an Androgen-Regulated Process Essential for Prostate Cancer Cell Viability.', *EBioMedicine*, 8, pp. 103–116.

Muzumdar, M. D., Tasic, B., Miyamichi, K., Li, L. and Luo, L. (2007) 'A global double-fluorescent Cre reporter mouse.', *Genesis*, 45(9), pp. 593–605.

Nakazawa, Y., Hiraki, M., Kamiya, R. and Hirono, M. (2007) 'SAS-6 is a Cartwheel Protein that Establishes the 9-Fold Symmetry of the Centriole', *Curr. Biol.*, 17(24), pp. 2169–2174.

Nazarenko, I., Rana, S., Baumann, A., McAlear, J., Hellwig, A., Trendelenburg, M., Lochnit, G., *et al.* (2010) 'Cell surface tetraspanin Tspan8 contributes to molecular pathways of exosome-induced endothelial cell activation', *Cancer Res.*, 70(4), pp. 1668–1678.

Neesse, A., Michl, P., Frese, K. K., Feig, C., Cook, N., Jacobetz, M. A., Lolkema, M. P., *et al.* (2011) 'Stromal biology and therapy in pancreatic cancer.', *Gut*, 60(6), pp. 861–8.

Neesse, A., Algül, H., Tuveson, D. A. and Gress, T. M. (2015) 'Stromal biology and therapy in pancreatic cancer: a changing paradigm.', *Gut*, 64(9), pp. 1476–84.

Nicholl, M. B., Ledgewood, C. L., Chen, X., Bai, Q., Qin, C., Cook, K. M., Herrick, E. J., *et al.* (2014) 'IL-35 promotes pancreas cancer growth through enhancement of proliferation and inhibition of apoptosis: evidence for a role as an autocrine

growth factor.', *Cytokine*, 70(2), pp. 126–33.

Nielsen, M. F. B., Mortensen, M. B. and Detlefsen, S. (2016) 'Key players in pancreatic cancer-stroma interaction: Cancer-associated fibroblasts, endothelial and inflammatory cells.', *World J. Gastroenterol.*, 22(9), pp. 2678–700.

Nigg, E. A. (2002) 'Centrosome aberrations: cause or consequence of cancer progression?', *Nat. Rev. Cancer*, 2(11), pp. 815–25.

Nigg, E. A. (2006) 'Origins and consequences of centrosome aberrations in human cancers', *Int. J. Cancer*, 119(12), pp. 2717–2723.

Nigg, E. A. and Holland, A. J. (2018) 'Once and only once: mechanisms of centriole duplication and their deregulation in disease', *Nat. Rev. Mol. Cell Biol.*, 19(5), pp. 297–312.

Nigg, E. A. and Raff, J. W. (2009) 'Centrioles, Centrosomes, and Cilia in Health and Disease', *Cell*, 139(4), pp. 663–678.

Nigg, E. A. and Stearns, T. (2011) 'The centrosome cycle: Centriole biogenesis, duplication and inherent asymmetries', *Nat. Cell Biol.*, 13(10), pp. 1154–1160.

Nilsson, E., Ghassemifar, R. and Brunk, U. T. (1997) 'Lysosomal heterogeneity between and within cells with respect to resistance against oxidative stress.', *Histochem. J.*, 29(11–12), pp. 857–65.

Noctor, G. and Foyer, C. H. (2002) 'ASCORBATE AND GLUTATHIONE: Keeping Active Oxygen Under Control', *Annu. Rev. Plant Physiol. Plant Mol. Biol.*, 49(1), pp. 249–279.

Nuha M, M. A. M., Hiba S, E. and Christina Wasunna, M. (2015) 'In-vitro "Depletion" of Mitochondrial Cytochrome C Oxidase Subunit II Affects the Patterns of Gene Expression across Multiple Cancer Pathways', *J. Mol. Biomark. Diagn.*, s2.

Nussey, S. and Whitehead, S. (2001) 'Chapter 2 The endocrine pancreas', in *Endocrinol. An Integr. Approach.* Oxford: BIOS Scientific Publishers.

O'Connell, C. B. and Khodjakov, A. L. (2007) 'Cooperative mechanisms of mitotic spindle formation', *J. Cell Sci.*, 120(10), pp. 1717–1722.

O'Connell, K. F., Caron, C., Kopish, K. R., Hurd, D. D., Kemphues, K. J., Li, Y. and White, J. G. (2001) 'The C. elegans zyg-1 gene encodes a regulator of centrosome duplication with distinct maternal and paternal roles in the embryo.', *Cell*, 105(4), pp. 547–58.

O'Neill, C., Gilligan, K. and Dwyer, R. (2019) 'Role of Extracellular Vesicles (EVs) in Cell Stress Response and Resistance to Cancer Therapy', *Cancers (Basel).*, 11(2), p. 136.

Ohnishi, H., Miyata, T., Yasuda, H., Satoh, Y., Hanatsuka, K., Kita, H., Ohashi, A., *et al.* (2004) 'Distinct Roles of Smad2-, Smad3-, and ERK-dependent Pathways in Transforming Growth Factor-β1 Regulation of Pancreatic Stellate Cellular Functions', *J. Biol. Chem.*, 279(10), pp. 8873–8878.

Ohnishi, N., Miyata, T., Ohnishi, H., Yasuda, H., Tamada, K., Ueda, N., Mashima, H., *et al.* (2003) 'Activin A is an autocrine activator of rat pancreatic stellate cells: potential therapeutic role of follistatin for pancreatic fibrosis.', *Gut*, 52(10), pp. 1487–93.

Ohta, M., Ashikawa, T., Nozaki, Y., Kozuka-Hata, H., Goto, H., Inagaki, M., Oyama, M., *et al.* (2014) 'Direct interaction of Plk4 with STIL ensures formation of a single procentriole per parental centriole.', *Nat. Commun.*, 5, p. 5267.

Omary, M. B., Lugea, A., Lowe, A. W. and Pandol, S. J. (2007) 'The pancreatic stellate cell: a star on the rise in pancreatic diseases.', *J. Clin. Invest.*, 117(1), pp. 50–9.

Orozco, C. A., Martinez-Bosch, N., Guerrero, P. E., Vinaixa, J., Dalotto-Moreno, T., Iglesias, M., Moreno, M., *et al.* (2018) 'Targeting galectin-1 inhibits pancreatic cancer progression by modulating tumor-stroma crosstalk.', *Proc. Natl. Acad. Sci. U. S. A.*, 115(16), pp. E3769–E3778.

Ostrowski, M., Carmo, N. B., Krumeich, S., Fanget, I., Raposo, G., Savina, A., Moita, C. F., *et al.* (2010) 'Rab27a and Rab27b control different steps of the exosome secretion pathway', *Nat. Cell Biol.*, 12(1), pp. 19–30.

Özdemir, B. C., Pentcheva-Hoang, T., Carstens, J. L., Zheng, X., Wu, C. C., Simpson, T. R., Laklai, H., *et al.* (2014) 'Depletion of carcinoma-associated fibroblasts and fibrosis induces immunosuppression and accelerates pancreas cancer with reduced

survival', *Cancer Cell*, 25(6), pp. 719–734.

Paintrand, M., Moudjou, M., Delacroix, H. and Bornens, M. (1992) 'Centrosome organization and centriole architecture: their sensitivity to divalent cations.', *J. Struct. Biol.*, 108(2), pp. 107–28.

Pällmann, N., Livgård, M., Tesikova, M., Zeynep Nenseth, H., Akkus, E., Sikkeland, J., Jin, Yixin, *et al.* (2019) 'Regulation of the unfolded protein response through ATF4 and FAM129A in prostate cancer', *Oncogene*.

Pan, B. T., Teng, K., Wu, C., Adam, M. and Johnstone, R. M. (1985) 'Electron microscopic evidence for externalization of the transferrin receptor in vesicular form in sheep reticulocytes.', *J. Cell Biol.*, 101(3), pp. 942–8.

Pan, B. T. and Johnstone, R. M. (1983) 'Fate of the transferrin receptor during maturation of sheep reticulocytes in vitro: Selective externalization of the receptor', *Cell*, 33(3), pp. 967–978.

Pandharipande, P. V, Heberle, C., Dowling, E. C., Kong, C. Y., Tramontano, A., Perzan, K. E., Brugge, W., *et al.* (2015) 'Targeted screening of individuals at high risk for pancreatic cancer: results of a simulation model.', *Radiology*, 275(1), pp. 177–87.

Pandol, S. J. (2011) 'Digestive Enzymes and Their Functions', in *The exocrine pancreas*. Morgan & Claypool Life Sciences.

Panic, M., Hata, S., Neuner, A. and Schiebel, E. (2015) 'The centrosomal linker and microtubules provide dual levels of spatial coordination of centrosomes.', *PLoS Genet.*, 11(5), p. e1005243.

Park, S.-Y., Park, J.-E., Kim, T.-S., Kim, J. H., Kwak, M.-J., Ku, B., Tian, L., *et al.* (2014) 'Molecular basis for unidirectional scaffold switching of human Plk4 in centriole biogenesis.', *Nat. Struct. Mol. Biol.*, 21(8), pp. 696–703.

Parkin, D. M. (2011) 'Tobacco-attributable cancer burden in the UK in 2010', *Br. J. Cancer*, 105, pp. S6–S13.

Parolini, I., Federici, C., Raggi, C., Lugini, L., Palleschi, S., De Milito, A., Coscia, C., *et al.* (2009) 'Microenvironmental pH is a key factor for exosome traffic in tumor cells', *J. Biol. Chem.*, 284(49), pp. 34211–34222.

Pellegata, N. S., Sessa, F., Renault, B., Bonato, M., Leone, B. E., Solcia, E. and Ranzani, G. N. (1994) 'K-ras and p53 gene mutations in pancreatic cancer: ductal and nonductal tumors progress through different genetic lesions.', *Cancer Res.*, 54(6), pp. 1556–60.

Pelletier, L., O'Toole, E., Schwager, A., Hyman, A. A. and Müller-Reichert, T. (2006) 'Centriole assembly in Caenorhabditis elegans', *Nature*, 444(7119), pp. 619–623.

Peng, T., Zhou, W., Guo, F., Wu, H. S., Wang, C. Y., Wang, L. and Yang, Z. Y. (2017) 'Centrosomal protein 55 activates NF-κB signalling and promotes pancreatic cancer cells aggressiveness', *Sci. Rep.*, 7(1).

Phillips, P. A., Wu, M. J., Kumar, R. K., Doherty, E., McCarroll, J. A., Park, S., Pirola, R. C., *et al.* (2003) 'Cell migration: a novel aspect of pancreatic stellate cell biology.', *Gut*, 52(5), pp. 677–82.

Phillips, P. A., McCarroll, J. A., Park, S., Wu, M.-J., Pirola, R., Korsten, M., Wilson, J. S., *et al.* (2003) 'Rat pancreatic stellate cells secrete matrix metalloproteinases: implications for extracellular matrix turnover.', *Gut*, 52(2), pp. 275–82.

Piel, M., Meyer, P., Khodjakov, A., Rieder, C. L. and Bornens, M. (2000) 'The respective contributions of the mother and daughter centrioles to centrosome activity and behavior in vertebrate cells.', *J. Cell Biol.*, 149(2), pp. 317–30.

Pihan, G. A., Purohit, A., Wallace, J., Knecht, H., Woda, B., Quesenberry, P. and Doxsey, S. J. (1998) 'Centrosome defects and genetic instability in malignant tumors', *Cancer Res.*, 58(17), pp. 3974–3985.

Pihan, G. A., Purohit, A., Wallace, J., Malhotra, R., Liotta, L. and Doxsey, S. J. (2001) 'Centrosome defects can account for cellular and genetic changes that characterize prostate cancer progression.', *Cancer Res.*, 61(5), pp. 2212–9.

Pihan, G. A., Wallace, J., Zhou, Y. and Doxsey, S. J. (2003) 'Centrosome abnormalities and chromosome instability occur together in pre-invasive carcinomas.', *Cancer Res.*, 63(6), pp. 1398–404.

Pinzani, M., Gesualdo, L., Sabbah, G. M. and Abboud, H. E. (1989) 'Effects of platelet-derived growth factor and other polypeptide mitogens on DNA synthesis and

growth of cultured rat liver fat-storing cells', *J. Clin. Invest.*, 84(6), pp. 1786–1793.

Piper, R. C. and Katzmann, D. J. (2007) 'Biogenesis and Function of Multivesicular Bodies', *Annu. Rev. Cell Dev. Biol.*, 23(1), pp. 519–547.

Poruk, K. E., Gay, D. Z., Brown, K., Mulvihill, J. D., Boucher, K. M., Scaife, C. L., Firpo, M. A., *et al.* (2013) 'The clinical utility of CA 19-9 in pancreatic adenocarcinoma: diagnostic and prognostic updates.', *Curr. Mol. Med.*, 13(3), pp. 340–51.

Poulton, J. S., Cuningham, J. C. and Peifer, M. (2014) 'Acentrosomal Drosophila epithelial cells exhibit abnormal cell division, leading to cell death and compensatory proliferation.', *Dev. Cell*, 30(6), pp. 731–45.

Provenzano, P. P., Cuevas, C., Chang, A. E., Goel, V. K., Von Hoff, D. D. and Hingorani, S. R. (2012) 'Enzymatic targeting of the stroma ablates physical barriers to treatment of pancreatic ductal adenocarcinoma.', *Cancer Cell*, 21(3), pp. 418–29.

Puri, N. and Roche, P. A. (2008) 'Mast cells possess distinct secretory granule subsets whose exocytosis is regulated by different SNARE isoforms.', *Proc. Natl. Acad. Sci. U. S. A.*, 105(7), pp. 2580–5.

Pylayeva-Gupta, Y., Das, S., Handler, J. S., Hajdu, C. H., Coffre, M., Koralov, S. B. and Bar-Sagi, D. (2016) 'IL35-Producing B Cells Promote the Development of Pancreatic Neoplasia.', *Cancer Discov.*, 6(3), pp. 247–55.

Qian, D., Lu, Z., Xu, Q., Wu, P., Tian, L., Zhao, L., Cai, B., *et al.* (2017) 'Galectin-1-driven upregulation of SDF-1 in pancreatic stellate cells promotes pancreatic cancer metastasis.', *Cancer Lett.*, 397, pp. 43–51.

Qu, J. L., Qu, X. J., Zhao, M. F., Teng, Y. E., Zhang, Y., Hou, K. Z., Jiang, Y. H., *et al.* (2009) 'Gastric cancer exosomes promote tumour cell proliferation through PI3K/Akt and MAPK/ERK activation', *Dig. Liver Dis.*, 41(12), pp. 875–880.

Quintyne, N. J., Reing, J. E., Hoffelder, D. R., Gollin, S. M. and Saunders, W. S. (2005) 'Spindle multipolarity is prevented by centrosomal clustering', *Science (80-.).*, 307(5706), pp. 127–129.

Raaijmakers, J. A., van Heesbeen, R. G. H. P., Meaders, J. L., Geers, E. F., Fernandez-Garcia, B., Medema, R. H. and Tanenbaum, M. E. (2012) 'Nuclear envelope-

associated dynein drives prophase centrosome separation and enables Eg5-independent bipolar spindle formation.', *EMBO J.*, 31(21), pp. 4179–90.

Raaijmakers, J. A. and Medema, R. H. (2014) 'Function and regulation of dynein in mitotic chromosome segregation', *Chromosoma*, 123(5), pp. 407–422.

Rabinowits, G., Gerçel-Taylor, C., Day, J. M., Taylor, D. D. and Kloecker, G. H. (2009) 'Exosomal microRNA: A diagnostic marker for lung cancer', *Clin. Lung Cancer*, 10(1), pp. 42–46.

Rahib, L., Smith, B. D., Aizenberg, R., Rosenzweig, A. B., Fleshman, J. M. and Matrisian, L. M. (2014) 'Projecting cancer incidence and deaths to 2030: The unexpected burden of thyroid, liver, and pancreas cancers in the united states', *Cancer Res.* American Association for Cancer Research Inc., pp. 2913–2921.

Rahier, J., Wallon, J. and Henquin, J. C. (1981) 'Cell populations in the endocrine pancreas of human neonates and infants', *Diabetologia*, 20(5), pp. 540–546.

Raimondi, S., Lowenfels, A. B., Morselli-Labate, A. M., Maisonneuve, P. and Pezzilli, R. (2010) 'Pancreatic cancer in chronic pancreatitis; aetiology, incidence, and early detection.', *Best Pract. Res. Clin. Gastroenterol.*, 24(3), pp. 349–58.

Raimondi, S., Maisonneuve, P. and Lowenfels, A. B. (2009) 'Epidemiology of pancreatic cancer: an overview.', *Nat. Rev. Gastroenterol. Hepatol.*, 6(12), pp. 699–708.

Raimondo, F., Morosi, L., Chinello, C., Magni, F. and Pitto, M. (2011) 'Advances in membranous vesicle and exosome proteomics improving biological understanding and biomarker discovery', *Proteomics*, 11(4), pp. 709–720.

Rana, S., Yue, S., Stadel, D. and Zöller, M. (2012) 'Toward tailored exosomes: The exosomal tetraspanin web contributes to target cell selection', *Int. J. Biochem. Cell Biol.*, 44(9), pp. 1574–1584.

Raposo, G., Nijman, H. W., Stoorvogel, W., Liejendekker, R., Harding, C. V, Melief, C. J. and Geuze, H. J. (1996) 'B lymphocytes secrete antigen-presenting vesicles.', *J. Exp. Med.*, 183(3), pp. 1161–72.

Raposo, G. and Stoorvogel, W. (2013) 'Extracellular vesicles: Exosomes, microvesicles, and friends', *J. Cell Biol.* Rockefeller University Press, pp. 373–383.

Rayess, H., Wang, M. B. and Srivatsan, E. S. (2012) 'Cellular senescence and tumor suppressor gene p16.', *Int. J. cancer*, 130(8), pp. 1715–25.

Redmann, M., Benavides, G. A., Berryhill, T. F., Wani, W. Y., Ouyang, X., Johnson, M. S., Ravi, S., *et al.* (2017) 'Inhibition of autophagy with bafilomycin and chloroquine decreases mitochondrial quality and bioenergetic function in primary neurons', *Redox Biol.*, 11, pp. 73–81.

Reiter, R., Gais, P., Steuer-Vogt, M. K., Boulesteix, A.-L., Deutschle, T., Hampel, R., Wagenpfeil, S., *et al.* (2009) 'Centrosome abnormalities in head and neck squamous cell carcinoma (HNSCC)', *Acta Otolaryngol.*, 129(2), pp. 205–213.

Rhim, A. D., Oberstein, P. E., Thomas, D. H., Mirek, E. T., Palermo, C. F., Sastra, S. A., Dekleva, E. N., *et al.* (2014) 'Stromal elements act to restrain, rather than support, pancreatic ductal adenocarcinoma', *Cancer Cell*, 25(6), pp. 735–747.

Rhys, A. D., Monteiro, P., Smith, C., Vaghela, M., Arnandis, T., Kato, T., Leitinger, B., *et al.* (2018) 'Loss of E-cadherin provides tolerance to centrosome amplification in epithelial cancer cells', *J. Cell Biol.*, 217(1), pp. 195–209.

Rhys, A. D. and Godinho, S. A. (2017) 'Dividing with extra centrosomes: A double edged sword for cancer cells', in *Adv. Exp. Med. Biol.* Springer, Cham, pp. 47–67.

Ring, D., Hubble, R. and Kirschner, M. (1982) 'Mitosis in a cell with multiple centrioles', *J. Cell Biol.*, 94(3), pp. 549–556.

Ringuette Goulet, C., Bernard, G., Tremblay, S., Chabaud, S., Bolduc, S. and Pouliot, F. (2018) 'Exosomes Induce Fibroblast Differentiation into Cancer-Associated Fibroblasts through TGFβ Signaling.', *Mol. Cancer Res.*, 16(7), pp. 1196–1204.

Roberts, N. J., Jiao, Y., Yu, J., Kopelovich, L., Petersen, G. M., Bondy, M. L., Gallinger, S., *et al.* (2012) 'ATM mutations in patients with hereditary pancreatic cancer.', *Cancer Discov.*, 2(1), pp. 41–6.

Rodrigues-Martins, A., Riparbelli, M., Callaini, G., Glover, D. M. and Bettencourt-Dias, M. (2008) 'From centriole biogenesis to cellular function: Centrioles are essential for cell division at critical developmental stages', *Cell Cycle*, 7(1), pp. 11–16.

Rogers, G. C., Rusan, N. M., Roberts, D. M., Peifer, M. and Rogers, S. L. (2009) 'The

SCFSlimb ubiquitin ligase regulates Plk4/Sak levels to block centriole reduplication', *J. Cell Biol.*, 184(2), p. 225.

Rohrmann, S., Linseisen, J., Nöthlings, U., Overvad, K., Egeberg, R., Tjønneland, A., Boutron-Ruault, M. C., *et al.* (2013) 'Meat and fish consumption and risk of pancreatic cancer: Results from the European Prospective Investigation into Cancer and Nutrition', *Int. J. Cancer*, 132(3), pp. 617–624.

Roig, J., Mikhailov, A., Belham, C. and Avruch, J. (2002) 'Nercc1, a mammalian NIMA-family kinase, binds the Ran GTPase and regulates mitotic progression.', *Genes Dev.*, 16(13), pp. 1640–58.

Roig, J., Groen, A., Caldwell, J. and Avruch, J. (2005) 'Active Nercc1 protein kinase concentrates at centrosomes early in mitosis and is necessary for proper spindle assembly.', *Mol. Biol. Cell*, 16(10), pp. 4827–40.

Romancino, D. P., Paterniti, G., Campos, Y., De Luca, A., Di Felice, V., D'Azzo, A. and Bongiovanni, A. (2013) 'Identification and characterization of the nano-sized vesicles released by muscle cells', *FEBS Lett.*, 587(9), pp. 1379–1384.

Rosendahl, A. H., Perks, C. M., Zeng, L., Markkula, A., Simonsson, M., Rose, C., Ingvar, C., *et al.* (2015) 'Caffeine and Caffeic Acid Inhibit Growth and Modify Estrogen Receptor and Insulin-like Growth Factor I Receptor Levels in Human Breast Cancer.', *Clin. Cancer Res.*, 21(8), pp. 1877–87.

Rozenblum, E., Schutte, M., Goggins, M., Hahn, S. A., Panzer, S., Zahurak, M., Goodman, S. N., *et al.* (1997) 'Tumor-suppressive pathways in pancreatic carcinoma.', *Cancer Res.*, 57(9), pp. 1731–4.

Ryan, D. P., Hong, T. S. and Bardeesy, N. (2014) 'Pancreatic Adenocarcinoma', *N. Engl. J. Med.*, 371(11), pp. 1039–1049.

Sah, R. P., Nagpal, S. J. S., Mukhopadhyay, D. and Chari, S. T. (2013) 'New insights into pancreatic cancer-induced paraneoplastic diabetes.', *Nat. Rev. Gastroenterol. Hepatol.*, 10(7), pp. 423–33.

Sahu, R., Kaushik, S., Clement, C. C., Cannizzo, E. S., Scharf, B., Follenzi, A., Potolicchio, I., *et al.* (2011) 'Microautophagy of cytosolic proteins by late endosomes.', *Dev.*

Cell, 20(1), pp. 131–9.

Salisbury, J. L., D'Assoro, A. B. and Lingle, W. L. (2004) 'Centrosome amplification and the origin of chromosomal instability in breast cancer.', *J. Mammary Gland Biol. Neoplasia*, 9(3), pp. 275–83.

Sánchez-Huertas, C. and Lüders, J. (2015) 'The augmin connection in the geometry of microtubule networks.', *Curr. Biol.*, 25(7), pp. R294-9.

Sander, E. E., ten Klooster, J. P., van Delft, S., van der Kammen, R. A. and Collard, J. G. (1999) 'Rac downregulates Rho activity: reciprocal balance between both GTPases determines cellular morphology and migratory behavior.', *J. Cell Biol.*, 147(5), pp. 1009–22.

Sato, N., Mizumoto, K., Nakamura, M., Nakamura, K., Kusumoto, M., Niiyama, H., Ogawa, T., *et al.* (1999) 'Centrosome abnormalities in pancreatic ductal carcinoma.', *Clin. Cancer Res.*, 5(5), pp. 963–70.

Sato, N., Mizumoto, K., Nakamura, M., Maehara, N., Minamishima, Y. A., Nishio, S., Nagai, E., *et al.* (2001) 'Correlation between centrosome abnormalities and chromosomal instability in human pancreatic cancer cells', *Cancer Genet. Cytogenet.*, 126(1), pp. 13–19.

Sato, T., Akasu, H., Shimono, W., Matsu, C., Fujiwara, Y., Shibagaki, Y., Heard, J. J., *et al.* (2015) 'Rheb protein binds CAD (carbamoyl-phosphate synthetase 2, aspartate transcarbamoylase, and dihydroorotase) protein in a GTP- And effector domain-dependent manner and influences its cellular localization and carbamoylphosphate synthetase (CPSase) activity', *J. Biol. Chem.*, 290(2), pp. 1096–1105.

Sausen, M., Phallen, J., Adleff, V., Jones, S., Leary, R. J., Barrett, M. T., Anagnostou, V., *et al.* (2015) 'Clinical implications of genomic alterations in the tumour and circulation of pancreatic cancer patients.', *Nat. Commun.*, 6, p. 7686.

Savina, A., Furlán, M., Vidal, M. and Colombo, M. I. (2003) 'Exosome release is regulated by a calcium-dependent mechanism in K562 cells', *J. Biol. Chem.*, 278(22), pp. 20083–20090.

Savina, A., Fader, C. M., Damiani, M. T. and Colombo, M. I. (2005) 'Rab11 promotes docking and fusion of multivesicular bodies in a calcium-dependent manner', *Traffic*, 6(2), pp. 131–143.

Scarpa, A., Capelli, P., Mukai, K., Zamboni, G., Oda, T., Iacono, C. and Hirohashi, S. (1993) 'Pancreatic adenocarcinomas frequently show p53 gene mutations.', *Am. J. Pathol.*, 142(5), pp. 1534–43.

Schneider, E., Schmid-Kotsas, A., Zhao, J., Weidenbach, H., Schmid, R. M., Menke, A., Adler, G., *et al.* (2001) 'Identification of mediators stimulating proliferation and matrix synthesis of rat pancreatic stellate cells.', *Am. J. Physiol. Cell Physiol.*, 281(2), pp. C532-43.

Schneiderhan, W., Diaz, F., Fundel, M., Zhou, S., Siech, M., Hasel, C., Moller, P., *et al.* (2007) 'Pancreatic stellate cells are an important source of MMP-2 in human pancreatic cancer and accelerate tumor progression in a murine xenograft model and CAM assay', *J. Cell Sci.*, 120(3), pp. 512–519.

Schnelderhan, W., Diaz, F., Fundel, M., Zhou, S., Siech, M., Hasel, C., Möller, P., *et al.* (2007) 'Pancreatic stellate cells are an important source of MMP-2 in human pancreatic cancer and accelerate tumor progression in a murine xenograft model and CAM assay', *J. Cell Sci.*, 120(3), pp. 512–519.

Schuh, M. and Ellenberg, J. (2007) 'Self-organization of MTOCs replaces centrosome function during acentrosomal spindle assembly in live mouse oocytes.', *Cell*, 130(3), pp. 484–98.

Schumacher, J. M., Ashcroft, N., Donovan, P. J. and Golden, A. (1998) 'A highly conserved centrosomal kinase, AIR-1, is required for accurate cell cycle progression and segregation of developmental factors in Caenorhabditis elegans embryos.', *Development*, 125(22), pp. 4391–402.

Schutte, M., Hruban, R. ., Geradts, J., Maynard, R., Hilgers, W., Rabindran, S. K., Moskaluk, C. A., *et al.* (1997) 'Abrogation of the Rb/p16 tumor-suppressive pathway in virtually all pancreatic carcinomas', *Cancer Res.*, 57(15), pp. 3126–3130.

Sedgwick, A. E. and D'Souza-Schorey, C. (2018) 'The biology of extracellular

microvesicles.', *Traffic*, 19(5), pp. 319–327.

Segat, D., Cassaro, M., Dazzo, E., Cavallini, L., Romualdi, C., Salvador, R., Vitale, M. P., *et al.* (2010) 'Pericentriolar material analyses in normal esophageal mucosa, Barrett's metaplasia and adenocarcinoma.', *Histol. Histopathol.*, 25(5), pp. 551–60.

Serçin, Ö., Larsimont, J.-C., Karambelas, A. E., Marthiens, V., Moers, V., Boeckx, B., Le Mercier, M., *et al.* (2015) 'Transient PLK4 overexpression accelerates tumorigenesis in p53-deficient epidermis.', *Nat. Cell Biol.*, 18(1), pp. 100–110.

Shek, F. W.-T., Benyon, R. C., Walker, F. M., McCrudden, P. R., Pender, S. L. F., Williams, E. J., Johnson, P. A., *et al.* (2002) 'Expression of transforming growth factor-beta 1 by pancreatic stellate cells and its implications for matrix secretion and turnover in chronic pancreatitis.', *Am. J. Pathol.*, 160(5), pp. 1787–98.

Shimizu, Y., Yasui, K., Matsueda, K., Yanagisawa, A. and Yamao, K. (2005) 'Small carcinoma of the pancreas is curable: new computed tomography finding, pathological study and postoperative results from a single institute.', *J. Gastroenterol. Hepatol.*, 20(10), pp. 1591–4.

Shono, M., Sato, N., Mizumoto, K., Maehara, N., Nakamura, M., Nagai, E. and Tanaka, M. (2001) 'Stepwise progression of centrosome defects associated with local tumor growth and metastatic process of human pancreatic carcinoma cells transplanted orthotopically into nude mice', *Lab. Investig.*, 81(7), pp. 945–952.

Siegel, R. L., Miller, K. D. and Jemal, A. (2019) 'Cancer statistics, 2019.', *CA. Cancer J. Clin.*, 69(1), pp. 7–34.

Sigoillot, F. D., Kotsis, D. H., Serre, V., Sigoillot, S. M., Evans, D. R. and Guy, H. I. (2005) 'Nuclear localization and mitogen-activated protein kinase phosphorylation of the multifunctional protein CAD.', *J. Biol. Chem.*, 280(27), pp. 25611–20.

Silkworth, W. T., Nardi, I. K., Scholl, L. M. and Cimini, D. (2009) 'Multipolar spindle pole coalescence is a major source of kinetochore mis-attachment and chromosome mis-segregation in cancer cells', *PLoS One*.

Sillibourne, J. E., Tack, F., Vloemans, N., Boeckx, A., Thambirajah, S., Bonnet, P.,

Ramaekers, F. C. S., *et al.* (2010) 'Autophosphorylation of Polo-like Kinase 4 and Its Role in Centriole Duplication', *Mol. Biol. Cell*, 21(4), p. 547.

Sincock, P. M., Fitter, S., Parton, R. G., Berndt, M. C., Gamble, J. R. and Ashman, L. K. (1999) 'PETA-3/CD151, a member of the transmembrane 4 superfamily, is localised to the plasma membrane and endocytic system of endothelial cells, associates with multiple integrins and modulates cell function.', *J. Cell Sci.*, 112 (Pt 6), pp. 833–44.

Sir, J.-H., Pütz, M., Daly, O., Morrison, C. G., Dunning, M., Kilmartin, J. V. and Gergely, F. (2013) 'Loss of centrioles causes chromosomal instability in vertebrate somatic cells', *J. Cell Biol.*, 203(5), pp. 747–756.

Smith, E., Hégarat, N., Vesely, C., Roseboom, I., Larch, C., Streicher, H., Straatman, K., *et al.* (2011) 'Differential control of Eg5-dependent centrosome separation by Plk1 and Cdk1.', *EMBO J.*, 30(11), pp. 2233–45.

Sonnen, K. F., Schermelleh, L., Leonhardt, H. and Nigg, E. A. (2012) '3D-structured illumination microscopy provides novel insight into architecture of human centrosomes', *Biol. Open*, 1(10), pp. 965–976.

Sonnen, K. F., Gabryjonczyk, A.-M., Anselm, E., Stierhof, Y.-D. and Nigg, E. A. (2013) 'Human Cep192 and Cep152 cooperate in Plk4 recruitment and centriole duplication', *J. Cell Sci.*, 126(14), pp. 3223–3233.

Stankovic-Valentin, N. and Melchior, F. (2018) 'Control of SUMO and Ubiquitin by ROS: Signaling and disease implications.', *Mol. Aspects Med.*, 63, pp. 3–17.

Starita, L. M., Machida, Y., Sankaran, S., Elias, J. E., Griffin, K., Schlegel, B. P., Gygi, S. P., *et al.* (2004) 'BRCA1-Dependent Ubiquitination of -Tubulin Regulates Centrosome Number', *Mol. Cell. Biol.*, 24(19), pp. 8457–8466.

Stenmark, H. (2009) 'Rab GTPases as coordinators of vesicle traffic', *Nat. Rev. Mol. Cell Biol.*, pp. 513–525.

Stephens, P. J., Greenman, C. D., Fu, B., Yang, F., Bignell, G. R., Mudie, L. J., Pleasance, E. D., *et al.* (2011) 'Massive genomic rearrangement acquired in a single catastrophic event during cancer development', *Cell*.

Stevens, N. R., Raposo, A. A. S. F., Basto, R., St Johnston, D. and Raff, J. W. (2007) 'From stem cell to embryo without centrioles.', *Curr. Biol.*, 17(17), pp. 1498–503.

Stoka, V., Turk, V. and Turk, B. (2016) 'Lysosomal cathepsins and their regulation in aging and neurodegeneration', *Ageing Res. Rev.* Elsevier, pp. 22–37.

Sumoza-Toledo, A. and Penner, R. (2011) 'TRPM2: A multifunctional ion channel for calcium signalling', *J. Physiol.* John Wiley & Sons, Ltd (10.1111), pp. 1515–1525.

Sun, G. D., Kobayashi, T., Abe, M., Tada, N., Adachi, H., Shiota, A., Totsuka, Y., *et al.* (2007) 'The endoplasmic reticulum stress-inducible protein Niban regulates eIF2α and S6K1/4E-BP1 phosphorylation', *Biochem. Biophys. Res. Commun.*, 360(1), pp. 181–187.

Sun, Y. and Liu, J. (2014) 'Potential of cancer cell-derived exosomes in clinical application: A review of recent research advances', *Clin. Ther.*, pp. 863–872.

Sung, B. H., Ketova, T., Hoshino, D., Zijlstra, A. and Weaver, A. M. (2015) 'Directional cell movement through tissues is controlled by exosome secretion', *Nat. Commun.*, 6, p. 7164.

Svensson, K. J., Christianson, H. C., Wittrup, A., Bourseau-Guilmain, E., Lindqvist, E., Svensson, L. M., Mörgelin, M., *et al.* (2013) 'Exosome uptake depends on ERK1/2-heat shock protein 27 signaling and lipid Raft-mediated endocytosis negatively regulated by caveolin-1.', *J. Biol. Chem.*, 288(24), pp. 17713–24.

Szczepanski, M. J., Szajnik, M., Welsh, A., Whiteside, T. L. and Boyiadzis, M. (2011) 'Blast-derived microvesicles in sera from patients with acute myeloid leukemia suppress natural killer cell function via membrane-associated transforming growth factor-β1', *Haematologica*, 96(9), pp. 1302–1309.

Tafani, M., Sansone, L., Limana, F., Arcangeli, T., De Santis, E., Polese, M., Fini, M., *et al.* (2016) 'The Interplay of Reactive Oxygen Species, Hypoxia, Inflammation, and Sirtuins in Cancer Initiation and Progression', *Oxid. Med. Cell. Longev.* Hindawi Limited.

Tahara, H., Sato, K., Yamazaki, Y., Ohyama, T., Horiguchi, N., Hashizume, H., Kakizaki, S., *et al.* (2013) 'Transforming growth factor-α activates pancreatic stellate cells

and may be involved in matrix metalloproteinase-1 upregulation.', *Lab. Invest.*, 93(6), pp. 720–32.

Tai, Y. L., Chen, K. C., Hsieh, J. T. and Shen, T. L. (2018) 'Exosomes in cancer development and clinical applications', *Cancer Sci.* Blackwell Publishing Ltd, pp. 2364–2374.

Takahashi, K., Yan, I. K., Kogure, T., Haga, H. and Patel, T. (2014) 'Extracellular vesicle-mediated transfer of long non-coding RNA ROR modulates chemosensitivity in human hepatocellular cancer', *FEBS Open Bio*, 4(1), pp. 458–467.

Tamai, K., Tanaka, N., Nakano, T., Kakazu, E., Kondo, Y., Inoue, J., Shiina, M., *et al.* (2010) 'Exosome secretion of dendritic cells is regulated by Hrs, an ESCRT-0 protein', *Biochem. Biophys. Res. Commun.*, 399(3), pp. 384–390.

Tanaka, Y., Kamohara, H., Kinoshita, K., Kurashige, J., Ishimoto, T., Iwatsuki, M., Watanabe, M., *et al.* (2013) 'Clinical impact of serum exosomal microRNA-21 as a clinical biomarker in human esophageal squamous cell carcinoma', *Cancer*, 119(6), pp. 1159–1167.

Tang, N. and Marshall, W. F. (2012) 'Centrosome positioning in vertebrate development', *J. Cell Sci.*

Tanida, I., Ueno, T. and Kominami, E. (2008) 'LC3 and autophagy', *Methods Mol. Biol.*, 445, pp. 77–88.

Taylor, D. D. and Gercel-Taylor, C. (2008) 'MicroRNA signatures of tumor-derived exosomes as diagnostic biomarkers of ovarian cancer', *Gynecol. Oncol.*, 110(1), pp. 13–21.

Telkoparan, P., Erkek, S., Yaman, E., Alotaibi, H., Bayik, D. and Tazebay, U. H. (2013) 'Coiled-Coil Domain Containing Protein 124 Is a Novel Centrosome and Midbody Protein That Interacts with the Ras-Guanine Nucleotide Exchange Factor 1B and Is Involved in Cytokinesis', *PLoS One*, 8(7).

Terino, M., Plotkin, E. and Karagozian, R. (2018) 'Pancreatoblastoma: an Atypical Presentation and a Literature Review', *J. Gastrointest. Cancer*, 49(3), pp. 361–364.

Thakur, B. K., Zhang, H., Becker, A., Matei, I., Huang, Y., Costa-Silva, B., Zheng, Y., *et al.*

(2014) ‘Double-stranded DNA in exosomes: a novel biomarker in cancer detection’, *Cell Res.*, 24(6), pp. 766–769.

Thayer, S. P., di Magliano, M. P., Heiser, P. W., Nielsen, C. M., Roberts, D. J., Lauwers, G. Y., Qi, Y. P., *et al.* (2003) ‘Hedgehog is an early and late mediator of pancreatic cancer tumorigenesis.’, *Nature*, 425(6960), pp. 851–6.

Théry, C., Amigorena, S., Raposo, G. and Clayton, A. (2006) ‘Isolation and characterization of exosomes from cell culture supernatants and biological fluids.’, *Curr. Protoc. cell Biol.*, Chapter 3, p. Unit 3.22.

Théry, C., Witwer, K. W., Aikawa, E., Alcaraz, M. J., Anderson, J. D., Andriantsitohaina, R., Antoniou, A., *et al.* (2018) ‘Minimal information for studies of extracellular vesicles 2018 (MISEV2018): a position statement of the International Society for Extracellular Vesicles and update of the MISEV2014 guidelines’, *J. Extracell. Vesicles*, 7(1), p. 1535750.

Théry, C., Ostrowski, M. and Segura, E. (2009) ‘Membrane vesicles as conveyors of immune responses’, *Nat. Rev. Immunol.*, pp. 581–593.

Thomas, D. and Radhakrishnan, P. (2019) ‘Tumor-stromal crosstalk in pancreatic cancer and tissue fibrosis’, *Mol. Cancer*. BioMed Central Ltd.

Thul, P. J., Akesson, L., Wiking, M., Mahdessian, D., Geladaki, A., Ait Blal, H., Alm, T., *et al.* (2017) ‘A subcellular map of the human proteome’, *Science (80-.).*, 356(6340).

Tian, T., Wang, Y., Wang, H., Zhu, Z. and Xiao, Z. (2010) ‘Visualizing of the cellular uptake and intracellular trafficking of exosomes by live-cell microscopy’, *J. Cell. Biochem.*, 111(2), pp. 488–496.

Tiwari, N., Wang, C.-C., Brochetta, C., Ke, G., Vita, F., Qi, Z., Rivera, J., *et al.* (2008) ‘VAMP-8 segregates mast cell-preformed mediator exocytosis from cytokine trafficking pathways.’, *Blood*, 111(7), pp. 3665–74.

Tjomsland, V., Pomianowska, E., Aasrum, M., Sandnes, D., Verbeke, C. S. and Gladhaug, I. P. (2016) ‘Profile of MMP and TIMP Expression in Human Pancreatic Stellate Cells: Regulation by IL-1α and TGFβ and Implications for Migration of Pancreatic Cancer Cells.’, *Neoplasia*, 18(7), pp. 447–56.

Tkach, M., Kowal, J., Zucchetti, A. E., Enserink, L., Jouve, M., Lankar, D., Saitakis, M., *et al.* (2017) 'Qualitative differences in T-cell activation by dendritic cell-derived extracellular vesicle subtypes.', *EMBO J.*, 36(20), pp. 3012–3028.

Townsend, D. M., Tew, K. D. and Tapiero, H. (2003) 'The importance of glutathione in human disease', *Biomed. Pharmacother.*, pp. 145–155.

Trajkovic, K., Hsu, C., Chiantia, S., Rajendran, L., Wenzel, D., Wieland, F., Schwille, P., *et al.* (2008) 'Ceramide triggers budding of exosome vesicles into multivesicular endosomes.', *Science*, 319(5867), pp. 1244–7.

Tramacere, I., Scotti, L., Jenab, M., Bagnardi, V., Bellocco, R., Rota, M., Corrao, G., *et al.* (2010) 'Alcohol drinking and pancreatic cancer risk: a meta-analysis of the dose-risk relation.', *Int. J. cancer*, 126(6), pp. 1474–86.

Tsang, W. Y., Bossard, C., Khanna, H., Peränen, J., Swaroop, A., Malhotra, V. and Dynlacht, B. D. (2008) 'CP110 suppresses primary cilia formation through its interaction with CEP290, a protein deficient in human ciliary disease.', *Dev. Cell*, 15(2), pp. 187–97.

Tsou, M.-F. B., Wang, W.-J., George, K. A., Uryu, K., Stearns, T. and Jallepalli, P. V (2009) 'Polo kinase and separase regulate the mitotic licensing of centriole duplication in human cells.', *Dev. Cell*, 17(3), pp. 344–54.

Tsou, M.-F. B. and Stearns, T. (2006) 'Mechanism limiting centrosome duplication to once per cell cycle', *Nature*, 442(7105), pp. 947–951.

Tsuchiya, R., Noda, T., Harada, N., Miyamoto, T., Tomioka, T., Yamamoto, K., Yamaguchi, T., *et al.* (1986) 'Collective review of small carcinomas of the pancreas.', *Ann. Surg.*, 203(1), pp. 77–81.

Tung, K., Ernstoff, M., Allen, C. and Shu, S. (2019) 'A Review of Exosomes and their Role in The Tumor Microenvironment and Host-Tumor "Macroenvironment"', *J. Immunol. Sci.*, 3(1), pp. 4–8.

Turchinovich, A., Weiz, L., Langheinz, A. and Burwinkel, B. (2011) 'Characterization of extracellular circulating microRNA', *Nucleic Acids Res.*, 39(16), pp. 7223–7233.

Uhlen, M., Zhang, C., Lee, S., Sjöstedt, E., Fagerberg, L., Bidkhori, G., Benfeitas, R., *et al.*

(2017) ‘A pathology atlas of the human cancer transcriptome’, *Science (80-.).*, 357(6352).

Umezu, T., Ohyashiki, K., Kuroda, M. and Ohyashiki, J. H. (2013) ‘Leukemia cell to endothelial cell communication via exosomal miRNAs.’, *Oncogene*, 32(22), pp. 2747–55.

Vaccaro, V., Sperduti, I. and Milella, M. (2011) ‘FOLFIRINOX versus gemcitabine for metastatic pancreatic cancer.’, *N. Engl. J. Med.*, 365(8), pp. 768–9; author reply 769.

Vaizel-Ohayon, D. and Schejter, E. D. (1999) ‘Mutations in centrosomin reveal requirements for centrosomal function during early Drosophila embryogenesis.’, *Curr. Biol.*, 9(16), pp. 889–98.

Valadi, H., Ekström, K., Bossios, A., Sjöstrand, M., Lee, J. J. and Lötvall, J. O. (2007) ‘Exosome-mediated transfer of mRNAs and microRNAs is a novel mechanism of genetic exchange between cells.’, *Nat. Cell Biol.*, 9(6), pp. 654–9.

Varmark, H., Llamazares, S., Rebollo, E., Lange, B., Reina, J., Schwarz, H. and Gonzalez, C. (2007) ‘Asterless is a centriolar protein required for centrosome function and embryo development in Drosophila.’, *Curr. Biol.*, 17(20), pp. 1735–45.

Verweij, F. J., Bebelman, M. P., Jimenez, C. R., Garcia-Vallejo, J. J., Janssen, H., Neefjes, J., Knol, J. C., *et al.* (2018) ‘Quantifying exosome secretion from single cells reveals a modulatory role for GPCR signaling’, *J. Cell Biol.*, 217(3), pp. 1129–1142.

Villarroya-Beltri, C., Gutiérrez-Vázquez, C., Sánchez-Cabo, F., Pérez-Hernández, D., Vázquez, J., Martin-Cofreces, N., Martinez-Herrera, D. J., *et al.* (2013) ‘Sumoylated hnRNPA2B1 controls the sorting of miRNAs into exosomes through binding to speVillarroya-Beltri, C., Gutiérrez-Vázquez, C., Sánchez-Cabo, F., Pérez-Hernández, D., Vázquez, J., Martin-Cofreces, N., … Sánchez-Madrid, F. (2013). Sumoylated hnRNPA2B’, *Nat. Commun.*, 4, p. 2980.

Villarroya-Beltri, C., Baixauli, F., Mittelbrunn, M., Fernández-Delgado, I., Torralba, D., Moreno-Gonzalo, O., Baldanta, S., *et al.* (2016) ‘ISGylation controls exosome secretion by promoting lysosomal degradation of MVB proteins’, *Nat. Commun.*, 7.

Vitre, B., Holland, A. J., Kulukian, A., Shoshani, O., Hirai, M., Wang, Y., Maldonado, M., *et al.* (2015) 'Chronic centrosome amplification without tumorigenesis.', *Proc. Natl. Acad. Sci. U. S. A.*, 112(46), pp. E6321–E6330.

Vlassov, A. V, Magdaleno, S., Setterquist, R. and Conrad, R. (2012) 'Exosomes: Current knowledge of their composition, biological functions, and diagnostic and therapeutic potentials', *Biochim. Biophys. Acta - Gen. Subj.*, pp. 940–948.

Vlijm, R., Li, X., Panic, M., Rüthnick, D., Hata, S., Herrmannsdörfer, F., Kuner, T., *et al.* (2018) 'STED nanoscopy of the centrosome linker reveals a CEP68-organized, periodic rootletin network anchored to a C-Nap1 ring at centrioles', *Proc. Natl. Acad. Sci.*, 115(10), pp. E2246–E2253.

Voichitoiu, A.-D., Mihaela Radu, B., Pavelescu, L., Cretoiu, D., Teona Deftu, A., Suciu, N. and Maria Cretoiu, S. (2019) 'Extracellular Vesicles in Cancer', in *Extracell. Vesicles [Working Title]*. IntechOpen.

Vonlaufen, A., Joshi, S., Qu, C., Phillips, P. A., Xu, Z., Parker, N. R., Toi, C. S., *et al.* (2008) 'Pancreatic stellate cells: Partners in crime with pancreatic cancer cells', *Cancer Res.*, 68(7), pp. 2085–2093.

Vonlaufen, A., Phillips, P. A., Yang, L., Xu, Z., Fiala-Beer, E., Zhang, X., Pirola, R. C., *et al.* (2010) 'Isolation of quiescent human pancreatic stellate cells: A promising in vitro tool for studies of human pancreatic stellate cell biology', *Pancreatology*, 10(4), pp. 434–443.

Wang, J. D., Jin, K., Chen, X. Y., Lv, J. Q. and Ji, K. W. (2017) 'Clinicopathological significance of SMAD4 loss in pancreatic ductal adenocarcinomas: A systematic review and meta-analysis', *Oncotarget*, 8(10), pp. 16704–16711.

Wang, L. M., Silva, M. A., D'Costa, Z., Bockelmann, R., Soonawalla, Z., Liu, S., O'Neill, E., *et al.* (2016) 'The prognostic role of desmoplastic stroma in pancreatic ductal adenocarcinoma', *Oncotarget*, 7(4), pp. 4183–4194.

Wang, X., Xu, C., Hua, Y., Sun, L., Cheng, K., Jia, Z., Han, Y., *et al.* (2016) 'Exosomes play an important role in the process of psoralen reverse multidrug resistance of breast cancer', *J. Exp. Clin. Cancer Res.*, 35(1), pp. 1–10.

Wang, Y., Jin, F., Higgins, R. and McKnight, K. (2014) 'The current view for the silencing of the spindle assembly checkpoint', *Cell Cycle*.

Waterman-Storer, C. M., Worthylake, R. A., Liu, B. P., Burridget, K. and Salmon, E. D. (1999) 'Microtubule growth activates Rac1 to promote lamellipodial protrusion in fibroblasts', *Nat. Cell Biol.*

Watts, C. A., Richards, F. M., Bender, A., Bond, P. J., Korb, O., Kern, O., Riddick, M., *et al.* (2013) 'Design, Synthesis, and Biological Evaluation of an Allosteric Inhibitor of HSET that Targets Cancer Cells with Supernumerary Centrosomes', *Chem. Biol.*, 20(11), pp. 1399–1410.

Weaver, B. A. A., Silk, A. D., Montagna, C., Verdier-Pinard, P. and Cleveland, D. W. (2007) 'Aneuploidy Acts Both Oncogenically and as a Tumor Suppressor', *Cancer Cell*.

Webber, J., Steadman, R., Mason, M. D., Tabi, Z. and Clayton, A. (2010a) 'Cancer exosomes trigger fibroblast to myofibroblast differentiation', *Cancer Res.*, 70(23), pp. 9621–9630.

Webber, J., Steadman, R., Mason, M. D., Tabi, Z. and Clayton, A. (2010b) 'Cancer exosomes trigger fibroblast to myofibroblast differentiation', *Cancer Res.*, 70(23), pp. 9621–9630.

Webber, J. and Clayton, A. (2013) 'How pure are your vesicles?', *J. Extracell. Vesicles*, 2(1), p. 19861.

Wei, G., Jie, Y., Haibo, L., Chaoneng, W., Dong, H., Jianbing, Z., Junjie, G., *et al.* (2017) 'Dendritic cells derived exosomes migration to spleen and induction of inflammation are regulated by CCR7', *Sci. Rep.*, 7, p. 42996.

Welton, J. L., Webber, J. P., Botos, L.-A., Jones, M. and Clayton, A. (2015) 'Ready-made chromatography columns for extracellular vesicle isolation from plasma.', *J. Extracell. vesicles*, 4, p. 27269.

Weng, S., Wang, Hua, Chen, W., Katz, M. H., Chatterjee, D., Lee, J. E., Pisters, P. W., *et al.* (2012) 'Overexpression of protein phosphatase 4 correlates with poor prognosis in patients with stage II pancreatic ductal adenocarcinoma', *Cancer*

Epidemiol. Biomarkers Prev., 21(8), pp. 1336–1343.

De Wever, O., Demetter, P., Mareel, M. and Bracke, M. (2008) 'Stromal myofibroblasts are drivers of invasive cancer growth', *Int. J. Cancer*. Wiley Subscription Services, Inc., A Wiley Company, pp. 2229–2238.

Whitehead, C. M. and Rattner, J. B. (1998) 'Expanding the role of HsEg5 within the mitotic and post-mitotic phases of the cell cycle.', *J. Cell Sci.*, 111 (Pt 17), pp. 2551–61.

Whiteman, D. C., Webb, P. M., Green, A. C., Neale, R. E., Fritschi, L., Bain, C. J., Parkin, D. M., *et al.* (2015) 'Cancers in Australia in 2010 attributable to modifiable factors: Introduction and overview', *Aust. N. Z. J. Public Health*, 39(5), pp. 403–407.

Whiteside, T. L. (2013) 'Immune modulation of T-cell and NK (natural killer) cell activities by TEXs (tumour-derived exosomes)', in *Biochem. Soc. Trans.*, pp. 245–251.

Wickman, G., Julian, L. and Olson, M. F. (2012) 'How apoptotic cells aid in the removal of their own cold dead bodies', *Cell Death Differ.*, 19(5), pp. 735–742.

Wigley, W. C., Fabunmi, R. P., Lee, M. G., Marino, C. R., Muallem, S., DeMartino, G. N. and Thomas, P. J. (1999) 'Dynamic association of proteasomal machinery with the centrosome.', *J. Cell Biol.*, 145(3), pp. 481–90.

Wilentz, R. E., Geradts, J., Maynard, R., Offerhaus, G. J., Kang, M., Goggins, M., Yeo, C. J., *et al.* (1998) 'Inactivation of the p16 (INK4A) tumor-suppressor gene in pancreatic duct lesions: loss of intranuclear expression.', *Cancer Res.*, 58(20), pp. 4740–4.

Willms, E., Cabañas, C., Mäger, I., Wood, M. J. A. and Vader, P. (2018) 'Extracellular vesicle heterogeneity: Subpopulations, isolation techniques, and diverse functions in cancer progression', *Front. Immunol.* Frontiers Media S.A.

Witwer, K. W., Aikawa, E., Alcaraz, M. J., Anderson, J. D., Andriantsitohaina, R., Antoniou, A., Arab, T., *et al.* (2018) 'Minimal information for studies of extracellular vesicles 2018 (MISEV2018): a position statement of the International Society for Extracellular Vesicles and update of the MISEV2014 guidelines AU -

Théry, Clotilde', *J. Extracell. Vesicles*, 7, p. 1535750.

Wojcik, E. J., Glover, D. M. and Hays, T. S. (2000) 'The SCF ubiquitin ligase protein slimb regulates centrosome duplication in Drosophila.', *Curr. Biol.*, 10(18), pp. 1131–4.

Wong, Y. L., Anzola, J. V., Davis, R. L., Yoon, M., Motamedi, A., Kroll, A., Seo, C. P., *et al.* (2015) 'Reversible centriole depletion with an inhibitor of Polo-like kinase 4', *Science*, 348(6239), p. 1155.

Wood, L. D. and Hruban, R. H. (2012) 'Pathology and Molecular Genetics of Pancreatic Neoplasms', *Cancer J.*, 18(6), pp. 492–501.

Wortzel, I., Dror, S., Kenific, C. M. and Lyden, D. (2019) 'Exosome-Mediated Metastasis: Communication from a Distance', *Dev. Cell*, pp. 347–360.

Wu, J., Mikule, K., Wang, W., Su, N., Petteruti, P., Gharahdaghi, F., Code, E., *et al.* (2013) 'Discovery and mechanistic study of a small molecule inhibitor for motor protein KIFC1', *ACS Chem. Biol.*, 8(10), pp. 2201–2208.

Xie, S., Qin, J., Liu, S., Zhang, Y., Wang, J., Shi, X., Li, D., *et al.* (2016) 'Cep70 overexpression stimulates pancreatic cancer by inducing centrosome abnormality and microtubule disorganization', *Sci. Rep.*, 6.

Xu, R., Rai, A., Chen, M., Suwakulsiri, W., Greening, D. W. and Simpson, R. J. (2018) 'Extracellular vesicles in cancer — implications for future improvements in cancer care', *Nat. Rev. Clin. Oncol.* Nature Publishing Group, pp. 617–638.

Xu, Z., Vonlaufen, A., Phillips, P. A., Fiala-Beer, E., Zhang, X., Yang, L., Biankin, A. V., *et al.* (2010) 'Role of pancreatic stellate cells in pancreatic cancer metastasis', *Am. J. Pathol.*, 177(5), pp. 2585–2596.

Yachida, S., Jones, S., Bozic, I., Antal, T., Leary, R., Fu, B., Kamiyama, M., *et al.* (2010) 'Distant metastasis occurs late during t1. Yachida, S. et al. Distant metastasis occurs late during the genetic evolution of pancreatic cancer. Nature 467, 1114–7 (2010).he genetic evolution of pancreatic cancer.', *Nature*, 467(7319), pp. 1114–7.

Yamamoto, Y., Matsuyama, H., Furuya, T., Oga, A., Yoshihiro, S., Okuda, M., Kawauchi, S., *et al.* (2004) 'Centrosome hyperamplification predicts progression and tumor recurrence in bladder cancer', *Clin. Cancer Res.*, 10(19), pp. 6449–6455.

Yang, J., Adamian, M. and Li, T. (2006) 'Rootletin Interacts with C-Nap1 and May Function as a Physical Linker between the Pair of Centrioles/Basal Bodies in Cells', *Mol. Biol. Cell*, 17(2), pp. 1033–1040.

Ying, X., Wu, Q., Wu, X., Zhu, Q., Wang, Xinjing, Jiang, L., Chen, X., *et al.* (2016) 'Epithelial ovarian cancer-secreted exosomal miR-222-3p induces polarization of tumor-associated macrophages.', *Oncotarget*, 7(28), pp. 43076–43087.

Yokode, M., Akita, M., Fujikura, K., Kim, M.-J., Morinaga, Y., Yoshikawa, S., Terada, T., *et al.* (2018) 'High-grade PanIN presenting with localised stricture of the main pancreatic duct: A clinicopathological and molecular study of 10 cases suggests a clue for the early detection of pancreatic cancer.', *Histopathology*, 73(2), pp. 247–258.

Yoshimori, T., Yamamoto, A., Moriyama, Y., Futai, M. and Tashiro, Y. (1991) 'Bafilomycin A1, a specific inhibitor of vacuolar-type H+-ATPase, inhibits acidification and protein degradation in lysosomes of cultured cells', *J. Biol. Chem.*, 266(26), pp. 17707–17712.

Yuan-Chen, C., Perihan, N., Jörg, B., Zee-Fen, C. and Gary, M. B. (2008) 'GEF-H1 Couples Nocodazole-induced Microtubule Disassembly to Cell Contractility via RhoA', *Mol. Biol. Cell*.

Yue, S., Mu, W., Erb, U. and Zöller, M. (2015) 'The tetraspanins CD151 and Tspan8 are essential exosome components for the crosstalk between cancer initiating cells and their surrounding', *Oncotarget*, 6(4), pp. 2366–2384.

Yukawa, M., Yamauchi, T., Kurisawa, N., Ahmed, S., Kimura, K. ichi and Toda, T. (2018) 'Fission yeast cells overproducing HSET/KIFC1 provides a useful tool for identification and evaluation of human kinesin-14 inhibitors', *Fungal Genet. Biol.*, 116, pp. 33–41.

Yuyama, K., Sun, H., Mitsutake, S. and Igarashi, Y. (2012) 'Sphingolipid-modulated exosome secretion promotes clearance of amyloid-?? by microglia', *J. Biol. Chem.*, 287(14), pp. 10977–10989.

Zack, T. I., Schumacher, S. E., Carter, S. L., Cherniack, A. D., Saksena, G., Tabak, B., Lawrence, M. S., *et al.* (2013) 'Pan-cancer patterns of somatic copy number

alteration', *Nat. Genet.*

Zhang, H., Freitas, D., Kim, H. S., Fabijanic, K., Li, Z., Chen, H., Mark, M. T., *et al.* (2018) 'Identification of distinct nanoparticles and subsets of extracellular vesicles by asymmetric flow field-flow fractionation.', *Nat. Cell Biol.*, 20(3), pp. 332–343.

Zhang, H. G. and Grizzle, W. E. (2014) 'Exosomes: A novel pathway of local and distant intercellular communication that facilitates the growth and metastasis of neoplastic lesions', *Am. J. Pathol.*, pp. 28–41.

Zhang, L., Zhang, S., Yao, J., Lowery, F. J., Zhang, Q., Huang, W. C., Li, P., *et al.* (2015) 'Microenvironment-induced PTEN loss by exosomal microRNA primes brain metastasis outgrowth', *Nature*, 527(7576), pp. 100–104.

Zhang, W., Zhai, L., Wang, Y., Boohaker, R. J., Lu, W., Gupta, V. V, Padmalayam, I., *et al.* (2016) 'Discovery of a novel inhibitor of kinesin-like protein KIFC1.', *Biochem. J.*, 473(8), pp. 1027–35.

Zhang, X., Chen, Q., Feng, J., Hou, J., Yang, F., Liu, J., Jiang, Q., *et al.* (2009) 'Sequential phosphorylation of Nedd1 by Cdk1 and Plk1 is required for targeting of the TuRC to the centrosome', *J. Cell Sci.*, 122(13), pp. 2240–2251.

Zhang, X., Wang, B., Wang, C., Chen, L. and Xiao, Y. (2015) 'Monitoring Lipid Peroxidation within Foam Cells by Lysosome-Targetable and Ratiometric Probe', *Anal. Chem.*, 87(16), pp. 8292–8300.

Zhang, Y.-F., Zhou, Y.-Z., Zhang, B., Huang, S.-F., Li, P.-P., He, X.-M., Cao, G.-D., *et al.* (2019) 'Pancreatic cancer-derived exosomes promoted pancreatic stellate cells recruitment by pancreatic cancer', *J. Cancer*, 10(18), pp. 4397–4407.

Zhitomirsky, B., Farber, H. and Assaraf, Y. G. (2018) 'LysoTracker and MitoTracker Red are transport substrates of P-glycoprotein: implications for anticancer drug design evading multidrug resistance', *J. Cell. Mol. Med.*, 22(4), pp. 2131–2141.

Zilfou, J. and Lowe, S. (2009) 'Tumor suppressive functions of p53.', *Cold Spring Harb Perspect Biol.*, 1(5).

Zomer, A., Maynard, C., Verweij, F. J., Kamermans, A., Schäfer, R., Beerling, E., Schiffelers, R. M., *et al.* (2015) 'In Vivo imaging reveals extracellular vesicle-

mediated phenocopying of metastatic behavior.', *Cell*, 161(5), pp. 1046–1057.

Zyss, D. and Gergely, F. (2009) 'Centrosome function in cancer: guilty or innocent?', *Trends Cell Biol.*, pp. 334–346.